THE SIGNIFICANCE OF DRUG INDUCED DNA DAMAGE OF TELOMERES IN HUMAN TUMOUR CELLS

Jessie Chandika Jeyapalan

UNIVERSITY OF
NEWCASTLE UPON TYNE

Thesis submitted to the University of Newcastle upon Tyne
for the degree of Doctor of Philosophy
February 2005

Gerontology- SCMS
Newcastle General Hospital
University of Newcastle upon Tyne

Dedicated to my dad

ACKNOWLEDGEMENTS

I would like to thank Prof Thomas von Zglinicki and Dr Mike Tilby for giving me the opportunity to work on this project, for their guidance, encouragement and support during my time here. Also thanks to Cancer Research UK for funding this project.

I would like to acknowledge past and present members of the MRC, Biogerontology and Cancer Research buildings for their help and making my time here a more enjoyable experience. A special thanks goes out to Barbara Keys, whose technical support and advice was greatly appreciated, especially during the initial stages of the project. I would like to thank Mandy Lee for her companionship and her mechanical skills; 'aunty' Carmen Martin Ruiz for being able to solve nearly all my problems and having the best ideas; Gabriele Saretzki for her helpful discussions; Alan Leake for his engaging conversations whilst working on the flow cytometer and Jaimie Sixsmith for being an understanding fellow scouser even though supporting the rival football team.

A huge thanks goes to the Hancock gang and the CF crew (apologises for not naming individually) for their friendship and making the hours away from my PhD over the years more entertaining. All will be missed dearly. Thanks (and apologises) also to past and present housemates who have to put up with my enthusiasm for hosting frequent planned and unplanned social gatherings. A very special thanks has to go to Karen Perrow (Pez) for her handy hints and wisdom; Susan Darroch for her constant encouragement and support over the years and Claudia Duerrwaechter (Dirtywater) for her enthusiasm, cynicism and sarcasm, that is beyond my understanding but nevertheless kept me amused, especially over the last few months. Thanks also to

Claudia for sharing the same interests and the 'never be able to use in everyday conversation' language lessons.

I would like to acknowledge Jennie Barclay, Eleri Short, Natalie Carter, Robbie Birchall and Clare Anderson, though living all over the world, whose frequent visits, phone calls and e mails have been greatly appreciated.

Finally I would like to give a huge thanks to my sister Jennie (Bennie) and mum for their love and support.

ABSTRACT

Telomere shortening is a major mechanism to induce telomere uncapping and thus to signal growth arrest and/ or apoptosis and can be caused by different mechanisms, one of which is damage to DNA, to which telomeres appear to be particularly sensitive. Contradictory data exists on the relationship between conventionally used chemotherapeutic drugs and the telomere/ telomerase complex. The aim of the work described in this thesis was to determine whether or not damage to telomeres played a significant role in the cytotoxic action of the anti-cancer drugs cisplatin and etoposide. Two cell lines were used with either short (neuroblastoma cell line SHSY5Y) or long (lymphoblastic T cell line 1301) telomeres. Cytotoxic effects of the drugs were assessed by growth inhibition assays and measurement of apoptosis and cell cycle progression by flow cytometry. Etoposide caused readily detectable DNA strand breakage and led to formation of nuclear foci of phosphorylated histone γ-H2A.X. Cisplatin treatment did not induce strand breaks after initial drug exposure but strand breaks and DNA damage foci were detected after further incubation.

For cells with either long or short telomeres, no detectable changes in total telomere length or overhang length were observed before apoptosis became manifest. Preferential occurrences of single strand breaks in the G-rich strand of telomeres were not found. Through the development of a dual staining method it was established that drug-induced histone H2A.X foci did not colocalise to the telomeres. Telomerase was transiently activated by lower concentrations of etoposide and its activity decreased only after onset of apoptosis.

Taken together, the results show no indication that telomeres and/ or telomeric damage play any preferential role as signal transducers towards apoptosis and/ or growth arrest in either of these cell lines. Also, the protective function of telomerase seems to be telomere independent. The data are consistent with a model of drug-induced growth arrest and apoptosis being triggered by damage elsewhere in the genome.

ABBREVIATIONS

(v/v)	volume per volume
(w/v)	weight per volume
ALT	Alternative lengthening of telomeres
AP	Apurinic/ apyrimidinic
BER	Base excision repair
Bp	Base pairs
BrdU	2-bromo-5-deoxuridine
BSA	Bovine serum albumin
CDK	Cyclin dependent kinase
CKI	Cyclin dependent kinase inhibitor
CPD	Cyclobutane pyrimidine dimers
CSPD	Chemiluminescent substrate
D-loop	Displacement loop
DAPI	4'-6-Diamidino-2-phenylindole
DMSO	Dimethyl sulphoxide
DNA	Deoxyribonucleic acid
DNA-PK	DNA dependent protein kinase
DSB	Double strand break
ELISA	Enzyme linked immunosorbent assay
FADD	Fas associated death domain
FADU	Fluorescence detected alkaline DNA unwinding
FCS	Foetal calf serum
FISH	Fluorescent *in situ* hybridisation
FITC	Fluorescein isothiocyanate
HR	Homologous recombination

hTERT	Catalytic subunit of telomerase
hTR	Telomerase RNA template
ICP-MS	Inductively coupled plasma- mass spectrometry
IR	Ionising radiation
Kbp	Kilobase pair
Mb	Megabase
MMR	DNA mismatch repair
MW	Molecular weight
NER	Nucleotide excision repair
NHEJ	Non homologous end joining
NIMA	Never in mitosis A
NT	Nucleotide
OD	Optical density
P	Phosphorus
PARP	Poly ADP ribose polymerase
PAS	Particle analysing system
PBS	Phosphate buffered saline
PCR	Polymerase chain reaction
PD	Population doubling
PFGE	Pulsed field gel electrophoresis
PIMMS	Plasma ionisation multicollector mass spectrometer
PIN2	Protein interacting with the never in mitosis A protein kinase
PNA	Peptide nucleic acid
PNK	Polynucleotide kinase
PPB	Parts per billion
PPM	Parts per million

PPT	Parts per trillion
POT1	Protection of telomeres1
Pt	Platinum
Rb	Retinoblastoma
RF	Radio frequency
RNA	Ribonucleic acid
SA- β Gal	Senescence associated- Beta galactosidase
SDS	Sodium dodecyl sulphate
SIPS	Stress induced premature senescence
SSC	Sodium chloride, sodium citrate
SRB	Sulphorhodamine B
SSB	Single strand break
TAP	Telomeric associated proteins
TBP	TATA binding protein
TCA	Trichloroacetic acid
TIN2	TRF1 interacting protein 2
TNF	Tumour necrosis factor
TRAP	Telomeric repeat amplification protocol
TRF1	TTAGGG repeat binding factor 1
TRF2	TTAGGG repeat binding factor 2
TTD	Trichothiodystrophy
UV	Ultraviolet
XP	Xeroderma pigmentosum

PUBLICATIONS

Parts of the research in production of this thesis has led to the publishing of the following papers:

Martin-Ruiz, C., Saretzki, G., Petrie, J., Ladhoff, J., Jeyapalan, J., Wei, W., Sedivy, J. and von Zglinicki T. (2004) Stochastic variation in telomere shortening rate causes heterogeneity of human fibroblast replicative life span. *J Biol Chem.,* **17**, 17826-33.

Jeyapalan, J., Leake, A., Ahmed, S., Saretzki, G., Tilby, M. and von Zglinicki, T. (2004) The role of telomeres in etoposide induced tumour cell death. *Cell Cycle.,* **3**, 1169-74.

Published abstracts:

Ottley, C.J., Pearson, D.G., Jeyapalan, J.C., Tilby, M.J., Nowell, G.M. von Zglinicki, T. (2001) Determination of P and Pt in clinical DNA samples by ICPMS and PIMMS. *International Conference of Plasma Source Mass Spectrometry* **8th**, p56.

Jeyapalan, J.C., Tilby, M.J. and von Zglinicki, T. (2003) Cisplatin induced neuroblastoma cell death and the involvement of telomeres. *British Journal of Cancer* **88** (Suppl 1), S39.

Jeyapalan, J.C., Tilby, M.J. and von Zglinicki, T. (2004) The role of telomeres in etoposide induced cell death. *Proceedings of the American Association for Cancer Research* **45**, A991.

Awards:

Cancer Research UK Student of the Year 2004

TABLE OF CONTENTS

LIST OF TABLES

LIST OF FIGURES

CHAPTER ONE

INTRODUCTION

1.1 Cancer

Cancer is a complex genetic disease that is the most common cause of death in the UK (26% of all deaths) and the lifetime risk of developing cancer is over one in three. 270,000 new cases were diagnosed in 2000 in the UK. Cancer is more likely to develop later on in life with 65% of cases diagnosed in people over the age of 65 (Cancer Research UK, Scientific Yearbook, 2003-2004).

Cancer is a disease which is distinguished by uncontrolled cell growth. During the early years of a person's life, normal cells divide more rapidly until the person becomes an adult then cells divide only to replace worn-out or dying cells and to repair injuries. As cancer cells continue to grow and divide, they differ from normal cells and they can travel to other parts of the body where they begin to grow and replace normal tissue which is called metastasis. This process occurs as the cancer cells get into the bloodstream or lymph vessels of our body. Cancer cells must not only be capable of dividing indefinitely but need to live as well by gaining nutrients and move through the extracellular matrix to metastasize (Hanahan and Weinberg, 2000). There are more than two hundred types of cancer but four of them account for half of all new cases (breast, lung, colorectal and prostate). Different types of cancers behave differently and therefore have to be treated individually. Cancer usually forms as tumours. Exceptions exist for example leukaemia which involves the blood and blood-forming organs. Though not all tumours are cancerous, non cancerous tumours are known as being benign. Benign tumours are generally slow growing expansive masses that compress rather than invade surrounding tissue.

There are many different types of cancer and more than one cause can often be involved (multi-factorial). Cancer causing agents (carcinogens) are widespread and can be present in food, air, water, chemicals or the sunlight. There are many risk factors that can increase the chance of getting cancer which includes age, sex, genetic makeup and family medical history. Other risk factors are linked to lifestyle and environment such as smoking, alcohol, diet and sun exposure. Certain virus infections can increase the risk of getting associated cancers e.g. Epstein Barr Virus.

Tumour development is a complex process that arises as a result of genetic alteration that leads to loss of control over cellular proliferation. This can occur by the gain of function of a gene (proto-oncogene) that is involved in signalling pathways governing cell survival, proliferation and differentiation. When a proto-oncogene function has been deregulated or is altered by being mutated or expressed at abnormally high levels (oncogene) this contributes to converting a normal cell into a cancer cell leading to uncontrolled mitosis.

Typical oncogenes have dominant activity and may be viral or cellular in origin. DNA viruses and retroviruses can carry oncogenes which are similar to cellular genes, however they only play a part to a small fraction of cancers but have greatly contributed to the understanding of oncogenes. Most oncogenes are cellular genes that have either been altered in their coding sequence by mutation, had their copy number increased or had chromosomal rearrangements. These include growth factors and receptors, membrane transducers, cell cycle regulators and inhibitors of apoptosis.

Another mechanism to deregulate cellular proliferation is through the loss of genes. Tumour suppressor genes are genes whose loss or downregulation contributes to the formation of malignancy. There are multiple genetic mechanisms that can account for this loss, including deletion, mutation and chromosomal silencing, but the common

end feature is lack of gene function which is thought to produce a physiological state that enhances the process of tumorigenesis. One of the best known tumour suppressor genes is p53.

Initially the conversion of normal cells into tumour cells (transformation) was achieved in rodents by introduction of several cooperating oncogenes (Land and Weinberg, 1983; Ruley, 1983). In humans, transformation was achieved by physical or chemical agents (Kang *et al.*, 1998), the use of an entire viral genome (Flore *et al.*, 1998) and the selection of rare, spontaneously arising immortalised cells (Yoakum *et al.*, 1985; Rhim *et al.*, 1985; Hurlin *et al.*, 1989; Burger *et al.*, 1998). This was until the cloning of the catalytic component of human telomerase (hTERT) was achieved (See Section 1.8). Using this subunit the immortalisation of cells by the extension of telomeric repeats was accomplished (Bodnar *et al.*, 1998; Vaziri and Benchimol, 1998). The ectopic expression on the catalytic subunit of hTERT in combination with two oncogenes (SV40 large T oncoprotein and H-ras) directly converted normal epithelial and fibroblast cells into tumour cells (Hahn *et al.*, 1999). This suggests that telomere maintenance, allowing cells to proliferate indefinitely contributes to transformation.

1.2 Cell Cycle Checkpoints

One important role of certain tumour suppressor genes involves regulation of the cell cycle. During development from stem to fully differentiated cells in the body divide (mitosis) and enter a stage between two successive cell divisions (interphase). Interphase is indispensable for the next mitosis, as cells in this stage are constantly synthesizing RNA, producing protein and growing in size. This sequence of activities exhibited by the cell is called the cell cycle (Figure 1.1).

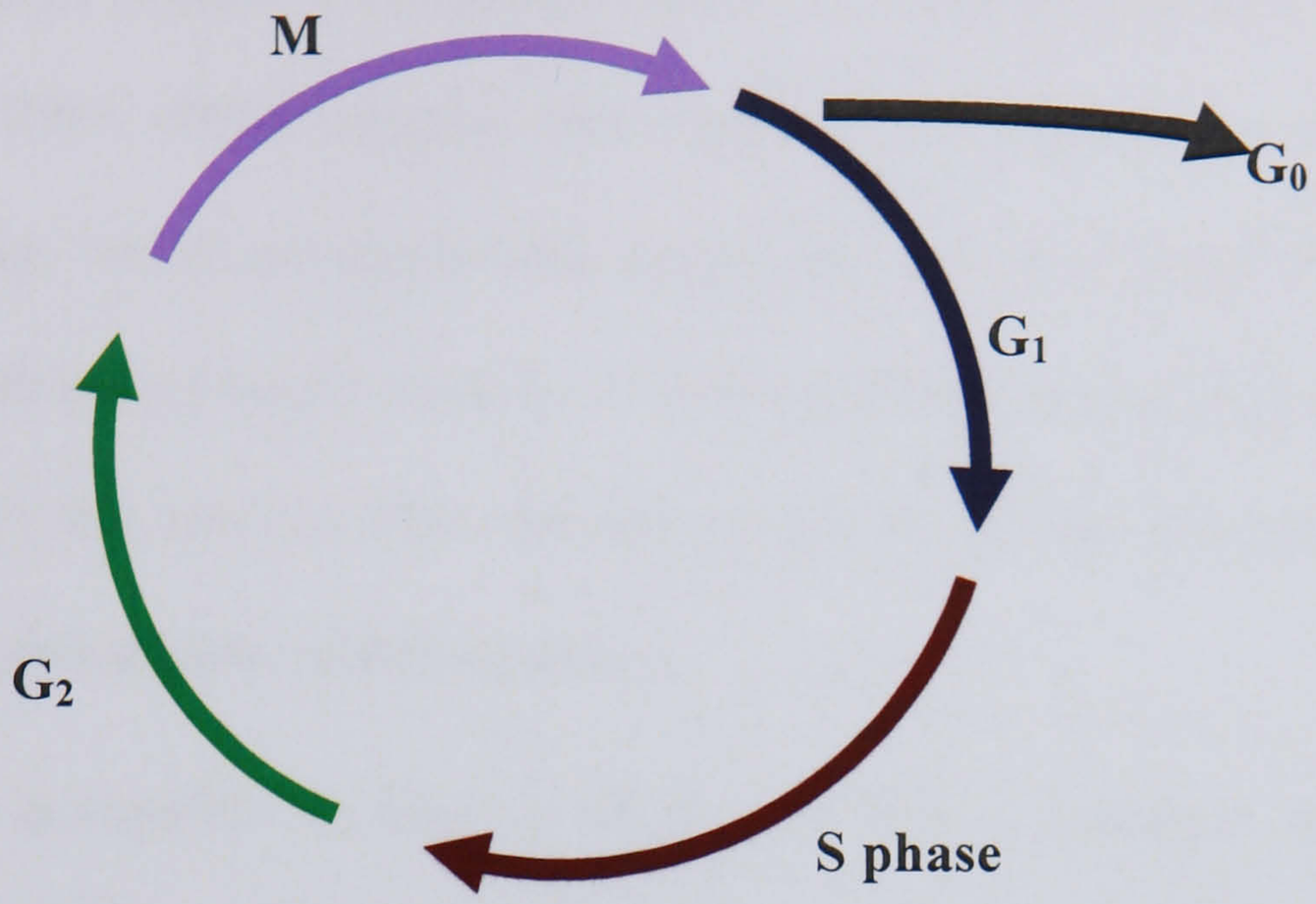

Figure 1.1 Schematic diagram of the cell cycle. The cell cycle is an ordered set of events that culminating in cell growth and division into two daughter cells.

During the cell cycle it is essential that the cells genome is copied, fully and accurately and segregation of the sister chromatids is error free. Many of the risk factors described in Section 1.1 increase the risk of obtaining cancer by interacting and modifying DNA. DNA contains cell's genetic information, in the form of a sequence of bases which are copied and transcribed into messenger RNA that are subsequently used to synthesise proteins. Therefore if DNA is modified by damage or copied incorrectly this will not allow the cell to function correctly increasing the risk of many human pathologies, including cancer.

DNA is highly susceptible to damage which can lead to mutation or cell death. Sources of DNA damage consist of chemical or physical agents found outside the cells or also agents that arise inside cells e.g. reactive oxygen species. Different types of DNA damaging agents produce different kinds of lesions in DNA. For example ultraviolet light produces DNA dimers in which chemical bonds are formed between adjacent cytosines or thymines, whereas cisplatin cross-links the DNA.

Damage to DNA causes several cellular responses. The ATM gene is activated by DNA double strand breaks (of different origins) in an early response and activates cell cycle checkpoints, DNA repair, stress response genes and apoptosis through signal transduction cascades (Figure 1.2). ATM is a serine/ threonine protein kinase whose phosphorylation targets and downstream effector molecules include p53, MDM2, CHK2, NBS1 and BRCA1. CHK2 is a protein kinase which is activated by post translational modifications, after DNA damage. CHK2 is phosphorylated in an ATM dependent and independent manner.

Multiple pathways are involved in the maintenance of genetic integrity, most of which link to the cell cycle. The inactivation of these pathways as part of a multi-step process contributes significantly to the origin of cancers.

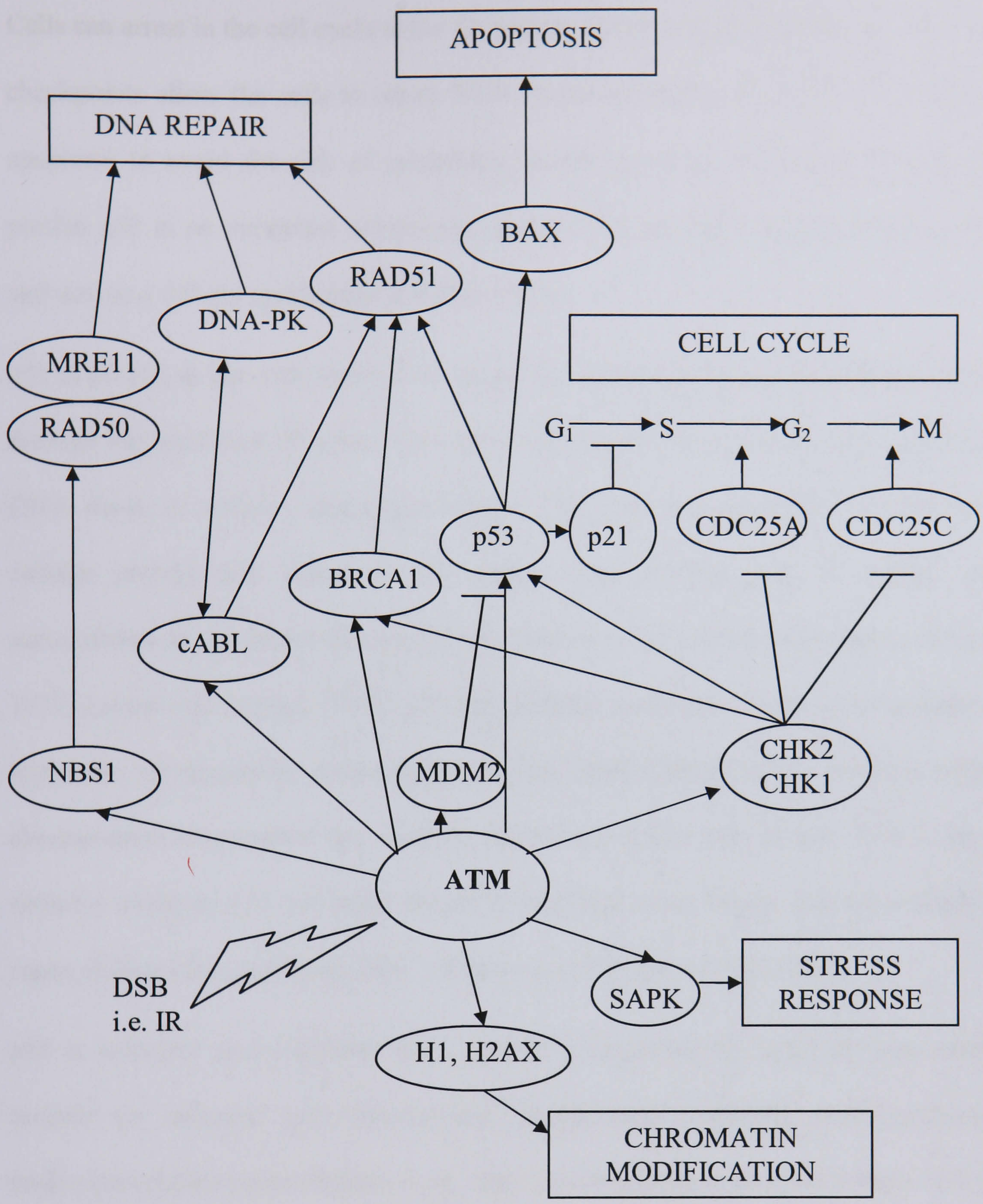

Figure 1.2 The ATM pathway. The ATM signalling pathway in response to double strand breaks induced for example by ionising radiation (IR) (Adapted from Daboussi *et al.*, 2002).

Cells can arrest in the cell cycle at G_0/ G_1 and/ or G_2/ M and by arresting the cell cycle, checkpoints allow the cells to repair DNA. Some cell types may primarily undergo apoptosis to avoid the risk of generating altered progeny. The tumour suppressor protein p53 is an important component of the DNA damage response (Lane, 1992) and acts as a cellular gatekeeper (Levine, 1997).

p53 is pivotal in the cells response to stress by protecting the cell from further stress through the activation of genes that play a role in cell cycle checkpoints, apoptosis, DNA repair or cellular senescence (Figure 1.3). p53 was identified in 1979 as a cellular protein that bound to the simian virus (SV40) large T antigen and accumulated in the nuclei of cancer cells (DeLeo *et al.*, 1979; Lane and Crawford, 1979; Linzer and Levine, 1979). p53 has multiple functions in cell cycle regulation, apoptosis, development, differentiation, gene amplification, DNA recombination, chromosomal segregation and cellular senescence (Oren and Rotter, 1999). More recently wildtype p53 has been shown to facilitate DNA repair and base excision repair (Adimoolam and Ford, 2003; Offer *et al*, 1999; Zhou *et al.*, 2001).

p53 is activated and regulated by a number of mechanisms and pathways which include for example post translational modification including phosphorylation/ dephosphorylation (Scheidtmann *et al.*, 1991) and acetylation (Gu and Roeder, 1997). p53 is mutated or lost in ~50% of all human cancers (Hollstein *et al.*, 1991; Levine *et al.*, 1991) and mice deficient in the gene encoding p53 (*TP53*) are susceptible to spontaneous tumour formation (Donehower *et al.*, 1992). Whereas in humans, germline mutations in the p53 gene lead to the cancer prone Li- Fraumeni syndrome (Malkin *et al.*, 1990; Srivastava *et al.*, 1990).

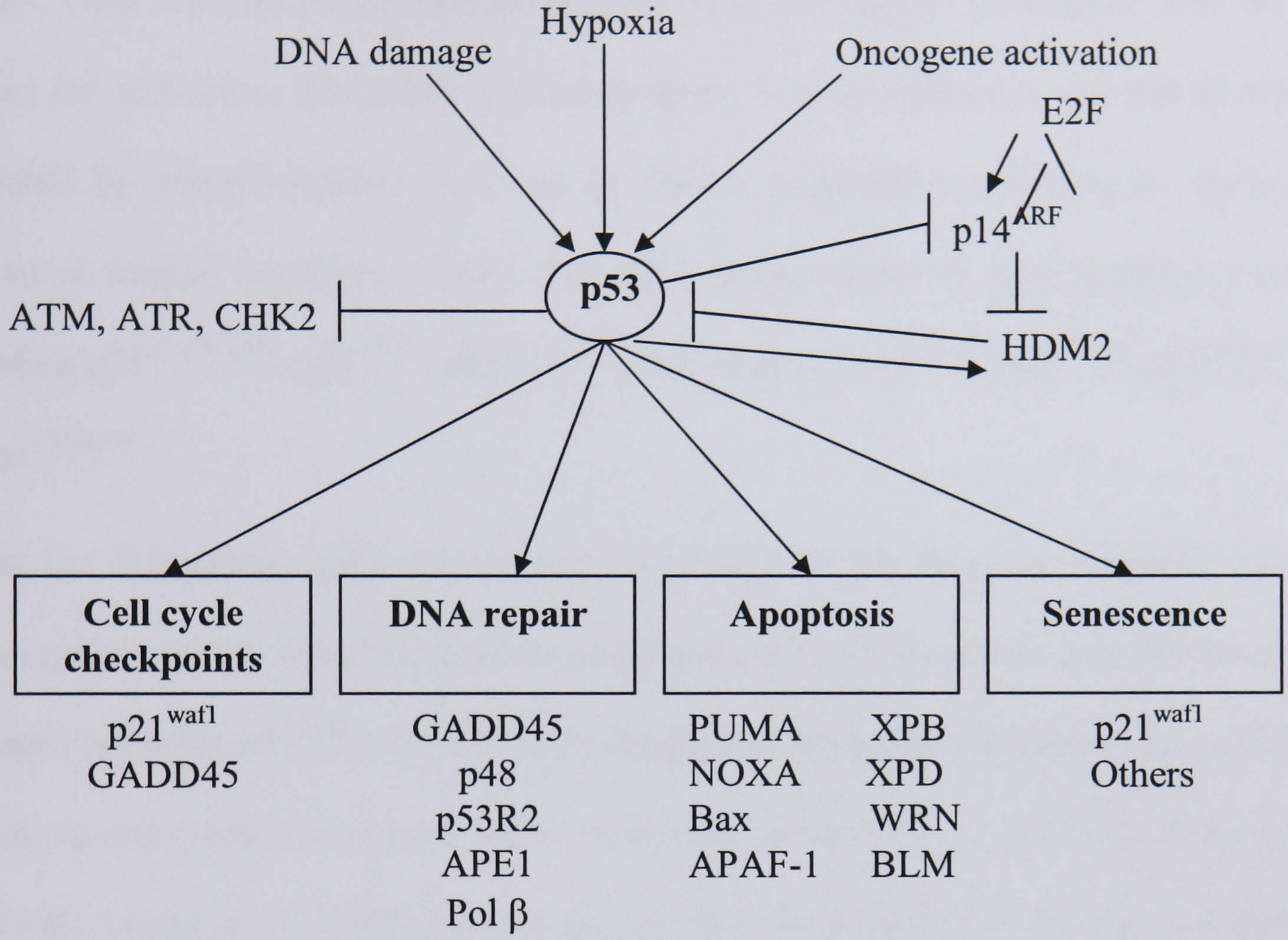

Figure 1.3 p53 stress pathways. Once p53 has been activated through stress it in turn activates genes to encode proteins (examples listed above) involved in cell cycle checkpoints, DNA repair, apoptosis and senescence (Adapted from Hofseth *et al.*, 2004).

Progression through the cell cycle is controlled by a family of proteins found in the cytoplasm termed cyclin dependent kinases (CDK). CDK holoenzymes are comprised of a catalytic subunit, the CDK and a member of a family of regulatory subunits, the cyclins. CDK are inactive in their monomeric form and require association with the cyclins for activation. The CDK- cyclin complex is both negatively and positively regulated by phosphorylation and can be further regulated by binding to cyclin dependent kinase inhibitors (CKI). The CKI compromise of two families, one including $p21^{WAF1/CIP1}$, $p27^{KIP1}$ and $p57^{KIP2}$, the other of $p15^{INK4B}$, $p16^{INK4A}$, $p18^{INK4C}$ and $p19^{INK4D}$.

At the G_1/ S boundary cells are checked on whether or not they can continue onto DNA replication. DNA damage leads to arrest in G_1 via p53 dependent transactivation of genes, primarily $p21^{CIP1}$. The CIP/ KIP family members share broad specificity for binding to and inhibition of most CDK/ cyclin complexes (Zhu *et al.*, 1995; Chen *et al.*, 1996; Adams *et al.*, 1996) but only p21 is involved in the DNA damage induced arrest. DNA damage is also linked to the CDC25A- CDK2 pathways, which has recently been reported (Falck *et al.*, 2001). Normally CDC25A activates CDK2, a kinase essential for S phase. CHK2 phosphorylates and promotes the destruction of CDC25A and this constitutes an S phase checkpoint.

A G_2/ M checkpoint exists which prevents cells from entering mitosis in response to DNA damage, providing an opportunity for repair and stopping the proliferation of damaged cells. This checkpoint is less clearly defined and its control has been shown to be either p53 dependent (Agarwal *et al.*, 1995; Stewart *et al.*, 1995) or independent (Kastan *et al.*, 1991).

There are three different outcomes of checkpoint activation;

(i) arrest to allow repair to occur or senescence if permanent (Section 1.6)

(ii) DNA repair to remove DNA damage (Section 1.4)

(iii) apoptosis to eliminate seriously damaged cells (Section 1.3)

1.3 Apoptosis

DNA damage can lead to cell death by creating too many DNA strand breaks, by cross-linking DNA strands, by introducing large number of mutations or creating lesions that block replication. DNA damage can also cause cell death indirectly by triggering a form of cellular suicide called apoptosis.

Apoptosis is a programmed cell death, that is an active, metabolic pathway that occurs under a variety of physiological and pathological conditions. Apoptosis has an important role in tissue homeostasis and the immune system. Apoptotic cells can be distinguished by their morphological characteristics which include blebbing of the plasma membrane, cell shrinkage and condensation of chromatin (Arends and Wyllie, 1991). An endonucleolytic pathway is activated which leads to cleavage of the DNA resulting in a distinct nucleosomal ladder of fragments (Wyllie *et al.*, 1980). This is followed by cell shrinkage and disintegration of the cell into multiple membrane enclosed vesicles 'apoptotic bodies' which are targets for phagocytes to remove (Wyllie, 1997).

Apoptosis can be triggered by several stimuli, including intracellular stress and receptor mediated signalling. A large number of genes and proteins have been implicated in the control of apoptosis. Caspases (cysteine aspartate proteases) play central roles in apoptotic signalling and execution (Thornberry, 1999). Caspases are

synthesized as zymogens and upstream signals convert these precursors into mature proteases.

There are two types of caspases; initiator caspases which are activated via oligomerisation induced autoprocessing (Butt *et al.*, 1998; Li *et al.*, 1997) and effector caspases which are activated by other proteases including initiator caspases. The initiator caspases transduce various signals into protease activity and are linked to death inducing signalling complexes. Effector capases cleave various cytoplasmic or nuclear substrates which gives many of the morphological features of apoptotic cell death (Degen *et al.*, 2000). There are two major pathways that have been identified according to their initiator caspase: the death receptor (Medema *et al.*, 1997) and the mitochondrial pathway (Green and Reed, 1998).

Stimulation of death receptors of the tumour necrosis factor (TNF) receptor superfamily such as CD95 (apo-1/ Fas) or TRAIL receptors results in receptor aggregation and recruitment of the adaptor molecule Fas- associated death domain (FADD) and caspase 8. Upon recruitment caspase 8 becomes activated and initiates apoptosis by direct cleavage of downstream effector caspases (Schulze-Osthoff *et al.*, 1998). The mitochondrial pathway is initiated by the release of apoptogenic factors such as cytochrome c from the mitochondrial intermembrane space (Kroemer and Reed, 2000). The release of cytochrome c into the cytosol triggers caspase-3 activation through formation of the cytochrome-c/Apaf-1/caspase 9 containing apoptosome complex (Adrain and Martin, 2001). Both pathways are interconnected at different levels (Roy and Nicholson, 2000).

Apoptosis can be induced by a variety of DNA damaging agents whereby p53 plays a critical role. One of its roles is to act as a transcriptional activator of genes encoding apoptotic effectors. For example human p53 directly activates transcription of several

genes encoding members of the Bcl-2 family, which include multidomain pro- and anti-apoptotic proteins (Cory and Adams, 2002). Loss of apoptosis due to loss of p53 has been implicated in tumourigenesis (Igney and Krammer, 2002) and also to the resistance of cancer cells to therapies that induce DNA damage (Lowe *et al.*, 1993). Overexpression of anti- apoptotic proteins such as Bcl-2 can additionally favour tumour cell survival following DNA damage based therapy.

The mitochondrial apoptotic pathway is thought to be the major pathway induced by DSB by decline of Bcl-2 and stabilisation of p53, which stimulates the promoter of the Fas receptor gene thus activating the FAS/CD95/Apo-1 apoptotic pathway (Figure 1.4). Damage may also activate the MAPK pathway leading to upregulation of Fos and Jun (Ap-1).

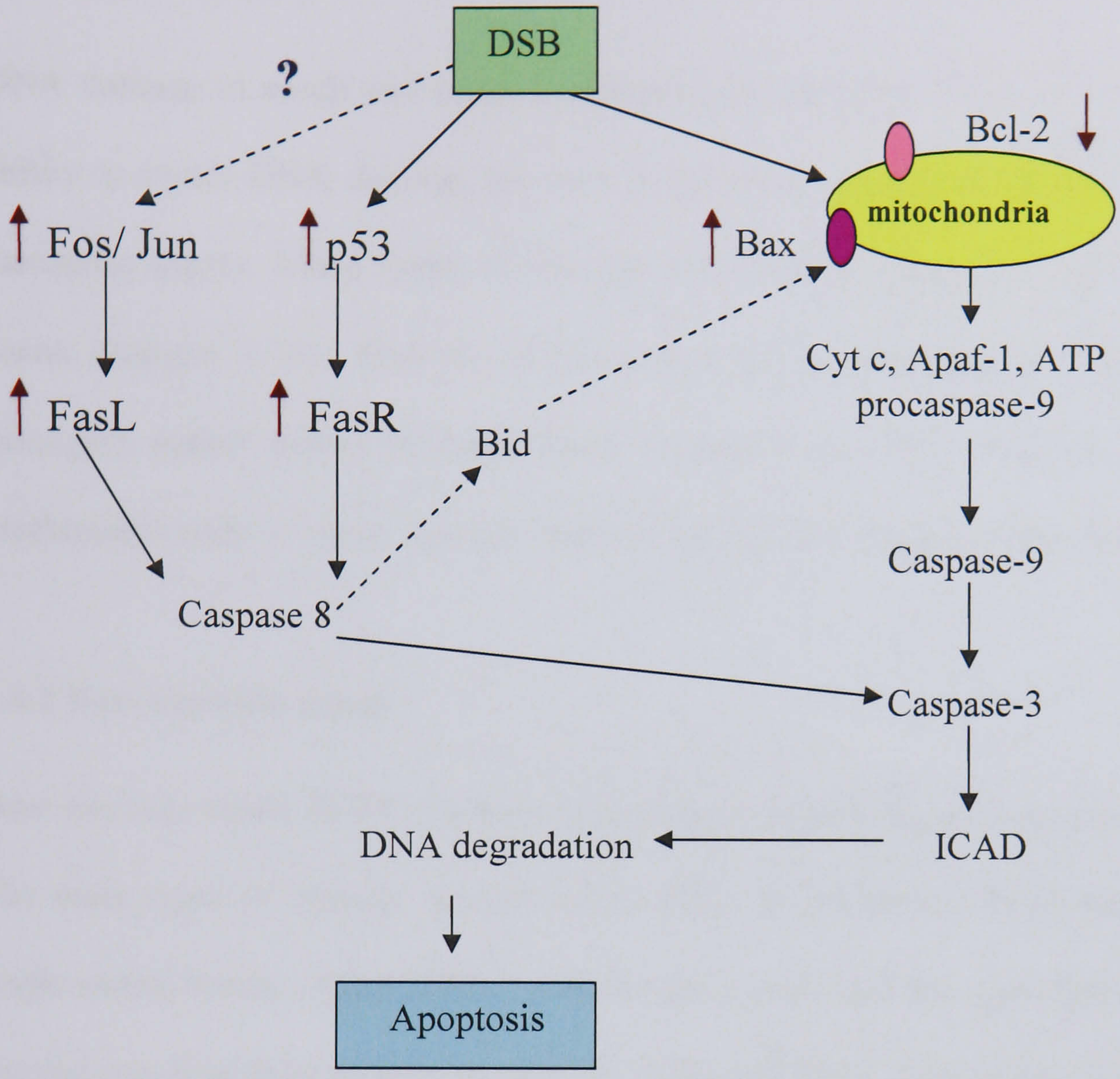

Figure 1.4 Apoptotic pathway induced by non repaired DNA double strand breaks. This occurs via the mitochondrial pathway. It is unknown whether Fos/ Jun upregulation is directly activated by DSB (Adapted from Bernd, 2003).

1.4 DNA repair

1.4.1 Introduction

DNA damage in a cell can cause mutations and cell death. Cells that have lost the ability to repair DNA damage are very sensitive to mutations and killing by DNA damaging agents. Many types of damage can occur in cells which include loss of bases, changes in the structure of bases and DNA strand breaks. Different DNA damaging agents induce different kinds of lesions in DNA therefore a variety of mechanisms exist to repair specific types of damage and these are described below.

1.4.2 Base excision repair

Base excision repair (BER) involves the damaged base being excised from the DNA. The main types of damage recognised by BER are oxidative, DNA alkylation and single strand breaks (SSB). BER is a multistep process and the repair pathway can be divided into five steps (i) base removal by a specific DNA glycosylase, (ii) incision at the resulting abasic site by an apurinic/ apyrimidinic (AP) endonuclease, (iii) processing of the produced blocked termini, (iv) filling in the gap and (v) resealing of the damaged DNA strand. The first step is characterised by the action of a DNA glycosylase, which after recognition of the specific modified base, cleaves the N-glycosidic bond giving rise to an AP site. This lesion is acted upon by AP endonucleases or an AP lyase which generates a single strand break. The BER can then proceed through two pathways a short and long patch BER, which are differentiated by the repair gap size and enzymes involved.

1.4.3 Nucleotide excision repair

Nucleotide excision repair (NER) deals with a wide range of structurally unrelated lesions and it acts on removing lesions that distort the DNA double helix which interferes with base pairing and blocks DNA replication and transcription. For example, NER repairs damage induced by UV light which induces pyrimidine dimers that cause a kink or bend in the DNA molecule. Cross-linking agents such as cisplatin, also distort DNA and are substrates for repair by NER. NER is a complicated multistep process that requires numerous proteins. NER involves recognition of damaged DNA, the sequential action of helicases and endonucleases open the double helix and enzymes cleave the damaged strand a few bases away from the lesion. This is followed by removal of the DNA segment containing the lesion and gap polymerisation using the intact strand as a template, with DNA ligase sealing the newly made patch into the DNA.

1.4.4 Mismatch repair

DNA mismatch repair (MMR) corrects mismatched bases which DNA polymerases have inserted opposite normal bases which can cause mutations if not corrected (Kolodner and Marsischky, 1999). Like BER and NER, MMR is an excision repair process and it targets newly synthesized DNA strands. MMR is clearly defined in *E coli*, though less is known about the mechanism in humans. At least six genes have been identified which are implicated in MMR. hMSH2, hMSH3, hMSH6 are involved with primary recognition of the mismatched DNA. hMLH1, hPMS2 and hPMS1 are recruited after the initial DNA recognition (Fink *et al.*, 1998).

1.4.5 DNA double strand break repair

DNA double strand breaks (DSB) can arise spontaneously or by DNA damaging agents for e.g. ionising radiation and is thought to be the most lethal type of DNA lesion. There are two main DSB repair pathways, homologous recombination (HR) and non homologous end joining (NHEJ). The difference between the processes is the fact that NHEJ requires little or no sequence homology and is a process that may or may not be error free, whereas HR requires DNA homology. The contribution of both processes to human DSB repair is controversial (Kanaar *et al.*, 1998; Haber, 2000; Johnson and Jasin., 2001) but is generally believed that NHEJ plays a more important role than HR in mitotically replicating cells (Jackson and Jeggo, 1995), especially during G_1 and early S phase (Lee *et al.*, 1997; Takata *et al.*, 1998). NHEJ is a damage tolerance mechanism because it does not result in the physical removal of the damage from the DNA but allows cells with unrepaired lesions to replicate their DNA without stalling. Many proteins take part in the NHEJ mechanism and once at the site of the damage, DNA is aligned and endonucleases remove incompatible sites, which is followed by polymerisation, ligation then replication. After replication, the damage can be removed from the DNA by repair mechanisms such as NER.

1.4.6 Direct damage reversal

Two well known examples of direct reversal of damage are the repair of UV induced DNA dimers by photolyases and the repair of mutagenic methyl lesions by methyltransferases. DNA photolyases are monomeric proteins and two different types have been distinguished according to the type of DNA lesion they repair (Todo *et al.*, 1996), though none have been discovered in mammals. The major lesion induced by UV light are cyclobutane pyrimidine dimers (CPD) which are repaired by CPD

photolyases (Taylor and Nadji, 1991). Minor UV light induced lesions are 6,4 photoproducts which are repaired by 6,4 photolyases (Zhao *et al.*, 1997). Photolyases work in concert with chromophores and use the energy of visible light.

DNA repair methyltransferases remove mutagenic alkyl lesions from oxygens on the bases guanine (O^6-methylguanine) and thymine (O^4-methylthymine) by transfer of a methyl group from the DNA to themselves, restoring the base to normal. The methyl group remains on the methyltransferase and inactivates the protein allowing the enzyme to repair only one lesion. Therefore the enzymes are known as suicide enzymes.

1.4.7 DNA repair deficiencies

Deficiencies in DNA repair can have serious consequences for cells as it can lead to increases in mutation, genetic instability and cancer. At least 15 human diseases have been linked to inherited deficiencies in DNA repair. These disorders represent defects in ~35 different genes. In most but not all there is greatly elevated cancer incidence and have multi- system defects. The first DNA repair disease to be identified in humans was Xeroderma Pigmentosum (XP) (Kraemer *et al.*, 1987). The defining characteristics of XP patients are extreme sensitivity of the eyes and skin to sunlight, abnormal pigmentation and drying of the skin and increased rate and incidence of cancer. XP patients have a defect in at least 8 different genes related to NER. Mutations in some of the genes cause two other DNA repair related disorders Cockayne syndrome and Trichothiodystrophy (TTD).

An elevated risk of cancer has been shown in an inherited defect in mismatch repair, which causes a syndrome called hereditary nonpolyposis colorectal cancer in which patients have a higher risk of developing colon cancer. People with defects in other

DNA repair related genes like BRCA1, BRCA2 and p53 also have a higher risk of developing cancer. Additionally during the course of tumour development, mutations in DNA repair genes can occur.

1.5 Telomeres

1.5.1 Historical background

In the 1930s from a combination of genetic and cytological observations the proposal that the natural ends of chromosomes had specialised structures came about. From light microscope studies of *Drosophila melangaster* in 1938 Müller detected that terminal deletions and inversions were not recovered following x-irradiation, though interstitial deletions and inversions were easily recovered (Müller, 1938). This suggested a unique structure at the end of linear chromosomes which causes them to behave differently from a free end. Müller named this hypothetical structure telomeres as telo= end and mere = segment. Müllers original experiments were many years later confirmed in wildtype *Drosophila* (Roberts, 1974).

Müllers work was also verified and extended by the work of McClintock, who studied the fate of broken chromosomes in maize (McClintock, 1941). McClintock discovered that the end of broken chromosomes were very reactive and underwent aberrant recombination and fusion reactions with other chromosomes, frequently to form dicentrics.

McClintocks results were validated 50 years later in yeast and mice when it was demonstrated that without telomeric ends, chromosomes undergo aberrant end-to-end fusions forming multicentric chromosomes. These have a propensity to break during

mitosis, activating DNA damage checkpoints and in some cases leading to widespread cell death (Zakian, 1989).

1.5.2 Structure of telomeres

Telomeres were first sequenced in 1978 from the ciliate protozoan *Tetrahymena thermophila* (Blackburn, 1984) and then *Oxytricha* (Oka *et al.*, 1980; Klotbutcher *et al.*, 1981). This was due to the fact that ciliate chromosomes have a vast number of telomeres per cell as a result of genome fragmentation and telomere addition. Therefore giving a rich source of both telomeric DNA and the structural proteins and enzymes that protect and replicate this DNA. Since then the DNA sequence of the telomeres of a number of protozoans, yeasts, vertebrates and plants have been determined. There is considerable conservation of both structure and function of telomeres from ciliated protozoans to plants and animals.

In most organisms telomere DNA consists of a very simple short tandem repeat that is G rich in one strand and whose orientation and sequence is highly conserved within species. For example in *Tetrahymena* the telomere consists of the repeat TTGGGG. In humans, other vertebrates, slime moulds and some protozoans the hexameric repeat unit is almost exclusively TTAGGG (Brown, 1989; Cross *et al.*, 1989). Yeast has irregular repeat sequence for example a T is followed by one, two, or three G's (abbreviated $TG_{1\text{-}3}$). *Drosophila* the organism in which telomeres were first defined though has a different kind of telomere repeat sequence than most other eukaryotes. The 6 kilobase pair (kbp) repeated elements found on *Drosophila* chromosome ends are telomere specific retrotransposable elements that can be lost and readded onto chromosome ends (Mason and Biessmann, 1995).

The length of the telomeric repeat sequence also varies depending on the organism ranging from 24 base pairs (bp) to 150 kbp. Each organism has a characteristic mean length. In humans they are between 10-15 kbp in germline cells to 5-12 kbp in peripheral blood leucocytes. Though there is much heterogeneity and spontaneous changes in telomere length even for example in human cells (Lansdorp *et al.*, 1996) as telomeres do not carry genetic information thus being able to act as a disposable part. It has been suggested that human cells are unique among primates in having relatively short (~10-15 kbp) telomeres in somatic tissue (Kakuo *et al.*, 1999).

The DNA sequences adjacent to the tandem repeats are known as subtelomeric regions or telomere associated DNA (Blackburn and Szostak, 1984) which generally contain repetitive but more variable sequences than those of telomeres.

The 3' of telomeres, the G rich strand forms an overhang of about 100-200 nucleotides (nt) in length (Makarov *et al.*, 1997; Wright *et al.*, 1997). According to one analysis (Makarov *et al.*, 1997), G strand overhangs appear to be present at most chromosome ends. However, other experiments suggest that in cells lacking telomerase long G strand tails are only present on half of the chromosome ends, consistent with their being generated by incomplete lagging strand synthesis during DNA replication (Wright *et al.*, 1997).

Originally, telomeres were thought to be linear structures with the repeat sequence and 3' single strand G rich overhang. Though they contain many telomeric proteins and it has been proposed that mammalian telomeres develop a loop structure at the end (Griffith *et al.*, 1999) known as t or telomere loop. This telomere loop is thought to back up on itself forming the t-loop and a single strand overhang invades the telomeric double strand resulting in a displacement loop (d-loop). This loop is stabilised by telomeric associated proteins (Figure 1.5). The loop structure protects

the single stranded overhang from degradation and/ or interaction with signalling proteins and this protection is referred to as telomere capping (Blackburn, 2000).

1.5.3 Telomeric associated proteins

A number of telomeric associated proteins (TAP) have been identified that associate with telomeres (Figure 1.5). Some of these proteins associate exclusively with telomeres (telomere binding proteins) whereas others localise to additional subnuclear or subcellular sites. Although the functions of many of the proteins associated with telomeres are not fully known some may assist in the spatial organisation and packaging of telomeric sequences e.g. as heterochromatin (Hazelrigg *et al.*, 1984; Gottschling *et al.*, 1990) and it is thought that for example in yeast, telomeres participate in transcriptional activation or repression for instance by altering chromatin conformation (Reuter and Spierer, 1992). It has been proposed that telomeric associated proteins may also be involved in the control of telomere length (Hardy *et al.*, 1992) whereas others may aid in attaching telomeres to the nuclear matrix (de Lange, 1992). Evidence has been published indicating that telomeres are linked to the nuclear envelope in a manner involving components of DNA-PK (de Lange, 1992; Laroche *et al.*, 1998; Bianchi and de Lange, 1999; Smith and Jackson, 1999).

In mammalian cells double strand telomeric repeats are bound directly by two ubiquitously expressed proteins, TRF1 (TTAGGG repeat binding factor 1) (Smith and de Lange, 1997) and TRF2 (TTAGGG repeat binding factor 2) (Bilaud *et al.*, 1997). They both bind double stranded telomeric DNA via a DNA binding motif related to the proto-oncogene Myb (Broccoli *et al.*, 1997).

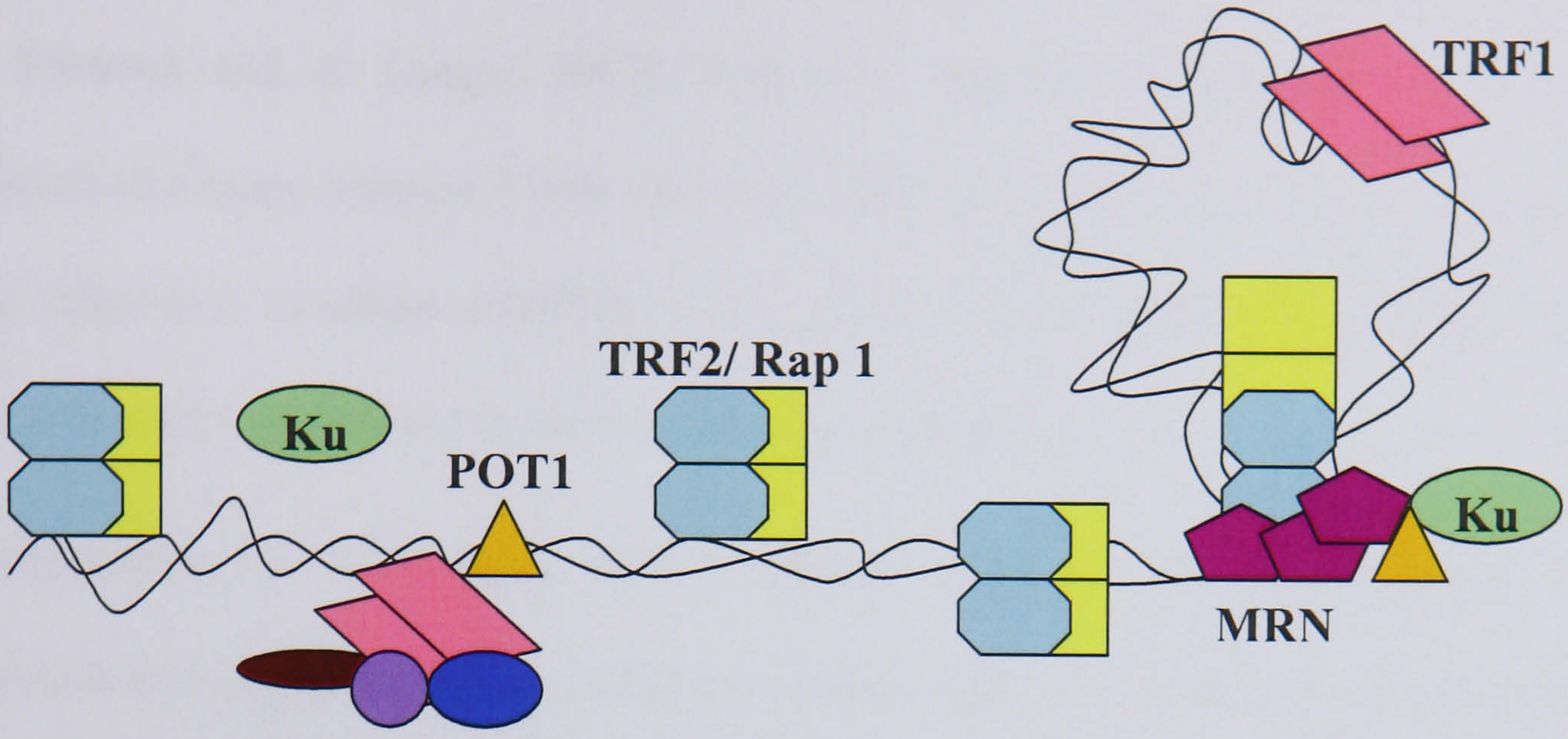

Figure 1.5 Structure of a human telomere. The human telomere has many telomeric associated proteins including proteins which bind to the telomeric DNA (Adapted from Harrington, 2004).

Overexpression of wildtype TRF1 reduces telomere length, whereas overexpression of dominant negative TRF1 increases telomere length in telomerase positive cells (van Steensel and de Lange, 1997). It is also thought TRF1 might contribute to formation of t loops because it was shown to catalyse telomeric synapsis resulting in a coiled telomeric structure (Griffith *et al.*, 1998). These results suggest that when TRF1 is bound to telomeres it inhibits telomere elongation.

Overexpression of a wildtype TRF2 reduces telomere length seemingly in a telomerase independent manner. However overexpression of dominant negative TRF2 induces unique phenotypes including loss of G rich overhangs, end to end fusions and ATM/ p53 dependent apoptosis or senescence depending on the cell type (van Steensel *et al.*, 1998). Inhibition of TRF2 leads to dysfunctional telomeres which are processed by DNA damage machinery (van Steensel *et al.*, 1998; Takai *et al.*, 2003; d'Adda di Fagagna *et al.*, 2003; Karlseder *et al.*, 1999). Therefore TRF1 is thought to function to regulate telomere length possibly by facilitating telomerase activity at telomeres, whereas TRF2 is thought to function independently to protect telomeres from non homologous end joining and other DNA repair or DNA damage response pathways. Though recent data suggests that TRF1 and TRF2 are linked and TRF1 also plays a role in telomere protection (Ye *et al.*, 2004).

TRF1 recruits a number of other proteins to the telomeres (Smogorzewska and de Lange, 2004). Two TRF1 interacting proteins were discovered by two hybrid interaction assays in yeast, tankyrase (Smith *et al.*, 1998) and TRF1 interacting protein 2 (TIN2) (Kim *et al.*, 1999). Tankyrase appears to have both telomeric and non telomeric functions in cells. Tankyrase under some circumstances interacts with acidic amino terminal region of TRF1 and a related TRF1 interacting protein TANK2 which is most abundant at the nuclear periphery and in the Golgi apparatus (Chi and

Lodish, 2000; Smith and de Lange, 2000; Kaminker *et al.*, 2001). The sequence of tankyrase includes 24 ankryin repeats responsible for protein-protein interactions and has homology to poly ADP ribose polymerase (PARP) catalytic domain. As recombinant tankyrase has PARP activity, as TRF1 was shown to be a target, it seems likely that post translational ADP ribosylation regulates some aspect of telomere dynamics (Smith *et al.*, 1998). This has been shown, as ADP-ribosylation of TRF1 impedes its DNA binding activity *in vitro* and tankyrase overexpression removes TRF1 from the telomeres and promotes it degradation. This *in vitro* ADP ribosylation of TRF1 by tankyrase is inhibited by TIN2 (Ye and de Lange, 2004; Kim *et al.*, 1999).

TIN2 is thought to protect TRF1 from tankyrase *in vivo* (Ye and de Lange, 2004; Kim *et al.*, 1999). TIN2 interacts with the homodimerisation region of TRF1 and has similar phenotypes as observed with overexpression of TRF1. Overexpression of wildtype TIN2 reduces telomere length, overexpression of truncated dominant negative TIN2 increases telomere length. TIN2 functions to recruit PIP1 (also known as PTOP) to the TRF1 complex (Liu *et al.*, 2004; Ye *et al.*, 2004a). PIP1 is a POT1 (protection of telomeres) interacting protein that mediates the binding of POT1 to the TRF1 complex (Liu *et al.*, 2004; Ye *et al.*, 2004a). POT1 binds the G rich telomeric single strand overhang (Baumann and Cech, 2001). An alternative splicing product of TRF1, PIN2 (protein interacting with the never in mitosis A (NIMA) protein kinase) contains an internal 20 amino acid deletion and forms homo and heterodimers with TRF1 (Shen *et al.*, 1997). TRF1 has also been shown to interact with Ku (Hsu *et al.*, 2000), PINX1 (Zhou and Lu, 2001), the BLM RecQ helicase (Opresko *et al.*, 2002) and ATM kinase (Kishi *et al.*, 2001). TRF1, TIN2, PIP1 AND POT1 are thought to be involved in telomere length homeostasis (Smogorzewska and de Lange, 2004).

TRF2 interacts directly with human RAP1 (Li *et al.*, 2000). It also interacts with RAD50/MRE11/NBS1 complex (Zhu *et al.*, 2000), ERCC1/ XPF (Zhu *et al.*, 2003), ATM kinase (Karlseder *et al.*, 2004), Ku (Song *et al.*, 2000) and WRN/ BLM helicases (Opresko *et al.*, 2002). A recent study has reported that TIN2 mediates an interaction between TRF1 and TRF2 (Ye *et al.*, 2004b).

RAD50/MRE11/NBS1 complex is a trimeric complex involved in the repair of double strand DNA breaks, which may also have a role in telomere maintenance as it associates with the telomeres at least during S phase which is thought to be due to an interaction between NBS1 and TRF2 (Zhu *et al.*, 2000).

Ku is a protein known to participate in specific DNA repair processes, particularly the repair of DNA double strand breaks, also associates with telomeres. Ku is a heterodimer and is abundantly localised throughout the nucleoplasm. It is a critical component of DNA dependent protein kinase (DNA-PK), a trimeric complex that is essential for the repair of double strand breaks by non homologous end joining and is thought to have a role to protect the terminal telomeric structure. Cells deficient in either of the two ku subunits are genomically unstable owing to frequent telomere-telomere fusions (Bailey *et al.*, 1999). Ku binds and stabilises the ends of broken DNA whereupon it recruits the catalytic subunit of DNA-PK (Smith and Jackson, 1999). Ku interacts with a number of nuclear proteins, the 70 kD ku subunit (ku70) specifically binds TRF1 (Hsu *et al.*, 2000) and TRF2 (Song *et al.*, 2000). Most Ku is recruited to the mammalian telomere by its binding to TRF1 (Hsu *et al.*, 1999).

One of the first responses of eukaryotic cells to oxidative and other types of DNA damage is the covalent post translational modification of nuclear proteins with poly (ADP-ribose). Poly (ADP) ribosylation is to a large extent catalysed by the nuclear enzyme PARP now called PARP1, which is a 113 kDa enzyme which utilises NAD^+

as a substrate. PARP1 is constitutively expressed at a level depending on the type of tissue or cell. However it is the contact with DNA single or double strand breaks, mediated by two zinc fingers located in the amino terminal DNA binding domain of the enzyme that causes activation of the catalytic centre, residing within the carboxy terminal NAD^+ binding domain. PARP1 has also been shown to have a role in controlling telomere length as mice lacking PARP display telomere shortening compared with wildtype mice (d'Adda di Fagagna *et al.*, 1999).

There may be many more TAP that have not yet been identified. As TAP function cooperatively to establish and maintain the telomere structure, it has been proposed that TAP are more important than telomere length in determining fate and phenotype of cells (Blackburn, 2000).

1.5.4 Function of telomeres

Telomeres play a number of important roles in the functioning and organisation of the genome. They protect the ends of eukaryotic chromosomes by having a capping function to protect from chromosomal fusion which would lead to genomic instability (Blackburn, 1999). Telomeres also protect the ends of chromosomes from being recognised as damaged DNA and from degradation. Telomeres are additional involved in chromosome pairing in meiosis and shield them from engaging in inappropriate kinds of recombination. More importantly, telomeres act as triggers of a checkpoint leading to growth arrest/ apoptosis/ senescence.

1.5.4.1 End replication problem

One of the most important roles of telomeres is that they ensure the complete replication of chromosomal DNA by recruiting a telomere specific DNA polymerase

to chromosome ends. Telomeric DNA is not completely replicated by the normal DNA replication machinery. In 1971 Olovnikov published a theoretical paper that in somatic cells the ends of the chromosomes are not fully replicated during DNA synthesis resulting in the shortening of linear DNA molecules with each cell division and that this may be the cause of progressive loss of essential genes and cell arrest in senescent cells (Olovnikov, 1971). In 1972 Watson also suggested that the termini of linear eukaryotic chromosomes could not be replicated known as the end replication problem (Watson, 1972).

In semi conservative DNA replication, DNA polymerase α synthesizes DNA in a 5' to 3' direction and requires a RNA primer to initiate DNA synthesis. Although one template strand can be copied in a continuous process, the other (the template for the lagging strand) is copied as a set of discrete Okazaki fragments. A problem occurs at the 3' end of the template for the lagging strand since there are no additional sequences beyond the end to which primers can anneal. DNA polymerase α is thus unable to fill in the gap between the last Okazaki fragment and the very 3' end of the template. The 5' end of the lagging daughter strand is consequently shorter than its template (Figure 1.6). The consequence of incomplete replication of terminal DNA fragment has been modelled and predicted to a form of the binomial distribution of deletion events at each independent chromosome end (Levy *et al.*, 1992).

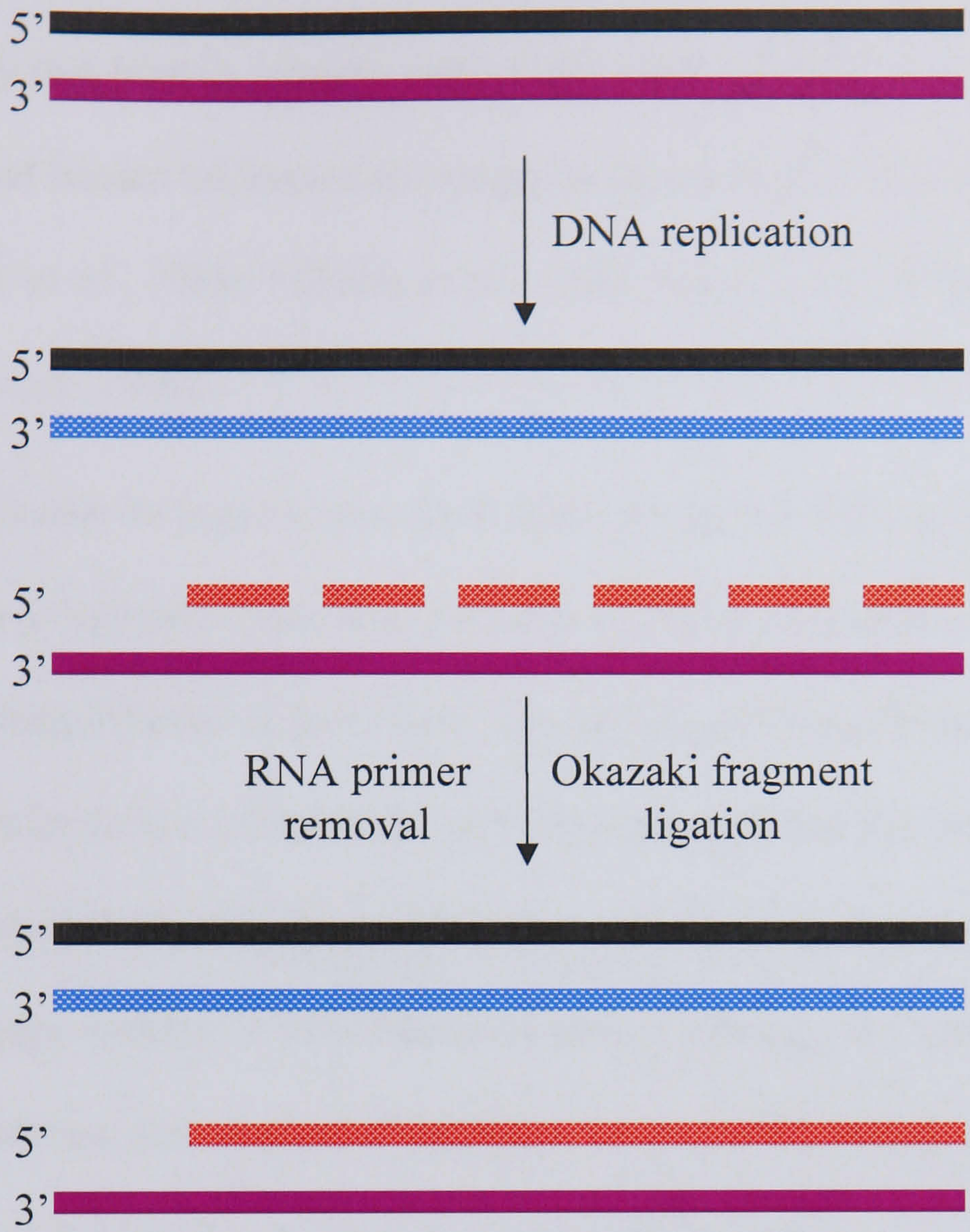

Figure 1.6 The end replication problem. A simple diagram showing that during each round of replication, the DNA molecules get shorter (Adapted from Greider, 1991).

1.5.4.2 Telomere shortening

The possibility that human somatic cells might show telomere loss stemmed from the observation that human telomeres are longer in sperm than in blood (Cooke and Smith, 1986; Allshire *et al.*, 1988; Allshire *et al.*, 1989; Cross *et al.*, 1989; de Lange *et al.*, 1990; Hastie *et al.*, 1990).

In 1990 Harley and colleagues provided evidence for the end replication problem by demonstrating in normal human somatic cells that telomeres shorten by 50-200 bp for each cell doubling (Harley *et al.*, 1990). Though the end replication problem can only account for the large loss of bp observed if one assumes that the last primer is located at a large distance to the end. Therefore other considerations came into account and as human telomeres contain a 100-200 nt G rich overhang, the action of a C strand specific exonuclease was suggested (Makarov *et al.*, 1997), which would shorten each telomere by half the overhang length per round of replication.

Alternatively telomeres are sensitive to DNA damage and telomere lengths have also seen to be affected by external influences particularly oxidative stress (Petersen *et al.*, 1998; von Zglinicki, 2000) which has been proposed to be responsible for the greater part of telomere loss in most cell strains. The G triplet is especially sensitive to modification by oxidative damage and telomeres are lost five to ten times faster than normal if fibroblasts are subjected to chronic hyperoxia (von Zglinicki *et al.*, 1995; Vaziri *et al.*, 1999) or to concentrations of H_2O_2 (von Zglinicki *et al.*, 2000).

The mitochondrial respiratory chain is a major source of reactive oxidative species internally and externally they are produced by ionising radiation e.g. x rays, cosmic radiation etc. Telomeres are deficient in repair of oxidatively generated single strand breaks (Petersen *et al.*, 1998) and these single strand breaks translate into accelerated

telomere shortening as soon as the cells replicate their DNA (Sitte *et al.*, 1998). DNA polymerases have a major problem if single strand breaks are present as replication fork stalls. Additionally DNA repair in telomeres by nucleotide excision repair was seen to be less efficient than in the endogenous gene dihydrofolate reductase but more efficiently repaired than the inactive non coding X chromosome associated 754 region (Kruk *et al.*, 1995).

A dramatic effect of telomere shortening is the arrest of cell proliferation (Section 1.6) or apoptotic cell death (Section 1.3).

1.6 Cellular Senescence and Immortalisation

1.6.1 The Hayflick limit

Hayflick established that human diploid fibroblast show a spontaneous decline in growth rate on continuous culture related not to time but to an increasing number of population doublings (PD) eventually terminating (after 50-70 PD) in a quiescent but viable state termed replicative senescence (Hayflick, 1965). Senescent cells have a characteristic morphology, with an increase in volume, they lose their original shape and gain a flattened cytoplasm. This is accompanied by changes in nuclear structure, gene expression, protein processing and metabolism (Campisi, 2000; Narita *et al.*, 2003). Senescent cells show beta galactosidase activity at a more neutral pH i.e. pH 6 than young cells (Dimri *et al.*, 1995). There is evidence now showing that replicative senescence is an irreversible cell cycle block in G_0 triggered via a concerted activation of the p53/ p21/ p19 and p16/ pRb pathway (Stein *et al.*, 1999).

The cells in a population fail to divide in response to a variety of normal growth stimuli after a characteristic number of divisions and they remain metabolically active

but with an aberrant pattern of gene expression (West *et al.*, 1989). Although the maximum division capacity in culture of a human somatic cell population from a young normal individual varies significantly from donor to donor and cell type to cell type, it typically falls in the range of 50-100 PD. This limit decreases as a function of donor age and there is evidence to support the notion that replicative senescence is related to *in vivo* ageing (Campisi, 2000). Ageing is usually defined as the progressive loss of function accompanied by decreasing fertility and increasing mortality with advancing age (Kirkwood and Austad, 2000). A positive correlation can also be drawn between species longevity and cell lifespan (Goldstein and Singal, 1974).

1.6.2 The telomere hypothesis of cell ageing and immortalisation

The shortening of telomeres gave rise to the telomere hypothesis of cell ageing and immortalisation (Figure 1.7) proposing that critically short telomeres may act as a mitotic clock to signal the cell cycle at senescence as it utilises cell divisions as the unit of time rather than chronological or metabolic age (Harley, 1991) and it has been suggested this may be adaptive in long lived species as a mechanism for tumour suppression (Campisi, 1997).

When cells reach the Hayflick limit or M1 (mortality stage 1) stage, cells irreversibly enter senescence. Some rare events can abolish the M1 barrier of proliferation, the best studied alterations are the expression of viral oncogenes that inactivate p53 and retinoblastoma (Rb) (Shay *et al.*, 1991; Shay *et al.*, 1993). Though the infrequent accumulation of these genetic aberrations leaves only a few cells that proliferate beyond the Hayflick limit (Harley, 1991) resulting in further telomere shortening.

A second checkpoint is reached at a critical telomere length called crisis (mortality stage 2 or M2). At this stage almost all cells die due to extensive chromosomal

aberrations caused by very short and dysfunctional telomeres. However some immortal cells activate telomerase (Harley, 1991) and these subpopulation of cells escape from crisis giving rise to cells which now have an unlimited proliferative capacity (immortalised). The characteristic feature of such immortal cells is the ability to maintain their telomeres. Evidence to support this hypothesis was achieved with the cloning of the catalytic component of human telomerase (hTERT) (See Section 1.8). Using this subunit the immortalisation of cells by the extension of telomeric repeats was accomplished (Bodnar *et al.*, 1998; Vaziri and Benchimol, 1998) rescuing some cell types from senescence.

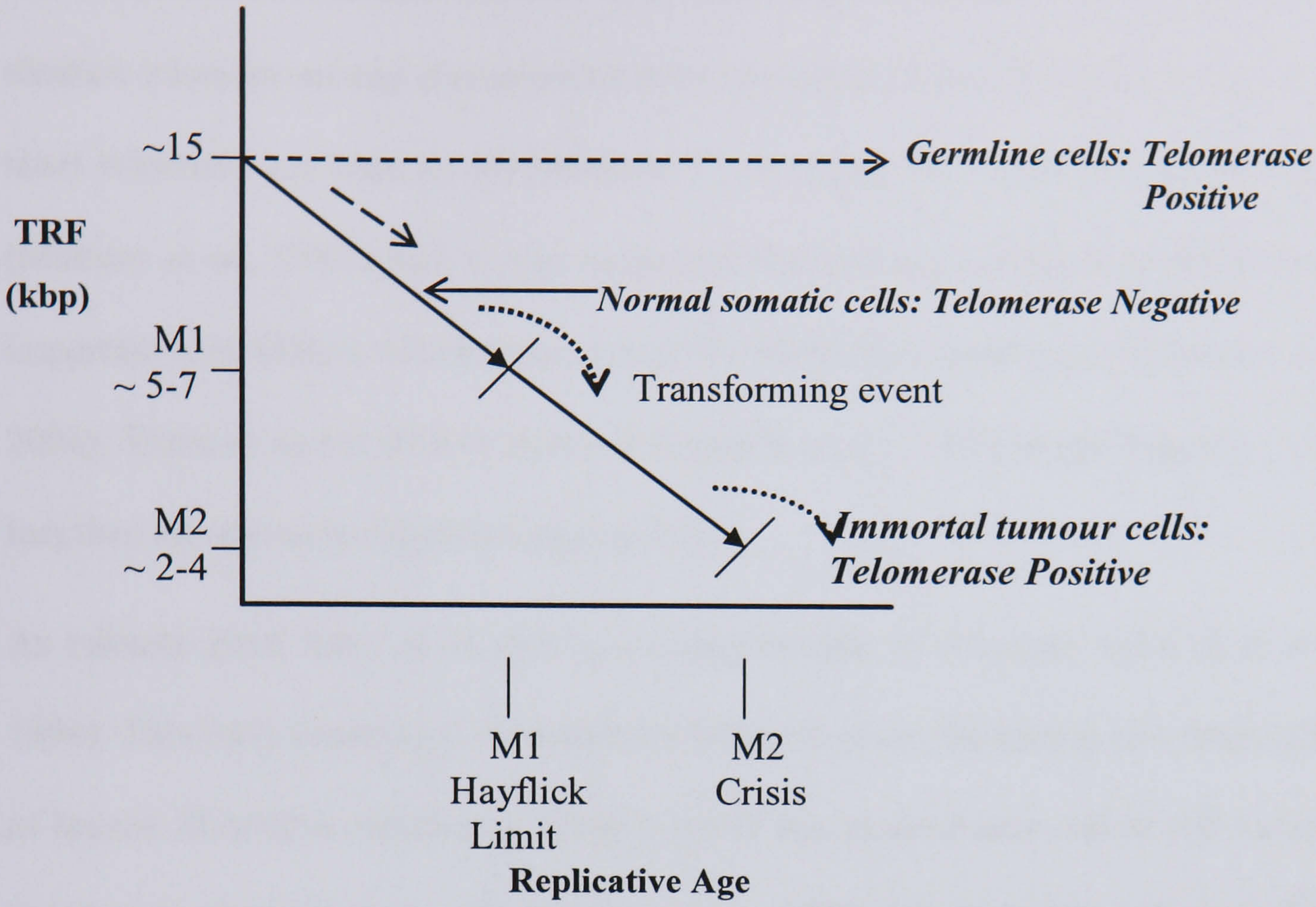

Figure 1.7 The telomere hypothesis of cell ageing and immortalisation. Telomeres shorten with every cell division until M1 (Hayflick limit). Some cells proliferate beyond M1 until they reach crisis or M2. Cells that escape M2 acquire an indefinite growth capacity (Harley, 1991).

Though even in replicating human cells there is evidence that telomeric length does not necessarily determine whether cells senescence (Ouellette *et al.*, 2000). The shortest telomere on any chromosome does not signal immediate arrest because very short telomeres are seen on chromosome 17 for many PD before senescence occurs (Martens *et al.*, 2000) and it was suggested that average telomere length plays an important role. Others indicate that one or few telomeres signal arrest (Hemann *et al.*, 2001). There is recent data (d'Adda di Fagagna *et al.*, 2003) suggesting that >1 but less than all telomeres together signal arrest.

As cultures grow there is an ever increasing fraction of senescent cells (Kill *et al.*, 1994). This early senescence is caused by faster telomere shortening and heterogenity of human fibroblasts replicative lifespan exists due to stochastic cell to cell variation in telomere shortening rates (Martin Ruiz *et al.*, 2004). Other evidence suggests that at the single telomere level there is stochastic variation in telomere length with ultrashort telomeres present in cells (Baird *et al.*, 2003). It has now been established that the length of telomeres does not directly trigger senescence but a concept known as telomere uncapping (Blackburn, 2000) and dysfunctional telomeres (Chin *et al.*, 1999).

1.6.3 Telomere capping/ uncapping

Expression of a dominant negative form of TRF2 protein causes loss of the overall telomere length in the double stranded region (van Steensel *et al.*, 1998; Takai *et al.*, 2003). When this protein is overexpressed in normal fibroblasts the result is the induction of rapid senescence (Smogorzewska and de Lange, 2003). TRF2 has been suggested to be required for telomere capping in mammals (de Lange, 2001) as it enables the telomeres to form the loop structure (Griffith *et al.*, 1999). The ends of

telomeric DNA form a structure which is termed the T loop which is stabilised by a number of telomere binding proteins (Griffith *et al.*, 1999). It has been suggested that a minimum number of telomere repeats is required to form this T loop and maintain a functional telomere (Martens *et al.*, 2000). This loop structure is thought to serve as a protective 'cap' allowing cell division to proceed and if this loop structure is disrupted or opened this is referred to as uncapping (Blackburn, 2000).

Blackburn suggests that the probability of telomere uncapping increases as it length shortens which corresponds to the fact that different strains of fibroblasts undergo senescence at different average telomere lengths (Martens *et al.*, 2000; Serra and von Zglinicki, 2002). Using TRF2, evidence suggests that the forced uncapping of telomeres activates the senescence program (Smogorzewska and de Lange, 2002). Senescence has been shown to be signalled and maintained via formation of DNA damage foci at telomeres which means telomeres remain in an uncapped state in senescent cells (d'Adda di Fagagna *et al.*, 2003).

The telomeric loop structure protects the single stranded G rich overhang from degradation or interaction with signalling protein (von Zglinicki, 2000). The uncapping of the telomeres exposes the single stranded telomeric overhang which could instigate the signal transduction pathway towards senescence (Saretzki *et al.*, 1999; von Zglinicki, 2001). Studies have shown that it is not only telomeres that shorten during every PD but also telomeric overhangs (Stewart *et al.*, 2003; Keys *et al.*, 2004) and this exposure of the chromosme end could lead to activation of the DNA damage machinery (d'Adda di Fagagna *et al.*, 2003).

1.7 Relationship Between Telomere-Dependent and Stress-Induced Senescence

There are many instances whereby senescence like growth arrest is induced in a telomere independent mechanism after stress, which is thought to be a form of a premature senescence (Toussaint *et al.*, 2000). This has been termed stress induced premature senescence (SIPS). For example, overexpression of oncogenes such as activated RAS induce senescence like arrest in primary or mouse cells (Lin *et al.*, 1998; Dimri *et al.*, 2002; Ferbeyre *et al.*, 2002). This has a p16 dependency (Benanti and Galloway, 2004), which corresponds with an arrest in human epithelial cells in response to suboptimal culture conditions (Stampfer and Yaswen, 2003). DNA damaging stresses can induce a senescence like growth arrest including drugs generating DNA double strand breaks (Robles and Adami, 1998). Ionising radiation and a number of chemotherapeutic agents induce a senescence like phenotype in cell lines derived from human tumours (Wang *et al.*, 1998; Chang *et al.*, 1999; Michishita *et al.*, 1999; Park *et al.*, 2000; Suzuki *et al.*, 2001; Elmore *et al.*, 2002; Han *et al.*, 2002; Haq *et al.*, 2002). Typically these forms of senescence do not involve significant telomere shortening and cannot be prevented by ectopic hTERT expression (Wei and Sedivy, 1999; Gorbunova *et al.*, 2002). This form of stress induced senescence which is telomere independent has phenotypic markers of replicative senescence in the fact that they express senescence associated beta galactosidase and express senescence associated proteins (Dierick *et al.*, 2002).

Telomeres are also particularly sensitive to stress/ DNA damage and have lower repair efficiencies (Kruk *et al.*, 1995; Petersen *et al.*, 1998). There is much evidence to suggest a link between the interaction of DNA damaging drugs and telomeres. Firstly, telomeres are specifically sensitive to DNA damage induced by UV (Kruk *et*

al., 1995), oxidative stress (von Zglinicki *et al.*, 1995; Stewart *et al.*, 2003) and possibly, chemotherapeutic drugs (Yoon *et al.*, 1998). Second, dysfunctional telomeres trigger growth arrest and/ or apoptosis via telomere-specific induction of DNA damage foci, also termed senescence-associated DNA damage foci (d'Adda di Fagagna *et al.*, 2003). Third, inhibition of telomerase sensitises mice cells (Lee *et al.*, 2001) and human cells (Ludwig *et al.*, 2001; Misawa *et al.*, 2002) towards cytotoxic drugs. Accordingly, overexpression of the catalytic subunit of telomerase increased the resistance of cells against chemotherapeutic drugs (Ludwig *et al.*, 2001; Zhang *et al.*, 2003). The modification of telomerase expression and/ or activity was detected after drug induced DNA damage (Spiropoulou *et al.*, 2004). Therefore, as telomeres are also influenced by stress it has been suggested that telomere dependent senescence is also a stress response (von Zglinicki, 2002) (Figure 1.8).

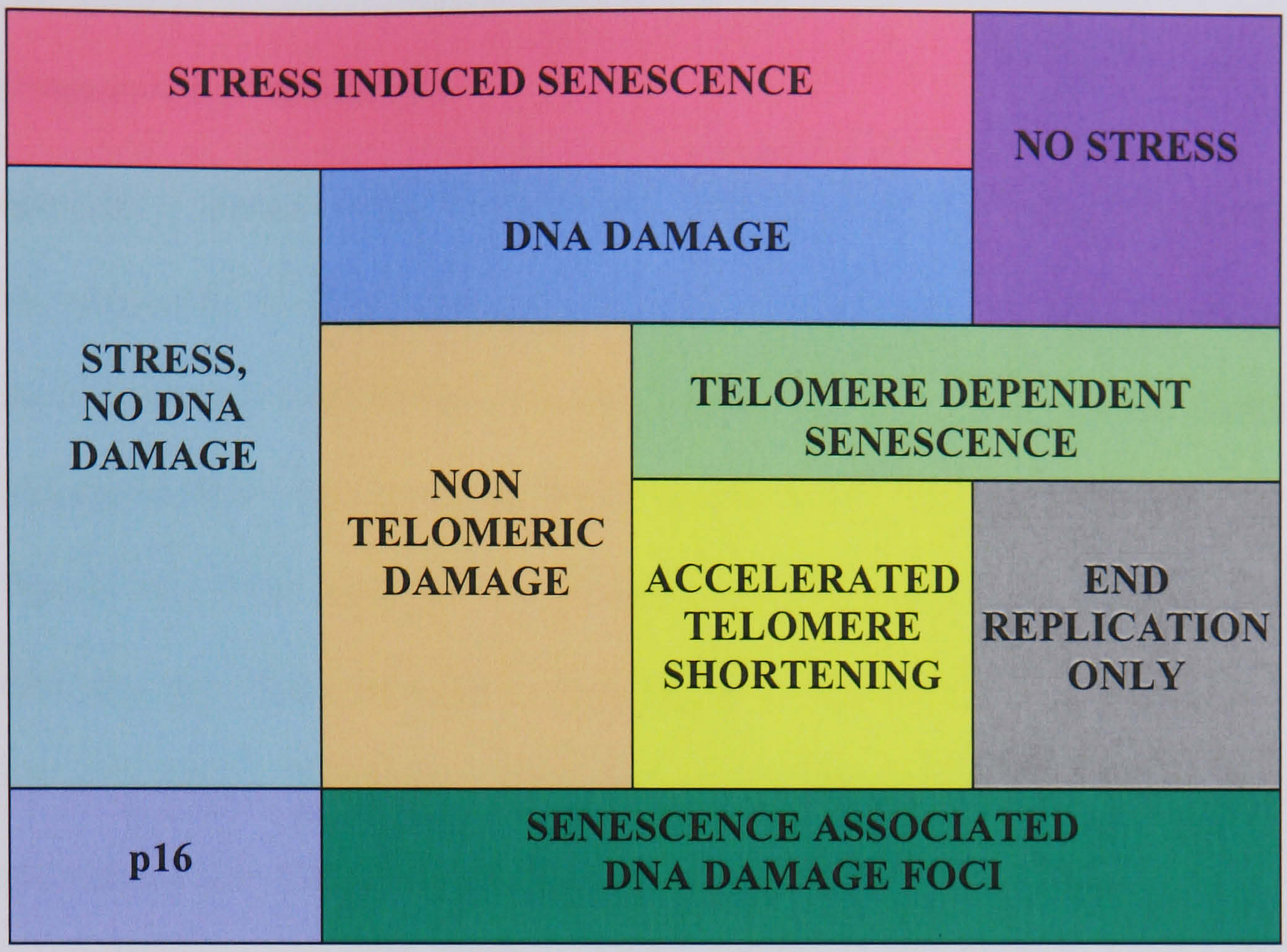

Figure 1.8 Relationship between telomere-dependent and stress-induced senescence. The diagram indicates the different categories and how they interlink.

1.8 Telomerase

1.8.1 Components of telomerase

A compensatory system exists for telomere shortening due to the end replication problem, sensitivity to DNA damage and other mechanisms by the activation of telomerase, a reverse transcriptase enzyme. Telomerase is an RNA-protein complex which utilises its RNA as a template for the addition of TTAGGG repeats in human cells (Figure 1.9). First discovered in *Tetrahymena* (Blackburn and Greider, 1985) telomerase has now been detected in extracts from almost all organisms with the exception of bacteria and viruses which have circular genomes and *Drosophila* which have retrotransposons instead of telomeres (Mason and Biessmann, 1995).

In humans telomerase is composed of two essential components an integral RNA (hTR) which provides the template for the synthesis of telomere repeats, as it contains a domain that is complementary to one hexameric unit of the DNA telomeric repeat sequence TTAGGG and a protein subunit (hTERT) which provides catalytic activity and is homologous to the reverse transcriptases (Feng *et al.*, 1995; Harrington *et al.*, 1997; Nakayama *et al.*, 1998). Telomerase binds to the 3' of DNA strands and extends them by copying its own RNA template in multiples of the hexamer repeat sequence.

Both hTR and hTERT are necessary for reconstitution of telomerase activity *in vitro* (Weinrich *et al.*, 1997; Beattie *et al.*, 1998). While hTR is widely expressed in embryonic and somatic tissue, hTERT is highly regulated and it was thought that it was not detectable in most somatic cells (Meyerson *et al.*, 1997; Nakamura *et al.*, 1997). Though a recent study indicated that maintenance of proper telomere structure is performed by telomerase operating in presenescenct cells (Masutomi *et al.*, 2003).

This work has shown that hTERT is expressed (only during S phase) and active in normal human fibroblasts. When the hTERT was eliminated from these cells, the cells underwent premature senescence (Masutomi *et al.*, 2003).

There is evidence showing that ectopic expression of hTERT is sufficient for restoring telomerase activity in a number of telomerase negative cell lines including foreskin fibroblasts, mammary endothelial cells and umbilical endothelial cells (Weinrich *et al.*, 1997; Bodnar *et al.*, 1998; Counter *et al.*, 1998; Vaziri and Benchimol, 1998; Wen *et al.*, 1998). Although the additional inactivation of the Rb/ p16 pathway is required for the hTERT mediated immortalisation of keratinocytes (Kiyono *et al.*, 1998).

Telomerase maintains a dynamic equilibrium and prevents the chromosomes from shortening to a critical length and prevents cells from receiving the signal to stop dividing. Cells that produce telomerase include germ cells and cancer cells, these cells are essentially immortal whereas normal somatic cells lack telomerase activity. The introduction of telomerase prior to either M1 or M2 is sufficient for immortalisation indicating that telomeres are associated with both M1 and M2 stage of growth arrest in human fibroblasts (Morales *et al.*, 1999).

1.8.2 Alternative lengthening of telomeres

Cells exist which are telomerase negative but are still able to maintain the length of their telomeres and have unlimited replicative potential, indicating the existence of one or more non telomerase mechanisms for telomere maintenance termed Alternative Lengthening of Telomeres (ALT) (Bryan and Reddel, 1997).

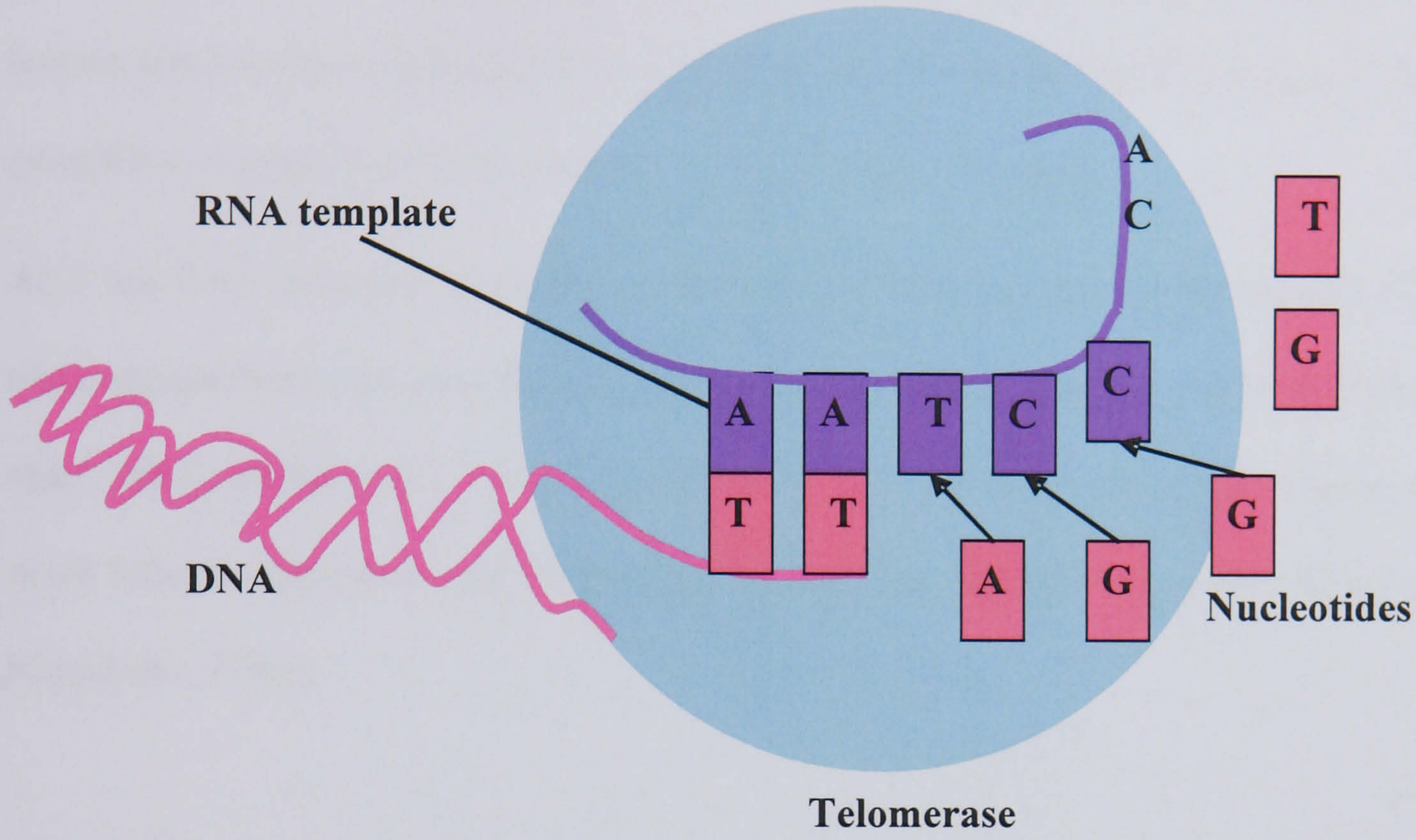

Figure 1.9 Telomere elongation. Telomeres are extended by the enzyme telomerase.

ALT cells have a heterogeneous telomere length phenotype with long telomere length and wide length distribution (Bryan *et al.*, 1995; Grobelny *et al.*, 2001; Murnane *et al.*, 1994) compared to telomerase positive human cancers, which are homogenous and have shorter lengths (de Lange, 1995; Park *et al.*, 1998). Approximately 85% of human tumours have telomerase activity (Shay and Bacchetti, 1997). Though it is not possible to suggest that the remaining 15% have ALT activated.

ALT has been detected in a number of tumours including osteosarcoma, soft tissue sarcoma, glioblastoma and carcinomas of the lung, kidney, adrenal and breast (Bryan *et al.*, 1997; Mehle *et al.*, 1996; Scheel *et al.*, 2001). There is evidence to suggest that some tumours have both ALT and telomerase activity (Bryan *et al.*, 1997; Strahl and Blackburn, 1996).

1.8.3 Telomere length independent survival function of telomerase

There is evidence to suggest that telomerase acts as a survival factor and plays a role in resistance of cancers to chemotherapeutic drugs (Ludwig *et al.*, 2001; Zhang *et al.*, 2003; Sharma *et al.*, 2003; Shin *et al.*, 2004). This has been supported by other investigations for example the upregulation of telomerase activity has been detected after DNA damaging drug treatments (Moriarty *et al.*, 2002; Klapper *et al.*, 2003; Sato *et al.*, 2000). Telomerase could promote survival either by compensating for telomeric damage or by some telomere independent mechanism. However, there are arguments in favour of a telomere independent mechanism:

1) Overexpression of telomerase has been shown to induce the expression of a number of DNA damage responses and repair genes (Sharma *et al.*, 2003; Shin *et al.*, 2004).

2) Telomerase interacts with proteins involved in survival and apoptosis (Cao *et al.*, 2002; Haendeler *et al.*, 2003; Zhang *et al.*, 2003; Dudognon *et al.*, 2004).

3) If maintenance of telomere length and/ or structure by telomerase were important for the resistance of tumour cells to cytotoxins, one should expect that telomerase knockdown would result in compromised telomeres, followed by early induction of apoptosis or growth arrest. In fact, telomerase knock down induces apoptosis (Fu *et al.*, 2000) in tumour cells and increased the sensitivity of cells to DNA damaging drugs (Ludwig *et al.*, 2001; Kondo *et al.*, 1998). Though this occurs without any change in telomere length (Saretzki *et al.*, 2001; Ludwig *et al.*, 2001).

4) Telomerase has been linked with various other pathways due to it being localised to different cellular compartments such as nucleolus, cytoplasm and mitochondria (Wong *et al.*, 2002; Haendeler *et al.*, 2003; Santos *et al.*, 2004).

1.8.4 Telomerase as a prognostic marker

In some forms of cancer telomerase could be used as a prognostic marker for example in neuroblastoma. 94% of neuroblastomas (Hiyama *et al.*, 1995) express telomerase suggesting an important role for telomerase in neuroblastoma development.

Neuroblastoma (NB) arises from the embryonal neural crest and is the most common solid extracranial malignancy of infancy and childhood affecting 1 in 7000. They are tumours that are markedly heterogeneous in terms of their biological, morphological and clinical characteristics (Maris and Matthay, 1999). It is an unpredictable cancer as some cases are highly aggressive and poorly responsive to current therapeutic schemes and others will spontaneously regress. Therefore leading to favourable and unfavourable prognosis even if multimodal therapy has occurred.

In order to predict the biological behaviour of an individual tumour there are several parameters to predict prognosis of neuroblastoma patients. These parameters include MYCN gene amplification where loss of heterozygosity for 1p32-36 and the subsequent increase in MYCN copy number predict poor outcome in all age and stage groups (Brodeur *et al.*, 1984; Ambros *et al.*, 1996; Caron *et al.*, 1996).

A low Trk A expression is another powerful prognostic marker that identifies a favourable group of tumours (Nakagawara *et al.*, 1993). Trk A is a proto-oncogene that is a transmembrane glycoprotein tyrosine kinase that is expressed selectively in the developing nervous system and whose product is a signal transducing receptor for nerve growth factor (Kaplan *et al.*, 1991). Trk is expressed in many primary neuroblastomas and is associated inversely with amplification of the N-myc proto-oncogene. Ha-ras p21 expression (Tanaka *et al.*, 1991) and cellular DNA content are other markers. All these markers though do not give a complete accurate prognostic grouping (Bown *et al.*, 1999).

Telomerase activity has been shown to be a powerful independent prognostic factor in neuroblastoma (Brinksmidt *et al.*, 1998; Poremba *et al.*, 1999; Poremba *et al.*, 2000) or in association with another parameter for e.g. Trk A expression (Nozaki *et al.*, 2000). Neuroblastomas have been classed into groups of high and low telomerase activity and the expression profile assessed by microarray to determine any genes that could be used as a novel targets in aggressive neuroblastomas (Hiyama *et al.*, 2003). Therefore since telomerase activity has prognostic significance in neuroblastoma it is particularly relevant that a study of telomeric damage caused by cisplatin and etoposide should focus on this disease.

1.9 Conventional Anticancer Therapeutics

The best result from any cancer treatment is the complete eradication of all cells from the body giving a patient a normal life expectancy. The number of treatment choices depends on the type of cancer, the stage of the cancer, and other individual factors such as the age, health status of the patient. The four major types of treatment for cancer are surgery, radiation, chemotherapy, and biological therapies. Though there are hormone therapies (tamoxifen) and transplant options (bone marrow) available. If a tumour is amenable to surgery, then surgery is the most effective tool in the anti-cancer treatment. Anti-cancer agents are rarely used singly to treat cancer as only a few tumours are sensitive enough to be cured by single agents. Effective chemotherapy usually depends on the identification of suitable combinations to treat a specific type of tumour (Frei *et al.*, 1998), as combination treatments minimise drug resistance and the dose limiting toxicity to the patient.

Conventional anti-cancer drugs have been designed with DNA as their target. Some target DNA synthesis though a problem lies in that tumour cells are not the only proliferating cells in the body i.e. cells that line the alimentary tract, bone marrow cells that generate red blood cells and cells to fight infection and epidermal cells including those that generate hair are all highly proliferative. New generation drugs have targets removed from the direct synthesis of DNA and now affect the signals that promote or regulate the cell cycle, growth factors and their receptors, signal transduction pathways and pathways affecting DNA repair and apoptosis.

1.10 Cisplatin

1.10.1 History of cisplatin

Cis-diamminedichloroplatinum (II) (cisplatin) is a neutral, inorganic compound that is widely used for the treatment of a variety of tumours. Cisplatin is a square planar complex that contains a single platinum atom with two ammonia and two chloride groups that are bound in the *cis* configuration (Figure 1.10).

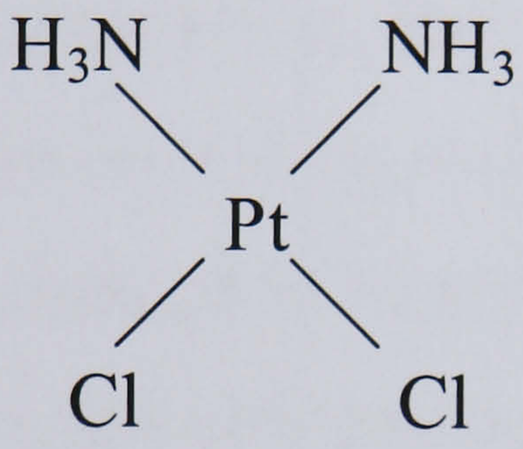

Figure 1.10 Structure of cisplatin. Two chloride and two ammonia groups attached to a single platinum atom.

Cisplatin was first synthesized by M. Peyrone in 1844 and was called 'Peyrone's chloride'. Its structure was discovered by Alfred Werner in 1893 and then it was only serendipitously revealed to be an anti-cancer compound by Barnett Rosenburg in the 1960's (Rosenburg *et al.*, 1965). Rosenburg was interested in the resemblance between mitotic spindle of dividing cells and the lines of magnetic force as visualised by iron filings around a magnet. Initially he designed an experiment to measure the effect of an electric field on the growth of the bacteria *Escherichia coli*. He showed that the bacteria growth was inhibited by the electric current though there was an increase in their normal length. However this effect was due to an electrolysis product formed by the interaction of dissolved platinum from the electrodes with ammonium in the culture medium. The product formed was identified as $(NH_4)_2(PtCl_6)$ and in

turn was converted by a photochemical reaction to cis-($PtCl_4(NH_3)_2$). As Rosenberg found that the platinum complexes were effective at inhibiting cell division (Rosenburg *et al.*, 1967) he decided to test the platinum complexes against the mouse tumour, Sarcoma 180 (Rosenburg *et al.*, 1969) and the compounds were also screened against the mouse leukaemia, L1210. The platinum complexes were found to be highly effective in eliminating tumours and were further tested in a number of animal models. In human trials, cisplatin was effective against a range of tumour types particularly testicular cancers (Higby *et al.*, 1974) and ovarian cancer (Wiltshaw and Carr, 1974) though it was limited to some extent by toxic side effects. These side effects include renal toxicity, bone marrow suppression, hearing loss, neurotoxicty etc (Calvert *et al.*, 1995), which have been made bearable by adjuvant therapies. For example, administration of continuous hypertonic saline along with diuretic drugs before and following cisplatin infusion has helped to reduce kidney damage (Hayes *et al.*, 1977). Similarly, several effective antiemetic drugs protect the patient from the worst of nausea and vomiting (Kidgell *et al.*, 1990). Today cisplatin is widely prescribed for a variety of tumours (germ-cell, advanced bladder carcinoma, adrenal cortex carcinoma, breast cancer, head and neck carcinoma, lung carcinoma, neuroblastoma). It is administered intravenously for one to 5 days in a row, followed by a rest period of 2-3 weeks.

1.10.2 Biochemical mechanism of action of cisplatin

Cisplatin's main intracellular target in mammalian cells is DNA, forming cisplatin-DNA adducts (Pinto and Lippard, 1985), though it can also react with RNA and protein. Cisplatin diffuses through the cell membrane and for the interaction to occur with DNA, the neutral cisplatin has to be activated through a series of aquation

reactions which involve the sequential replacement of the *cis*-chloro ligands of cisplatin with water molecules (Figure 1.11). A chloride ligand of the neutral cisplatin complex is displaced by a water ligand in the cytosol, to produce a monofunctionally active complex which can react with nucleophilic sites i.e. a single nitrogen on a DNA molecule. Displacement of the second chloride with water leads to the bifunctional active complex. The aquation process takes place in the cytosol as the presence of a high chloride ion concentration in extracellular fluid suppresses the aquation reaction. Cisplatin forms both monofunctional and bifunctional inter and intra-strand cross-links on DNA and the amounts of platinum bound to DNA have also been determined (Jamieson and Lippard, 1999). The nature and proportions of these adducts are shown in Figure 1.12. The major adduct formed is the bifunctional intra-strand cross-link between adjacent guanines (1,2d(GpG)) 60-65%. Other adducts formed are 1,2 intra-strand d(ApG) 20-25%, 1,3 intra-strand GpG 2%, monofunctional adducts 2% and 1,2 G,G inter-strand cross-links ~ 2% (Fichtinger-Schepman *et al.*, 1985).

1.10.3 Cisplatin cytotoxicty

Cisplatin is a potent inducer of apoptosis (Ormerod *et al.*, 1996; Henkels and Turci, 1997). It is unclear how the cisplatin-DNA adducts induces cytotoxicty, though it is widely thought that the cross-links formed are the cause of the drugs cytotoxicty and there is linear correlation between gross levels of platinum bound to DNA and the extent of cytotoxicty (Fraval and Roberts, 1979). Reports exist that indicate that inter-strand cross-links are the most cytotoxic lesion (Knox *et al.*, 1986). Though other evidence favours intra-strand adducts as lesions largely responsible for the cytotoxic action (Pinto and Lippard, 1985) which is consistent with the knowledge that the intra-strand adducts account for 85- 90% of total lesions (Kelland, 1993).

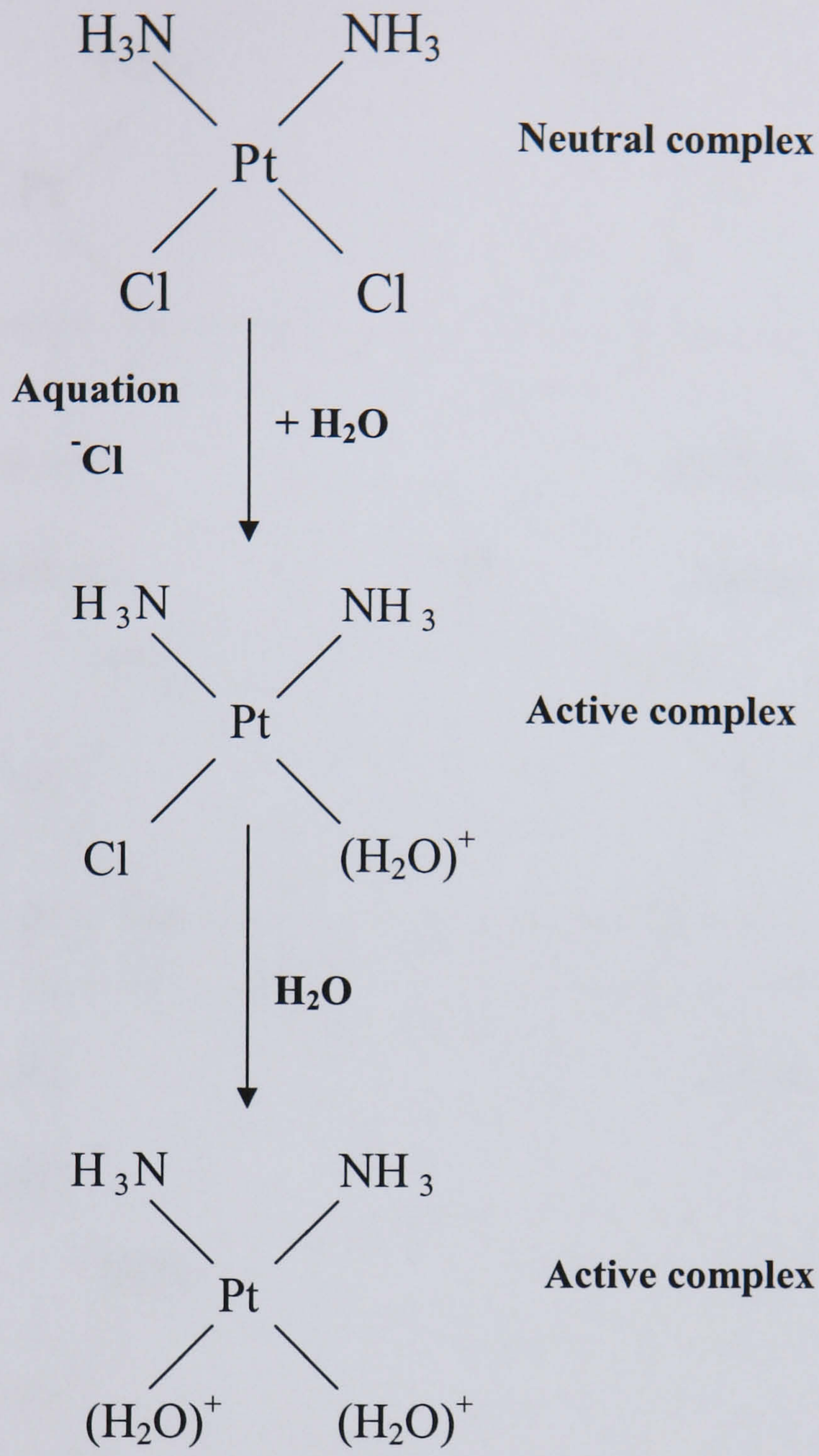

Figure 1.11 Formation of reactive cisplatin complexes *in vivo.* For cisplatin to be able to react with DNA the neutral complex is activated through a series of aquation reactions, whereby the *cis*-chloro ligands of cisplatin are replaced with water molecules.

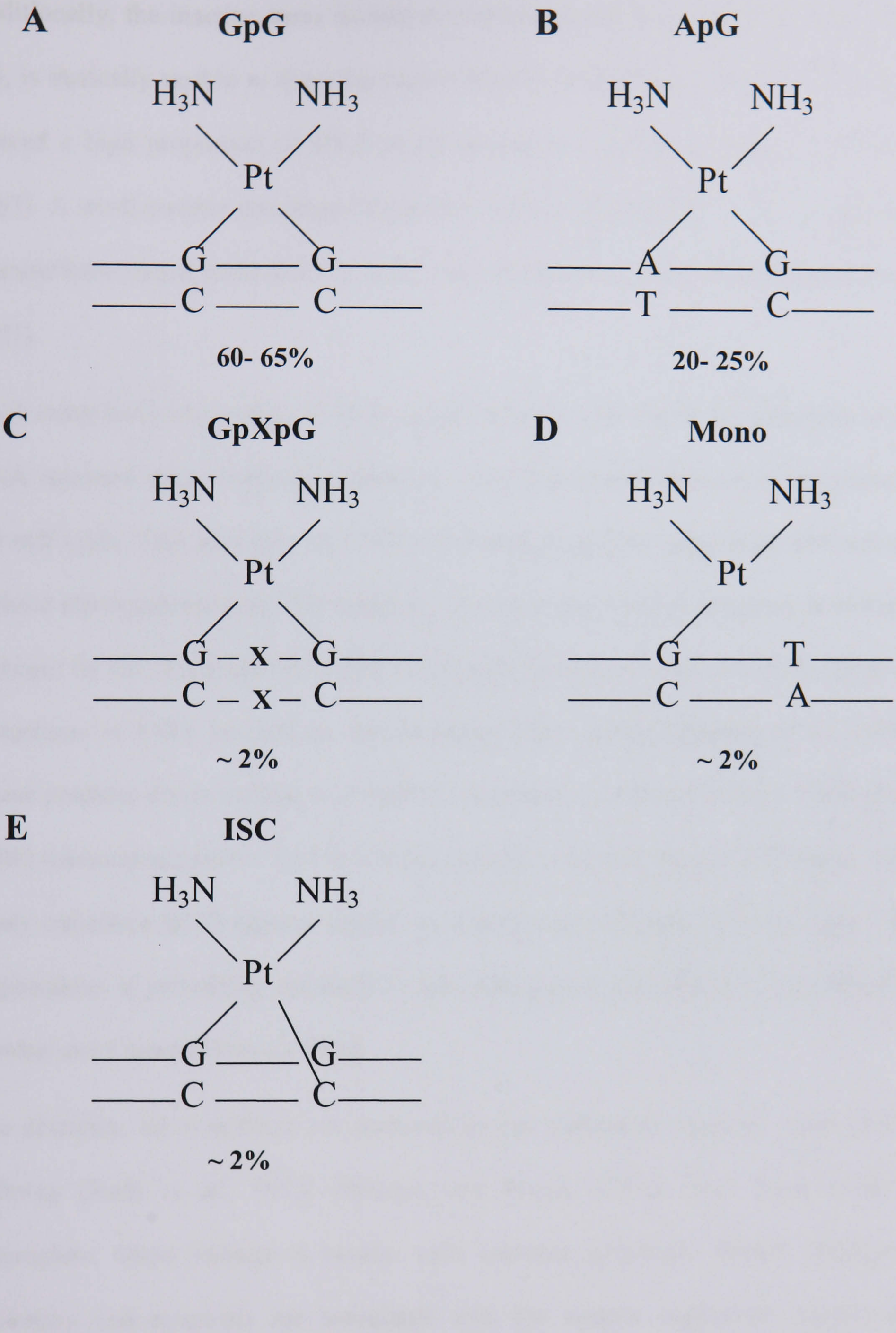

Figure 1.12 Spectrum of cisplatin- DNA adducts. Cisplatin binds to DNA to form the following cross-links; (A) 1, 2-(GpG)- intra-strand, (B) 1, 2-d (GpG)- intra-strand, (C) 1, 3-d (GpXpG)- intra-strand, (D) cisplatin bound monofunctionally to guanine, (E) inter-strand cross-link. The percentage of the specific type of adduct formation is denoted below each diagram.

Additionally, the inactive *trans* isomer of cisplatin, trans-diamminedichloroplatinum (II), is sterically unable to form the major d(GpG) and d(ApG) intra-strand adducts. Instead a high proportion of DNA mono-adducts are formed (Eastman and Barry, 1987). A small number rearrange themselves to form bifunctional 1,3 or 1,4 guanine-guanine intra-strand cross-links or DNA inter-strand cross-links (Eastman and Barry, 1987).

DNA cross-links are considered to be cytotoxic to the cell due to the alteration of the DNA structure when cisplatin is bound to it and apoptosis is induced at any phase of the cell cycle. This alteration in DNA is believed to prevent replication and activate cellular repair mechanisms. The sequence of events that leads to apoptosis is believed to begin by the recognition of DNA damage by proteins which bind to the physical distortions of DNA induced by the cisplatin- DNA adducts (Bellon *et al.,* 1991). These proteins which include the hMSH2 component of mismatch repair (Fink *et al.*, 1998) transcription factor 'TATA binding protein' (TBP) (Chaney and Vaisman, 1999) likely transduce DNA damage signals to downstream effectors but may have other implications in promoting cytoxicty by preventing their participation in transcription (Jordan and Carmo-Fonseca, 2000).

The cisplatin- DNA adducts are removed by the nucleotide excision repair (NER) pathway (Beck *et al.,* 1973; Hansson and Wood, 1989). Only when repair is incomplete, when damage is severe, cells undergo apoptosis. Repair, checkpoint activation and apoptosis are associated with the tumour suppressor protein p53 (Morgan and Kastan, 1997; Bullock and Fersht, 2001). Additionally, patients with a deficiency in NER, Xeroderma Pigmentosum (XP) were hypersensitive to cisplatin (Dijt *et al.*, 1988). Futhermore the transcribed strand has shown to be repaired more efficiently than the untranscribed strand due to the transcription coupled repair system

(Mellon and Hanavalt, 1989) and it has been shown that the major intra-strand d(GpG) adduct induced by cisplatin is poorly repaired compared to d(GpXpG) and monofunctional adducts (Page *et al.*, 1990; Szymkowski *et al.*, 1992).

1.10.4 Cisplatin drug resistance

Drug resistance is a major limitation in cisplatin cancer chemotherapy. Resistance can be either intrinsic (present at the onset of treatment) or acquired (occurring during treatment). Colorectal and non small cell lung tumours are examples of those exhibiting intrinsic resistance to cisplatin while ovarian and small cell lung cancers often develop acquired resistance (Kelland, 2000). Cisplatin resistance can be multifactoral, and the several mechanisms that can contribute to this property include changes in reduced intracellular drug accumulation (Kelland, 1993), increased inactivation by thiol containing molecules (Wolf *et al.*, 1987) and an increase in DNA repair (Lai *et al.*, 1988). Other possibly important mechanisms inhibit propagation of the DNA damage signal to the apoptotic machinery including loss of damage recognition, overexpression of HER-2/neu, activation of the PI3-K/Akt (also known as PI3-K/PKB) pathway, loss of p53 function, overexpression of antiapoptotic bcl-2, and interference in caspase activation (Siddick, 2003).

1.11 Etoposide

1.11.1 Topoisomerase II poisons

Topoisomerases are enzymes located in the nucleus of cells and induce topological changes in DNA during essential processes such as DNA replication, transcription, recombination and repair. Topoisomerase I (Wang, 1971) breaks single strand DNA, whilst topoisomerase II (Gellert *et al.*, 1976) cleaves double strands of DNA and can untangle inter-twined double strands of DNA (Wang, 1996). For example topoisomerase II has shown to be essential for the segregation of daughter chromosomes in mitosis in *S.* cerevisiae (Dubrana *et al.*, 2001).

Toposiomerase II enzymes are multi subunit proteins, which require ATP for overall catalytic activity and modulate DNA topology by passing an intact helix through a transient double strand backbone break (Li and Chen, 1994; Froelich-Ammon and Oshesoff, 1995). Topoisomerase II poisons stabilise the cleavable complex, preventing the removal of covalently bound enzyme and religation of the DNA. The topoisomerase II poisons appear to be particularly toxic during S phase when replication forks and transcription complexes are both present as compared to other phases when only transcription complexes are present (Estey *et al.*, 1987; D'Arpa *et al.*, 1990). Intact p53 is required for G_1 arrest by topoisomerase inhibitors etoposide and doxorubicin (Fan *et al.*, 1994). In normal human cells DNA topoisomerase inhibitors are efficient and reversible inducers of premature senescence (Michishita *et al.*, 1998).

1.11.2 History of etoposide

Etoposide (Figure 1.13) was the first agent recognised as a topoisomerase II inhibiting anti-cancer drug and is one of the most active anti-tumour agents against solid tumours.

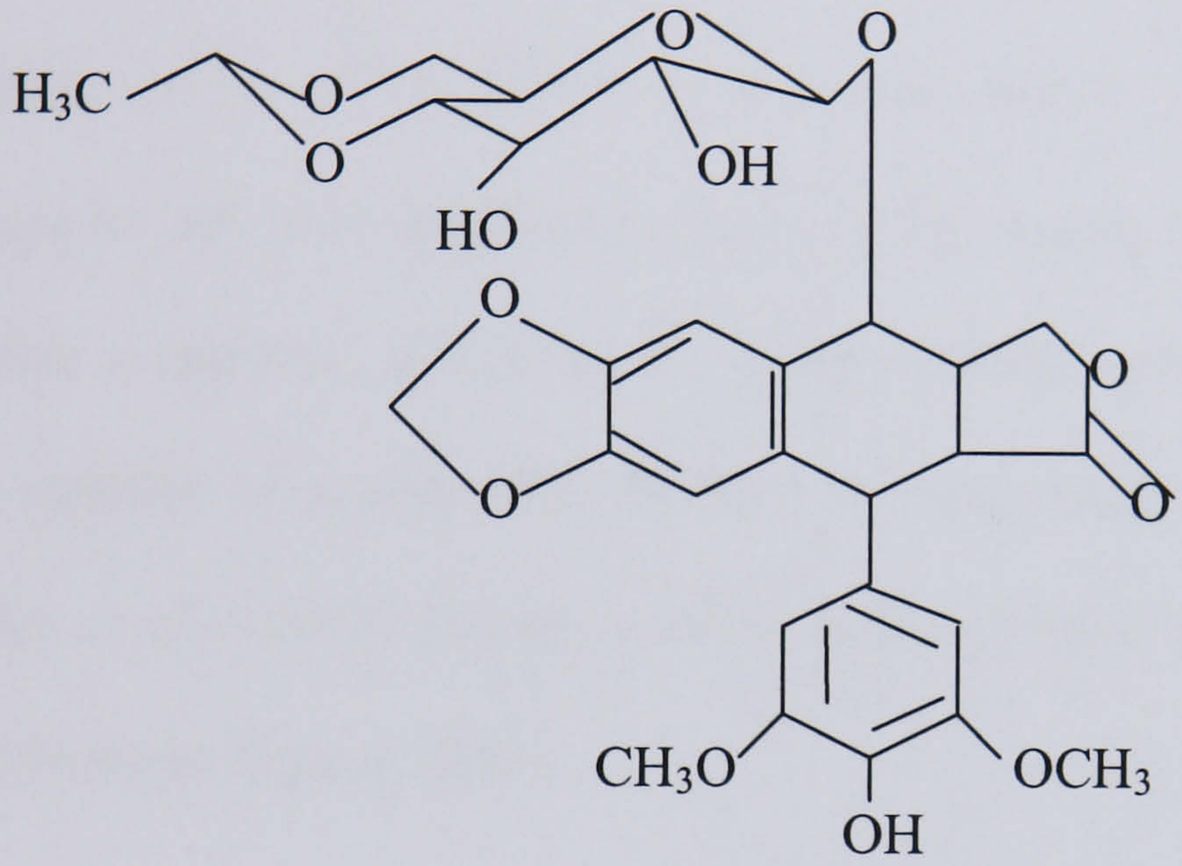

Figure 1.13 Structure of etoposide. Etoposide, a topoisomerase II inhibitor, is a derivative of podophyllotoxin.

Etoposide is the first drug choice for testicular cancer and small lung cancer though it is also used in treatments of lymphomas, Ewings sarcoma, Kaposi's sarcoma and ovarian cancer (Hande, 1998a). Etoposide is a derivative of the plant derived natural product, podophyllotoxin and was put into clinical trials in the 1970's.

1.11.3 Biochemical mechanism of action and cytotoxicty of etoposide

Etoposide is a typical topoisomerase II poison that stabilises the cleavable complex formation with DNA topoisomerase II without an intercalating action. Etoposide and

other topoisomerase II posions do not kill cells by blocking topoisomerase catalytic function. Rather they poison these enzymes by increasing the steady state concentration of their covalent DNA cleavable complexes. This action converts topoisomerase into physiological toxins that introduce high levels of transient protein associated breaks in the genome of treated cells (Kaufmann, 1998). Etoposide is known to cause DNA strand breaks and to induce apoptosis in diverse cell types (Okamoto-Kubo *et al.*, 1994; Bonelli *et al.*, 1996; Hande, 1998b; Michishita *et al.*, 1998). Etoposide has been reported to have topoisomerase II independent functions, as it contains a phenolic group which when oxidised yields reactive metabolites (quinones) capable of irreversible binding to macromolecular targets like DNA (Stoyanovsky *et al.*, 1993). Though it is not known if these play a significant role to etoposides pharmacological effects.

1.11.4 Etoposide drug resistance

Etoposide shows high affinity for P-glycoprotein and multidrug resistant cells show cross resistance to etoposide. Tumour cells resistant to topoisomerase II inhibitors often have low topoisomerase II levels whereas tumour cells with high levels of expression of topoisomerase II are sensitive to topoisomerase II inhibitors (Davies *et al.*, 1988). Overexpression of topoisomerase II in tumour samples has been reported in several types of tumours including lung cancer, ovarian cancer and lymphoma (Koomagi *et al.*, 1996).

1.12 Telomerase Inhibition as a Potential Therapeutic

Telomerase is active in early embryogenesis (Ulaner *et al.*, 1998) but is down regulated during differentiation. It is expressed in adult reproductive cells, at very low levels in somatic cells (except proliferative cells of renewal tissues) and is expressed in 85% of human cancers (Shay and Bacchetti, 1997). There has been much attention given to the development of telomerase inhibitors as potential anti-cancer agents because of the strong potential advantages of broad versatility (nearly all known cancers express telomerase) and comparatively high tumour specificity (as the few human somatic cells that have telomerase seem to be less reliant on it than tumour cells). Additionally inhibiting telomerase activity will allow telomere shortening to occur which is a major mechanism to induce telomere uncapping and thus to signal growth arrest and/ or apoptosis. Unfortunately, the disadvantage with telomerase inhibition, is the requirement to maintain the inhibition over a long time in order to allow telomere erosion and eventually cell death (Kipling, 1995), as telomeres only erode at a rate of 50 to 100 bases per population doubling (Harley *et al.,* 1990). This is especially relevant to tumours with long telomeres and provides circumstances highly favourable for the development of drug resistance. Alternatively, telomerase has been shown to have a telomere independent survival function (See Section 1.8.3) which may play a role in resistance of cancers to chemotherapeutic drugs and identifying the mechanisms involved could potentially be useful in future therapeutics.

It may be possible to overcome this serious problem of telomerase inhibition by exploiting synergistic interactions that are predicted to arise from the correct combination of telomerase inhibitors with certain established and novel anti-cancer drugs. It has been shown that inhibition of telomerase activity by expression of a

ribozyme targeted against hTERT increases the sensitivity of breast cancer cells to doxorubicin, a topoisomerase inhibitor (Ludwig *et al.*, 2001).

As telomerase is controlled on a number of levels, various strategies have been investigated as targets for telomerase inhibition using either a direct or an indirect action by i) chemoprevention, ii) targeting telomerase components and their regulatory mechanisms, iii) targeting the telomere and iv) synergistic approaches (Reviewed: Keith *et al.*, 2002; Saretzki., 2003). Inhibition of telomerase by different methods has lead not only to progressive telomere shortening and ensuing cell death (Herbert *et al.*, 1999) but also to telomere length independent apoptosis induction (Saretzki *et al.*, 2001).

Tumours using the ALT mechanism will be resistant to telomerase inhibitors. Repression of ALT in ALT+ immortalised cell lines results in senescence and cell death (Nakabayashi *et al.*, 1997; Perrem *et al.*, 2001) which may also be an attractive target and help prevent drug resistance. Bechter and colleagues inhibited telomerase activity in a human cancer cell line with a mismatch repair defect and observed an ALT like telomere elongation (telomerase independent) which showed a novel mechanism of resistance to anti-telomerase therapy (Bechter *et al.*, 2004).

1.13 Aims and Objectives

The aim of this study was to establish the significance of the telomere/ telomerase complex for the action of the conventional cytotoxic anti-cancer drugs cisplatin and etoposide. This aim was approached by using cells with either long or short telomeres and by assessing a number of parameters to detect evidence for significant levels of drug-induced effects on telomeres. An important aspect of the experiments was to distinguish between effects that resulted from apoptosis as opposed to effects that could have induced apoptosis. Thus, the investigation examined whether induction of apoptosis was preceded or accompanied by telomere shortening or other observable changes in the telomere/ telomerase complex after drug treatments.

The cell line used to investigate short telomeres was a neuroblastoma cell line, SHSY5Y with telomere lengths of ~4 kbp and for the long telomeres an acute lymphoblastic T cell line 1301 with telomere lengths of ~80 kbp was used. Both cell lines positively express telomerase. The study assessed two treatment regimes namely a short and a continuous exposure to both drugs. The short exposure drug treatment was 2 hours for cisplatin and 4 hours for etoposide and studies took place up to 48 hours after exposure. For the continuous drug exposure, studies took place at daily intervals up to 72 hours after initial drug exposure.

The main hypothesis to be tested was that drug induced DNA damage targets the telomere/ telomerase complex to a significant extent such that apoptosis and or growth arrest might largely be triggered from telomeres. If confirmed, this model would have important implications for the design of potentially effective anti-cancer therapies based on the combination of DNA damaging cytotoxic agents with telomerase inhibitors.

This work involved:

- Investigation of cytotoxicty of cisplatin and etoposide treatment on the SHSY5Y and 1301 cells
- Analysis of the cellular response to drug exposures by examining levels of apoptosis and kinetics of cell cycle
- Confirmation of DNA damage induction and response after cisplatin and etoposide exposure
- Examination of telomere restriction fragment length, length and integrity of single stranded G overhangs and telomeric single strand breaks after cisplatin and etoposide treatment
- Evaluation of telomerase activity after cisplatin and etoposide exposure
- Adaptation of an immunoFISH procedure to assess the co-localisation of telomeric DNA and DNA damage response foci

CHAPTER TWO

MATERIALS AND METHODS

2.1 Chemicals and Reagents

Unless otherwise stated, the chemicals used in these studies were obtained from Sigma-Aldrich Company Ltd (Poole, Dorset, UK) or VWR International (Poole, Dorset, UK).

2.2 Buffers and Solutions

Alkaline buffer	50 mM NaOH, 1 mM EDTA
B & W buffer	10 mM Tris-HCl pH 7.5, 1 mM EDTA, 2 M NaCl
Buffer C1	1.28 M sucrose, 40 mM Tris-Cl pH 7.5, 20 mM $MgCl_2$, 4% Triton X-100
Buffer G2	800 mM guanidine HCl, 300 mM Tris-Cl pH 8, 30 mM EDTA pH 8, 5% Tween-20, 0.5% Triton X-100
Buffer QBT	750 mM NaCl, 50 mM MOPS pH 7, 15% isopropanol, 0.15% Triton X-100
Buffer QC	1 M NaCl, 50 mM MOPS pH 7, 15% isopropanol
Buffer QF	1.25 M NaCl, 50 mM Tris-Cl pH 8.5, 15% isopropanol
Cell suspension buffer	10 mM Tris pH 7.2, 20 mM NaCl, 50 mM EDTA

Culture medium	Medium containing 10% (v/v) heat inactivated foetal calf serum, 1% (w/v) penicillin/ streptomycin, 1% (w/v) L- glutamine
Denaturation buffer	0.5 M NaOH, 1.5 M NaCl
Depurination buffer	0.25 M HCl
Diethanolamine solution	100 mM diethanolamine, 1 mM $MgCl_2$ pH 10
EDTA buffer	10 mM EDTA pH 8.2, 95% formamide
FADU alkali solution	200 mM NaOH, 40% FADU denaturation buffer
FADU denaturation buffer	9 M urea, 10 mM NaOH, 25 mM CDTA, 0.1% SDS
FADU lysis buffer	0.25 M meso-inositol, 1 M $MgCl_2$, 10 mM Na_2PO_4/ NaH_2PO_4, pH 7.2
H buffer	50 mM Tris-Cl, 10 mM $MgCl_2$, 100 mM NaCl, 1 mM dithioerythritol pH 7.5
Neutralisation buffer	0.5 M Tris-HCl, 1.5 M NaCl, pH 8
PBG	0.2% cold water fish gelatine, 0.5% BSA in PBS
Phosphate Buffered Saline (PBS)	10 mM Na/ KH_2PO_4, 140 mM NaCl, 2.7 mM KCl, pH 7.4
Plug wash buffer	20 mM Tris, 50 mM EDTA pH 8
Protein reaction buffer	100 mM EDTA pH 8, 0.2% sodium deoxycholate, 1% sodium laurylsarcosine
Sen β gal staining solution	150 mM NaCl, 2 mM $MgCl_2$, 40 mM citric acid, 12 mM sodium phosphate pH 6, water, X-Gal, potassium ferrocynaide
Sodium acetate buffer	80 mM NaOAc, 95% formamide
Sulphorhodamine B (SRB) solution	0.4% (w/v) SRB dissolved in 1% (v/v) acetic acid
TBS buffer pH 7	0.14 M NaCl, 50 mM Tris, 2.7 mM KCl, pH 7

TBS buffer pH 8.5	0.14 M NaCl, 50 mM Tris, 2.7 mM KCl, pH 8.5
TE buffer	10 mM Tris-Cl pH 8, 1 mM EDTA pH 8
1x SSC	0.015 M sodium chloride, 0.15 M sodium citrate
1x SSC/ 1% Triton X-100	0.015 M sodium chloride, 0.15 M sodium citrate/ 1% Triton X-100
0.1x SSC/ 1% Triton X-100	0.0015 M sodium chloride, 0.015 M sodium citrate, 1% Triton X-100
0.2x SSC/ 0.1% SDS	0.03 M sodium chloride, 0.003 M sodium citrate, 0.1% sodium lauryl sulphate (SDS)
0.5 x TBE	45 mM Tris, 45 mM boric acid, 2 mM EDTA

2.3 Cell Culture

2.3.1 Tissue culture supplies

Tissue culture flasks (25 cm^2, 75 cm^2 and 150 cm^2) were supplied from Corning Incorporated, USA. All other plasticware used were obtained from VWR International, UK. All reagents were acquired from Sigma-Aldrich, UK unless otherwise stated.

2.3.2 Equipment

All tissue culture procedures were carried out in a Trimat^2 class II microbiological safety cabinet (Medical Air Technology, UK) and cell flasks were incubated in a CO_2 tissue culture incubator (Binder GmbH, Germany). Cells were centrifuged in either a centrifuge equipped with a swing out rotor (Biofuge Primo R, Heraeus, Kendro Laboratory Products, UK) or microcentrifuge (Eppendorf 5415R, Germany). Culture media was pre-warmed in a 37°C waterbath (Grant Instruments, Jencons PLS, UK).

2.3.3 Cell lines/ strain

Cell lines/ strain used in this study are listed in Table 2.1.

Table 2.1 Characteristics of cell lines/ strain

Cell Lines/ Strain	Characteristics	Reference	Acquired
SHSY5Y	Human neuroblastoma	Ross *et al.*, 1983	ATCC, USA
1301	Human T cell lymphoblast	Hultdin *et al.*, 1998	Dako, Denmark
MRC5	Human lung fibroblasts	Holliday *et al.*,1972	ECACC, UK

2.3.4 Maintenance of cell lines/ strain

SHSY5Y and MRC5 cells are adherent whilst the 1301 are suspension cells. SHSY5Y and 1301 cell lines were maintained in RPMI 1640 medium, MRC5 in Dulbecco's Modified Eagle's Medium (DMEM). All medium contained 10% (v/v) heat inactivated foetal calf serum (S0275551800/500, Biowest, UK), 1% (w/v) L-glutamine (200 mM) and 1% (w/v) penicillin/ streptomycin. Cells were grown as asynchronous cultures at 37°C in a humidified atmosphere under air containing 5% CO_2. Mycoplasma testing was performed regularly using Mycoplasma Plus^{TM} PCR Primer Set (Stratagene, USA). Cells tested negative throughout.

2.3.5 Cryogenic storage

Exponentially growing adherent cells were trypsinised (unnecessary for suspension cells) and both adherent and suspension cells were centrifuged at 800 g for 5 minutes at room temperature. The supernatant was removed, cells were washed in Dulbecco's phosphate buffered saline (PBS), recentrifuged and the cells resuspended in foetal calf serum (FCS) containing 5% (v/v) dimethyl sulfoxide (DMSO) at a density of $1x10^6$ cells/ ml. DMSO is a cryoprotectant that reduces damage to cell structure by altering the nature of ice formation. 2 ml aliquots of cell suspension were immediately

transferred to cryo-vials and placed in a Nalgene™ Cryo 1°C freezing container filled with isopropanol. They were kept for 24 hours in a -80°C freezer to allow them to freeze slowly, before being stored in liquid nitrogen.

2.3.6 Resuscitation of frozen cells

Cryo-vials were removed from the liquid nitrogen bank and quickly thawed by being placed in a 37°C water bath for 1 to 2 minutes. The thawed cell suspension was then immediately seeded into a 75 cm^2 flask with 30 ml prewarmed medium. After 6 hours for adherent cells the medium was replaced to remove DMSO, cell debris etc. The medium was also replaced for the suspension cells after 6 hours, by centrifugation at 800 g for 5 minutes at room temperature.

2.3.7 Routine cell culture

Adherent cells were always sub-cultured before reaching confluence, unless otherwise indicated. Adherent cells were harvested using trypsin/ EDTA. Initially the culture medium was removed, cells were washed in PBS and 5 ml of trypsin/ EDTA was added which covered the surface of the flask. Cells were exposed to trypsin for 5 minutes or until they had detached from the flask, at 37°C in the tissue culture incubator. Inactivation of the trypsin/ EDTA was achieved by adding an equal volume of culture medium. Cells were counted (Section 2.3.8) and were either reseeded into tissue culture flasks or collected by centrifugation at 800 g for 5 minutes.

Suspension cells were sub-cultured when they were visibly at a high density. Cells were collected and centrifuged at 800 g for 5 minutes, the supernatant removed and cells were resuspended in fresh culture medium. Cells were counted (Section 2.3.8)

and were either reseeded into tissue culture flasks or collected by centrifugation at 800 g for 5 minutes.

2.3.8 Calculation of cell density

Cells were counted using a Fuchs Rosenthal haemocytometer (VWR International, UK) and a standard microscope (DMIL, Leica Microsystems, UK). 20 µl of cell suspension was added to a haemocytometer to which the coverslip had been attached. Three lots of eight squares were counted and averaged. In order to avoid counting a cell twice, the cells touching the upper and right hand perimeter lines were ignored whereas those touching the lower and left hand lines were counted. With the coverslip in place the depth of the chamber is 0.2 mm, hence the volume of eight squares is calculated as followed:

$$\text{Eight squares} = 1\ \text{mm} \times 0.5\ \text{mm} \times 0.2\ \text{mm} = 0.1\ \text{mm}^3 = 0.1\ \mu\text{l}$$

The total number of cells per ml can be calculated from the following equation:

$$\text{Total number of cells per ml} = \text{average of three cell counts} \times 10^4$$

2.3.9 Calculation of population doubling

For the MRC5 mortal cell strain, each time the cells were sub-cultured the population doubling (PD) level was calculated by comparing the amount of cells seeded with the number of cells obtained, using the following equation:

$$PD = \frac{\ln (n2/ n1)}{\ln 2}$$

where n1 was the number of cells seeded and n2 was the number of cells harvested.

2.4 Drug Preparation

2.4.1 Safety procedures

Cisplatin and etoposide were the drugs used throughout the investigations. Both are known human carcinogens and were handled according to the local rules for use of potent carcinogens. All handling of powder or solutions of these drugs were performed in a Trimat^2 class II microbiological safety cabinet (Medical Air Technology, UK).

2.4.2 Cisplatin

Cisplatin was obtained from Sigma-Aldrich Company Ltd, UK. Cisplatin was weighed into ~5 mg aliquots and dissolved in DMSO to give a 100 mM solution. The DMSO solution was immediately diluted in culture medium to give a concentration of 1 mM. This was then further diluted to achieve the concentrations required for use. For drug treatments the final concentration of DMSO was always less than 1% (v/v).

2.4.3 Etoposide

Etoposide was obtained from Sigma-Aldrich Company Ltd, UK. Etoposide was dissolved in methanol to give a final concentration of 17 mM and placed in a Wheaton glass vial (Sigma-Aldrich Company Ltd, UK) which was covered in parafilm and stored at -20°C. Immediately prior to use etoposide stock solution was diluted in medium to the required concentration.

2.5 Sulphorhodamine B (SRB) Growth Inhibition Assay

2.5.1 Introduction

The Sulphorhodamine B (SRB) assay measures cellular protein content of wells of a 96 well cell culture plate (Skenhan *et al.*, 1990). Cells were inoculated into 96 well plates, allowed to attach and then exposed to drugs for the appropriate length of time. The drug was removed and the cells are left to grow for a further 6 days. After fixation the number of cells adhering to each well was measured by staining with the SRB dye. SRB is a bright pink aminoxanthene dye, which contains two sulfonic groups that can bind electrostatically to basic amino acid residues under mildly acidic conditions. Excess dye is removed by washing and bound dye was solublised in order to make reliable measurement of the optical density, which is directly proportional to the number of cells. The drug concentration causing 50% reduction in number of cells present at the end of the growth period was determined (IC_{50}). For the SRB growth inhibition assay it was important that the cells in the control wells remained in active growth throughout the period of culture. Therefore initially, experiments were carried out to determine optimum inoculum densities.

2.5.2 SRB staining procedure

2.5.2.1 Trichloroacetic acid (TCA) fixation

Plates were removed from incubation and fixed by adding 50 µl of ice cold 50% (w/v) trichloroacetic acid (TCA) to each well and incubating for 1 hour at 4°C. Plates were immersed in water five times for washing, to remove TCA and air dried. Plates were stored at 4°C until ready to stain.

2.5.2.2 SRB staining

Plates were removed from 4°C and allowed to come to room temperature. Fixed cells were stained with 100 µl of SRB solution for 30 minutes at room temperature. Following staining, SRB was removed and any unbound dye on the plate was washed of with 1% acetic acid using a plate washer (Dynex Technologies/The Microtiter Company MRWAM60). Any residual solution was removed by flicking the plates over the sink and air drying. The SRB was solublised by adding 100 µl of 10 mM Tris (pH 10.5) per well and gently shaking on a plate shaker (Heidolph Titramax 100) for 10 minutes. Optical density (OD) was measured at 570 nm on a spectrophotometric plate reader (Dynex Technologies Plate Reader MRX Version 2.02).

2.5.3 Establishment of optimal inoculum conditions

Initially cell densities and growth curves are determined for specific cell lines, so that control cells can grow actively for several population doublings after the drug exposure has ended. Cells were inoculated into ten 96 well plates (NUNC, Life Technologies Ltd, Denmark) with a range of the following cell numbers per well in 200 µl of medium: 2000, 1000, 500, 250, 125, 62.5, 31.2, 15.6, 7.8 and 3.8, where there were 6 wells per inoculated density on each plate. To minimise any edge effects the outermost wells of the 96 well plates were not used (Row A and H, columns 1 and 12), though 200 µl of medium was added to test the background levels of the medium. The 96 well plates were incubated at 37°C in the tissue culture incubator. Daily, plates were fixed (Section 2.5.2.1) and stored at 4°C. Once all plates were fixed the 96 well plates were SRB stained and the opticall densities measured (Section 2.5.2.2). Growth curves were plotted.

2.5.4 Determination of IC_{50} values

For growth inhibition studies an optimum inoculum density was chosen from the growth curve results, whereby cells maintained active growth for at least 5 days. The IC_{50} is defined as the concentration of drug required to inhibit cell growth by 50% after the chosen post treatment incubation period. For these experiments a post incubation period of 6 days was used. The IC_{50} concentrations for a 2 hour drug exposure to cisplatin and a 4 hour drug exposure to etoposide were calculated. In six replicate 96 well plates, SHSY5Y cells were plated at a density of 125 cells in 200 µl of medium per well. The outermost wells of the 96 well plates were not used (Row A and H, columns 1 and 12) though 200 µl of medium was added to each. A day later cells were treated with a range of drug concentrations for either 2 hours (cisplatin) or 4 hours (etoposide). Control cells were treated with medium containing 1% DMSO. Following exposure to the drugs, the medium was removed and wells were washed three times with fresh medium to remove the drug. After final addition of 200 µl of medium to each well, the plates were incubated for 6 days. After 6 days the cells were fixed and stained (Section 2.5.2). The mean absorbance of the wells, for each drug concentration was then expressed as a percentage of the mean absorbance from the control (untreated cells).

2.6 DNA Extraction

2.6.1 Materials

DNA was extracted from cells using "Blood and Cell Culture DNA Midi Kits" (Qiagen, UK), with reagent solutions supplied with the kits (Section 2.2). This procedure yielded high molecular weight DNA of a high purity.

2.6.2 Method

Up to $2x10^7$ cells were centrifuged at 800 g for 5 minutes, washed in PBS and resuspended in PBS to a final concentration of 10^7 cells per ml. 2 ml of ice cold Buffer C1 (lysis buffer that stabilises and preserves the nuclei) and 6 ml of ice cold distilled water was added to the cell suspension. The tube was mixed by inverting and was incubated for 10 minutes on ice. The lysed cells were centrifuged at 4°C for 15 minutes at 1300 g and the supernatant discarded. 1 ml of ice cold Buffer C1 was added with 3 ml of ice cold distilled water and the pelleted nuclei were resuspended by vortexing. The nuclei were centrifuged again at 4°C for 15 minutes at 1300 g and the supernatant discarded. 5 ml of Buffer G2 (digestion buffer) was added and the nuclei resuspended by vortexing for 30 seconds at maximum speed. 95 µl of proteinase K was added and cells were incubated for 1 hour at 50°C. A Qiagen genomic tip 100/g was equilibrated with 4 ml of Buffer QBT (equilibration buffer). After digestion, samples were vortexed and applied to the genomic tip, where it passed through by gravity flow (Figure 2.1).

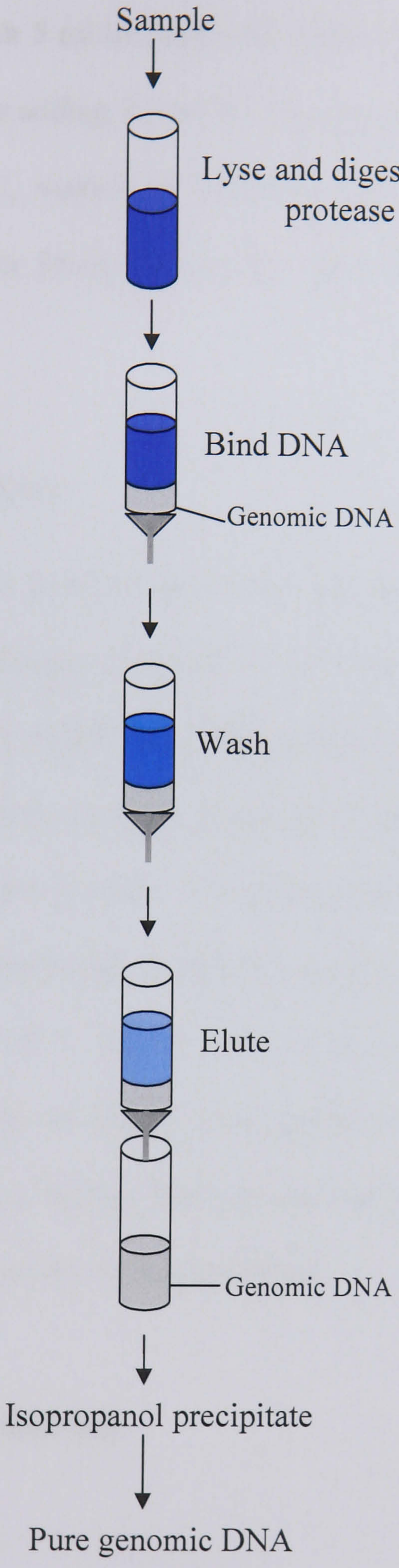

Figure 2.1 DNA extraction using Qiagen columns. Pure genomic DNA is isolated from cell pellets.

The genomic tip was washed three times with 7.5 ml of Buffer QC (wash buffer) and the DNA was eluted with 5 ml of Buffer QF (elution buffer) into a fresh tube. The DNA was precipitated by adding 3.5 ml of isopropanol, centrifuged at >5000 g for at least 15 minutes at 4°C, washed in 70% ice cold ethanol, vortexed briefly and centrifuged at >5000 g for 10 minutes at 4°C. DNA was dissolved in an appropriate volume of TE buffer.

2.6.3 Concentration of DNA

The concentration and the purity of the DNA were determined by the absorbance of UV light in a spectrophotometer (Unicam UV/VIS, Spectronic Analytical Instruments, UK). DNA was diluted in sterile water. Both protein and DNA absorb UV light but they have different absorbance spectra. The peak of light absorption is at 260 nm for DNA and at 280 nm for protein. The optical density was measured at both wavelengths. The concentration of the DNA was calculated from the absorbance at 260 nm (an absorbance of 1 OD at 260 nm in a 10 mm path length cuvette corresponds to 50 μg/ ml of DNA). The purity of the DNA was checked by determining the ratio OD_{260}/ OD_{280}. The ratio of pure DNA should be $\geq$ 1.8 and this value was typically observed for the isolated DNA.

2.7 Telomeric DNA Isolation

2.7.1 Introduction

Telomeres are composed of repeat sequences in which the strand with its 3' end at the terminus is G rich and forms a single stranded G-rich overhang. Wright and colleagues developed a technique for purifying human telomeres (Wright *et al.*, 1997). This procedure to purify human telomeres was based on the ability of biotinylated

oligonucleotides complementary to the G-rich telomeric repeat to anneal to the G rich overhang in otherwise double stranded DNA (Shay *et al.*, 1994).

Following annealing, DNA/ oligonucleotide complexes were bound to streptavidin coated magnetic beads and washed (Figure 2.2). Purified telomeres were eluted and analysed on pulsed field agarose gels.

2.7.2 Hinf1 restriction digestion of genomic DNA

Extracted double stranded genomic DNA (Section 2.6) was restriction digested to completion for 6 hours in 150 µl of Hinf1 (20- 40 units; Roche), H buffer (Boehringer) and water at 37°C in a block thermostat (BI 100, Kleinfield, Labortechnik, Germany). Hinf1 recognizes the sequence G/ANTC and generates fragments with 5' cohesive termini. DNA samples were then ethanol precipitated by the addition of 1/ 10 sodium acetate (3 M) and three times the volume of 100% ethanol. This ethanol precipitation solution was placed in -20°C freezer for 2 hours.

2.7.3 Mixing of biotinylated oligonucleotides and DNA

The precipitated DNA was pelleted by centrifugation and dissolved in 1x SSC/ 1% Triton X-100. The dissolved DNA was mixed with 5' biotinylated oligonucleotide (MWG) with the sequence $(CCCTAA)_6$ and annealed for 15 minutes each at 65°C, 55°C, 45°C, 35°C and 20°C. It was then combined with streptavidin coated magnetic beads (Dynal Inc, Norway) that had been preincubated for at least 1 hour in 5x Denhardts solution. The DNA bead suspension was rotated end over end at 4°C overnight.

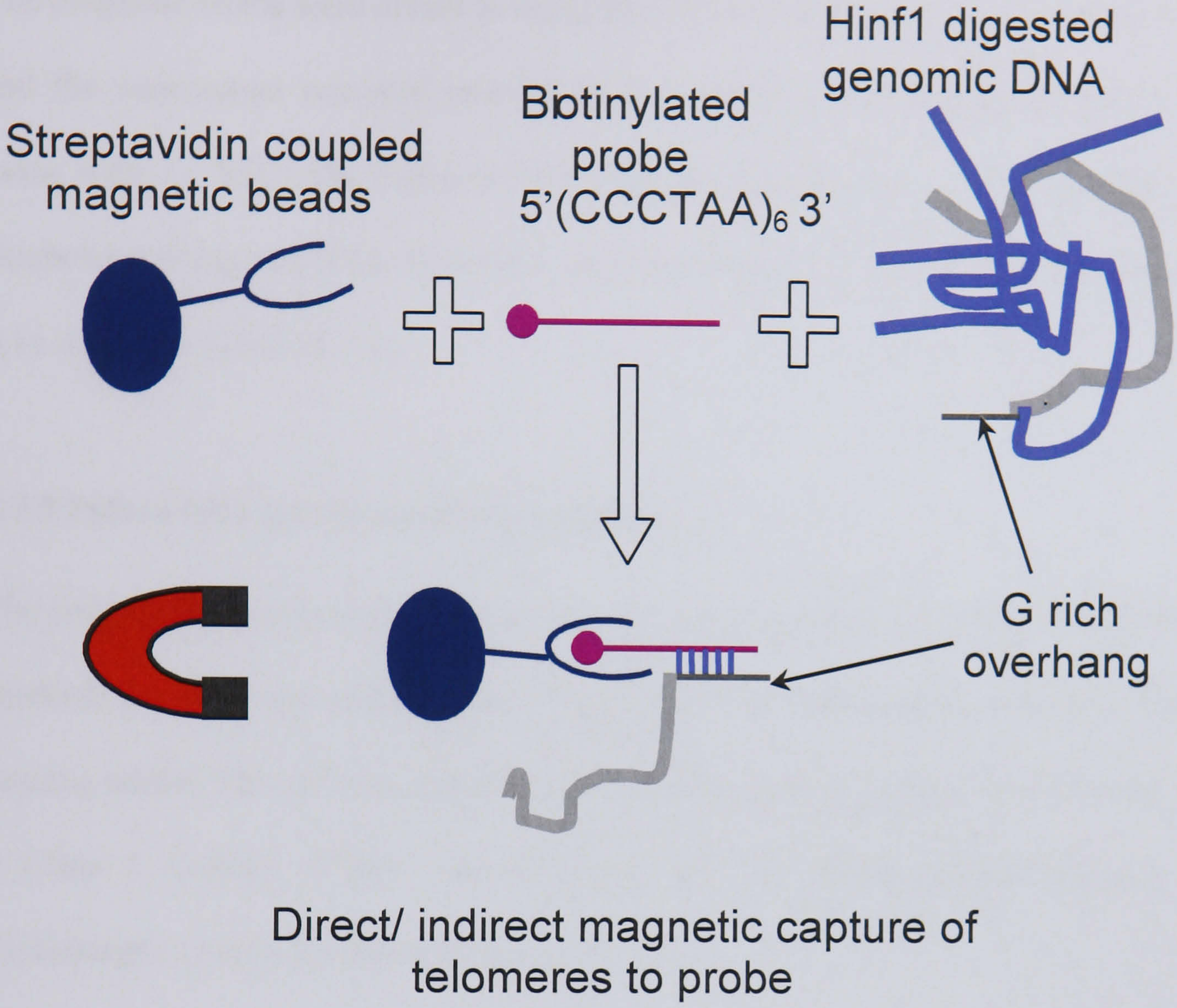

Figure 2.2 Isolation of telomeric DNA. This procedure uses a magnetic bead approach to purify telomeric DNA from the rest of the genomic DNA.

2.7.4 Elution of telomeres

The magnetic beads were drawn to the sides of a tube using a magnet (Systems 1000) and the supernatant removed and saved. The beads were resuspended and washed twice with 1x SSC/ 1% Triton X-100. The bound telomeres were eluted from the beads by melting the oligonucleotide/ telomere interaction at 65°C for 10 minutes in 0.1x SSC/ 1% Triton X-100.

2.7.5 Pulsed field gel electrophoresis (PFGE)

The isolated telomeres and supernatant were size separated by PFGE (CHEF-DRIII, BioRad) for 17 hours at 3.5 V in a 1% pulsed field agarose gel with 0.5x TBE as running buffer. The gel was stained for 30 minutes in 0.5 μg ethidium bromide/ ml in a Class I Cabinet (Clean Air Limited, UK) and photographed using a UV Alphaimager (Alpha Innotech Corporation, UK).

2.7.6 Southern blotting

Following staining with ethidium bromide, the gel DNA was partially depurinated in depurination buffer for 30 minutes, denatured in denaturation buffer for 1 hour and neutralised for 60 minutes in neutralisation buffer. The DNA was then transferred from the gel onto a Hybond N+ membrane by vacuum blotting for 90 minutes at 200 mbar (Vacum blotter Model 785, BioRad) in 10x SSC transfer buffer. The membrane was then rinsed in 1x SSC and the DNA was cross-linked to the membrane by exposing it to UV light on a transilluminator for 5 minutes.

2.7.7 Membrane hybridisation

2.7.7.1 Using an alkaline phosphatase labelled probe

The amino modified oligonucleotide $(TTAGGG)_4$ was conjugated to alkaline phosphatase using the LIGHSMITH Luminescence Engineering System for Oligonucleotides (Promega, UK). Briefly the amino modified oligonucleotide was activated and purified using a G-50 column. The activated oligonucleotide was then conjugated to alkaline phosphatase and purified with a S-100 column. The AP telomeric probe was stored in 50% glycerol at -20°C.

The hybridisation steps took place in glass tubes in a hybridisation oven (Hybridize HB-1000, Camlab, UK). The membrane was preincubated in Quantum Yield Blocking Solution (Promega, UK) for 1 hour at 50°C then removed. The $(TTAGGG)_4$ probe conjugated to alkaline phosphatase was diluted 1:1000 in low stringency hybridisation solution and hybridised for 1 hour at 50°C. The membrane was then washed 2 x 10 minutes in 1 x SSC/ 0.1% SDS at 50°C and this was repeated at 20° C. The SDS was removed by an additional wash in 1x SSC. The membrane was next incubated for 5 minutes in 200 µl diethanolamine solution and the chemiluminescent substrate (CSPD) (Tropix Inc, Massachusetts, USA) was diluted 1:100 in fresh diethanolamine solution and added to start the chemiluminescence reaction. The membrane was covered with clear film and exposed to Hyperfilm ECL (Amersham/ Pharmacia) at 37°C for 90 minutes. Alternatively the membrane was on occasion scanned using a Fuji Film Luminiscent Image Analyzer LAS 1000- Pro (Raytek, UK).

2.7.7.2 Using a digoxigenin labelled probe

Digoxygenin is a ligand that can be incorporated into DNA and detected after hybridisation with an anti- digoxgenin antibody enzyme conjugate. This procedure

used the "TeloTAGGG Telomere Length Assay" kit (Roche, UK) and hybridisation took place according to the manual. All reagents were provided in the kit. Briefly the membrane was prehybridised for 30 minutes at 42°C in Easy-Hyb solution in the hybridising oven (Hybridize HB-1000, Camlab, UK). Following this the dig labelled probe was diluted 1:1000 in fresh Easy-Hyb solution and left for 1 hour at 42°C. The membrane was removed and washed as follows:

2 x 5 minutes in 2 x SSC/ 0.1% SDS at 20°C
2 x 15 minutes in 0.2 x SSC/ 0.1% SDS at 50°C
1 x 5 minutes in washing buffer at 20°C

The membrane was then placed in blocking solution for 30 minutes at 20°C. This was poured off and the anti- digoxigenin antibody diluted 1:1000 in fresh blocking solution was added for 30 minutes at 20°C. The membrane was next washed four times for 10 minutes in washing buffer at 20°C and soaked in detection buffer for 5 minutes. The CSPD was diluted 1:100 in detection buffer and placed onto the membrane for 5 minutes without shaking. Excess liquid was drained and sandwiched between clear film and exposed at 37°C for 90 minutes on a Hyperfilm ECL.

2.8 Inductively Coupled Plasma-Mass Spectrometry (ICP-MS)

2.8.1 Equipment

ICP-MS Perkin Elmer Sciex Elan 6000 (Figure 2.3)
Department of Earth Sciences, Durham University

2.8.2 Introduction

Inductively coupled plasma- mass spectrometry was used to detect platinum (Pt) bound to DNA and phosphorus (P) levels as an indicator of DNA concentration, with high sensitivity. The inductively coupled plasma is an argon plasma maintained by the

interaction of a radio frequency (RF) power supply (generally 1150 W) and ionised argon gas. Power is transferred into the plasma gas by inductive heating. The argon gas passes continuously through the plasma torch which is located in a 2 or 3 turn induction coil carrying a very high frequency alternating current. Samples are nebulised and injected into the plasma. Singly charged ions are formed from the elemental species within a sample and are directed towards the quadropole mass spectrometer. The mass spectrometer separates the ions introduced from the ICP according to their mass to charge ratio (Thompson and Walsh, 1983). Ions of selected mass/ charge ratio are then directed to a detector which quantifies the number of ions present. Pt is naturally present as four main isotopes 194 Pt (32.97% abundance), 195 Pt (33.83% abundance), 196 Pt (25.24% abundance) and 198 Pt (7.18% abundance).

2.8.3 Preparation of DNA samples

DNA was extracted as in Section 2.6 with the following modifications. After cell resuspension in buffer G2, cells were sonicated for 2 minutes using a Vibracell™ ultrasonic processor equipped with a cup-horn (Roth Scientific, UK). 10 µl of RNase A (Qiagen, UK) was then added and left to stand at room temperature for 15 minutes before 95 µl of proteinase K addition and incubation for 1 hour at 50°C. Telomeric DNA was isolated as in Section 2.7.

2.8.4 Method

The Perkin Elmer Sciex Elan 6000 ICP-MS uses a standard cross flow nebuliser and Scott type double pass spray chamber. Nebuliser gas flow rates varied between 0.8 to 1.0 l/ minute and were optimised to keep the production of CeO^+ less than or equal to 3% of the total Ce^+ signal. All test samples were diluted into 1 ml of 3.5% (w/v) nitric

acid and incubated overnight (70°C) to hydrolyse the DNA so that the precipitated DNA is dissolved. Phosphorus levels and the four isotopes of platinum (Pt) were monitored (194, 195, 196 and 198) to evaluate possible isobaric interferences. Standard solutions of 50, 100, 200, 500 and 1000 parts per billion (PPB) of phosphorus and standard solutions of 0, 100, 500, 1000 and 2000 parts per trillion (PPT) of Pt were run at the beginning of the analytical session, during and at the end to check for instrumental drift. Platinum standard solutions were made from Johnson Matthey 1000 parts per million (PPM) stock solutions. Test samples were introduced manually into the ICP-MS and were ideally meant to give signals within the calibration range of the standard solutions.

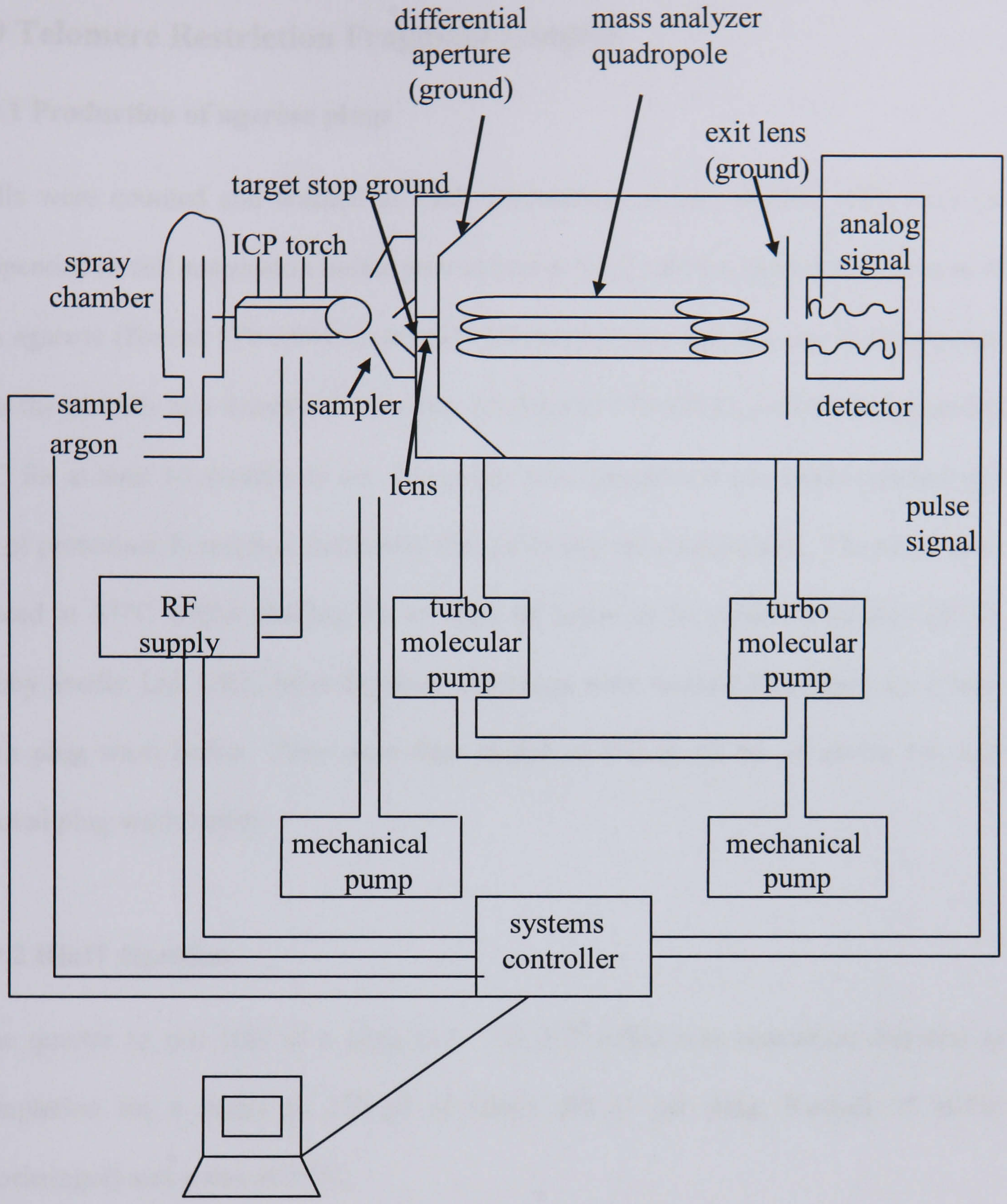

Figure 2.3 Inductively Coupled Plasma-Mass Spectrometry (ICP-MS). A schematic diagram of the quadropole Perkin Elmer Sciex Elan 6000 ICP-MS (Montaser, 1998).

2.9 Telomere Restriction Fragment Lengths

2.9.1 Production of agarose plugs

Cells were counted and washed in PBS. Depending on the amount, cells were re-suspended in cell suspension buffer prewarmed at 50°C and the appropriate amount of 2% agarose (Biorad 170-3594 Clean-cut). The suspension was then carefully pipetted into the moulds, at a density of 10^7 cells/ ml (Biorad 170-3713), which were placed at 4°C for at least 10 minutes to set. The plugs were transferred into tubes containing 5 ml of proteinase K reaction buffer and 250 µl 20 mg/ ml proteinase K. The tubes were placed at 37°C whilst shaking for at least 48 hours in an orbital incubator (S150, Bibby Sterlin Ltd, UK). After digestion the plugs were washed four times for 1 hour with plug wash buffer. They were then stored at 4°C in 50 ml of sterile 10- fold diluted plug wash buffer.

2.9.2 Hinf1 digestion

One quarter to one half of a plug (2.5- 5.0 $x10^5$ cells) was restriction digested to completion for 6 hours in 150 µl of Hinf1 (60 U per plug; Roche), H buffer (Boehringer) and water at 37°C.

2.9.3 Pulsed field gel electrophoresis

Restricted plugs were analysed in a 1% agarose gel (Ultrapure DNA grade agarose, Biorad) with marker, by pulsed field gel electrophoresis (CHEF-DRIII, Biorad) at 3.0 V/cm for SHSY5Y cells and 5.5 V/cm for 1301 cells for 17 hours with a switching time of 2 to 10 in 0.5x TBE. For the SHSY5Y cells the Hind III bacteriophage Lambda marker was used. The bacteriophage Lambda DNA is fragmented in a restriction digestion with Hind III endonuclease. The digestion reaction results in 8

double stranded DNA fragments at 23.1, 9.4, 6.6, 4.4, 2.3, 2.0, 0.6 and 0.1 kbp. Only 7 bands are visible on the gel due to small size of the 0.1 kbp fragment. For the 1301 cells the 0.1- 200 kbp pulse marker (Sigma Aldrich, UK) was used. This marker contains a mixture of 12 fragments consisting of Lambda DNA Hind III fragments plus uncut Lambda DNA and Lambda DNA concatemers. Its fragment sizes are 194, 145.5, 97, 48.5, 23.1, 9.4, 6.6, 4.4, 2.3, 2.0, 0.6 and 0.1 kbp.

2.9.4 Hybridisation

2.9.4.1 Preparation of 32P-γ-ATP labelled oligonucleotide probes

The following mix was prepared:

33 µl water

5 µl 10 x polynucleotide kinase (PNK) buffer (New England Labs Inc, USA)

1 µl oligonucleotide

1 µl T4 PNK

Total: 40 µl

10 µl (= 100 µCi/ 3.7 MBq) of 32P (~185TBq/ mmol; ~6000 Ci/ mmol) (Amersham Bioscience) was added and incubated for 1 hour at 37°C, then for a further 15 minutes at 70°C to inactivate the kinase. Eppendorfs were briefly centrifuged and a Microspin G column (Amersham Bioscience) was prepared by 1 minute centrifugation at 0.8 g. The probe preparation was passed through the column by 2 minutes centrifugation at 0.8 g and the elute added to 10 ml Rapid Hyb buffer (Amersham Bioscience).

2.9.4.2 Hybridisation of dried gels

Gels were dried at room temperature for 2 hours (Model 583 gel drier, Biorad), stained with ethidium bromide (0.5 µg/ ml) for 30 minutes in a Class I Cabinet (Clean Air Limited, UK) and photographed using a UV Alphaimager (Alpha Innotech Corporation, UK). Gels were denatured (denaturation buffer) for 30 minutes,

neutralised (neutralisation buffer) for 30 minutes and in-gel hybridised with 32P-γ-ATP $(CCCTAA)_4$ at 43°C for 16 hours. Gels were washed four times in 0.2x SSC at 43°C for 30 minutes each and then exposed to a phosphoimager screen overnight. Signals were visualised using a phosphoimager (Storm 820, Molecular Dynamics, Amersham).

2.9.4.3 Hybridisation of membranes

Gels were southern blotted to Hybond-N+ membranes by vacuum blotting at 200 mbar (Vacum blotter Model 785, BioRad) in 10x SSC transfer buffer. The membrane was then rinsed in 1x SSC and the DNA was cross-linked to the membrane by exposing it to UV light on a transilluminator for 5 minutes. The membrane was hybridised with 32P-γ-ATP $(CCCTAA)_4$ at 43°C for 16 hours. Blots were washed four times in 0.2x SSC/ 0.1% SDS at 43°C for 30 minutes each and then exposed to a phosphoimager screen overnight. Signals were visualised using a phosphoimager (Storm 820, Molecular Dynamics, Amersham).

2.9.5 Evaluation of telomere length by fragment size determination

The images after hybridisation and the UV gel pictures with the molecular weight markers on them were cropped and adjusted to the same size using Photoshop, Adobe software. The marker lanes were overlayed onto the telomere restriction fragment length image. The merged image could then be used to evaluate fragment size with AIDA densitometry software (Raytek, Sheffield, UK). The AIDA program was used in the 1D evaluation mode. Lanes were defined starting with the marker lanes. The peaks of all marker lanes were assigned to the Lambda phage Hind III DNA marker. For each telomere fragment profile a baseline and a peak position by centre was

determined enabling the program to calculate the average fragment length per lane as weighted mean of the optical density.

2.9.6 Minisatellite probing

To test for non-specific degradation of DNA, gels or membranes were rehybridised with the minisatellite probe $(CAC)_8$. The probe was made as in section 2.9.4.1 with the only modification in using the $(CAC)_8$ oligonucleotide instead of the telomeric sequence. To strip the gels of radioactivity dried gels were denatured (denaturation buffer) for 30 minutes, neutralised (neutralisation buffer) for 30 minutes. To strip the membranes of radioactivity 1 ml of 20% SDS was boiled in 100 ml of water and poured onto the membrane and left for 10 minutes. The SDS was removed from the blot by washing three times in 1x SSC. Dried gels or membranes were hybridised with 32P-γ-ATP $(CAC)_8$ at 43°C for 16 hours and washed and screened as in sections 2.9.4.2 and 2.9.4.3 respectively.

2.10 Telomeric Single Stranded Overhangs

The length of single-stranded terminal overhangs in telomeres was measured by in-gel hybridisation of telomeric probes onto non-denatured DNA. As in Section 2.9, treated cells were embedded in 0.65% low melting agarose plugs at a density of 10^7 cells/ ml before treatment with proteinase K. DNA was completely digested by Hinf1 (60 U per plug; Roche) at 37°C (Section 2.9.2). Plugs were analysed in a 1% agarose gel by pulsed field gel electrophoresis (Biorad) at 3 V/ cm for 17 hours with a switching time of 2 to 10 in 0.5 x TBE. In-gel hybridisation with 32P-γ-ATP $(CCCTAA)_4$ was performed on non denatured gels at 37°C for 16 hours. Gels were washed four times in 0.2 x SSC at 37°C for 30 minutes each and then exposed to a phosphoimager

screen overnight. Signals were visualised using a phosphoimager (Storm 820, Molecular Dynamics, Amersham). Under these conditions, only single-stranded G-rich DNA is available as target for hybridisation. The gel is then denatured (denaturation buffer) for 30 minutes, neutralised (neutralisation buffer) for a further 30 minutes and in-gel hybridised with 32P-γ-ATP $(CCCTAA)_4$ at 43°C to allow detection of the total telomeric signal. To assess overhang length, the ratio of the relative hybridisation signal intensity of overhangs alone/ whole telomeres were evaluated using AIDA densitometry software (Raytek, Sheffield, UK).

2.11 G Rich Strand Telomeric DNA Damage

Agarose plugs DNA were digested overnight at 37°C with Hinf1 as described in 2.9.2. Digested DNA was pre-incubated for 2 hours in alkaline buffer and then electrophoresed at 26 V for 20 hours for SHSY5Y cells and 40 V for 24 hours for 1301 cells in 0.7% agarose in alkaline buffer. Gels were then neutralised (neutralisation buffer) for 1 hour and dried at room temperature. Gels were hybridised (Section 2.9.4.1) with 32P-γ-ATP $(CCCTAA)_4$ at 43°C for 16 hours and washed four times in 0.2 x SSC at 43°C for 30 minutes each. They were then exposed to a phosphoimager screen overnight. Signals were visualised using a phosphoimager (Storm 820, Molecular Dynamics, Amersham).

2.12 Telomerase Activity

2.12.1 Introduction

Telomerase activity was determined by the TeloTAGGG Telomerase PCR Elisa (TRAP assay, Roche Applied Science, Germany) kit which uses an extension of the original method described by Kim and colleagues (Kim *et al.*, 1994). All reagents were supplied with the kit and composition of reagents was not specified. The assay works (Figure 2.4) by initially telomerase adding telomeric repeats (TTAGGG) to the 3' end of the biotinylated primer (P1- TS primer). Then the extended products were amplified by PCR using the P1-TS and reverse primers generating PCR products with the telomerase specific 6 nucleotide additions. An aliquot of the PCR product was denatured and hybridised to a digoxigenin telomeric specific repeat probe. The resulting product was immobilised via the biotin labelled primer to a streptavidin coated microtiter plate. The immobilised PCR product was then detected with an antibody against digoxigenin that was conjugated to peroxidase. Finally the probe was quantified by determination of peroxidase activity using a chromogenic substrate.

2.12.2 Lysis

Cells were harvested, counted and 1 million cells pelleted and lysed with 200 µl of lysis buffer. The cells were left on ice for 30 minutes and centrifuged at 14000 rpm for 30 minutes at 4°C. The supernatant was aliquoted into fresh tubes and frozen at -80°C until required.

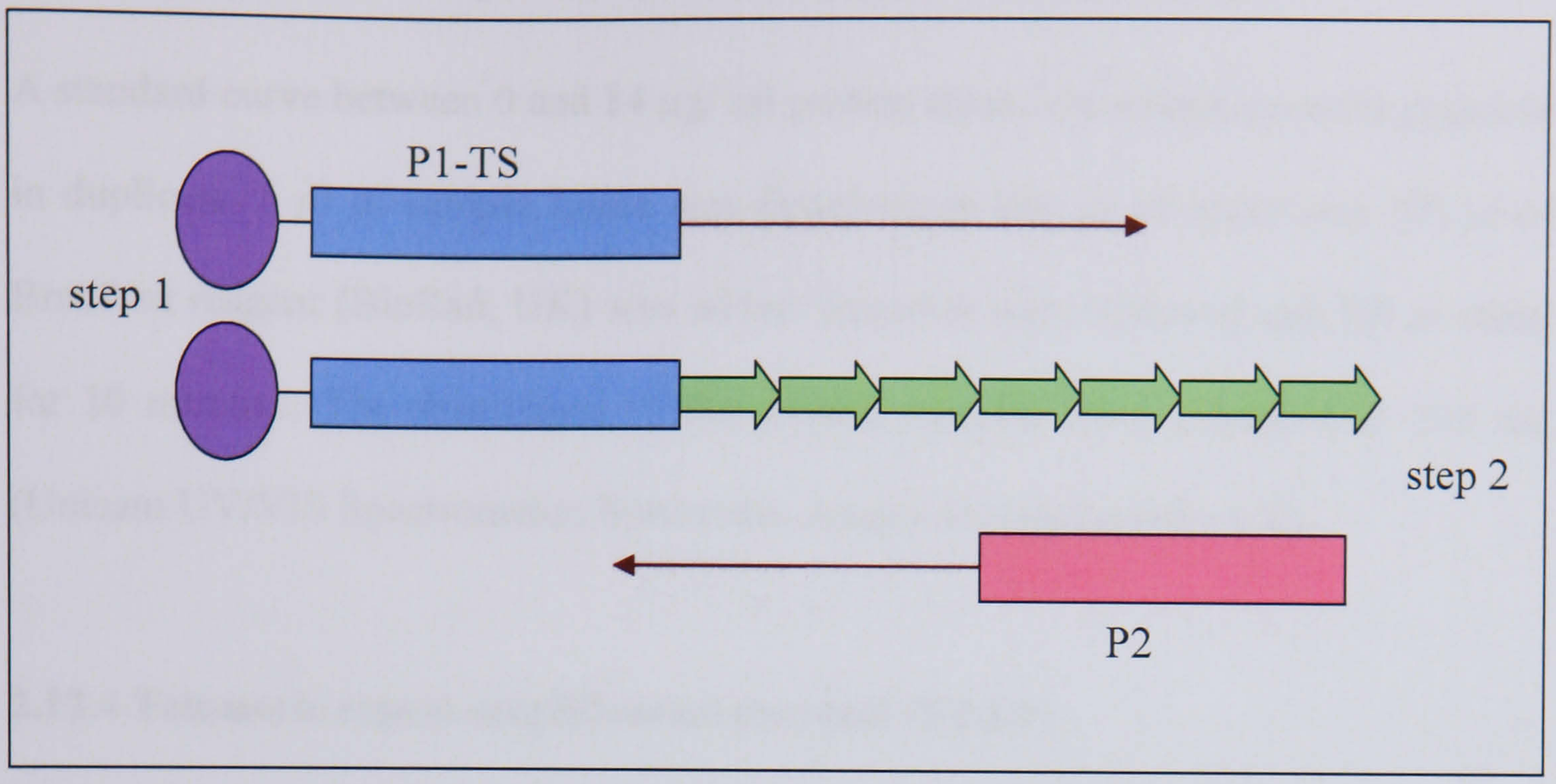

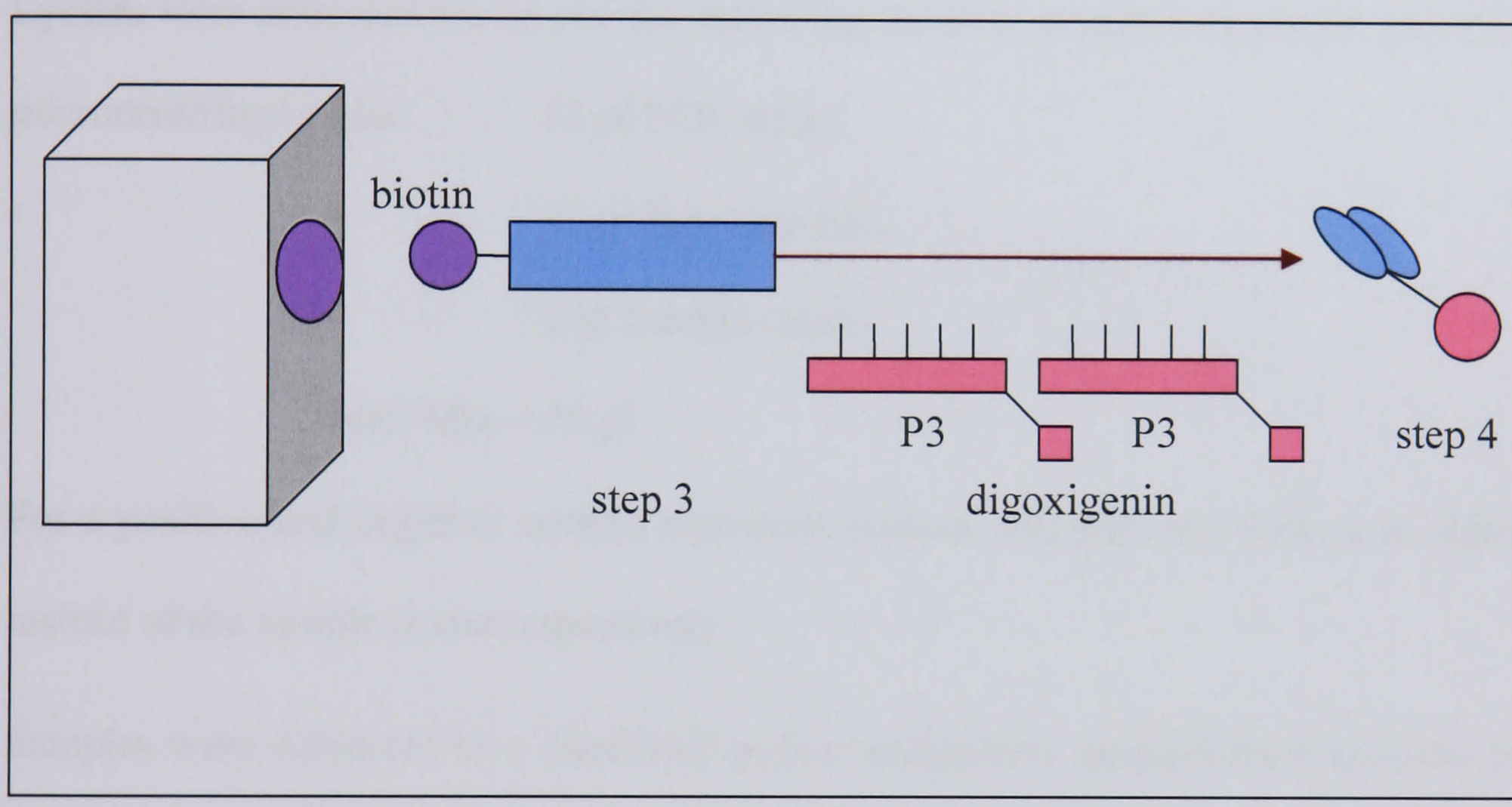

Figure 2.4 TeloTAGGG Telomerase PCR Elisa. Step 1: telomerase adds telomeric repeats to the P1-TS primer. Step 2: the elongation products are amplified by PCR. Step 3: the PCR product is denatured and hybridised to telomere repeat detection probe. Step 4: a coloured reaction product is formed.

2.12.3 Determination of protein concentration by Bradford assay

A standard curve between 0 and 14 µg/ ml protein stock concentrations were prepared in duplicate. 5 µl of sample lysate was dissolved in 800 µl of water and 200 µl of Bradford reagent (BioRad, UK) was added. Samples were vortexed and left to stand for 10 minutes. The absorbance of the protein samples were measured at 595 nm (Unicam UV/VIS Spectrometer, Spectronic Analytical Instruments, UK).

2.12.4 Telomeric repeat amplification protocol (TRAP)

Lysates were defrosted on ice and the following for each sample was placed into PCR microcentrifuge tubes:

23 µl PCR water,

25 µl Reaction mix,

2 µl Sample lysate

Total Mix = 50 µl

For a positive and negative control a positive tumour cell line and water was added instead of the sample lysate respectively.

Samples were subjected to a combined primer elongation/ amplification reaction by the following protocol in Table 2.2.

Table 2.2 Telomeric repeat amplification PCR procedure

Step	Time	Temperature	Steps/Cycles
1. Primer Elongation	10-30 min	25°C	Step 1
2. Telomerase Inactivation	5 min	94°C	Step 2
3. Amplification			
denaturation	30s	94°C	
annealing	30s	50°C	Cycles 1-30
polymerisation	90s	72°C	
	10 min	72°C	Step 3
4. Hold		4°C	Step 4

2.12.5 Hybridisation & ELISA

5 µl of the amplification product was added to 20 µl of denaturation reagent and incubated for 10 minutes at room temperature. 225 µl of hybridisation buffer was added to each sample and mixed by vortexing briefly. 100 µl of the mixture was added to a well of a 96 well plate that had been precoated with streptavidin (supplied with the kit). Wells were covered with self adhesive foil to prevent evaporation and the plate incubated on an orbital shaker (Janke & Kunkel Gmbh & Co, Germany) at 300 rpm for 2 hours. The hybridisation solution was removed completely and wells were washed three times with 250 µl of washing buffer for a minimum of 30 seconds each. 100 µl of a solution of peroxidase conjugated anti- digoxigenin antibody (a polyclonal antibody from sheep) was added per well. The plate was covered and incubated at room temperature for 30 minutes, shaking at 300 rpm. The solution was removed and washed five times for a minimum of 30 seconds each with washing buffer. 100 µl of TMB substrate (solution containing the peroxidase substrate 3,3',5,5' tetramethyl benzidine) was added to each well and incubated for colour development at room temperature for 10- 20 minutes whilst shaking at 300 rpm. 100 µl of stop reagent was added to the reacted substrate to stop colour development (blue to yellow) and absorbance of the samples were measured at 450 nm (reference wavelength of 690 nm) on a microtiter plate reader (Thermo Labsystems Multiscan EX, Model 355, UK) within 30 minutes of the addition of the stop reagent.

2.13 Flow Cytometry

2.13.1 Equipment

Partec Pas flow cytometer (Partec GmbH, Munster, Germany) (Figure 2.5)

Data handling was performed using FlowMax instrument software (Partec GmbH, Munster, Germany)

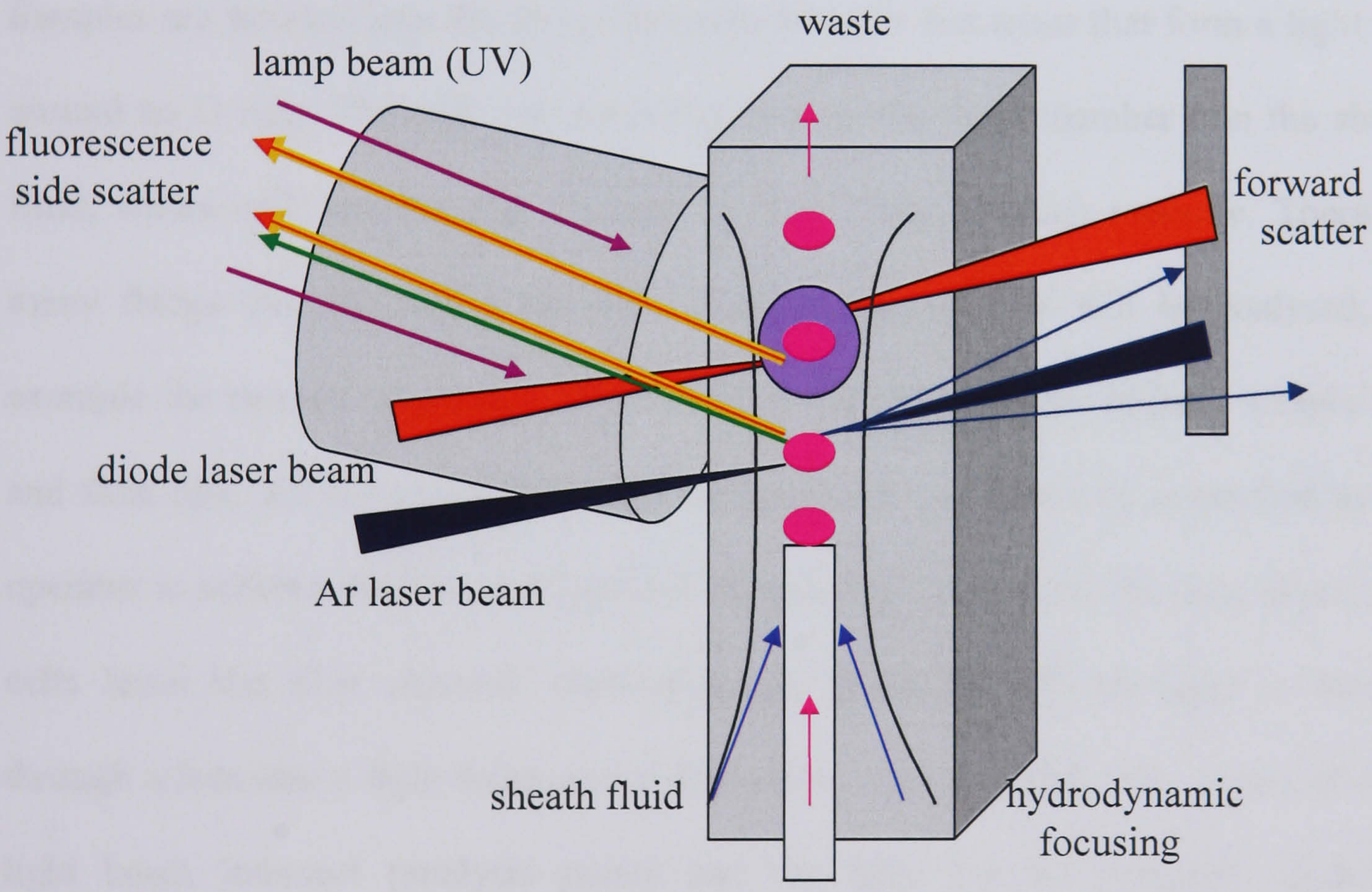

Figure 2.5 Principle of the Partec Particle Analysing System (PAS). A schematic diagram of the Partec Pas flow cytometer (Partec Pas web page).

2.13.2 Introduction

Flow cytometry detects for individual cells, light that has been scattered or emitted via fluorescence activation. The method can be used in numerous applications such as identifying cells labelled with fluorescent antibodies or size through light scatter.

There are key components of all flow cytometers;

1. A light or excitation source e.g. laser that emits light at a particular wavelength

2. A liquid flow that moves the suspended cells through the instrument, past the laser

3. A detector for detecting the brief flashes of light coming from the particles as they pass through the light beam

Samples are injected into the flow cytometer in small test tubes that form a tight seal around an O ring. The cells are pushed up and in the flow chamber join the sheath fluid, where cells are directed through the laser beam through pressure. There are many things that can affect the way in which the samples will be analysed, for example the amount of pressure driving the sample through the system, sample size and flow rate. All the parameters must be optimised and manually controlled by the operator to achieve the precise alignment of cells one at a time in the laser beam. The cells leave the flow chamber (hydrodynamic focusing) and the light is focused through a lens into a light beam as it approaches a liquid stream. The stream and the light beam intersect (analysis point) and the light can be reflected, absorbed, diffracted and/ or refracted to give the signal (Givan *et al.*, 2001). Photodetectors that vary in position, colour filters etc convert the light signal into an electrical impulse. Fluorescence based detection depends on the absorption of light by the cell and the reemission of this light at different frequencies. Filters block the original light source from reaching the detector, while the fluorescence emission is allowed through for

detection (Ormerod, 2000). Cells can be labelled with a fluorescent marker, which fluoresce only when light of the appropriate wavelength hits them. There are different spectral regions available to detect multicolour fluorescence in parallel, for example FL-1 is green, FL-2 is orange and FL-3 and red.

2.13.3 Setting up the flow cytometer

The precision and balance was checked using Partec 3 μM calibration beads (Partec Cat Code~05-4007) checking FSC/ SSC dotplots and FL-1, FL-2, FL-3 histograms and/ or dotplots for a narrow range signal (Figure 2.6). If the signal was wider than desired, the 3D position of the cuvette relative to the laser was adjusted using microscewdrivers. For cleaning and stabilising 2 ml of 1% Triton X 100 (dissolved in water), followed by 2 ml of PBS and 2 ml of water was passed through. 1x PBS was used as sheath fluid for the Partec Pas.

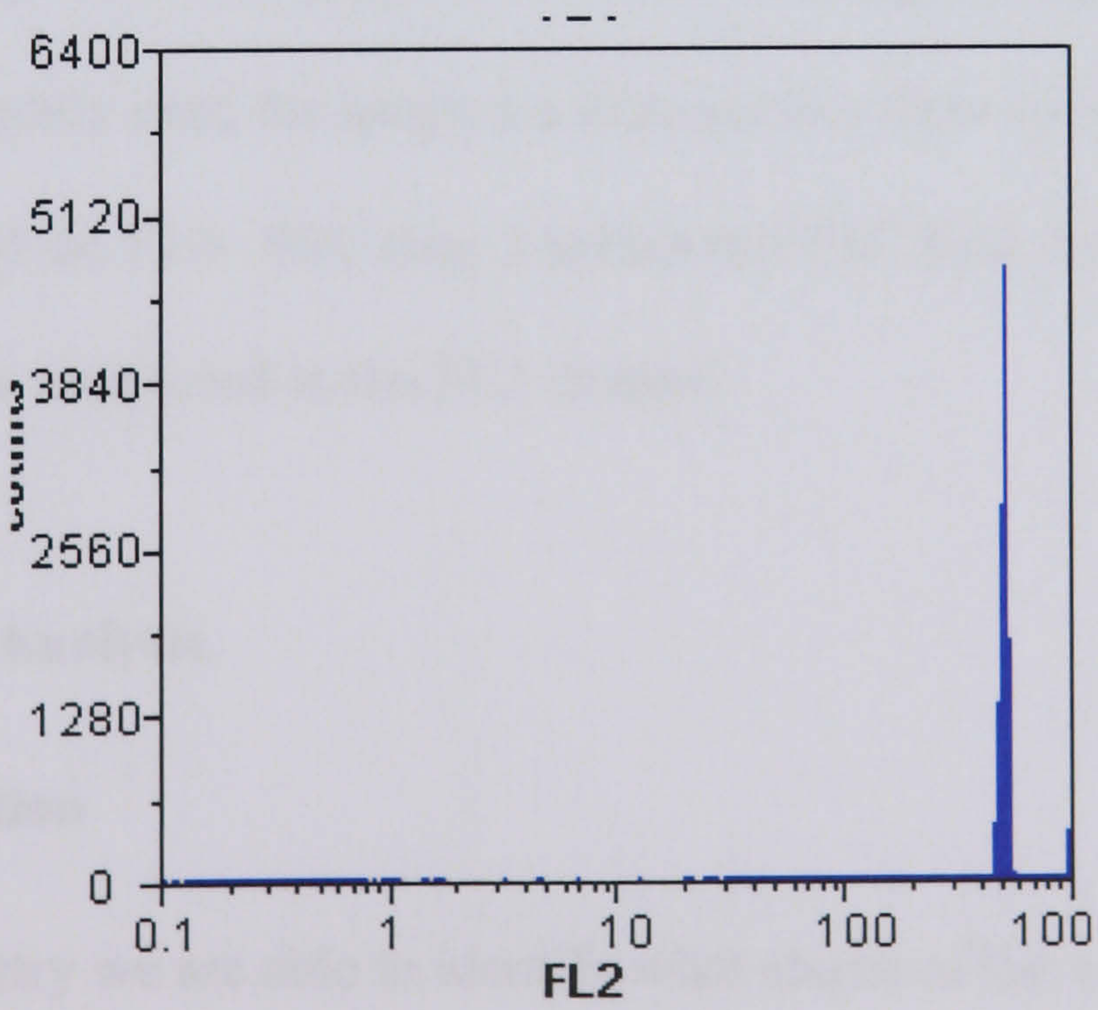

Figure 2.6 Calibration pasbeads. FL-2 histogram of the calibration beads showing a narrow signal range.

2.13.4 Measuring Apoptosis

2.13.4.1 Introduction

The pattern of light scattered is dependent on cell size (Forward Scatter; FSC), shape and internal structure (Light Scattered Sideways; SSC) giving relative measures of these cellular characteristics as cells flow through the beam. Apoptosis was assessed as the fraction of small, granular apoptotic cells that are distinguishable from viable cells by their lower forward and higher sideward light scatter (Sgonc and Gruber, 1998).

2.13.4.2 Method

After appropriate treatment non adherent and adherent cells were collected in RPMI plus 10% FCS, counted using a haemocytometer (Section 2.3.8) and stained with 10 µg/ ml propidium iodide for 15 minutes at 4°C to determine the number of cells with intact plasma membrane. Propidium iodide binds to double stranded DNA, but can only cross the plasma membrane of non viable cells, therefore cells that have lost membrane integrity show red propidium iodide staining throughout the nuclei. The cells were immediately used for apoptosis analysis in a flow cytometer. For apoptosis cells were analysed on FL4- SSC (log 3 scale) and FSC (log 4 scale) and propidium iodide staining was monitored in the FL2 channel.

2.13.5 Cell Cycle Analysis

2.13.5.1 Introduction

Using flow cytometry we are able to identify what stages of the cell cycle the cells are in after drug treatments by analysing the DNA content. This is due to the fact that the amount of DNA in the nucleus of a cell changes through the cell cycle from one copy

(n) to two (2n) during DNA replication. Cells in G_0 are not cycling at all and G_1 have just divided and/ or in preparation for further entry to the cell cycle. S phase cells are in the process of DNA synthesis and so have intermediary DNA content i.e. cells in late stage S phase will have double (diploid) whilst cells in early S phase will have one copy. G_2 cells have double the amount of DNA. Cells in mitosis are undergoing chromosome condensation. By staining the cells with DAPI or propidium idodide a DNA flow cytometry histogram (Figure 2.7) can be produced determining the cells position in the cell cycle based on its DNA content during DNA replication.

2.13.5.2 Method

Non adherent and adherent cells were collected, washed in PBS and fixed in 70% ice cold ethanol for 1 hour. Cells were washed in PBS, resuspended in DAPI stain/ PBS and analysed in the flow cytometer using UV excitation. Cells were analysed on FL4-SSC (linear scale) and FSC (log 4 scale).

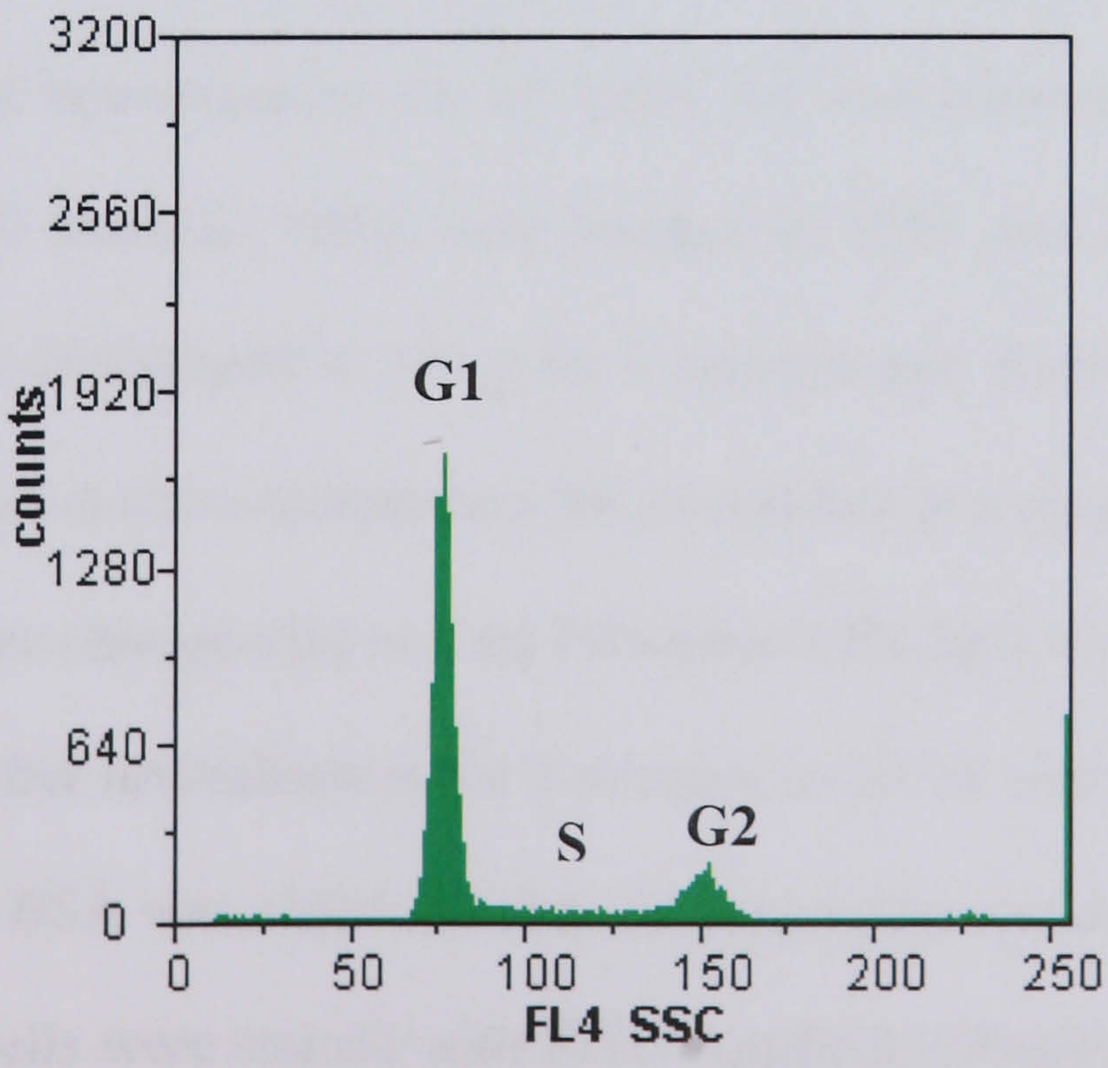

Figure 2.7 DNA cell cycle histogram. Peaks for each stage of the cell cycle can clearly be identified and from this, percentages of cells can be calculated.

2.13.6 BrdU Incorporation

2.13.6.1 Introduction

BrdU is a thymidine analogue and when added to culture medium it becomes incorporated into cellular DNA during replication, in the place of thymidine. Antibodies with specificity for BrdU are available. Thus after a short treatment with BrdU, the DNA can be partially denatured exposing the BrdU so that it can be stained with anti-BrdU antibody. As the cells have been fixed, the DNA can be stained with propidium iodide at the same time to see the total DNA content. BrdU incorporation allows us to distinguish cells that are proliferating from cells that may be blocked in S phase.

2.13.6.2 Method

Cells were incubated in medium supplemented with 20 μM 2-bromo-5-deoxuridine (BrdU) for 1 hour and harvested. Cells were centrifuged at 300 g for 5 minutes, resuspended in PBS and re-centrifuged for 5 minutes. The supernatant was aspirated and the pellet was loosened by tapping the tube. Cells were then fixed in 70% ice cold ethanol, to a final concentration of 10^7 cells/ ml and allowed to warm to room temperature for 20 minutes. Cells were washed in PBS plus 0.5% bovine serum albumin (BSA), re-centrifuged at 300 g for 5 minutes and denatured in 2 M HCl in PBS plus 0.5% BSA at room temperature for 20 minutes at a concentration of 150 μl/ 10^6 cells. Cells were resuspended in 1 ml PBS plus 0.5% BSA and centrifuged at 300 g for 5 minutes. After neutralisation for 2 minutes in 0.1 M sodium borate pH 8.5, 1 ml PBS plus 0.5% BSA was added and the cell suspension was divided into tubes for test and control. Cells were stained with FITC-AntiBrdU (Pharmingen Cat#33284X) or FITC-IgG control (Pharmingen Cat# 35404X) diluted in PBS plus 0.5% Tween-20

and 0.5% BSA at a concentration of 50 µl/ 10^6 cells and incubated in the dark at room temperature for 30 minutes. Cells were stained with the FITC-IgG control to detect any unspecific binding of the BrdU. Cellular DNA was stained with 10 µg/ ml propidium iodide for 30 minutes in the dark. Samples were diluted in PBS and then were analysed by flow cytometry. Data was displayed as a dotplot of FL-1 (log4 scale, detects BrdU) against FL-3 (linear scale, detects PI). Propidium iodide fluoresces red in FL-3, FITC-fluoresces green in FL-1.

2.14 Fluorescence Detected Alkaline DNA Unwinding Assay (FADU)

2.14.1 Introduction

The fluorescence detected alkaline DNA unwinding assay (FADU) is a procedure used to detect DNA damage, which is or can be converted to strand breaks (Birnboim and Jevcak, 1981). The assay is based upon the observation that DNA strand breaks accelerate DNA strand separation in alkaline conditions. DNA unwinding starts from strand breaks, which after alkaline denaturation, destabilises short duplex regions. The remaining double strand regions are selectively bound by a fluorescent intercalating dye. Therefore the fluorescence intensity of a sample is inversely correlated to the number of DNA strand breaks present.

Levels of single and double DNA strand breaks were assessed using a semi-automated FADU assay (Braebeck *et al.*, 2003). Briefly lysed cells were transferred onto 96 well plates and denatured in detergent/ urea buffer. An alkaline solution was added under controlled conditions to allow partial unwinding of the DNA starting from DNA strand interruptions. The fraction of DNA that remained double stranded

bound the DNA intercalating dye SYBR Green and the fluorescence intensity was measured.

2.14.2 Determination of DNA strand damage

Cells were treated with DNA damaging drugs, washed in PBS and lysed in FADU lysis buffer. The lysed cells were transferred onto a 96-well plate (replicates of 8-10) where at 4°C the FADU denaturation buffer was added, followed by the FADU alkali solution at 37°C for 90 minutes. DNA was stained with the intercalating dye SYBR Green (diluted 1:25,000 in 13 mM NaOH) and fluorescence was measured in a fluorescence reader Spectrafluor Plus (Tecan, Crailsheim, Germany) at λex 492 nm and λem 520 nm. The fluorescence intensity was inversely correlated to the number of DNA strand breaks present at the time of lysis. DNA damage percentage was calculated as $100x\ (P_0 - P_x)/P_0$, with P_0: fluorescence intensity of an untreated control sample and P_x: fluorescence intensity of the treated cell sample.

2.14.3 Determination of repair

To measure the amount of DNA which was being repaired after exposure to the drugs, cells were treated as in Section 2.14.2 with the following modifications. Cells were treated with a drug, after treatment was complete the medium was removed, cells were washed in PBS and placed at 37°C for a further 4 hours in serum free medium to minimise proliferation. The cells were then lysed and analysed as in Section 2.14.2.

2.15 Senescence Associated - β galactosidase (SA- β gal)

2.15.1 Introduction

Normal beta galactosidase histochemical procedures identify the lysosomal form of the enzyme. Such assays are performed at pH 4 and use the substrate 5-bromo-4chloro-3indolyl β-D-galactopyranoside (X-Gal). Whilst senescence associated beta galactosidase (SA- β gal) activity is optimal at pH 6 and is observed in the cytoplasm in the non lysosomal regions (Dimri *et al.*, 1995) of senescent cells. It is commonly used as a marker for senescence. A hallmark of senescence is a permanent arrest of cell cycle as senescent cells arrest at the G_1/ S transition with a G_1 content of DNA (Goldstein, 1990). Dimri and colleagues showed that staining for beta galactosidase was poor in young, non proliferating quiescent or terminally differentiated cells but stained more intensely once senescent. Additionally they tested human skin samples from a range of age donors and found an age related increase in the marker in dermal fibroblasts and epidermal keratinocytes (Dimri *et al.*, 1995).

2.15.2 Method

Cells were seeded onto petri dishes and allowed to grow until near confluence. Cells were washed twice with PBS and fixed with 1% formaldehyde/ PBS for 5 minutes at room temperature. Cells were washed twice with PBS, the Sen β gal staining solution (Section 2.2) was added and cells were incubated at 37°C for several hours. As a positive control MRC5 senescent fibroblasts underwent the same procedure. Images were obtained using a DMIL microscope (Leica Microsystems, UK).

2.16 Histone H2A.X Phosphorylation (γ-H2A.X)

2.16.1 Introduction

The DNA damage response was examined by staining with an antibody recognising the phosphorylated form of histone H2A.X (γ-H2A.X). γ-H2A.X accumulates in response to DNA damage, at discrete foci within nuclei. A number of other proteins accumulate at these foci which function as signal transducers between DNA strand breaks and the cellular repair, growth arrest and apoptosis machinery (d'Adda di Fagagna *et al.*, 2003). One of the first cellular responses to the introduction of double strand breaks is the phosphorylation of H2A.X. Serine 139 in the unique carboxy terminal tail of H2A.X is phosphorylated rapidly after damage and the number of H2A.X molecules phosphorylated increases with the severity of the damage. The phosphorylation is mediated by ATM (Rogakou *et al.*, 1999), ATR (Furuta *et al.*, 2003) and/ or DNA dependent protein kinase (DNA-PK) (Park *et al.*, 2003). Checkpoint and DNA repair proteins such as Rad50, Rad51 and Brca1 colocalise with γ-H2A.X (Paull *et al.*, 2000).

2.16.2 Method

Ethanol sterilised 16 mm circular coverslips were placed in a 12 well plate. 1 ml of cell suspension was added to each well and incubated for 24 hours at 37°C. The medium was aspirated from the wells and cells were washed twice for 5 minutes in PBS. Cells were fixed by incubating for 10 minutes at room temperature with 1 ml of 2% paraformaldehyde/ PBS. Cells were washed twice with PBS and permeabilised by adding 1 ml of PBG with 0.5% Triton X-100 for 45 minutes at room temperature whilst shaking slightly. The solution was removed and cells were incubated with anti-

phospho histone H2A.X (Ser 139) clone JBW103 mouse monoclonal IgG1 (Upstate, CAT#05-636) in PBG with 0.5% Triton X-100 (400 µl) for 1 hour at room temperature, shaking slightly. Cells were washed twice with PBG plus 0.5% Triton for 5 minutes and incubated with a dilution of Alexafluor 594 goat anti-mouse IgG (H+L) (Molecular probes, Cat# A11005) in PBG plus 0.5% Triton for 45 minutes up to 1 hour at room temperature as a secondary antibody. Cells were washed three times with PBS for 5 minutes and 400 µl of DAPI staining solution was added for 10 minutes at room temperature. DAPI (4'-6-Diamidino-2-phenylindole) is known to form fluorescent complexes with natural double-stranded DNA and is used as a specific nuclei counterstain. When DAPI binds to DNA, its fluorescence is strongly enhanced as it binds to the minor groove of the DNA helix around A-T clusters. Cells were further washed three times with PBS for 5 minutes, aspirated and sealed onto a glass slide containing a drop of anti-fade mounting medium (Vecta Shield). Slides were examined using a Zeiss epifluorescence microscope. The DAPI and Alexafluor 594 fluoresce at separate wavelengths of 372 nm (blue excitation) and 594 nm (red excitation) respectively. These images are then merged using the LeicaQfluro Imaging Capture Program.

2.17 ImmunoFISH

2.17.1 Introduction

To determine whether any sites of DNA damage localised to the telomeres, a protocol was devised that combines the immunological detection of γ-H2A.X foci with fluorescence *in situ* hybridisation (FISH) detection of telomeres using a telomere specific peptide nucleic (PNA) probe. This procedure enables detection of the damage and telomeres at different wavelengths through a fluorescence microscope.

To see both the telomeric DNA and the γ-H2A.X DNA damage foci simultaneously, initially a variety of procedures were attempted from published data and through personal communication. For the detection of DNA damage foci through immunohistochemistry and telomeric DNA using FISH, cells have to be in a fixed state. Originally it was endeavoured to use the same fixation method for both the immunohistochemistry and the FISH techniques and the individual procedures were primarily examined separately using the following reagents; paraformaldehyde, acetone and methanol/ acetic acid. Once it was determined which of the fixing reagents gave positive signals for both the DNA damage foci and telomeres individually, the procedures were combined for immunoFISH, with the telomeres being probed before the DNA damage foci. The results obtained using the various fixing reagents for the immunoFISH, either gave a signal for DNA damage foci but not the telomeres and vice versa. Therefore the procedure was modified whereby cells were fixed individually for each procedure using different fixation reagents, with the telomeres targeted before the damage response staining. Through further modification, the immunoFISH procedure was finalised by firstly staining for the DNA damage response, then probing for the telomeres and reapplying the secondary antibody to detect γ-H2A.X DNA damage foci.

2.17.2 Method

Cells on coverslips were fixed by incubating for 10 minutes at room temperature with 1 ml of 2% paraformaldehyde/ PBS. Cells were washed twice with PBS and permeabilised by adding 1 ml of PBG with 0.5% Triton X-100 for 45 minutes at room temperature whilst shaking slightly. The solution was removed and cells were incubated with anti-phospho histone H2A.X (Ser 139) clone JBW103 mouse

monoclonal (Upstate, CAT#05-636) in PBG with 0.5% Triton X-100 (400 µl) for 1 hour at room temperature, shaking slightly. Cells were washed twice with PBG plus 0.5% Triton for 5 minutes and incubated with a dilution of Alexafluor 594 goat anti-mouse IgG (H+L) (Molecular probes, Cat# A11005) in PBG plus 0.5% Triton for 45 minutes up to 1 hour at room temperature as a secondary antibody. Cells were washed three times with PBS for 5 minutes and 1 ml of fixative (methanol: acetic acid 3:1) was added for 15 minutes, washed in PBS and a further 1.3 ml of fixative was added for a further 15 minutes. Cells were then washed in PBS, washed in 1 ml fixative and baked at 60°C for 1 hour. Cells were rehydrated in 2x SSC at 37°C for 2 minutes and dehydrated in a series of 70%, 80%, 95% ethanol for 2 minutes each and air dried. Cells were treated with 20 µl of Cy-3 labelled telomere specific $(C_3TA_2)_3$ peptide nucleic acid (PNA) probe (4ng/ µl) (Applied Biosystems) containing 70% formamide/ 2x SSC. Both probe and cellular DNA were codenatured at 75°C for 10 minutes in a moist chamber containing 1x SSC and hybridised for 2 hours in a moist chamber at 37°C in 1x SSC, washed with 2x SSC/ 0.05% tween for 10 minutes shaking at room temperature. Cells were further incubated with a dilution of the fluorescein conjugated secondary antibody in PBG plus 0.5% Triton for 45 minutes at room temperature and washed three times for 5 minutes in PBS. Coverslips were mounted in Vectashield mounting solution containing DAPI as a DNA counterstain and examined using a Zeiss epifluorescence microscope. The DAPI, Alexafluor 594 and Cy-3 fluoresce at separate wavelengths of 372 nm (blue excitation), 594 nm (red excitation) and 494 nm (green excitation) respectively. The images are merged using the LeicaQfluro Imaging Capture Program.

CHAPTER 3

NEUROBLASTOMA APOPTOSIS INDUCTION AFTER CISPLATIN TREATMENT IS NOT TELOMERE DEPENDENT

3.1 Introduction

Cisplatin is a chemotherapeutic agent for the treatment of neuroblastoma, a common solid extracranial malignancy of childhood and infancy. Cisplatin binds to DNA to cause a biological effect by forming cisplatin- DNA adducts and is a potent inducer of apoptosis (Ormerod *et al.*, 1996; Henkels and Turchi, 1997). The major DNA adduct formed is the bifunctional intra-strand cross-links between adjacent guanines. It is unclear how the cisplatin- DNA adducts induce cytotoxicty, though this is widely attributed to the formation of various types of cross-links. There is a linear correlation between gross levels of platinum bound to DNA and the extent of cytotoxicty (Fraval and Roberts, 1979). Reports exist that strongly favour intra-strand adducts as lesions largely responsible for the cytotoxic action (Pinto and Lippard, 1985), which is consistent with the knowledge that the intra-strand adducts account for 85- 90% of total lesions (Kelland, 1993). Though other reports indicate that inter-strand cross-links are the most cytotoxic lesion (Knox *et al.*, 1986).

Telomeres, the DNA-protein structures that form the ends of chromosomes, play a number of important roles in the function and organisation of the genome. Their shortening with each round of DNA replication is caused by different mechanisms, one of these being their sensitivity to DNA damage. Thus, telomere shortening can be greatly accelerated or decelerated by controlling oxidative stress within the cells (von Zglinicki, 2002). Cisplatin has been shown to bind preferentially to runs of two or

more consecutive guanines (Grimaldi *et al.*, 1994). Human telomeric DNA is partially composed of guanines as its repeat sequence is TTAGGG. Therefore, cisplatin may preferentially target telomeric DNA. Telomeres end in single stranded overhangs of the G-rich strand, which appear to be essential for telomeric higher order structure (Griffith *et al.*, 1999) and for the generation of DNA damage signals from telomeres (Saretzki *et al.*, 1999; von Zglinicki, 2001; Stewart *et al.*, 2003). Telomerase, a reverse transcriptase that uses an RNA template to add telomeric repeats onto the ends of chromosomes (Greider and Blackburn, 1987; 1989) is expressed in 94% of neuroblastomas (Hiyama *et al.*, 1995) and has been shown to be a powerful independent prognostic factor (Brinksmidt *et al.*, 1998). Thus a specific role of the telomere/ telomerase complex in mediating cisplatin induced neuroblastoma cell death may be expected.

In fact, cisplatin induced cell killing of tumour cells was associated with a decline in detectable telomerase activity (Burger *et al.*, 1997; Kunifuji *et al.*, 2002; Zhang *et al.*, 2002) and a continuous cisplatin treatment induced loss of telomeres in HeLa cells (Ishibashi and Lippard, 1998). However, in testicular teratoma and haematopoietic cell lines the decline in telomerase activity following cisplatin treatment was shown to be a consequence of, rather than a cause for, apoptosis (Akiyama *et al.*, 1999; Cressey *et al.*, 2002). Telomerase inhibition by different methods has been shown to lead not only to progressive telomere shortening and cell death (Herbert *et al.*, 1999) but also to telomere length independent apoptosis induction (Saretzki *et al.*, 2001), while activation of telomerase was related to increased resistance to apoptosis (Holt *et al.*, 1999; Ludwig *et al.*, 2001). Telomerase inhibition was found to increase the sensitivity of various cell lines to cisplatin induced apoptosis, for example glioblastomas (Kondo *et al.*, 1998; Kondo *et al.*, 2001) and HEC-1 cells (Murakami *et*

al., 1999). However this was not detected in human breast tumour cells and overexpression of hTERT, the catalytic subunit of telomerase in human fibroblasts did not increase their cisplatin resistance (Ludwig *et al.*, 2001). Given these contradictory results, the aim of the work described in this chapter was to test the hypothesis that there is a role for the telomere/ telomerase complex in cisplatin induced neuroblastoma cell apoptosis. No indications for a causal involvement were found.

3.2 Methods

All methods used in this study are described in Chapter 2.

3.3 Results

3.3.1 Growth inhibitory effect of cisplatin on SHSY5Y cells

Initially it was very important to establish the relationship between cisplatin treatment and growth inhibitory effects as a basis for experiments on mechanism of action. Cell growth was assessed by cell counting and by the SRB assay after cisplatin treatment. The latter is widely used to assess the effect of cytotoxic drugs.

Growth curve data for the SHSY5Y cells (Figure 3.1 A) were used to determine the optimal inoculum density for the SRB assay. The cytotoxicty levels of cisplatin on the SHSY5Y cells were then examined by exposing cells to a short (2 hour) exposure drug treatment and incubating for a further 6 days before fixing and staining with the SRB reagents (Section 2.5). The control cells (untreated) optical density (OD) was set at 100%. The OD of the treated cells were converted into percentages of the control OD, plotted against cisplatin concentration (Figure 3.1 B) and the IC_{50} value calculated from this giving an IC_{50} value of 13.3 μM.

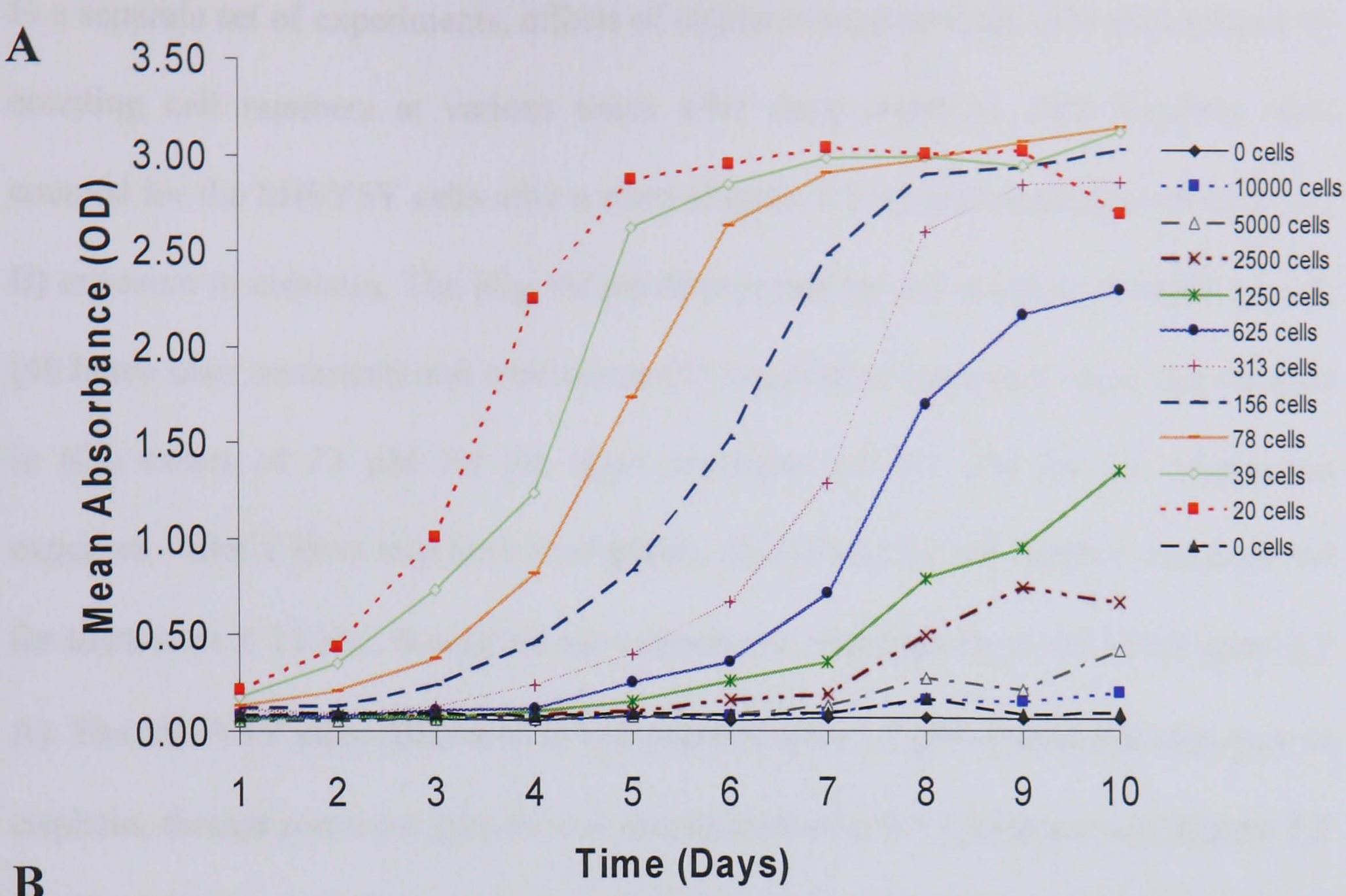

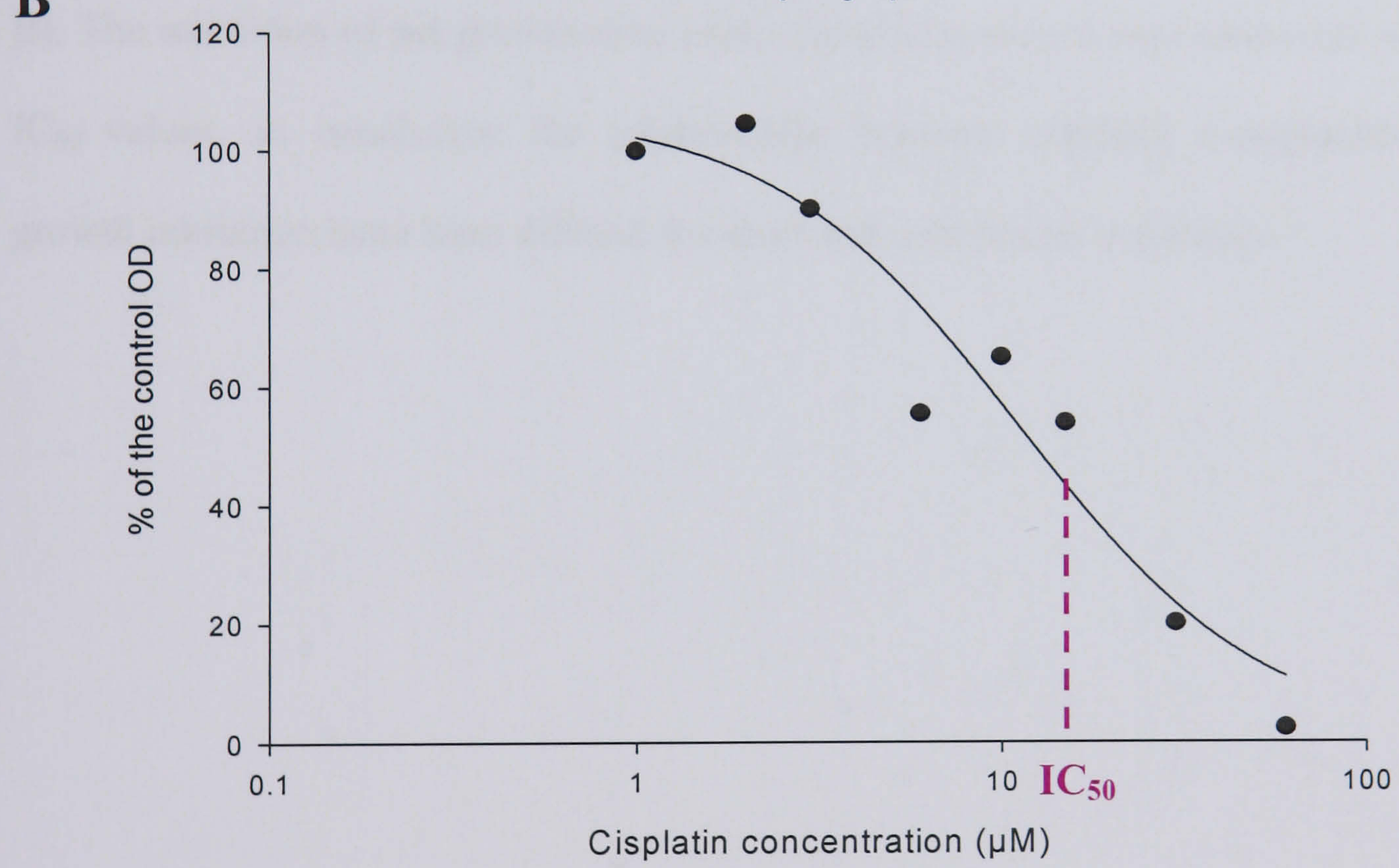

Figure 3.1 Determination of IC_{50} of SHSY5Y cells after cisplatin treatment. (A) Growth curves of SHSY5Y cells. Cells were grown at various densities in ten 96 well plates and each day plates were fixed and stained with sulphorhodamine B to give the optical densities. The OD was directly proportional to the number of cells and these values can be used to determine the optimum inoculum density to be used in further experiments. (B) SHSY5Y cells were exposed to a 2 hour drug treatment and incubated for 6 days before fixing and staining with sulphorhodamine B. Treated cells were converted into % of the control OD which was used to estimate the IC_{50} value.

In a separate set of experiments, effects of cisplatin on growth of cells was defined by counting cell numbers at various times after drug exposure. Cell numbers were counted for the SHSY5Y cells after a short (Figure 3.2 A) and continuous (Figure 3.2 B) exposure to cisplatin. The IC_{50} values determined by cell counting for both a short (48 hours after treatment) and continuous (72 hours after treatment) exposure resulted in IC_{50} values of 23 μM for the short exposure and 0.7 μM for the continuous exposure. After a short exposure to cisplatin, an increase in cell number was detected for treatments ≤ 15 μM, though no net growth was observed for ≥100 μM (Figure 3.2 A). The SHSY5Y cells decreased in cell number after ≥ 2 μM continuous exposure to cisplatin, though some net growth was established after 0.5 μM treatment (Figure 3.2 B). The inhibition of net growth after both cisplatin treatment regimens confirmed the IC_{50} values. In conclusion the relationships between cisplatin concentration and growth inhibition have been defined for short and continuous exposures.

A

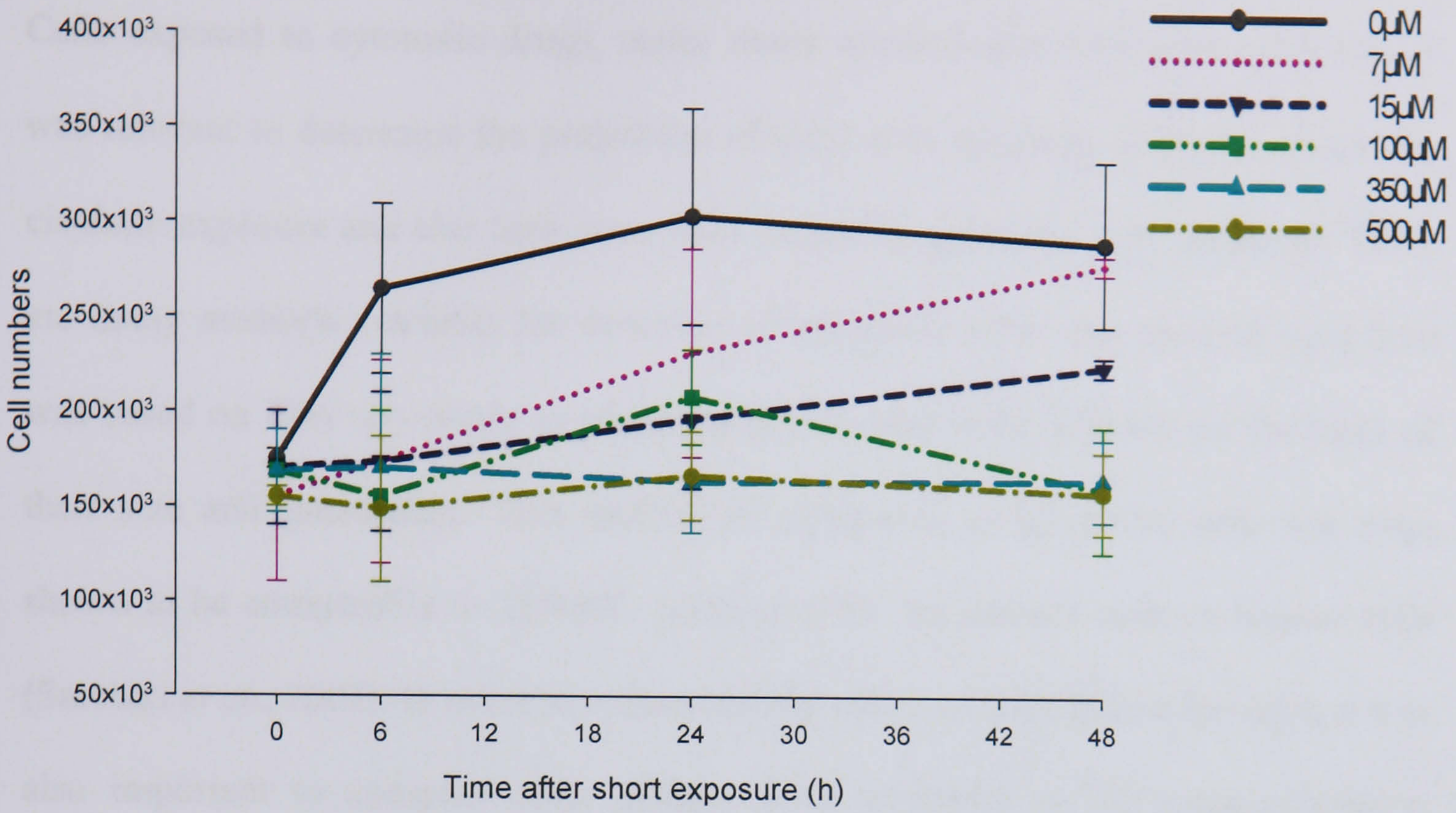

B

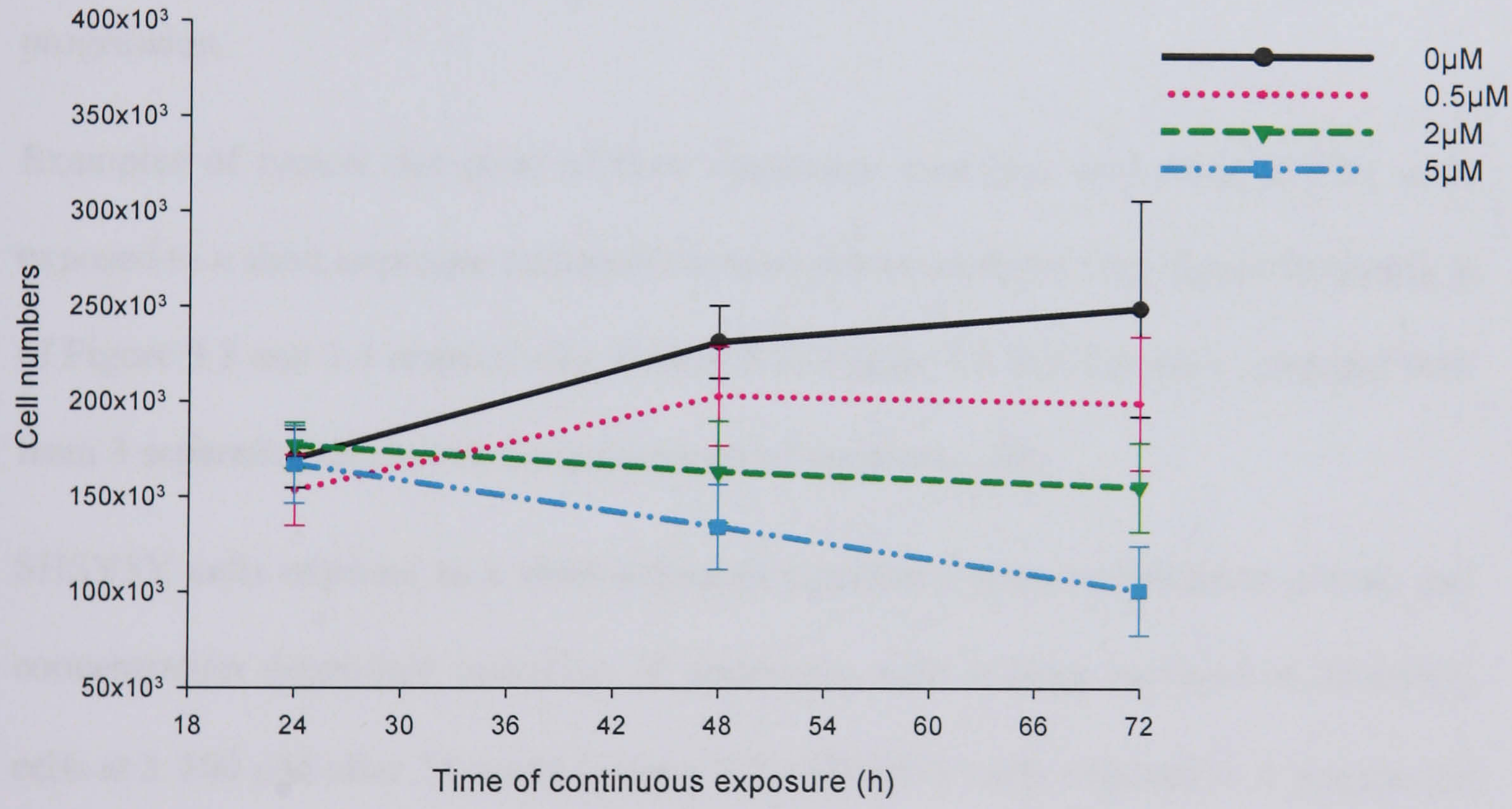

Figure 3.2 Cell numbers of SHSY5Y cells after a short and continuous exposure to cisplatin. SHSY5Y cells were exposed to cisplatin for 2 hours (A) or continuously (B) and cell numbers per flask were counted up to at least 48 hours after. Data are mean ± SEM from triplicate experiments.

3.3.2 Cisplatin induces apoptosis and S phase arrest in SHSY5Y cells

Cells exposed to cytotoxic drugs, under many circumstances undergo apoptosis. It was relevant to determine the proportion of cells with apoptotic features induced by cisplatin exposure and also how soon after treatment apoptotic cells appeared. There are many methods available for detection of apoptotic cells. The method used here was based on flow cytometry in which apoptotic cells were detected on the basis of their size and granularity. This method of estimation of apoptotic cells has been shown to be comparable to TUNEL- positive cells and sub-G1 cells in tumour cells (Saretzki *et al.*, 2001). In order to understand the effect of cisplatin on the cells, it was also important to compare other cellular drug responses to the drug exposures. Therefore it was essential to investigate the effect of cisplatin on cell cycle progression.

Examples of typical dot plots of flow cytometry apoptotic data for SHSY5Y cells exposed to a short exposure and continuous exposure treatment are shown in panels A of Figure 3.3 and 3.4 respectively. Panels B of Figure 3.3 and 3.4 show averaged data from 3 separate experiments for percentage of apoptotic cells.

SHSY5Y cells exposed to a short exposure cisplatin treatment exhibited a time and concentration dependent induction of apoptosis, with a large increase in apoptotic cells at ≥ 100 μM after 24 hours (Figure 3.3). SHSY5Y cells exposed to a continuous treatment of cisplatin also displayed a time and concentration dependent induction of apoptosis (Figure 3.4). Though the SHSY5Y cells not exposed to cisplatin (untreated) exhibited an increased frequency of apoptotic cells, this is thought to be due to adverse growth conditions i.e. confluency.

Measurement of the cellular DNA content in SHSY5Y cells after a short exposure

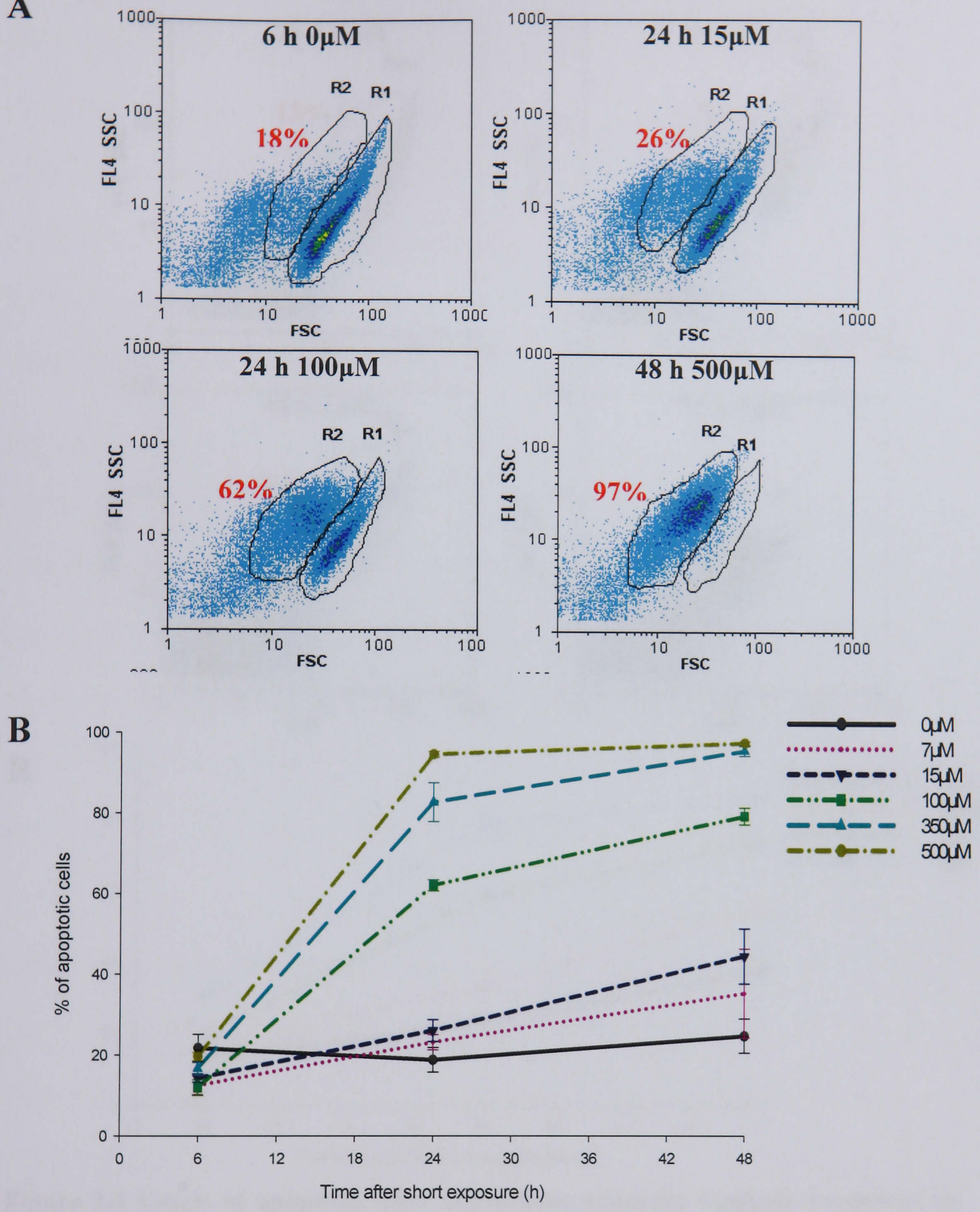

Figure 3.3 Levels of apoptosis after short exposure cisplatin treatment on SHSY5Y cells. Apoptotic cells were measured by flow cytometry according to their size (forward scatter; FSC) and granularity (light scattered sideways; SSC). (A) Examples of gated apoptotic cells R2, to non apoptotic cells R1 after cisplatin treatment. Time after treatment and concentration of cisplatin indicated. % of apoptotic cells are shown in red. (B) % of apoptotic cells after cisplatin treatment average graph. Data are mean ± SEM from triplicate experiments with three replicates in each experiment.

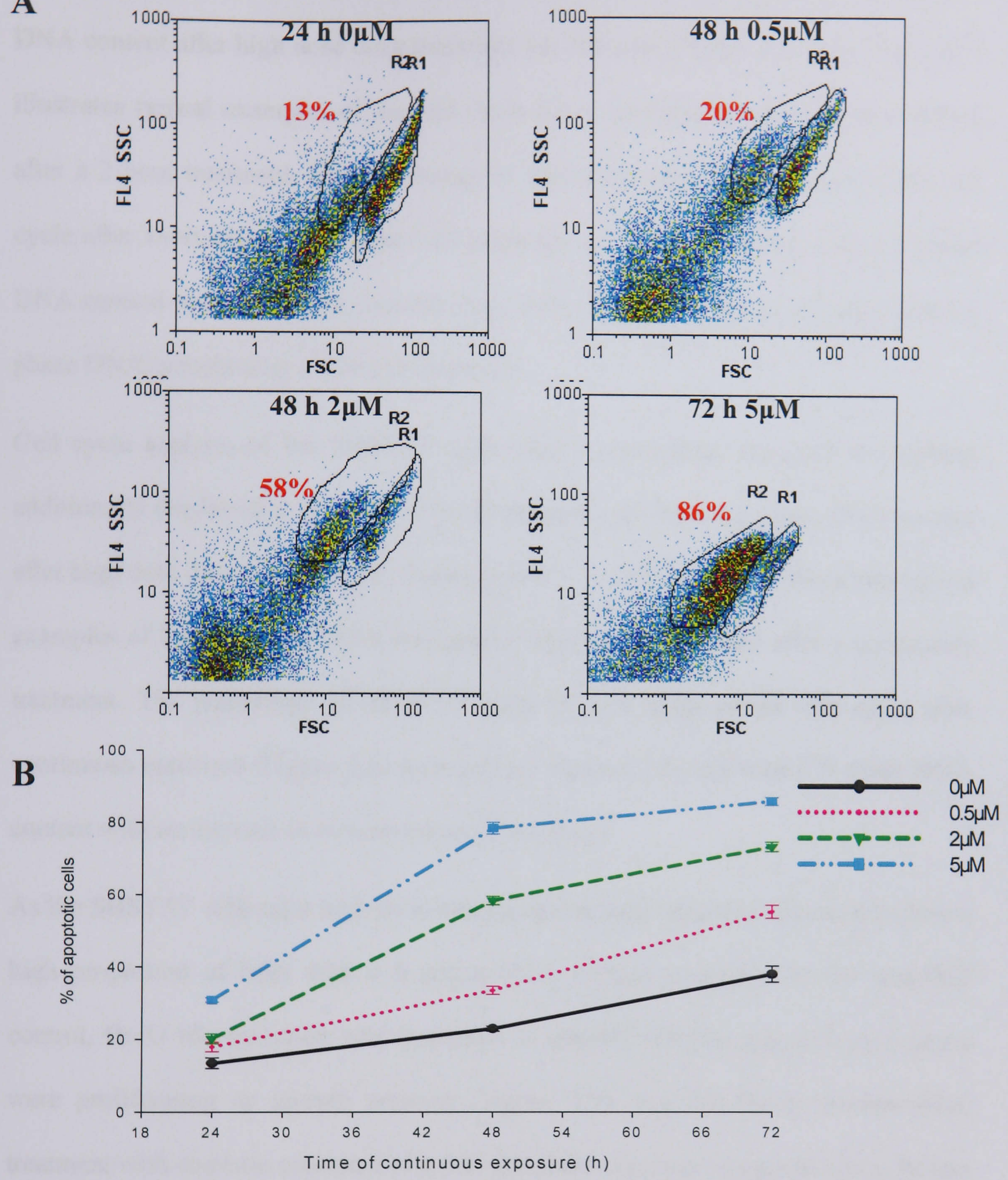

Figure 3.4 Levels of apoptosis after continuous exposure cisplatin treatment on SHSY5Y cells. Apoptotic cells were measured by flow cytometry according to their size (forward scatter; FSC) and granularity (light scattered sideways; SSC). (A) Examples of gated apoptotic cells R2, to non apoptotic cells R1 after cisplatin treatment. Time after treatment and concentration of cisplatin indicated. % of apoptotic cells are shown in red. (B) % of apoptotic cells after cisplatin treatment average graph. Data are mean ± SEM from triplicate experiments with three replicates in each experiment.

cisplatin treatment revealed significant increases of the fraction of cells with a S phase DNA content after high dose drug treatment i.e. 100 μM (Figure 3.5- 3.6). Figure 3.5 illustrates typical examples of the cell cycle DNA histograms which were obtained after a 2 hour treatment. The percentage of SHSY5Y cells in each stage of the cell cycle after short exposure (Figure 3.6) indicated an increase of cells with a S phase DNA content with increasing concentration, with the highest amount of cells with a S phase DNA content after a 100 μM treatment.

Cell cycle analysis of the SHSY5Y cells after a continuous exposure to cisplatin additionally displayed an increase of the fraction of cells with a S phase DNA content after high dose drug treatment i.e. 5 μM (Figure 3.7- 3.8). Figure 3.7 illustrates typical examples of the cell cycle DNA histograms which were obtained after a continuous treatment. The percentage of SHSY5Y cells in each stage of the cell cycle after continuous exposure (Figure 3.8) indicated an increase of cells with a S phase DNA content with an increase in concentration of treatment.

As the SHSY5Y cells after high dose treatments for both regimens appeared to have a high proportion of cells with a S phase DNA content compared to the untreated control, BrdU incorporation was examined to identify whether the cells in S phase were proliferating or growth arrested (Figure 3.9). For the BrdU incorporation, treatment with cisplatin consisted of a 500 μM short exposure treatment with a further incubation of 48 hours and a 5 μM continuous exposure to cisplatin for 48 hours. BrdU was added for 1 hour after treatment was complete. Figure 3.9 A illustrates the DNA content of the cells after the treatments, whilst Figure 3.9 B displays the FITC labelled anti- BrdU fluorescence. BrdU is incorporated in the untreated cells (compared to 0 μM IgG) as expected. Though 48 hours after high dose treatments BrdU was not incorporated suggesting that the cells were arrested in S phase.

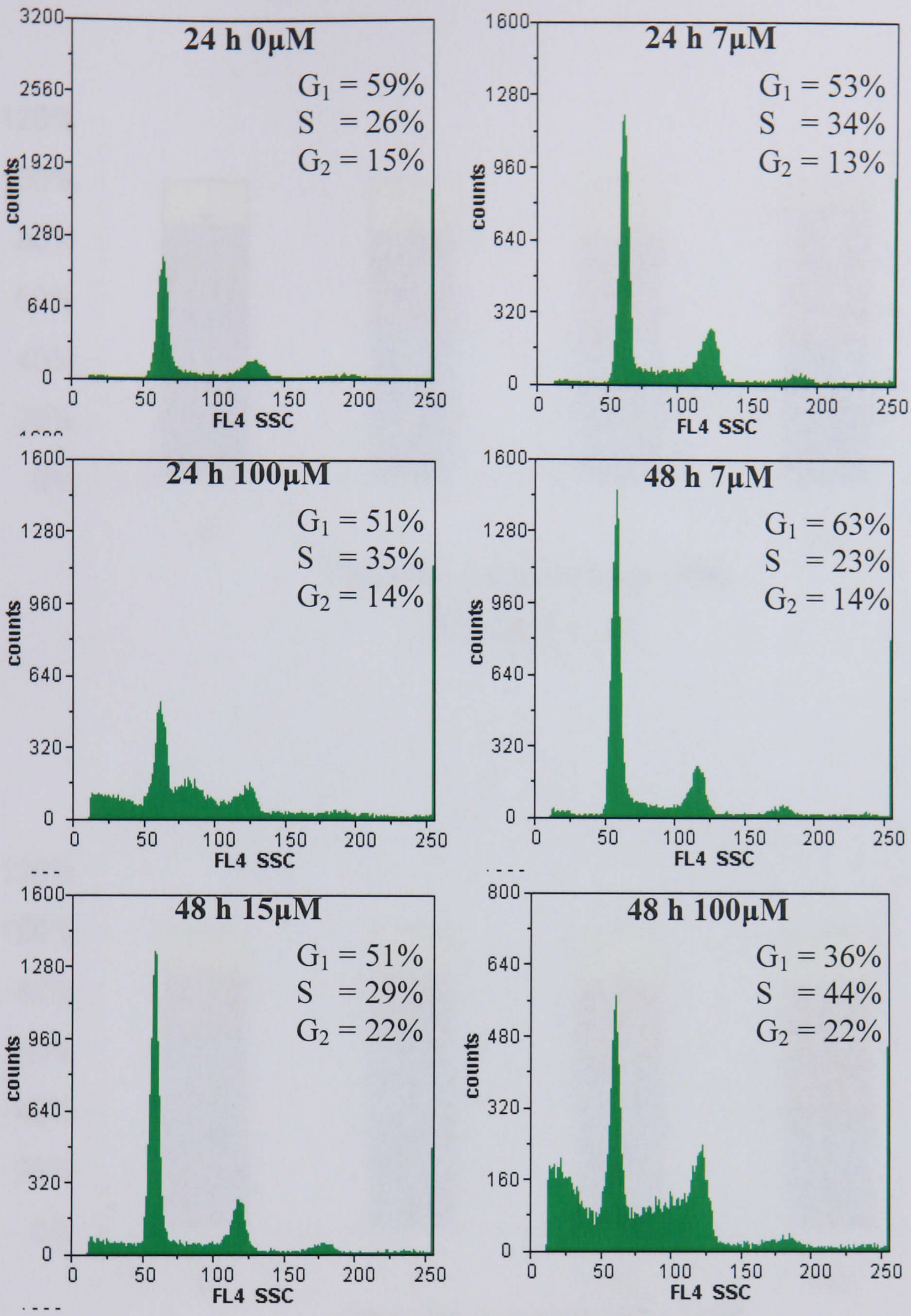

Figure 3.5 Cell cycle analysis of SHSY5Y cells exposed to cisplatin after a short exposure. % ratios of cell cycle stages were measured in DNA histograms from DAPI stained cells using UV light at the indicated times after treatment. Typical DNA histograms from DAPI stained cells at the indicated times after treatment are shown.

A

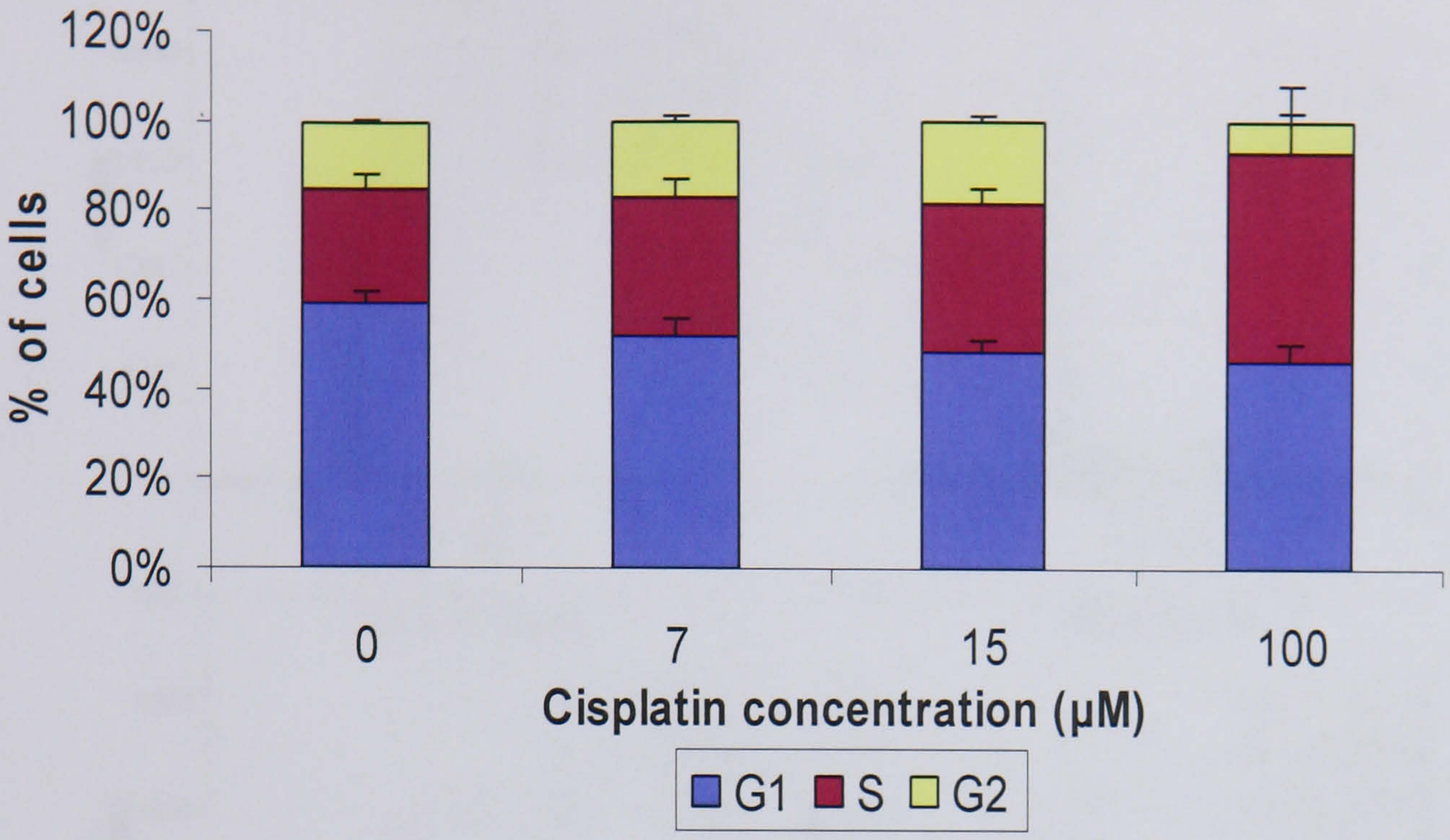

B

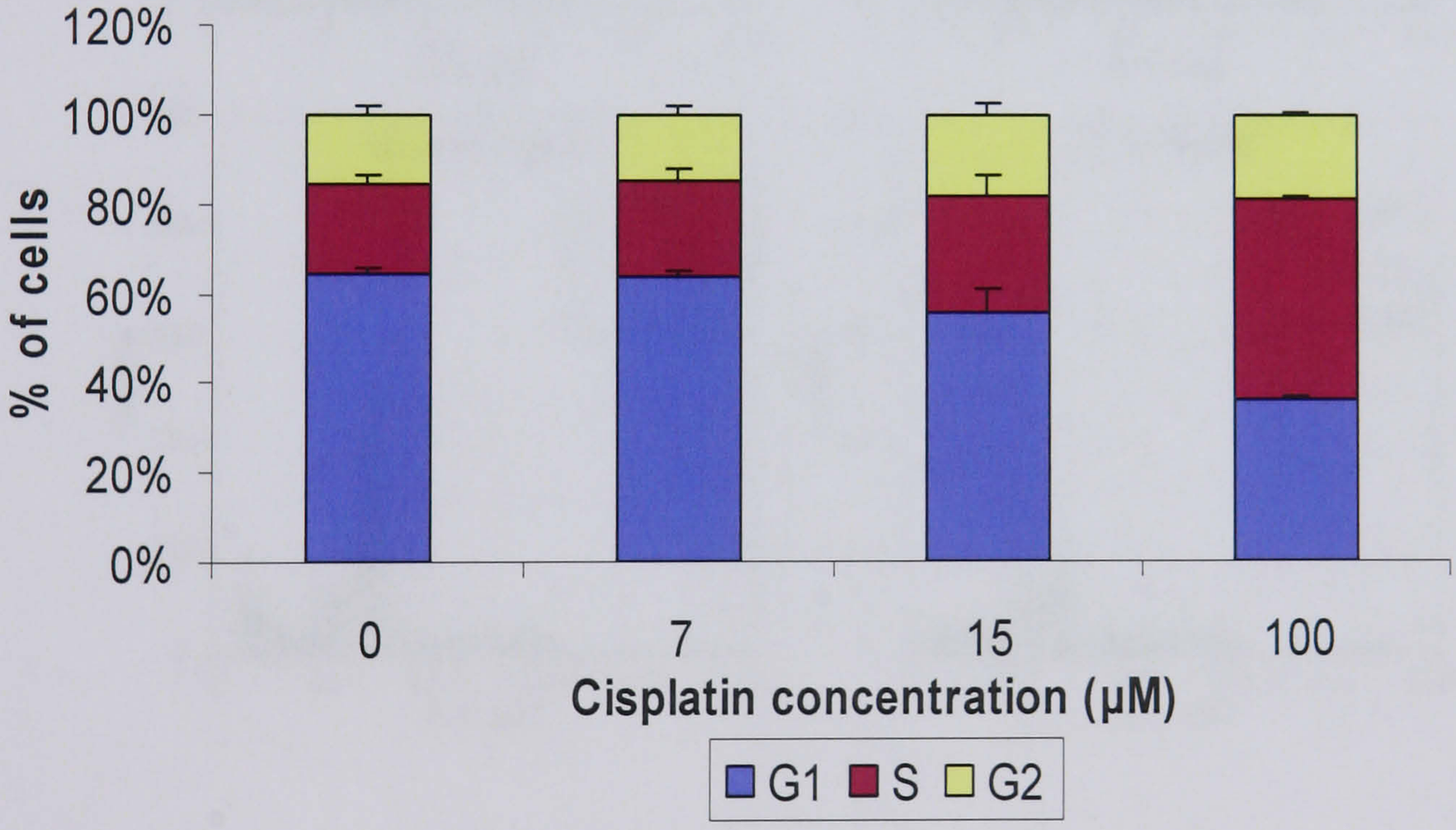

Figure 3.6 Stages of SHSY5Y cells in the cell cycle after a short exposure to cisplatin. Percentage of cells in G_1 (blue), S (purple) and G_2 (yellow) phase 24 hours (A) and 48 hours (B) after a short exposure cisplatin treatment at the indicated concentrations, assessed by flow cytometry. Data are mean ± SEM from triplicate experiments with three replicates in each experiment.

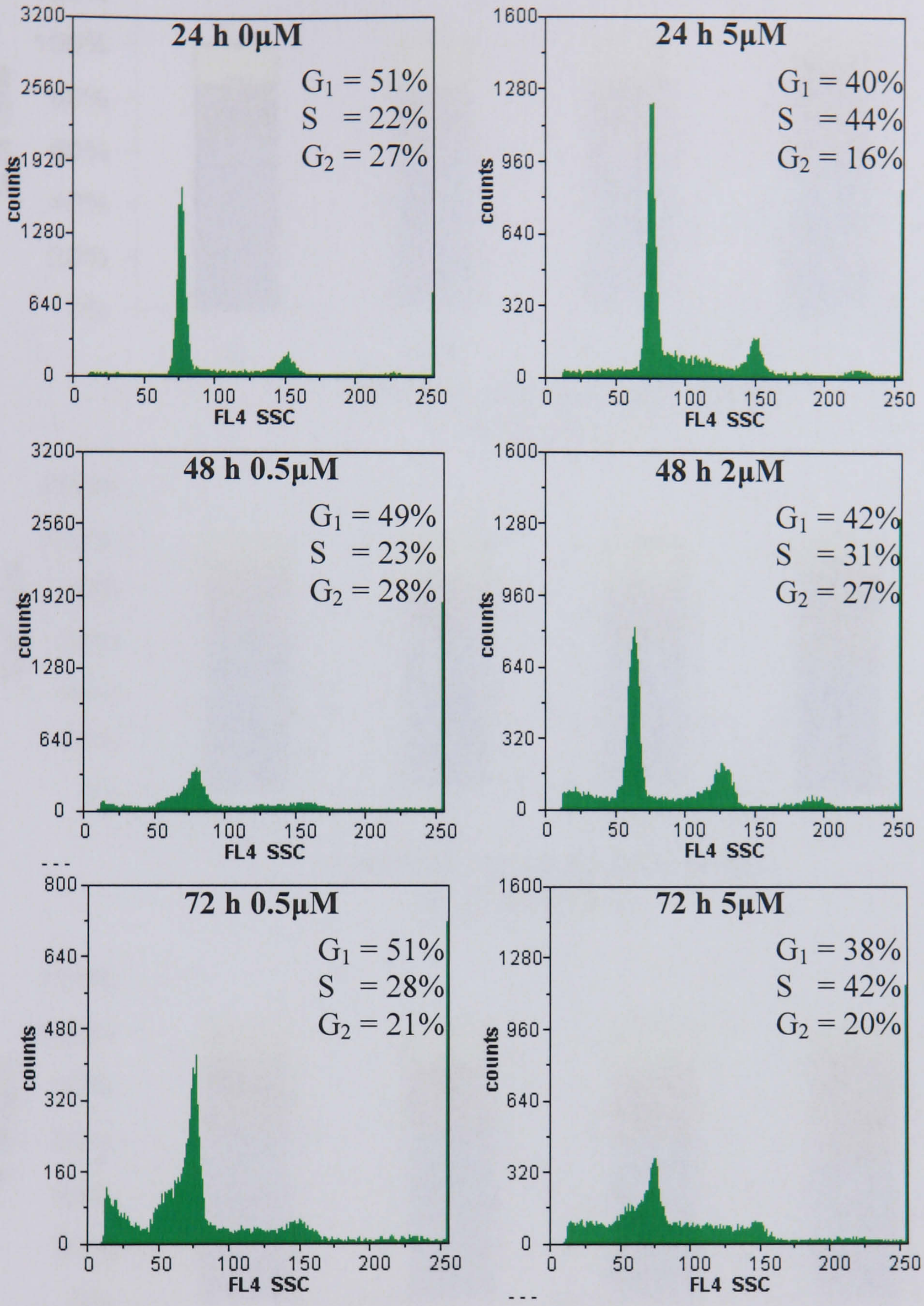

Figure 3.7 Cell cycle analysis of SHSY5Y cells exposed to cisplatin continuously. % ratios of cell cycle stages were measured in DNA histograms from DAPI stained cells using UV light at the indicated times after treatment. Typical DNA histograms from DAPI stained cells at the indicated times after treatment are shown.

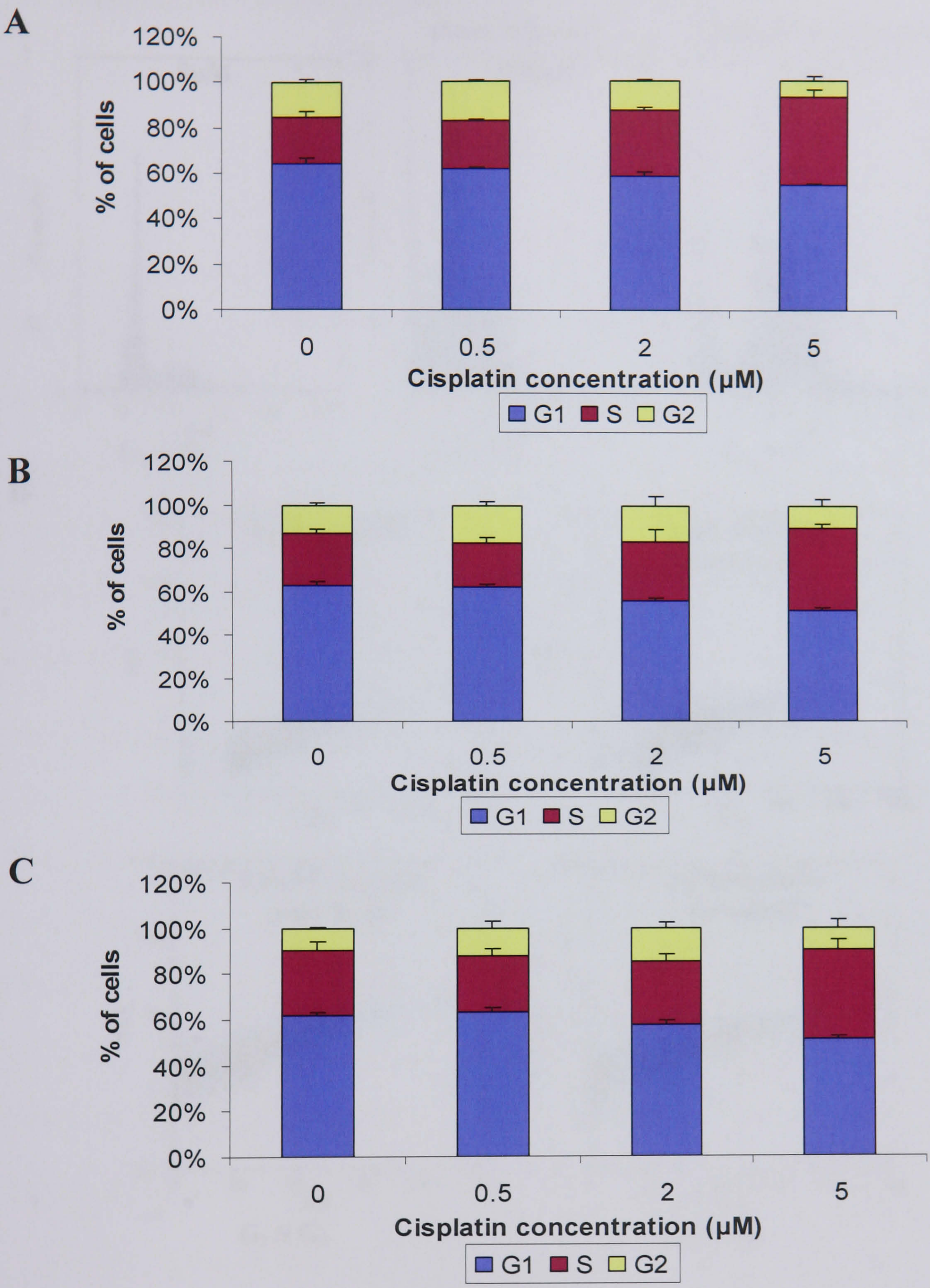

Figure 3.8 Stages of SHSY5Y cells in the cell cycle after a continuous exposure to cisplatin. Percentage of cells in G_1 (blue), S (purple) and G_2 (yellow) phase 24 hours (A), 48 hours (B) and 72 hours (C) after a continuous cisplatin treatment at the indicated concentrations assessed by flow cytometry. Data are mean ± SEM from triplicate experiments with three replicates in each experiment.

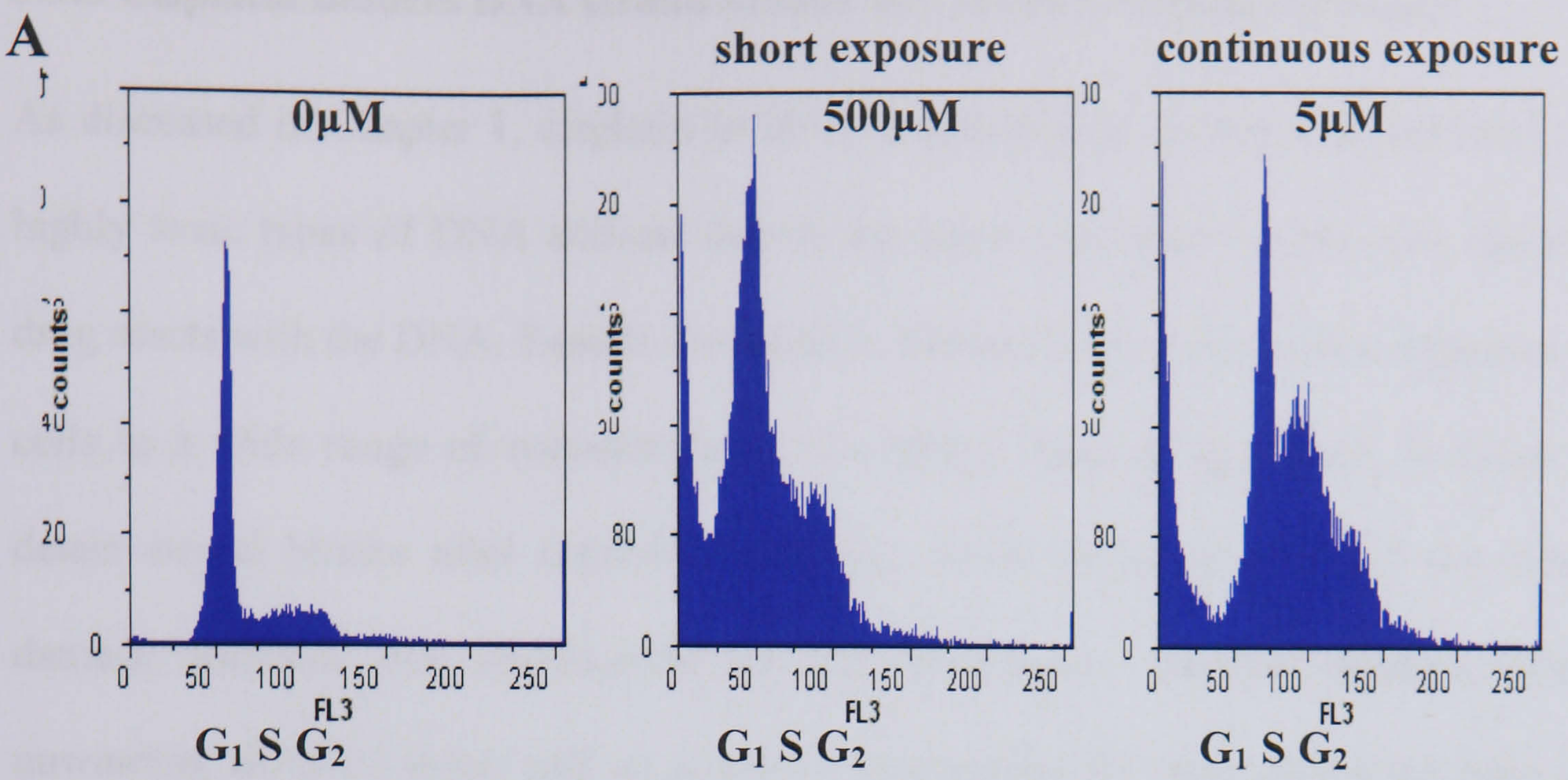

Figure 3.9 BrdU incorporation of cisplatin treated SHSY5Y cells. Cells were incubated with BrdU at 48 hours after onset of cisplatin treatment for 1 hour. DNA content histograms after a 500 μM short exposure, 5 μM continuous exposure and untreated by DAPI staining (A). FL1 vs FL3 scattergrams (B). FITC labelled anti-BrdU fluorescence is measured in FL1 and DNA content is measured in FL3. Cell cycle phase positions G_1, S, G_2/ M are indicated at the x- axis.

3.3.3 Cisplatin induces DNA strand breaks as a result of attempted repair

As discussed in Chapter 1, cisplatin in its *cis* conformation favours the formation of highly toxic types of DNA adducts due to the steric restriction on the way that the drug reacts with the DNA. Results described in Section 3.3.2 indicate that exposure of cells to a wide range of concentrations of cisplatin induced apoptosis. In order to detect strand breaks after cisplatin treatment, DNA strand breaks and the DNA damage response was investigated by the fluorescence detected alkaline DNA unwinding (FADU) assay and an antibody recognising the phosphorylated form of histone H2A.X (γ-H2AX) respectively. It was of importance to determine if cisplatin exposure of SHSY5Y cells resulted in strand breaks because strand breakage in telomeric DNA could be detected by available techniques.

The presence of DNA strand breaks were measured after exposure for 2 hours to cisplatin at 7, 100 and 500 μM. Samples were analysed immediately after the exposure period and following further incubation for 14 and 24 hours (Figure 3.10). Strand breaks were detectable at 14 and 24 hours after a short exposure treatment, though not immediately after treatment. This increase in strand breaks after an incubation period was statistically significant (ANOVA) compared to breaks measured immediately after treatment.

The level of DNA breaks was higher after 24 hours than 14 hours. Strand breaks present after treatment increased with cisplatin concentration up to 100 μM. The apparent decrease in strand breaks at 500 μM is attributed to the fact that many of the cells were in apoptosis (Figure 3.3).

The DNA damage response of SHSY5Y following exposure to cisplatin was examined by γ-H2A.X staining, immediately after a 100 μM and 500 μM, 2 hour

treatment (Figure 3.11 A) and after a further 24 hours (Figure 3.11 B). Immediately after the 2 hour exposure the cells did not show the presence of DNA damage foci. After 24 hours further incubation the majority of the cells stained positive for γ-H2A.X.

As cisplatin- DNA adducts primarily do not induce strand breaks, the delayed detection of H2A.X phosphorylation and DNA strand breaks in cisplatin treated cells is probably associated with DNA repair activities. As described in Chapter 1, NER is known to be involved in repair of cisplatin DNA intra-strand cross-links and this process involves strand incision. However, induction of H2A.X phosphorylation is generally associated with double strand breaks which are likely to form during repair of stalled replication forks or during repair of inter-strand cross-links.

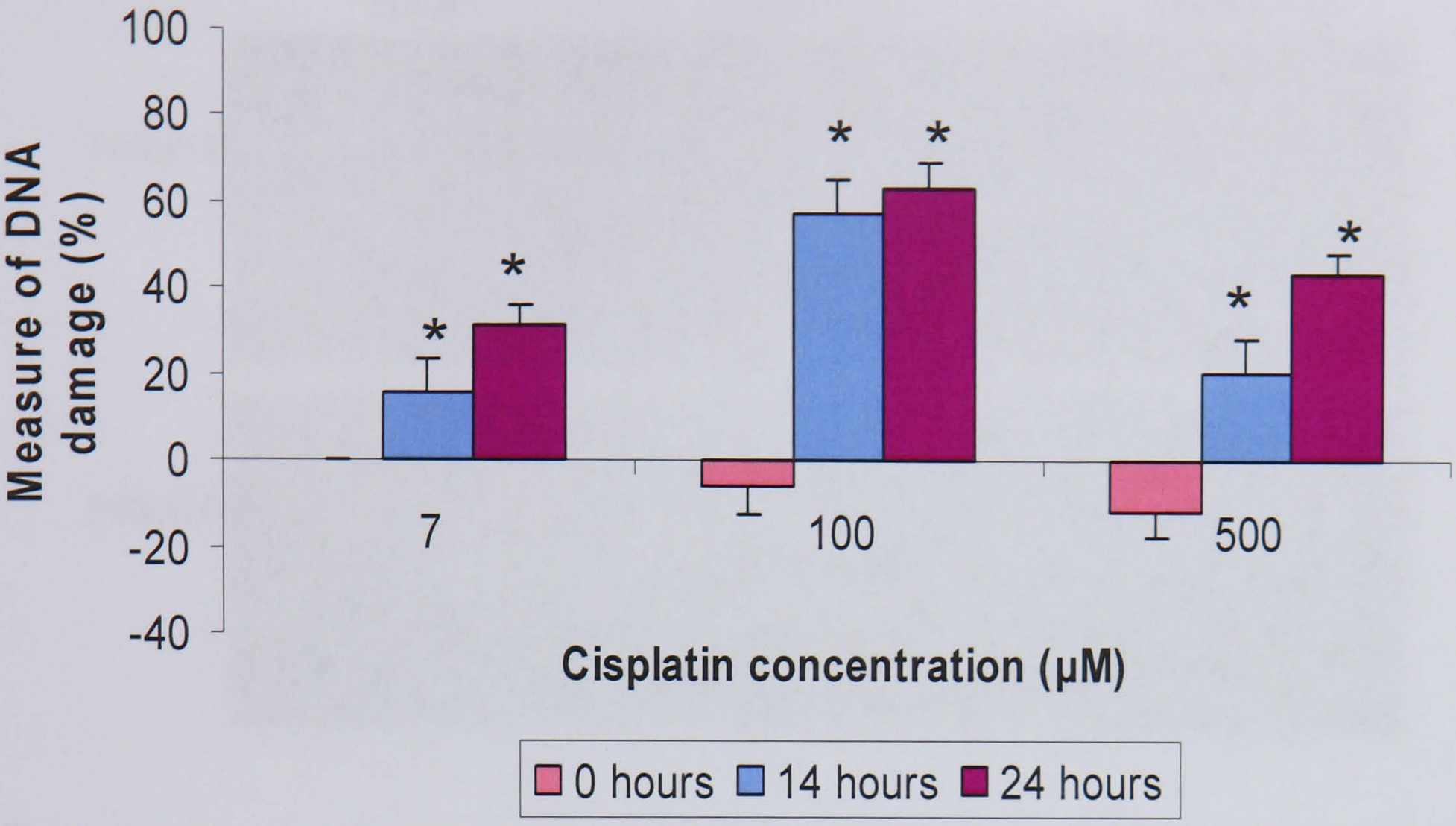

Figure 3.10 DNA strand breaks in cisplatin treated SHSY5Y cells. DNA strand breaks were measured immediately after a 2 hour exposure (pink), 14 hours later (blue) and 24 hours (purple) after 2 hour exposure by fluorescence detected alkaline DNA unwinding (FADU) assay. Data are mean +/- SEM from at least three experiments. Statistically significant differences towards the 0 hours after exposure treatment are marked by an asterisk ($p < 0.05$, ANOVA).

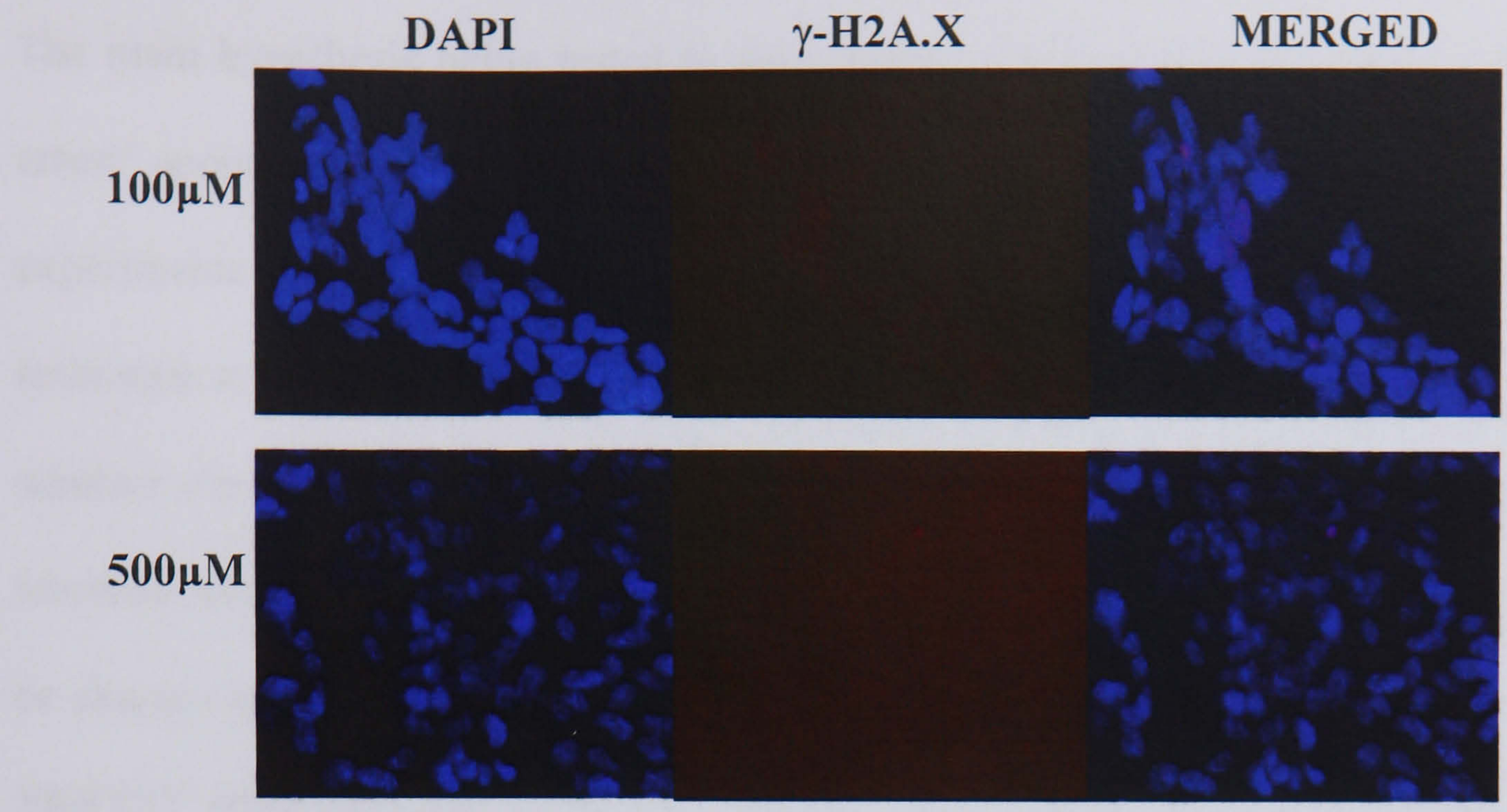

Figure 3.11 DNA damage response in cisplatin treated SHSY5Y cells. Cells were fixed after a 100 μM and 500 μM cisplatin treatment, immediately after a 2 hour exposure (A) and 24 hours after a 2 hour exposure (B) and stained with an antibody against the phosphorylated form of H2A.X (γ-H2A.X) and DAPI nuclear stain.

3.3.4 Cisplatin does not shorten telomeres in SHSY5Y cells

The main hypothesis being tested in this chapter was that cisplatin induces growth arrest/ apoptosis via the telomere/ telomerase complex. The aim of the following experiments was to determine telomere lengths using an in-gel hybridisation technique at various times after exposure of SHSY5Y cells to cisplatin and to find out whether cisplatin induced growth arrest/ apoptosis was preceded or accompanied by telomere shortening. In addition, non-specific degradation of DNA and the presence or absence of single strand breaks on the G rich telomeric strand was assessed. The SHSY5Y cells are a neuroblastoma cell line with telomere lengths of ~4 kbp. This cell line was chosen for this investigation as cisplatin is a conventionally used chemotherapeutic drug in the treatment of neuroblastoma.

SHSY5Y cells were exposed to cisplatin for either 2 hours (0, 7, 15, 100, 350 and 500 μM) or continuously (0, 0.5, 2, 5 μM). At 6, 24 and 48 hours after short exposure and 24, 48 and 72 hours after continuous exposure telomere restriction fragment lengths were assessed.

Figure 3.12 shows an example of typical data. Panel A illustrates images of ethidium bromide fluorescence from electrophoresis gels to indicate distribution of total cellular DNA and MW markers. The intensity signal was proportional to the amount of DNA loaded, which was kept constant throughout. Panel B demonstrates the telomere restriction fragment length gel. The calculated average telomere lengths are superimposed as white bars. Panel C shows the average of at least 3 separate determinations of mean telomere length plotted against time after exposure to a range of cisplatin concentrations. SHSY5Y cells exposed to cisplatin for 2 hours show no significant change in telomere length at any concentrations.

To assess the integrity of the total nuclear DNA, the telomere restriction fragment length gels were rehybridised with an interstitial minisatellite probe $(CAC)_8$ (Figure 3.13 A) and the average relative intensities of a high (L1) and a low (L2) molecular weight band, for at least three experiments were calculated (Figure 3.13 B). Degradation of DNA was not detected using this minisatellite marker.

Typical results for the presence of single strand breaks on the G rich telomeric strand after exposure to cisplatin for 2 hours are shown in Figure 3.14. There was no evidence of single stranded DNA breaks on the G rich telomeric strand for as long as 48 hours after treatment.

Similarly, after a continuous cisplatin treatment no telomere shortening was detected in the SHSY5Y cells (Figure 3.15), with no evidence of single stranded DNA damage on the telomeric G rich strand (Figure 3.16 A). The single stranded DNA telomeric G rich strand when reprobed with the interstitial minisatellite probe $(CAC)_8$ displayed no degradation of DNA (Figure 3.16 B).

A

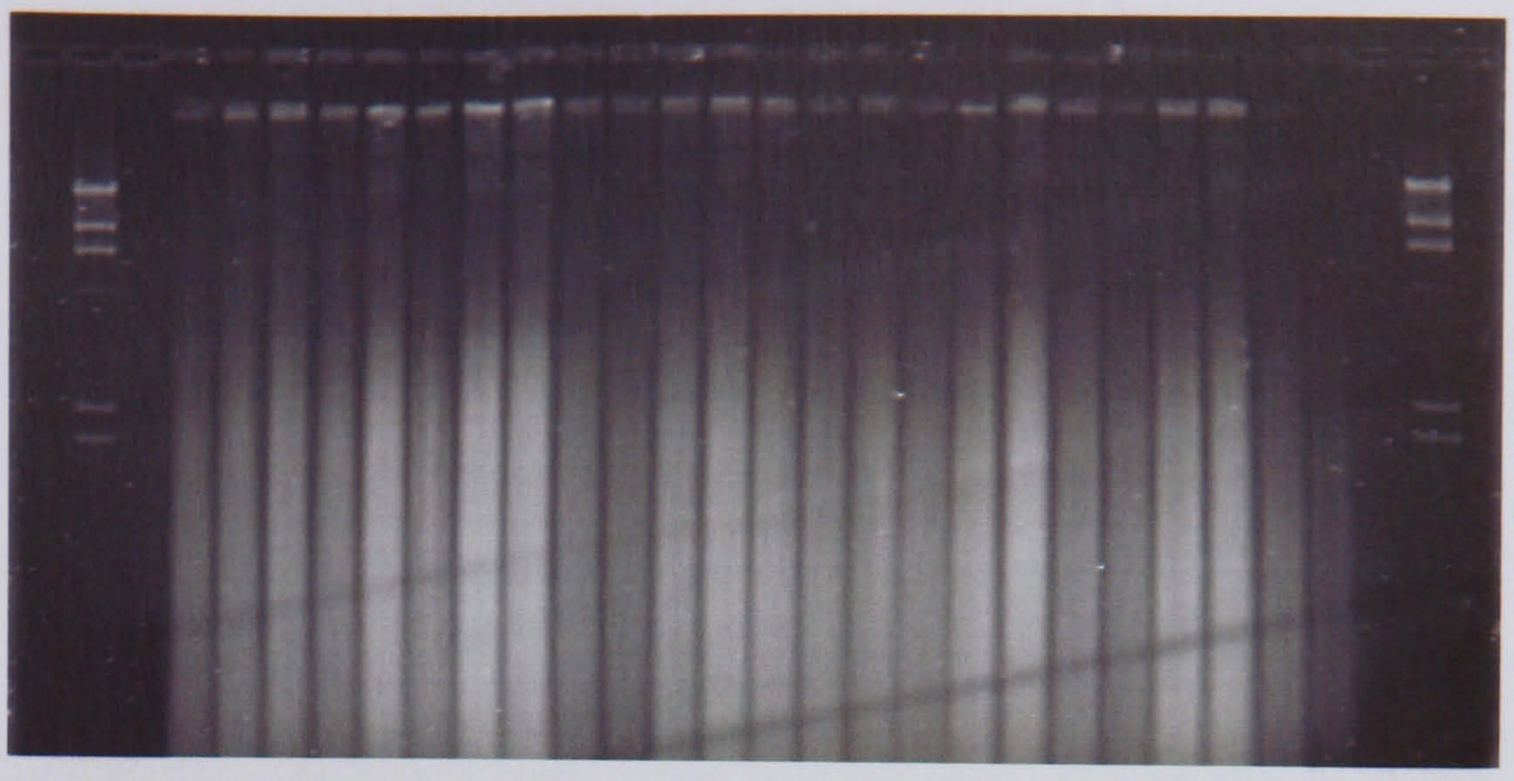

B

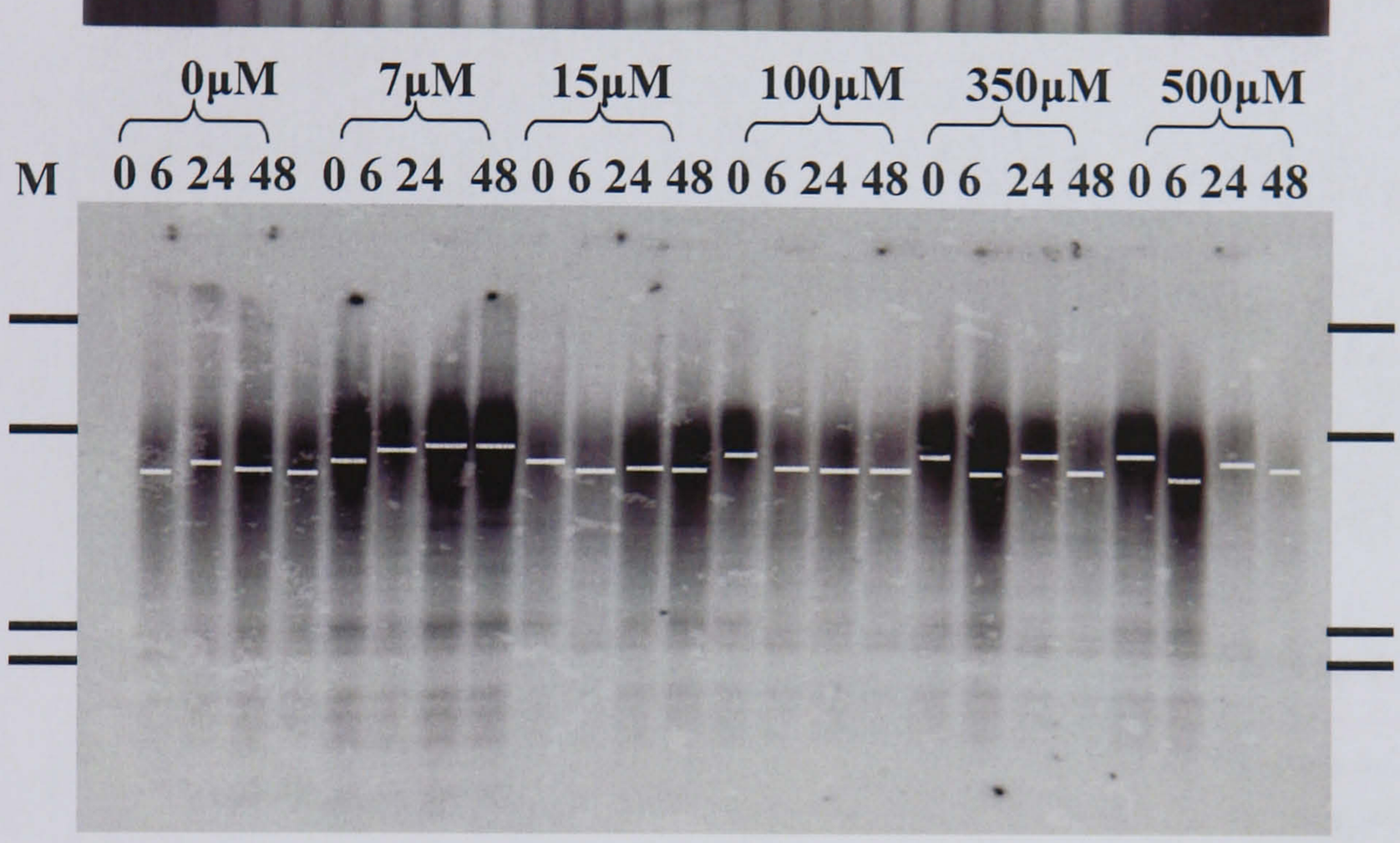

C

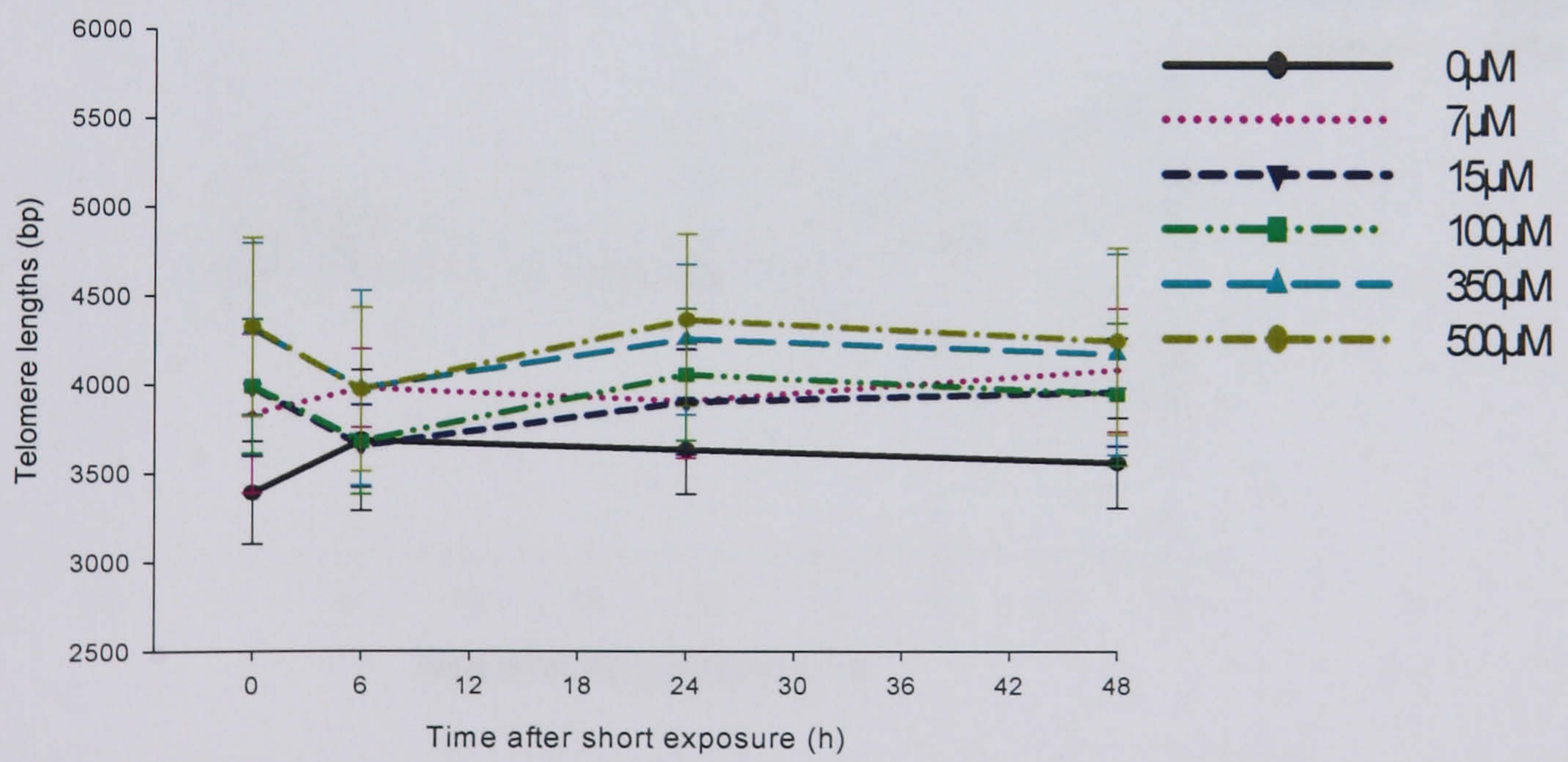

Figure 3.12 Telomere restriction fragment lengths after short exposure cisplatin treatment on SHSY5Y cells. (A) Ethidium bromide fluorescence of genomic DNA. (B) Telomere gel. Cisplatin concentrations (in μM) and times after onset of treatment (in h) are indicated on top of the figure. White bars indicate average telomere length. The positions of the size markers (23.1, 4.36, 2.32, 2.03 kbp) are shown by black bars. (C) Average telomere length. Gels were normalised to a standard and average fragment lengths of at least 4 experiments were calculated. Data are ± SEM.

A

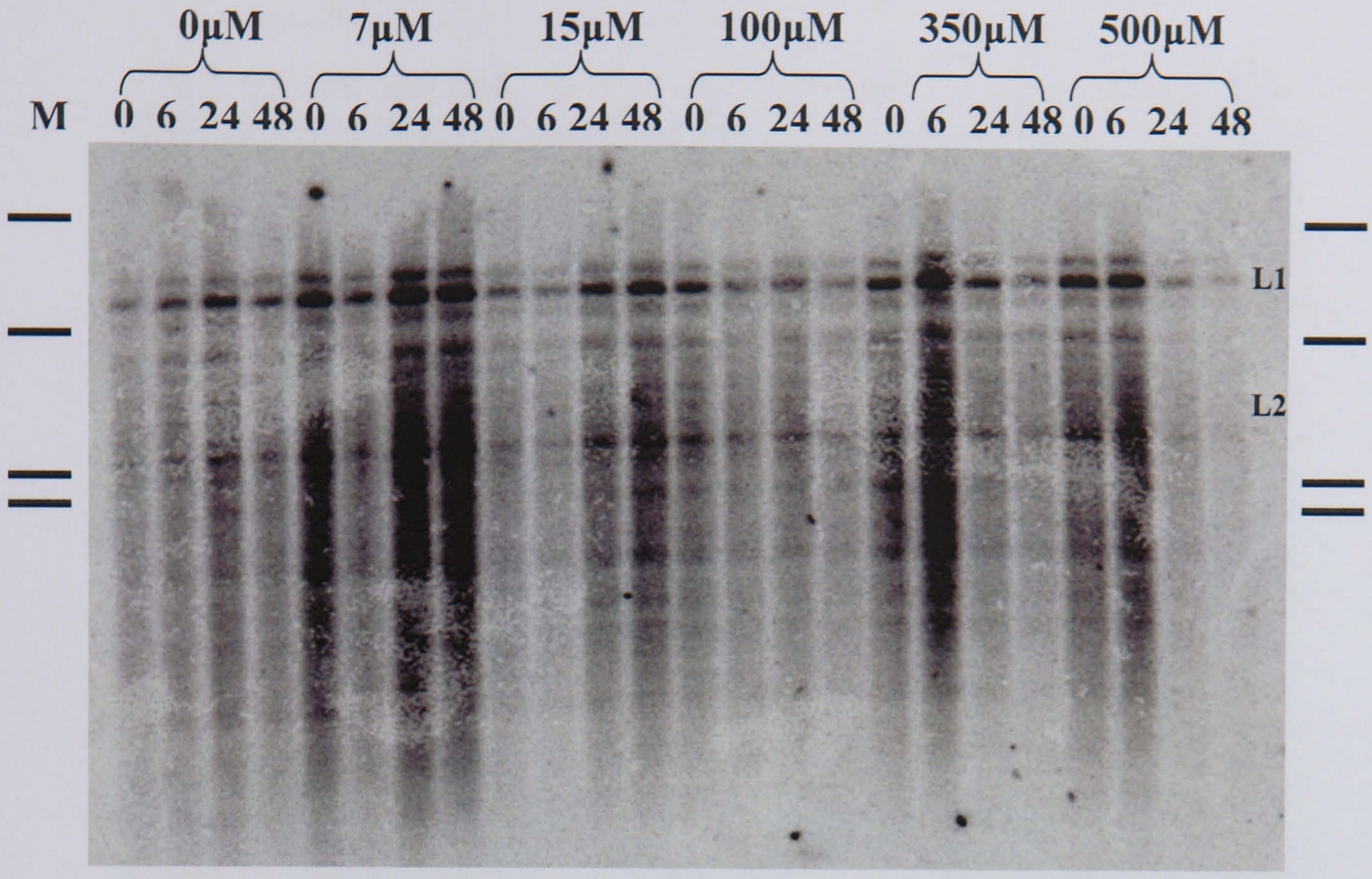

B

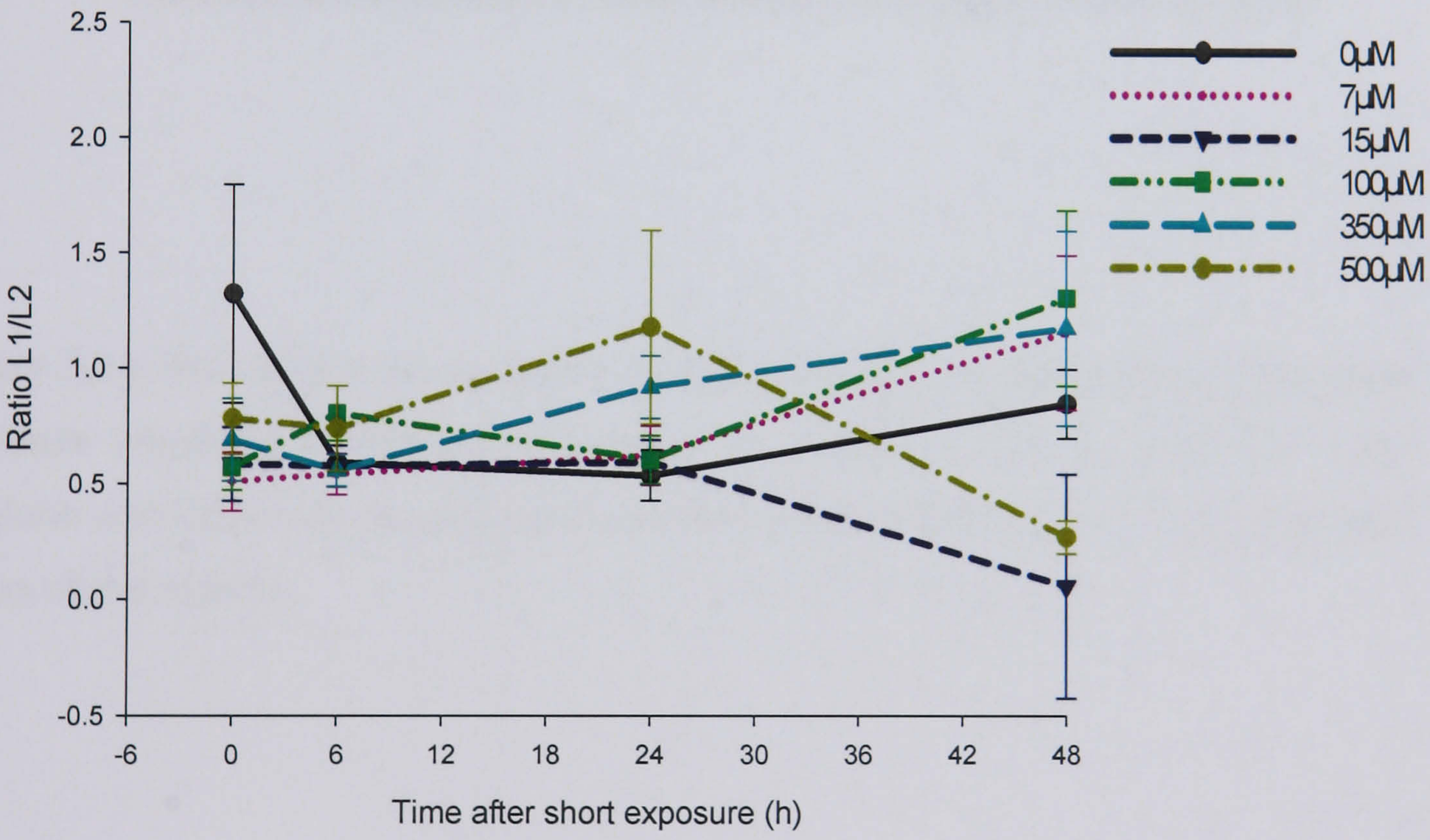

Figure 3.13 Determination of unspecific DNA degradation. Gels were rehybridised with $(CAC)_8$ minisatellite marker to test for unspecific DNA degradation (A). The positions of the size markers (23.1, 4.36, 2.32, 2.03 kbp) are shown by black bars. The intensity ratios between high (L1) and low molecular weight (L2) bands were compared over time and cisplatin concentration (B). Data are mean ± SEM from triplicate experiments.

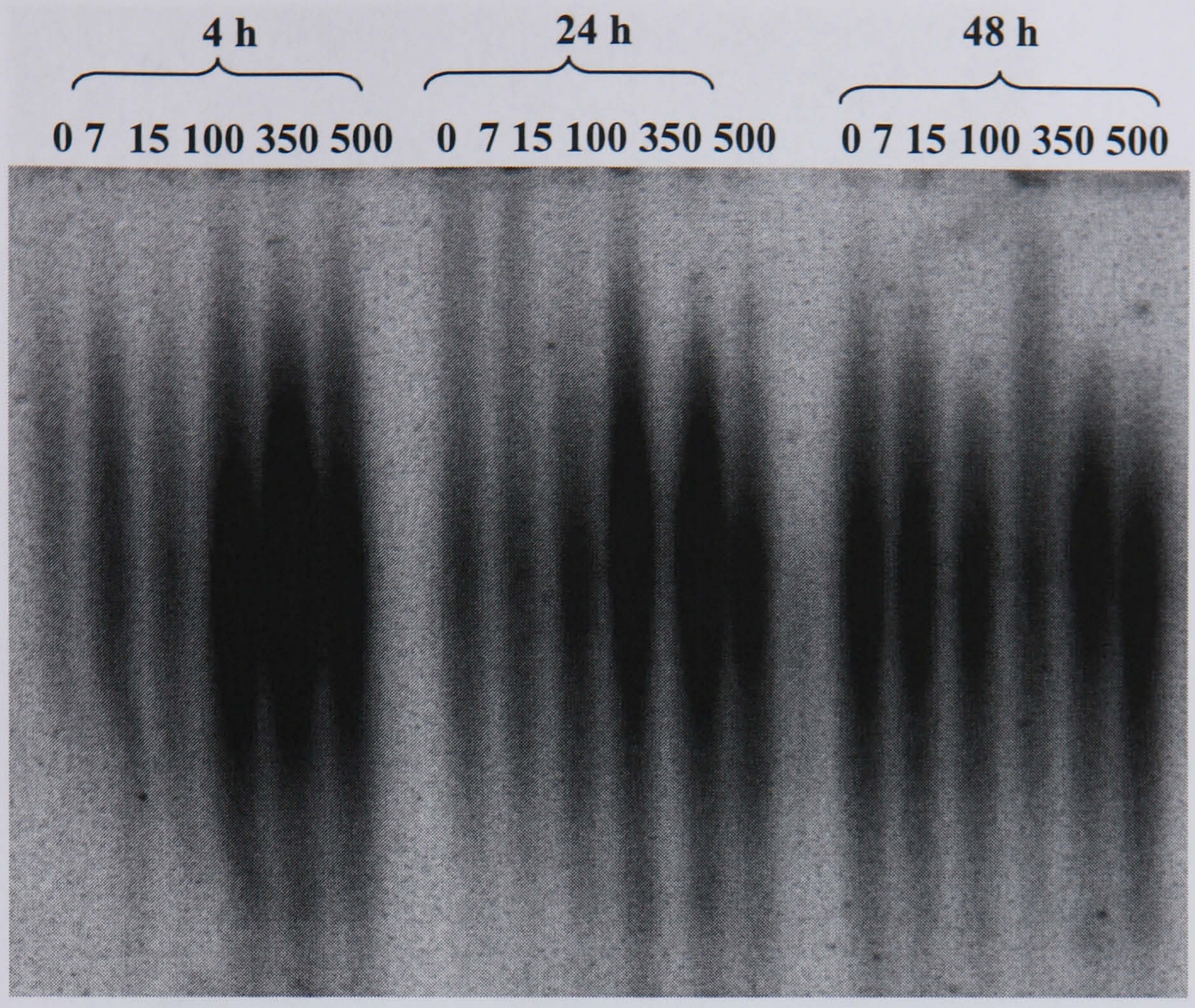

Figure 3.14 Denaturing gel to detect G rich telomeric strand breaks after short exposure cisplatin treatment. Examples of denaturing gel on SHSY5Y cells. Cisplatin concentrations (in μM) and times after onset of treatment (in h) are indicated on top of the figures.

A

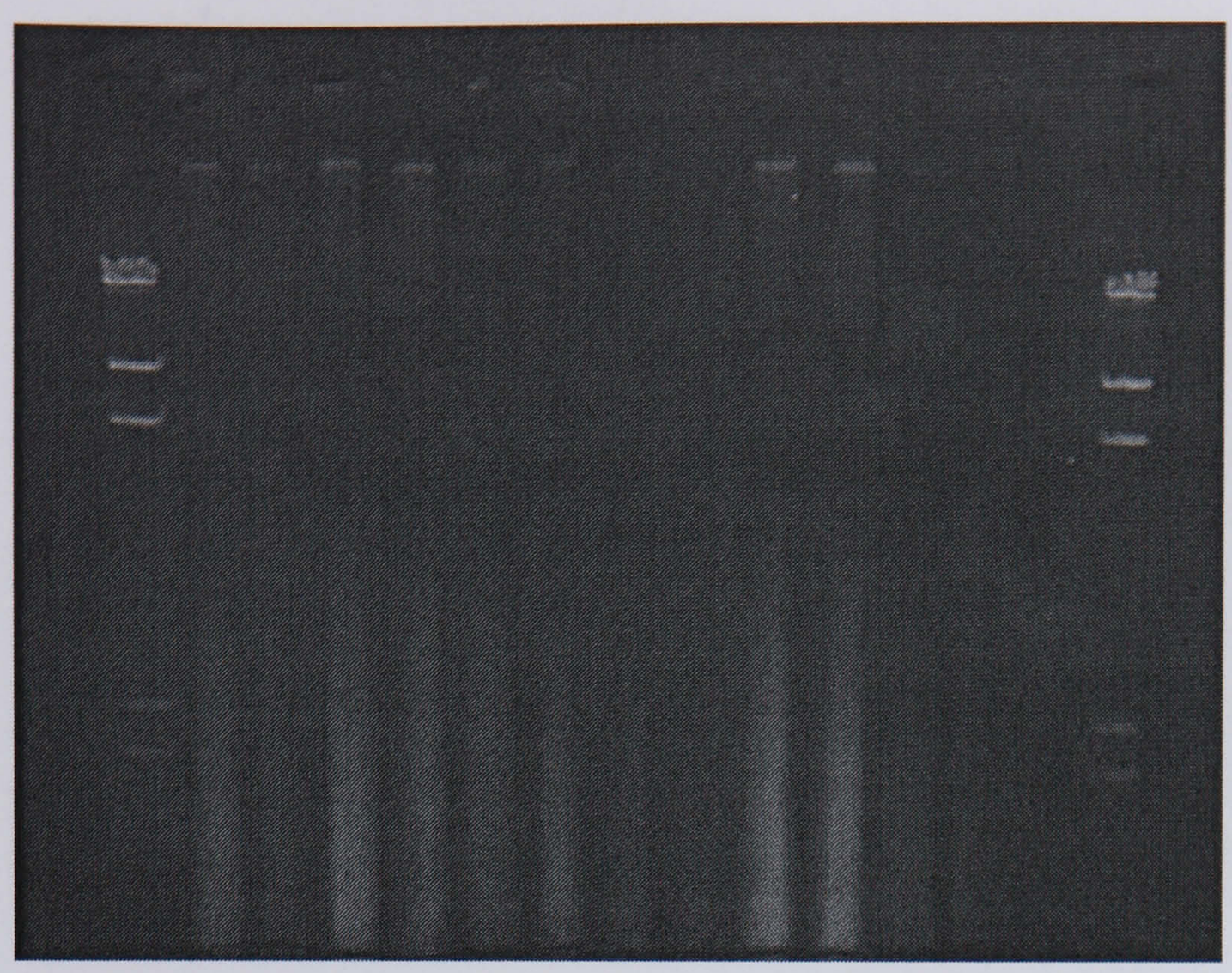

B

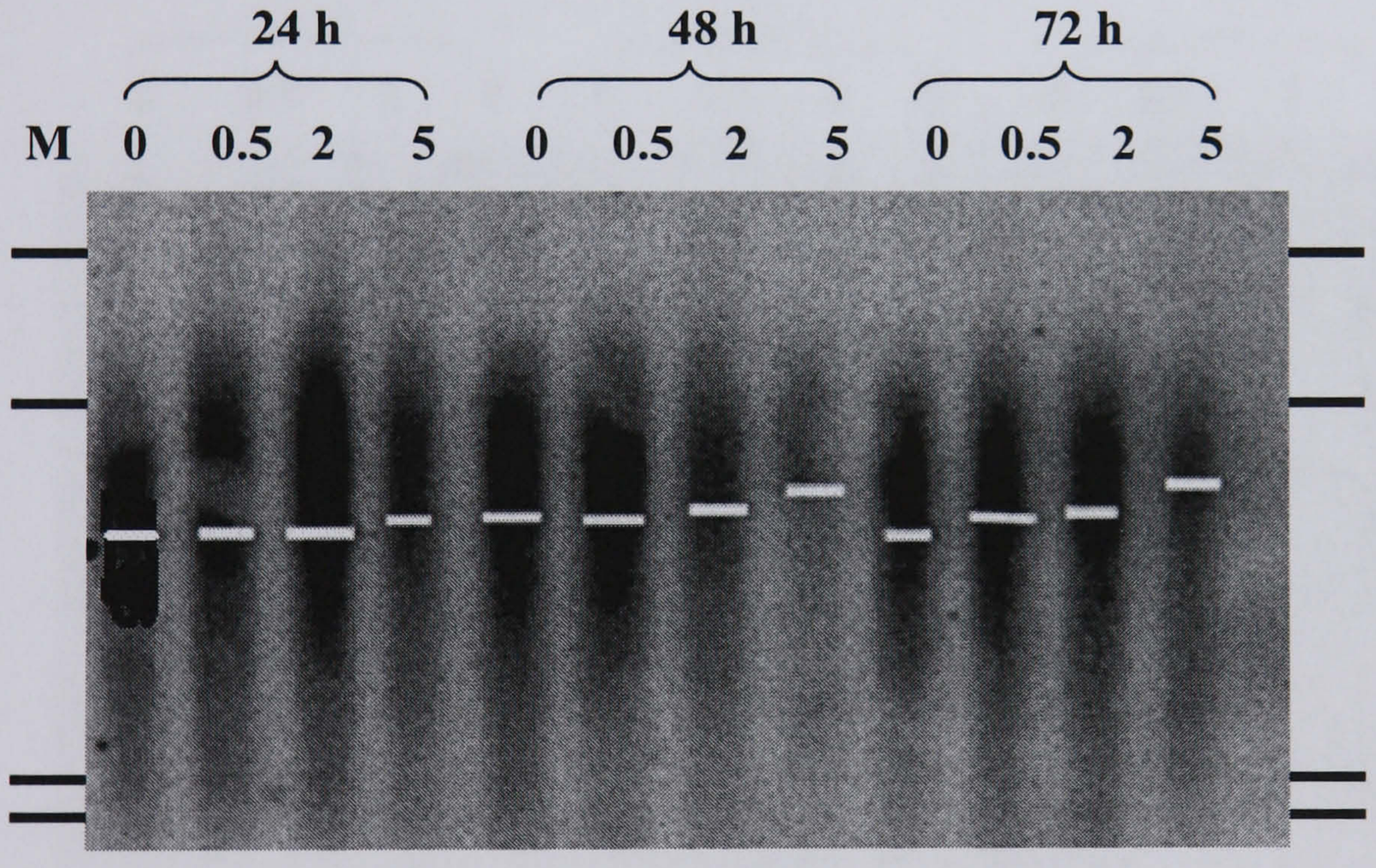

Figure 3.15 Telomere restriction fragment lengths after continuous exposure cisplatin treatment on SHSY5Y cells. (A) Ethidium bromide fluorescence of genomic DNA. (B) Telomere gel. Cisplatin concentrations (in μM) and times after onset of treatment (in h) are indicated on top of the figure. White bars indicate average telomere length. The positions of the size markers (23.1, 4.36, 2.32, 2.03 kbp) are shown by black bars.

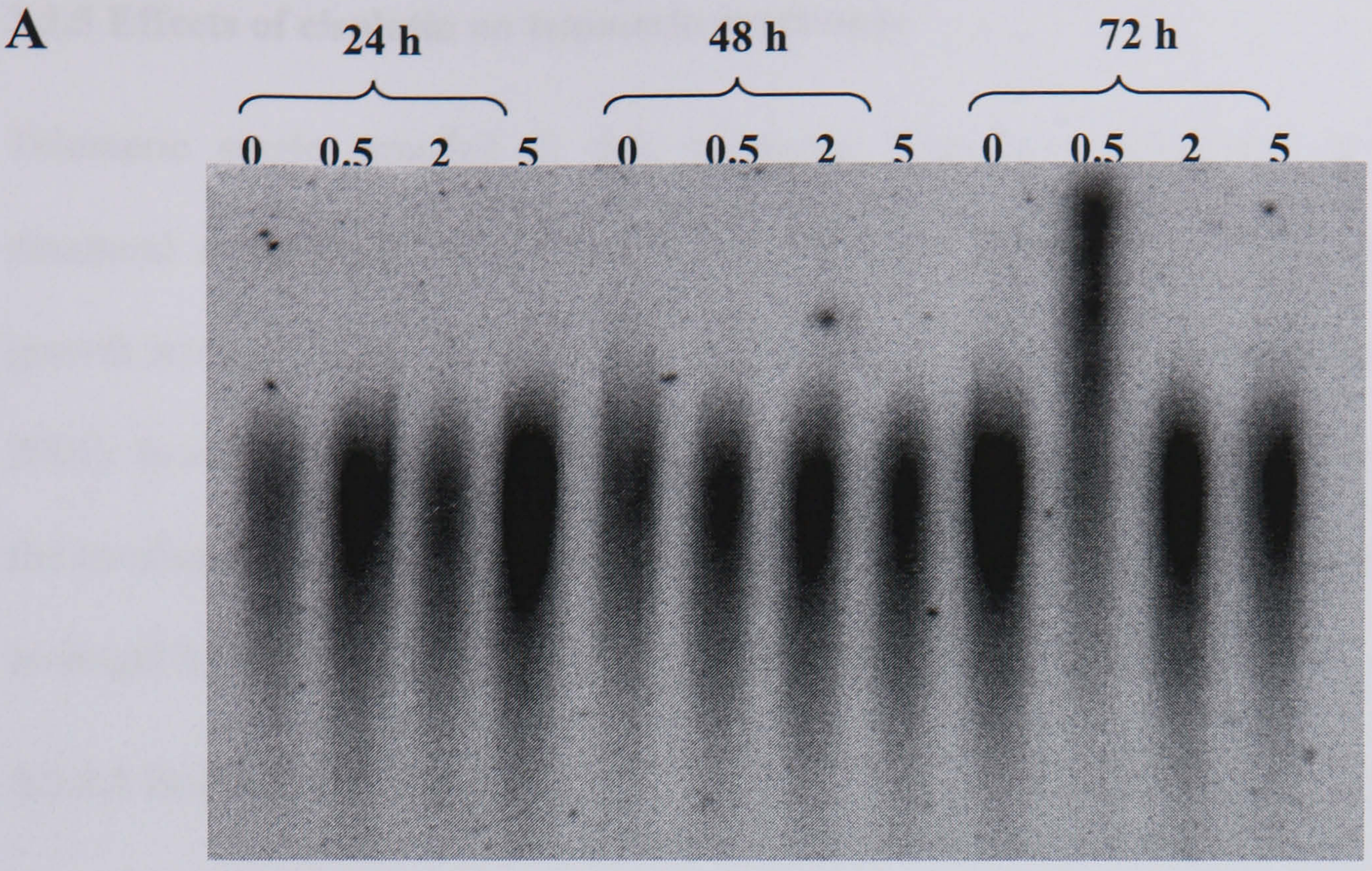

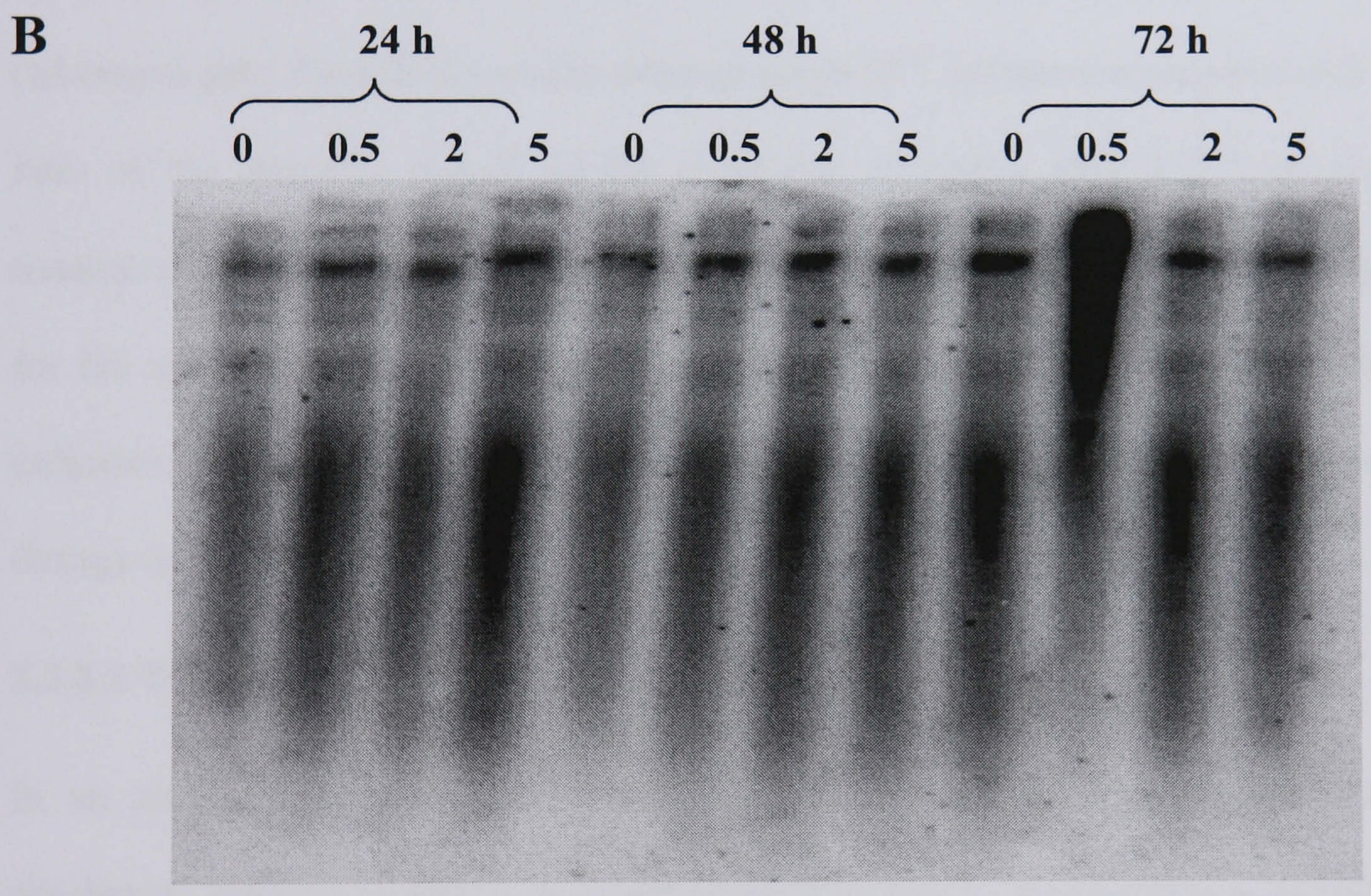

Figure 3.16 DNA degradation after continuous cisplatin treatment. (A) Denaturing gel to detect G rich telomeric strand breaks. (B) Gels were rehybridised with $(CAC)_8$ minisatellite marker to test for unspecific DNA degradation. Cisplatin concentrations (in μM) and times after onset of treatment (in h) are indicated on top of the figures.

3.3.5 Effects of cisplatin on telomeric overhangs

Telomeric single stranded G rich overhangs have been implicated in telomere structural maintenance (Griffith *et al.*, 1999) and generation of a DNA damage/ growth arrest response (Stewart *et al.*, 2003; Saretzki *et al.*, 1999; von Zglinicki *et al.*, 2001). In order to test whether cisplatin treatment might interfere with the integrity of the overhangs, the effect of exposure to cisplatin on the overhangs was examined by an in-gel hybridisation technique and a telomere isolation procedure.

3.3.5.1 In-gel hybridisation

Figure 3.17 shows typical data of overhang length measurements by in-gel hybridisation. Panel A illustrates probed non denatured (overhang) and denatured (telomere) gels. Panel B shows the average graph of 3 independent experiments of the ratio of the intensity signals of the overhang/ telomeres after a 2 hour cisplatin treatment. The ratio of non denatured/ denatured hybridisation signals was the same for the untreated compared to cells exposed to 500 μM cisplatin for 2 hours. This indicates that, at least under these conditions, SHSY5Y cells showed no significant change in overhang lengths.

3.3.5.2 Telomere isolation

In an alternative approach to investigating the effects of cisplatin on telomeric overhangs, isolated telomeres were extracted from restriction digested genomic DNA (supernatant) by a streptavidin coated magnetic bead approach with biotinylated oligonucleotides complimentary to the G-rich telomeric strand.

To purify telomeric DNA, isolated telomeres were extracted from restriction digested genomic DNA (supernatant) and were detected by being run on a pulsed field gel, then hybridised using a telomere specific probe (Figure 3.18 A). The procedure

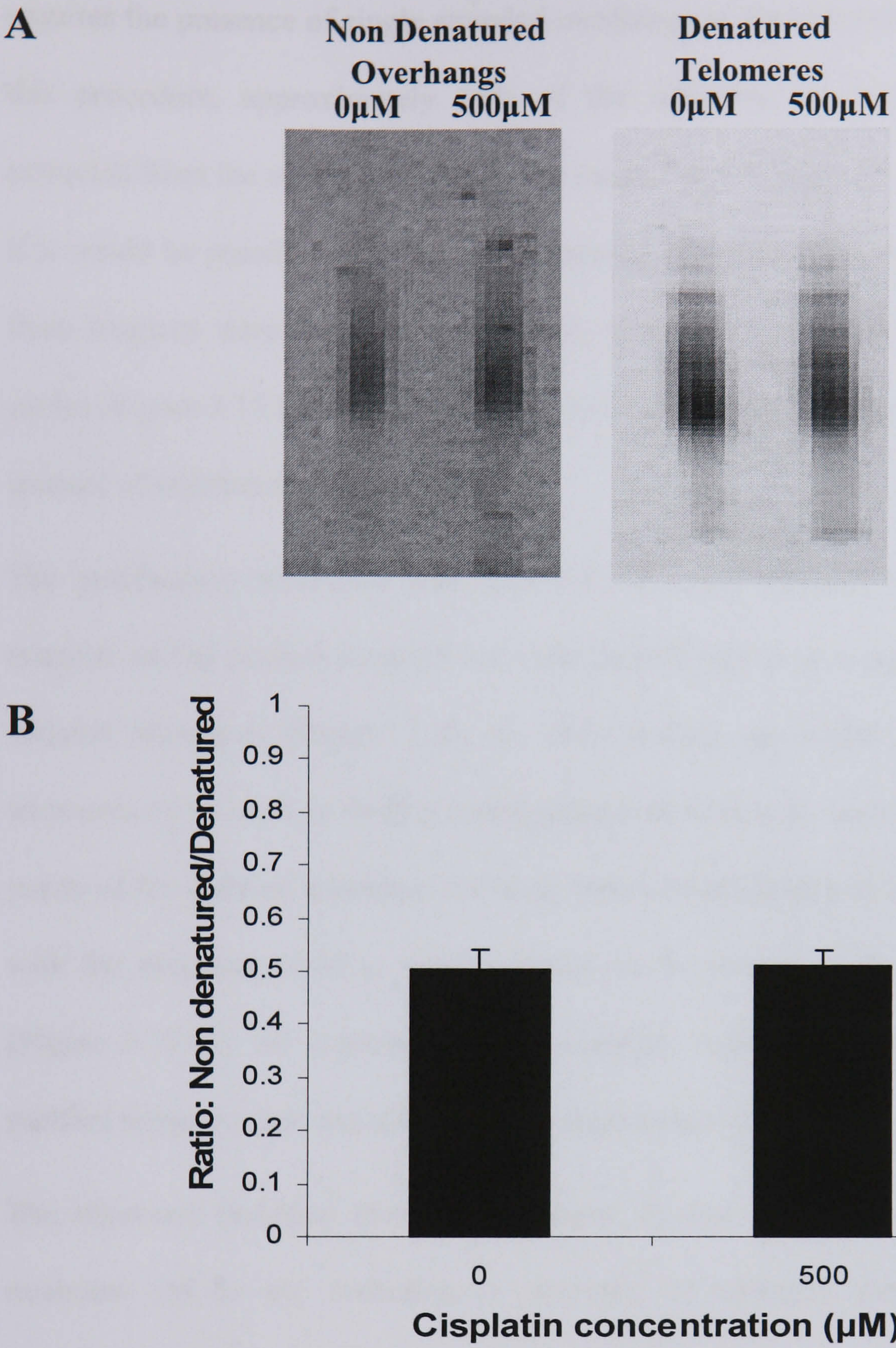

Figure 3.17 Telomeric G rich overhangs in SHSY5Y cells after short exposure cisplatin treatment. 2 hours after treatment with either 0 or 500 µM cisplatin a $(CCCTAA)_6$ probe was hybridised to a non denatured gel to detect G rich overhangs (left) and again to the same gel after DNA denaturation (right) to detect whole telomeres (A). The intensity ratios of non denatured/ denatured signals are compared after treatment to control (B).

requires the presence of single stranded overhangs at the telomeres in solution. Using this procedure, approximately 50% of the telomeric restriction fragments were extracted from the supernatant (Compare lanes 2 and 3, Figure 3.18 A). To determine if it would be possible to isolate the remaining telomeric DNA from the supernatant, fresh reagents were added and the whole procedure repeated a number of times in cycles (Figure 3.18 B). Repeating the procedure resulted in further isolation of a small amount of additional telomeric DNA.

The purification procedure was modified by using different amounts of starting material and up scaling reagents and cells accordingly to give an increase in yield of isolated telomeres (Figure 3.19 A). This scaling up would enable the isolated telomeres to be used in further investigations described in Section 3.3.6. To test the purity of the isolated telomeres the blots were rehybridised with a minisatellite probe with the sequence $(CAC)_8$, which should not be present in the purified telomeres (Figure 3.19 B). As expected, the minisatellite sequence was not detected in the purified telomeres but was present in the supernatant DNA.

The telomeric isolation procedure (Chapter 2) was used to determine if cisplatin treatment led to any reduction in recovery of telomeric DNA isolated by the hybridisation procedure (Figure 3.20). Any such reduction could indicate a drug-induced loss of single strand overhangs. SHSY5Y cells were treated with a short exposure treatment to either 100 μM or 500 μM cisplatin, the DNA was isolated and the telomeric DNA purified (Figure 3.20 A). The ratio of intensities of hybridisation signals for telomeres remaining in the supernatant (S) to telomeres isolated (T) was similar in drug treated and control cells (Figure 3.20 B). In conclusion, cisplatin treatment even at high concentrations does not induce degradation of the single stranded G rich telomeric overhang.

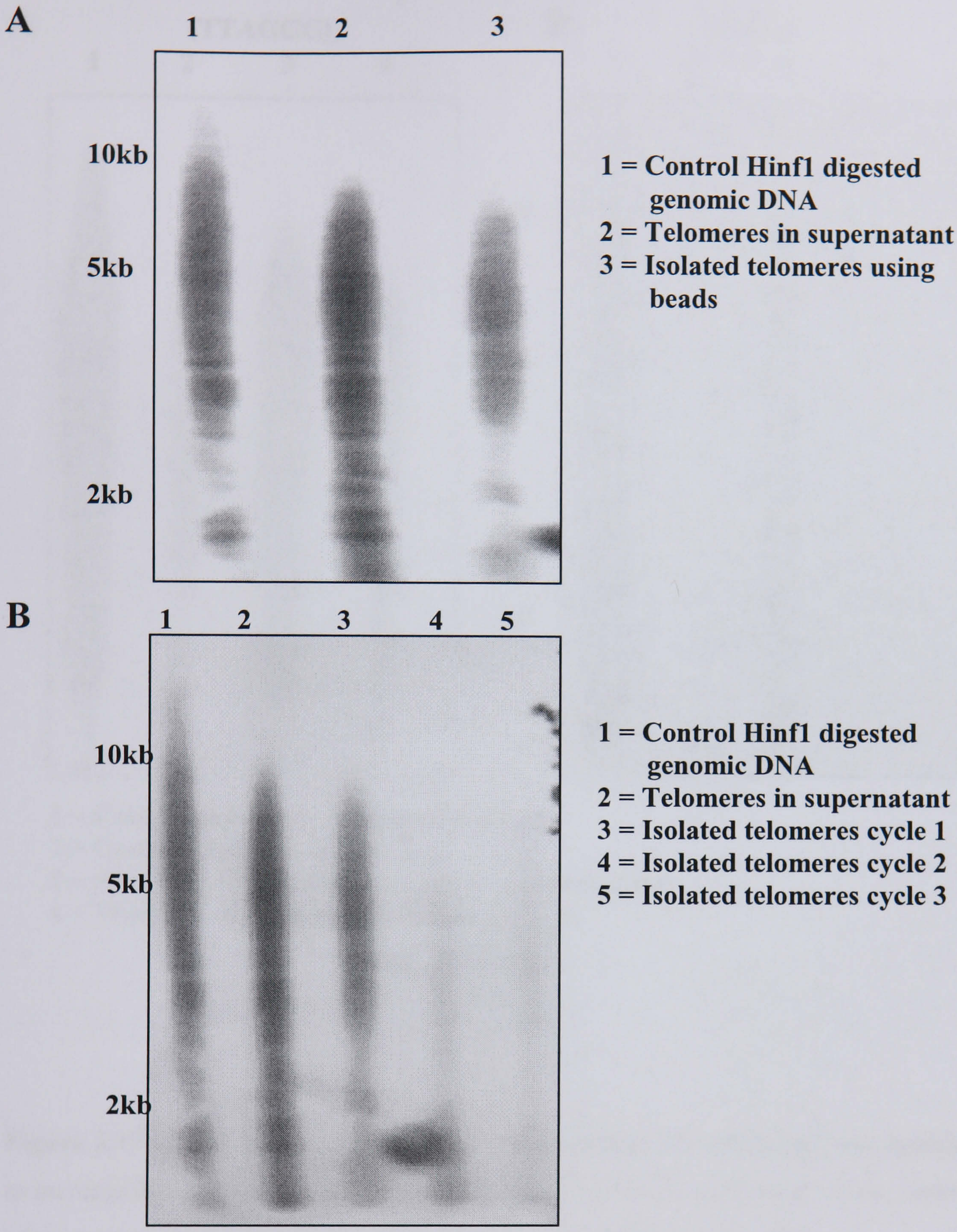

Figure 3.18 Telomeric DNA isolation. Telomeres were captured by solution hybridisation of single stranded G rich overhangs to magnetic bead coupled oligonucleotides and eluted from the magnetic beads. Samples were analysed by pulsed field gel electrophoresis, blotted, denatured and then hybridised with a telomere specific probe (A). Purification of the remaining telomeres in the supernatant using further cycles of the isolation procedure (B).

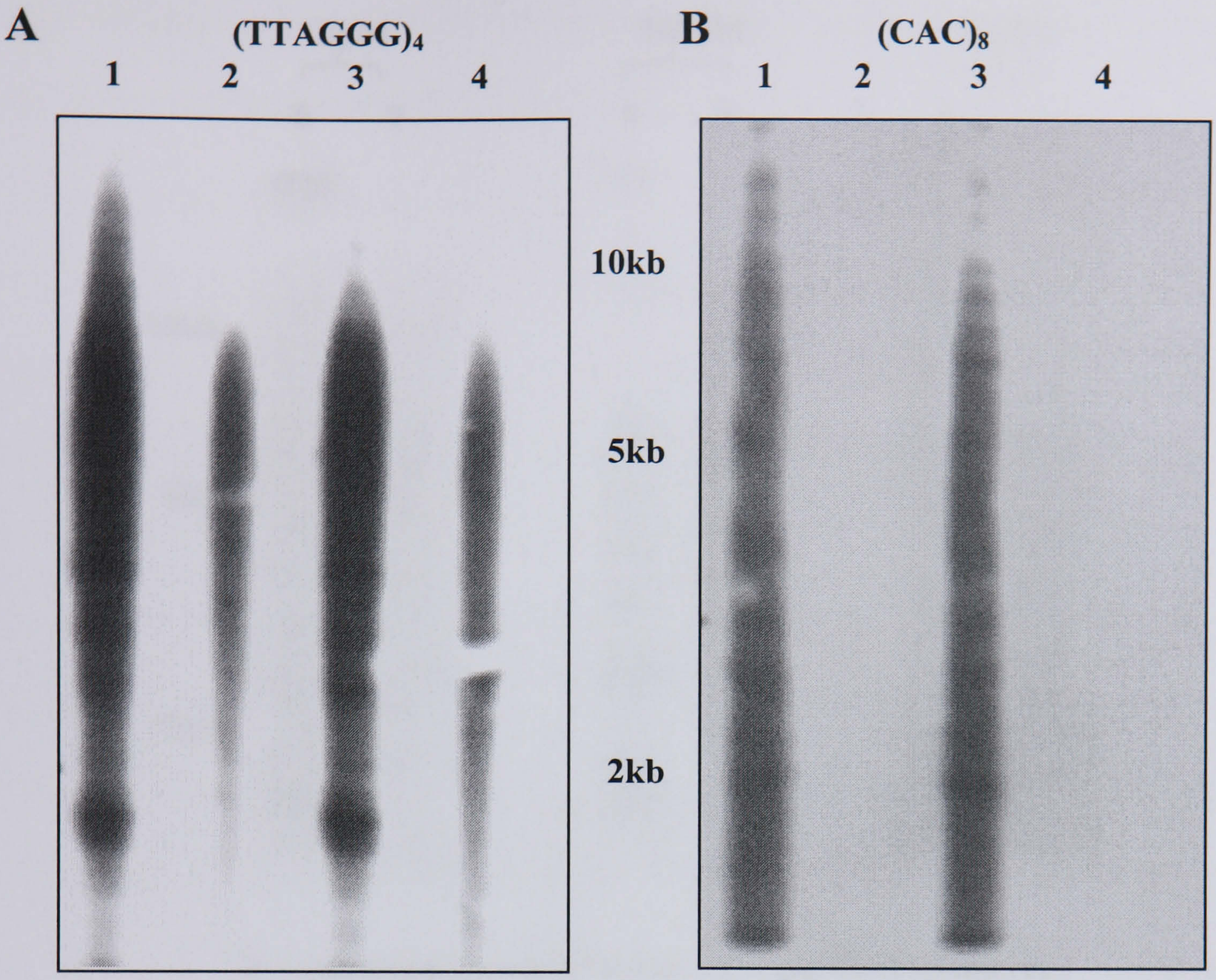

1 = Control: telomeres in supernatant
2 = Control: isolated telomeres
3 = Modified experiment: telomeres in supernatant
4 = Modified experiment: isolated telomeres

Figure 3.19 Modification of telomeric DNA isolation. The procedure was modified to increase the quantities of telomeric DNA (A). Confirmation of purity of the isolated telomeres by rehybridising blots with $(CAC)_8$ minisatellite marker (B).

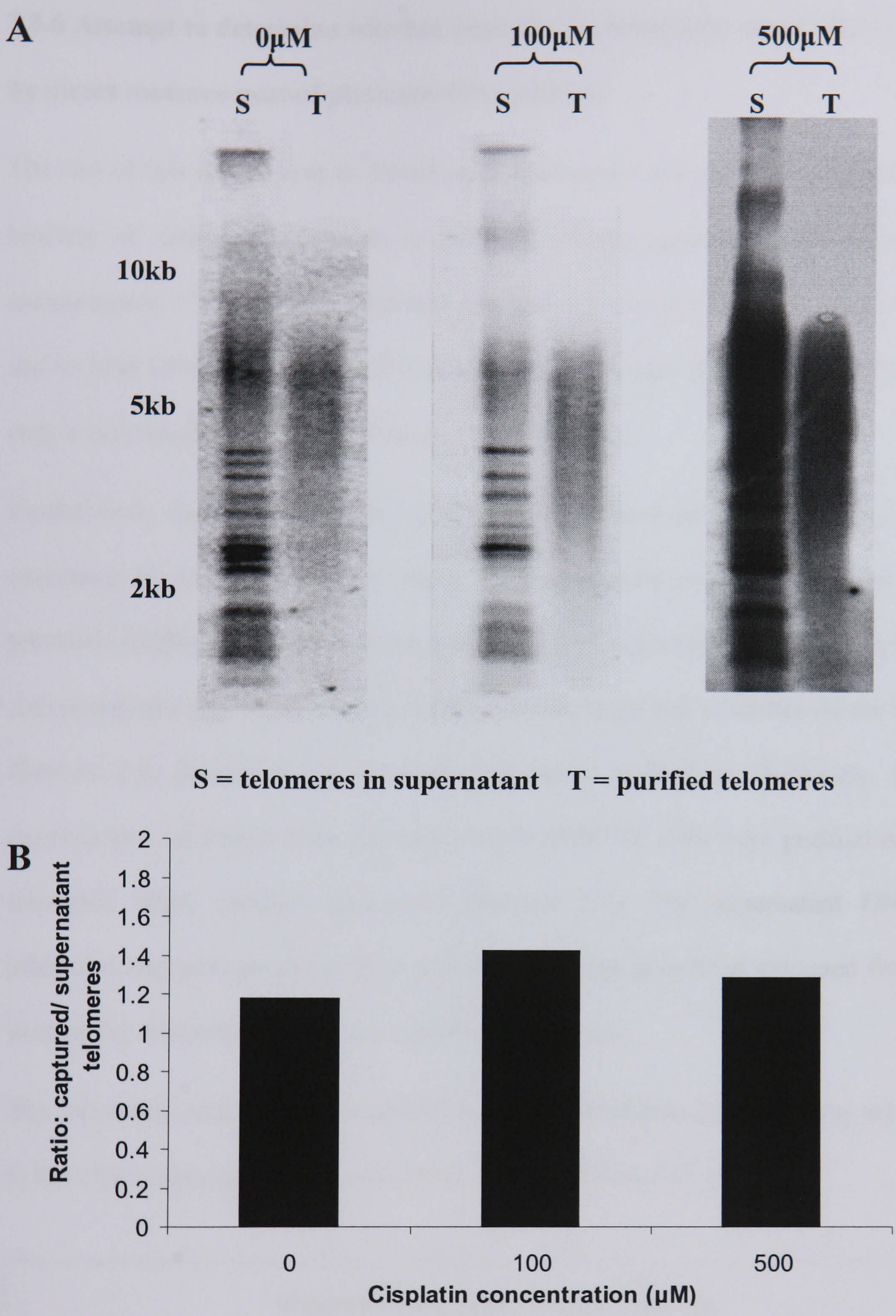

Figure 3.20 Telomeric DNA isolation after treatment with short exposure to cisplatin. (A) 2 hours after a short exposure cisplatin treatment with the indicated concentrations, telomeres were captured by solution hybridisation of single stranded G rich overhangs to magnetic bead-coupled oligonucleotides. (B) The ratio of isolated telomeres (T) to those remaining in the supernatant (S).

3.3.6 Attempt to determine whether cisplatin preferentially targets the telomeres by direct measurement of platinum-DNA adducts

The aim of this section was to determine if telomeres were preferential targets for the binding of cisplatin compared to the rest of the genomic DNA directly, by measurement of the levels of platinum that became bound to isolated telomeric DNA and to total DNA. As telomeric DNA constitutes around 0.01% of all genomic DNA, only a very small yield of this material was anticipated.

Furthermore, the levels of Pt that become bound to the total DNA following relevant exposures to cisplatin are very small. Therefore, measurement of adducts on the telomeric fragments would require quantification of extremely low levels of platinum. An appropriate high sensitivity of detection of platinum was available via the ICP-MS (Section 2.8) facility in the Geology Department at Durham University. In these experiments, telomeres from cisplatin treated SHSY5Y cells were purified using the telomeric DNA isolation procedure (Section 2.7). The supernatant DNA (the restriction digested genomic DNA that the telomeres have been extracted from) was used as the comparison DNA (i.e. rest of the genome).

The following calculation indicates the amount of telomeric DNA that was anticipated to have been obtained from 1 mg of total genomic DNA (10^8 cells).

Mean telomere repeat length = 5000 bp

As there are 92 telomeres per cell= 4.6×10^5 bp per genome

Genome size= 3×10^9 bp

Thus proportion of genome in telomere fragments= $4.6 \times 10^5 / 3 \times 10^9 = 1.53 \times 10^{-4}$

Therefore 1 mg of DNA contains:

1×10^{-3} g x 1.53×10^{-4} = **153 ng** of telomeric fragment

For the telomere isolation procedure, a maximum of 300 μg of total genomic DNA was used as starting material and it was anticipated from this that at least 30% of all telomeres were expected to be isolated.

Therefore 1 mg DNA = ~ 153 ng telomeric fragment

300 μg DNA = ~ 45 ng telomeric fragment

30% yield = ~ 13.5 ng telomeric fragment

The following calculation indicates the expected level of Pt in 13.5 ng of telomeric DNA (the anticipated yield from 300 μg of total genomic DNA).

If adduct level were 500 nmoles Pt/g DNA then assuming that adduct levels on telomeric DNA are similar to overall genome:

13.5 ng telomeric DNA would carry $13.5 \times 10^{-9} \times 500 \times 10^{-9} = 6.75 \times 10^{-15}$ moles Pt

At mass of Pt = 195

Therefore 6.75×10^{-15} moles Pt = $6.75 \times 10^{-15} \times 195 = 1.3 \times 10^{-12}$ g Pt

If dissolved in 0.1 ml water the concentration of Pt would be:

1.3×10^{-12} g Pt in 0.1 g = 13×10^{-12} g per g = **13 PPT**

It is essential to accurately quantify the concentration of DNA as well as Pt because adduct levels must be calculated as the ratio of the two values. It was not possible to measure the concentration of the purified telomeres by UV spectrophotometry due to low sensitivity of this method for small amounts of DNA. Additionally, the use of fluorescent intercalating dyes would have utilised DNA for estimation of concentration. The dye-DNA mixtures could not be re-utilised for Pt measurement because of the risk of the introduction of Pt contamination. Consequently, phosphorus was measured in the samples simultaneously with platinum as a method to accurately

calculate DNA concentration. In the past, chemical measurement of phosphorus has been used to provide definitive measurements of concentration of large quantities of DNA. However, for determination of low concentrations of DNA by ICP-MS, the presence of background levels of P exists as a serious problem since P is present in many commonly used solutions.

The telomeric DNA isolation procedure requires a buffer in which to dissolve the genomic DNA and a buffer to elute the telomeres from the magnetic beads (Section 2.7). These buffers are composed of 1x SSC/ 1% Triton X-100 and 0.1x SSC/ 1% Triton X-100 respectively. When extracting telomeric DNA for ICP-MS, these buffers or components in them may cause interference and high background levels of phosphorus or platinum. Therefore a variety of alternative buffers (Table 3.1) were examined for use in the telomere isolation procedure. The isolated supernatant and telomeric DNA were initially analysed by hybridisation to see whether or not the yield of telomeres purified varied from the possible buffer combinations (Section 2.7). The alternative buffers gave similar levels of isolated telomeres compared to the initial buffers used. Samples to be analysed for the ICP-MS were prepared in triplicate in a series of dilutions in 3.5% nitric acid and incubated overnight at 70°C (Section 2.84).

The variety of buffer and buffer components were measured by ICP-MS in two independent experiments to see if any of them contained high levels of P (in the absence of DNA) which would subsequently give inaccurate calculations for the concentration of DNA (Table 3.2). High purity water from Durham University that was known to be suitable for ICP-MS was used throughout for the DNA extraction and isolation of telomeric DNA procedures to avoid the risk of contamination.

Table 3.1 Combination of buffers tested in the telomere isolation procedure

	Buffers	
	Supernatant Dissolved In	**Telomeres Eluted In**
1	1 x SSC/ 1% Triton X-100	0.1 x SSC/ 1% Triton X-100
2	TE buffer	TE buffer
3	TE buffer	B & W buffer
4	1 x TBS pH= 8.5	1 x TBS pH= 8.5
5	EDTA buffer	EDTA buffer
6	1 x TBS pH= 8.5	EDTA buffer
7	Sodium acetate buffer	Sodium acetate buffer
8	1 x TBS pH= 8.5	Sodium acetate buffer
9	B & W buffer	EDTA buffer
10	B & W buffer	Sodium acetate buffer

Samples were also diluted in a very pure nitric acid which was again obtained from the ICP-MS facility at Durham University. High levels of P were detected in samples of reagents and the levels of P measured in samples varied between experiments (Table 3.2). This suggested that contamination of P had occurred, presumably related to the widespread use of phosphate buffers and detergents in biological laboratories. Furthermore, P suffers from many spectral and isobaric interferences in ICP-MS measurements and these can severely impair the detection limit.

From the results from Table 3.2, the buffers and solutions that induced high levels of P were eliminated from the telomere isolation procedure and the risk of contamination was kept at a minimum in the preparation steps.

Purified telomeres were isolated from cisplatin treated and untreated DNA and the samples measured using the ICP-MS for both Pt and P levels. The procedure for isolation of telomeres began with 300, 90 or 30 μg of genomic DNA. Telomeric DNA and remaining genomic DNA were isolated from these quantities and assessed by ICP-MS (Table 3.3).

Table 3.2 Measurement of phosphorus levels in buffers used in telomeric DNA isolation procedure using ICP-MS

		Experiment 1	Experiment 2
Sample	**Dilution Factor**	**Phosphorus Levels/ ppb**	**Phosphorus Levels/ ppb**
Special water from Durham	10	12.63	32.61
Special water from Durham	20	9.56	32.5
Special water from Durham	100	12.37	29.11
Nitric Acid from Durham	0	28.38	31.34
100% Triton	10	107.84	821.34
100% Triton	20	1196.47	517.71
100% Triton	100	486.49	216.15
1% Triton/ 1x SSC	10	19.09	57.21
1% Triton/ 1x SSC	20	10.73	48.06
1% Triton/ 1x SSC	100	8.23	34.33
1% Triton/ 0.1x SSC	10	18.24	66.07
1% Triton/ 0.1x SSC	20	13.04	53.27
1% Triton/ 0.1x SSC	100	6.83	32.91
1 x SSC	10	9.47	38.45
1 x SSC	20	11.38	32.37
1 x SSC	100	13.45	35.21
1 x TBS pH=7	10	8.13	34.24
1 x TBS pH=7	20	9.19	32.56
1 x TBS pH=7	100	18.9	35.81
1 x TBS pH=8.5	10	13.04	21.34
1 x TBS pH=8.5	20	16.1	26.43
1 x TBS pH=8.5	100	11.45	34.93
B& W Buffer	10	4.13	156.78
B& W Buffer	20	8.32	95.83
B& W Buffer	100	8.41	60.32
EDTA buffer	10	66.19	33.77
EDTA buffer	20	45.64	30.69
EDTA buffer	100	23.46	32.25
10mM EDTA	10	9.54	114.78
10mM EDTA	20	17.14	32.8
10mM EDTA	100	12.62	58.68
Sodium acetate buffer	10	64.87	36.23
Sodium acetate buffer	20	31.13	36.33
Sodium acetate buffer	100	20.85	33.3
80mM NaOAc	10	8.1	124.13
80mM NaOAc	20	9.63	110.29
80mM NaOAc	100	8.69	53.76
100% Formamide	10	113.25	25.5
100% Formamide	20	34.27	32.74
100% Formamide	100	32.58	11.59

Telomeric DNA and remaining genomic DNA were prepared from control cells (untreated) using a variety of buffers to estimate the range of background levels of Pt and to assess use of P for quantifying DNA (Table 3.3).

Telomeric DNA and remaining genomic DNA that were extracted from cells that had been incubated for 2 hours with high concentrations of cisplatin were analysed on the ICP-MS. This was undertaken using the combination of buffers (supernatant dissolved in B & W buffer and telomeres eluted in EDTA buffer) which gave a similar yield to the initial buffers used in the isolation procedure (≤ 50%) when assessed on a southern blot (Section 2.7) and low background levels of Pt and P (Table 3.3).

Table 3.3 shows that Pt and P levels for the treated telomeric DNA were very low even when the initial starting amount of DNA was 300 μg and would not be distinguishable from background levels using the ICP-MS. For that reason a high resolution instrument, Plasma Ionisation Multicollector Mass Spectrometer (PIMMS) was used which had a higher sensitivity to lower levels of Pt and P.

The calculations outlined above indicated that Pt levels in solutions of isolated telomeric DNA could be up to about 13 PPT. Using PIMMS, these levels of Pt on the telomeric DNA after cisplatin treatment would have been easily detectable (See Table 3.3).

Table 3.3 Total Pt concentration determined from measurement of Pt 195 and P concentration on cisplatin treated and untreated telomeres/ supernatant using a combination of buffers

	Dilution Factor	Pt 195 Conc/ ppt	P Conc/ ppb
DNA samples from untreated (control cells)			
B& W Supernatat-300µg DNA	3.85	2.07	1205.62
EDTA+95% Form Telomeres-300µg DNA	3.33	2.21	302.58
B& W Supernatat-30µg DNA	100	4.72	97.1
EDTA+95% Form Telomeres-30µg	100	5.83	22.48
B& W Supernatant -30µg DNA	100	5.02	66.72
NaOAc Telomere-30µg	100	5.02	17.7
B& W Supernatant -90µg DNA	20	4.06	284.26
NaOAc Telomere-90µg	20	5.68	17
TBS Supernatant-300µg DNA	3.33	6.79	152.64
EDTA+95% Form Telomeres-300µg	3.33	1.26	169.16
DNA samples after a 2 hour cisplatin treatment			
100µM cisplatin- B&W Sup-300µg DNA	3.33	567.19	1177.62
100µM cisplatin- EDTA+95% Form Telo-300µg DNA	3.33	6.27	263.39
100µM cisplatin- B&W Sup-30µg DNA	66.67	59.28	83.24
100µM cisplatin- EDTA+95% Form Telo-30µg DNA	66.67	5.39	17.49
500µM cisplatin- B&W Sup-30µg DNA	66.67	1100.67	317.53
500µM cisplatin- EDTA+95% Form Telo-30µg DNA	66.67	6.2	14.16

The telomeric preparations were expected to contain only about 14 PPB of P as shown by the following estimation:

13.5 ng telomeric DNA = $(13.5 \times 10^{-9} / 300) = 4.5 \times 10^{-11}$ moles of nt (or P)

At. mass of P = 32

Thus the yield of P = $4.5 \times 10^{-11} \times 32 = 1.44 \times 10^{-9}$ g P

If this were dissolved in 0.1 ml water. Wt of water = 0.1 g

Conc P = $1.44 \times 10^{-} \div 0.1 = 14.4 \times 10^{-8}$ g per g water = **14 PPB**

Thus the P concentrations of the expected levels of telomeric DNA were similar to the lowest concentrations of the background levels in the best of the buffers tested. Furthermore there was a high degree of variation in the background levels of P and even the water and nitric acid samples gave high background levels of P. This, as previously mentioned, is presumably related to the widespread use of phosphate buffers and detergents in the biological laboratory where the DNA extraction and isolation procedure was carried out. In general, the P levels determined in the various DNA samples did not agree with the expected values. However, since the background P levels were too high, attempts were not made to resolve this aspect. Therefore, since an accurate measure of DNA concentration was essential as well as an accurate measure of Pt concentration, the attempt to directly measure Pt in telomeric DNA was ceased.

3.3.7 Cisplatin decreases telomerase activity in SHSY5Y cells

Telomerase activity is activated in tumour cells and thus plays an important role in maintaining their telomeres at a stable length. Conventionally used anti- cancer drugs may induce their cytotoxic effects via the telomere/ telomerase complex and much contradictory data exists on the effect of cisplatin treatment on telomerase activity in a variety of cell lines. Therefore, telomerase activity was measured by the semi-quantitative TRAP PCR ELISA in SHSY5Y cells after a short exposure cisplatin treatment after further incubation for 6, 24 and 48 hours, at the concentration ranges 0- 500 μM as for all previous experiments (Chapter 2). The relative telomerase activity was calculated and for each experiment, activities measured in untreated control samples were set as 100%.

A decrease in relative telomerase activity was detected after cisplatin treatment (Figure 3.21). This decrease occurred after treatment with the highest cisplatin concentrations (i.e. ≥ 100 μM) and became significant after 24 hours with a 500 μM treatment where > 80% of the cells were apoptotic (See Section 3.2.2) and after 48 hours for ≥ 100 μM treatments (Figure 3.21). The statistically significant differences towards untreated controls were confirmed by one way analysis of variance (ANOVA). Treatments with concentrations ≤ 100 μM displayed a decrease in activity levels, though not to a significant degree compared to the untreated controls.

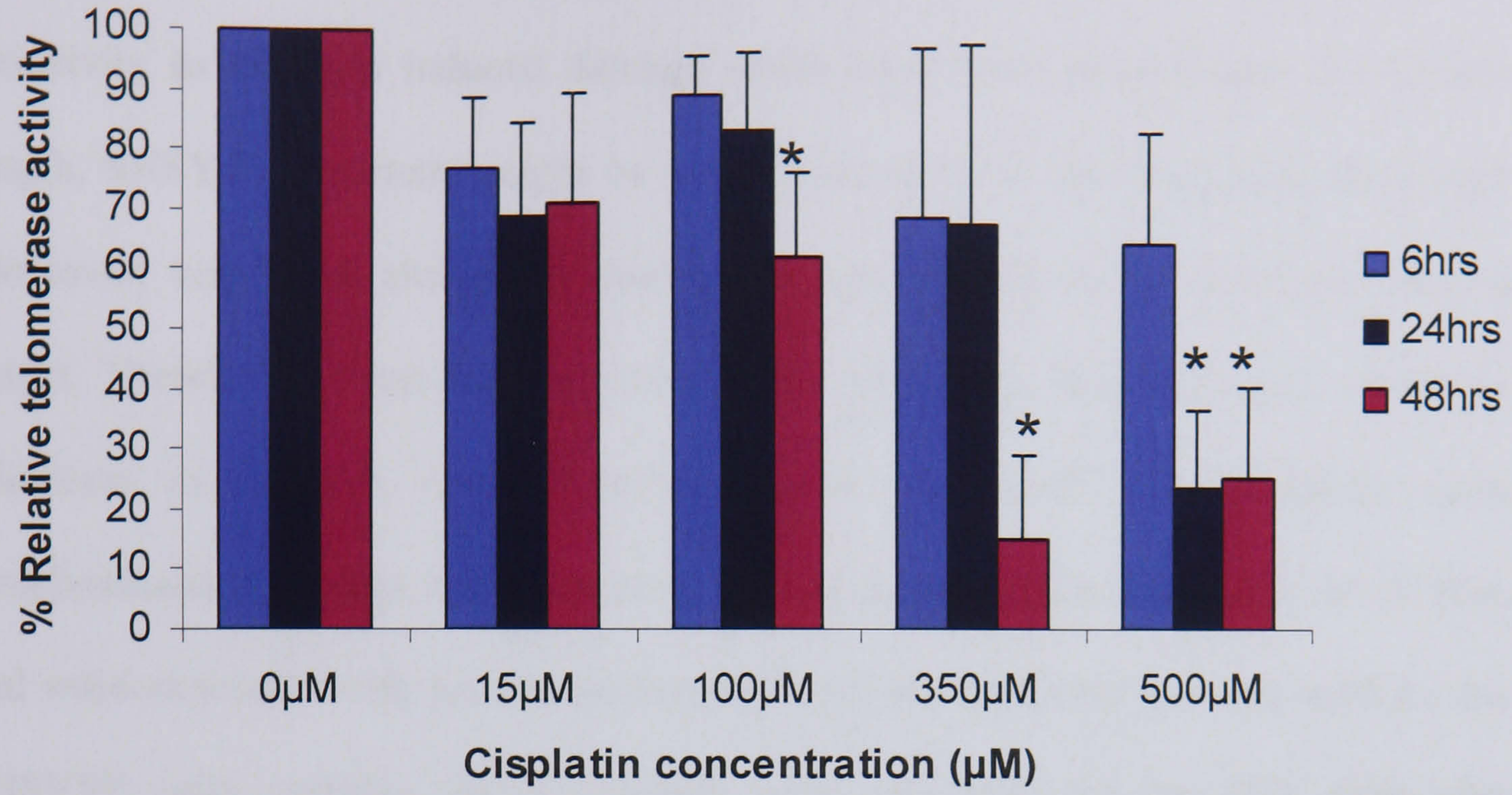

Figure 3.21 Telomerase activity in SHSY5Y cells after short exposure to cisplatin.

Relative telomerase activity was measured using a telomerase PCR ELISA or PCR ELISA^{plus}. Data are mean ± SEM from at least four independent experiments. For each experiment, activities measured in untreated control samples were set as 100%. Statistically significant differences towards untreated controls are marked by an asterisk ($p<0.05$, ANOVA).

3.3.8 Response of 1301 cells to cisplatin treatment

SHSY5Y cells have relatively short telomeres with mean lengths of ~4 kbp. As sensitivity to cisplatin induced damage could have been proportional to telomere length, SHSY5Y telomeres might be rather insensitive to the drug treatments used. Moreover, very small changes in average telomere length would have been hard to detect. Therefore, to test more rigorously the hypothesis that there was a role for telomeres in cisplatin induced growth arrest/ cell death, the tetraploid acute lymphoblastic T cell line 1301 was used. 1301 cells have telomere lengths of ~80 kbp and were exposed to the same conditions of cisplatin treatment as were used for the SHSY5Y cells. Initially, the IC_{50} values were calculated for the 1301 cells after cisplatin treatment by cell counting for both a short (Figure 3.22 A) and continuous exposure (Figure 3.22 B) and resulted in IC_{50} values of 2 μM for the short exposure and 0.6 μM for the continuous exposure. Net growth was detected only for the untreated cells after a short exposure treatment, whilst cell growth was observed for 0.5 μM after a continuous exposure.

The kinetics of apoptosis was measured in the 1301 cells, similar to the SHSY5Y cells, after a short (Figure 3.23) and continuous (Figure 3.24) exposure to cisplatin. Examples of typical dot plots of flow cytometry apoptotic data for 1301 cells exposed to cisplatin treatment are shown in panels A. Panels B of the figures show averaged data from three separate experiments for percentage of apoptotic cells.

1301 cells exposed to a short exposure cisplatin treatment exhibited a time and concentration dependent induction of apoptosis, with a large increase in apoptotic cells at ≥ 100 μM after 24 hours (Figure 3.23). 1301 cells exposed to a continuous treatment of cisplatin also displayed a time and concentration dependent induction of apoptosis, at concentrations ≥ 2 μM (Figure 3.24).

A

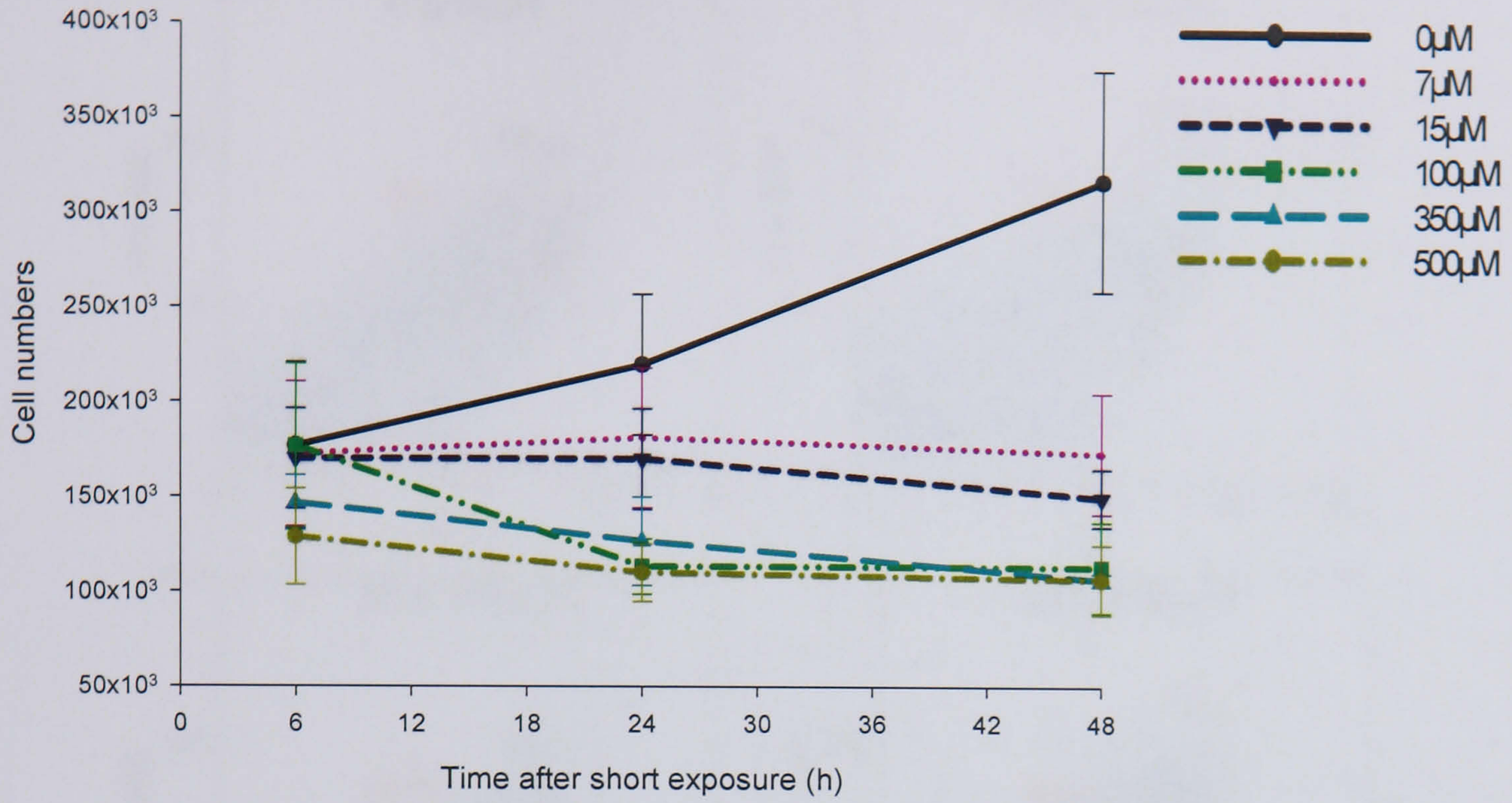

B

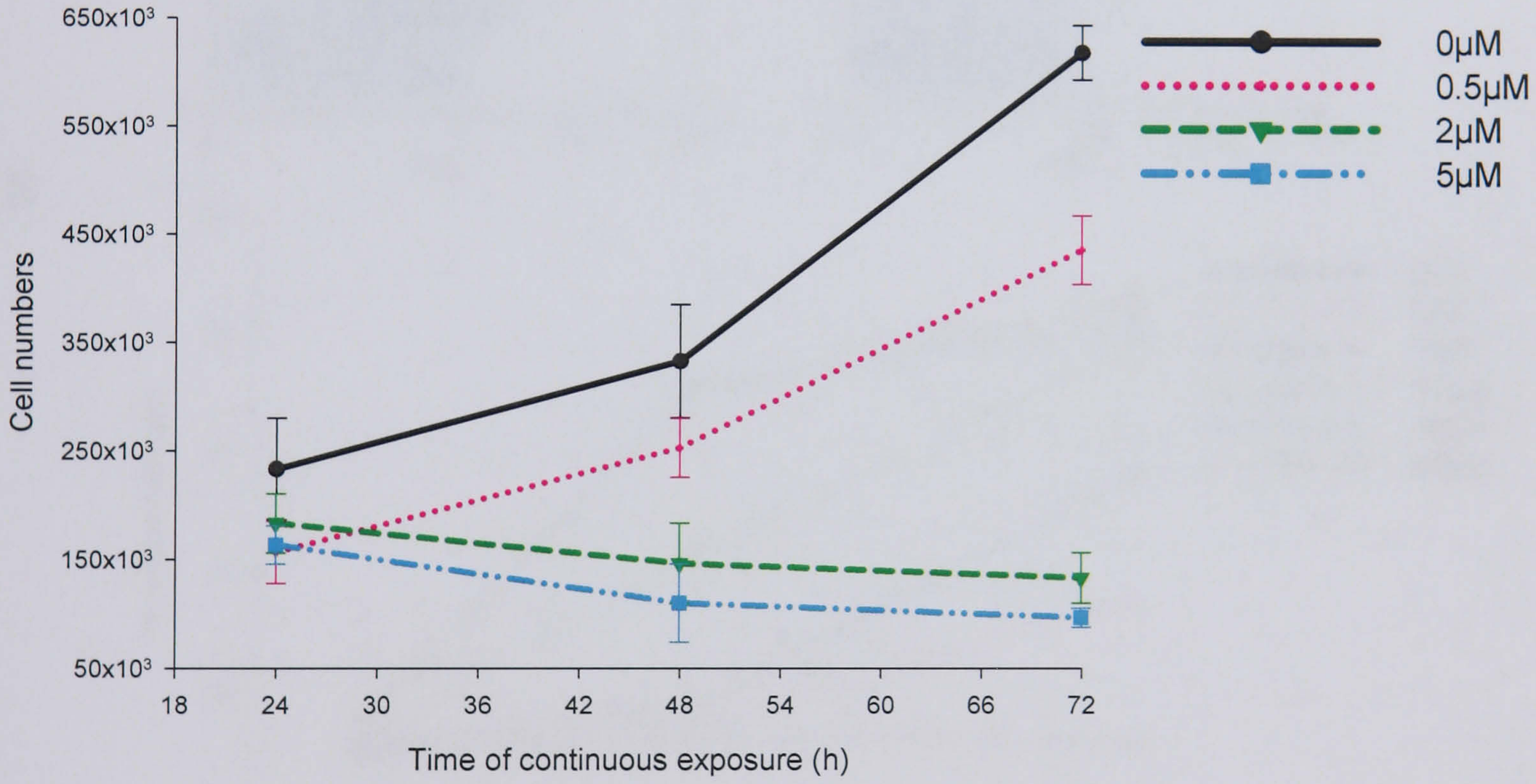

Figure 3.22 Cell numbers of 1301 cells after cisplatin treatment. Cell numbers per flask were counted after a short (A) and a continuous (B) exposure to cisplatin for at least 48 hours after treatment. Data are mean ± SEM from triplicate experiments.

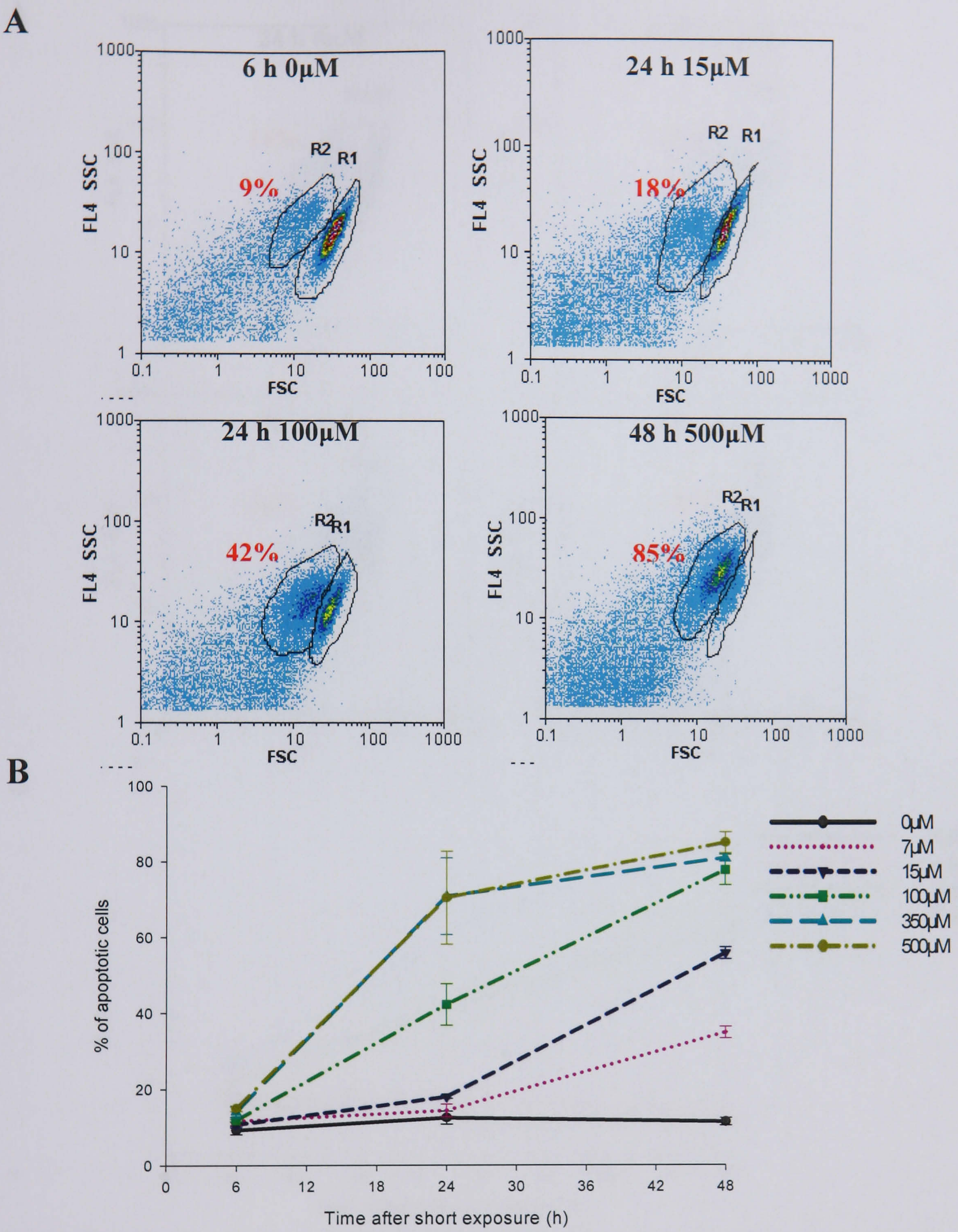

Figure 3.23 Levels of apoptosis after short exposure cisplatin treatment on 1301 cells. Apoptotic cells were measured by flow cytometry according to their size (forward scatter; FSC) and granularity (light scattered sideways; SSC). (A) Examples of gated apoptotic cells R2, to non apoptotic cells R1 after cisplatin treatment. Time after treatment and concentration of cisplatin indicated. % of apoptotic cells are shown in red. (B) % of apoptotic cells after cisplatin treatment average graph. Data are mean ± SEM from triplicate experiments with three replicates in each experiment.

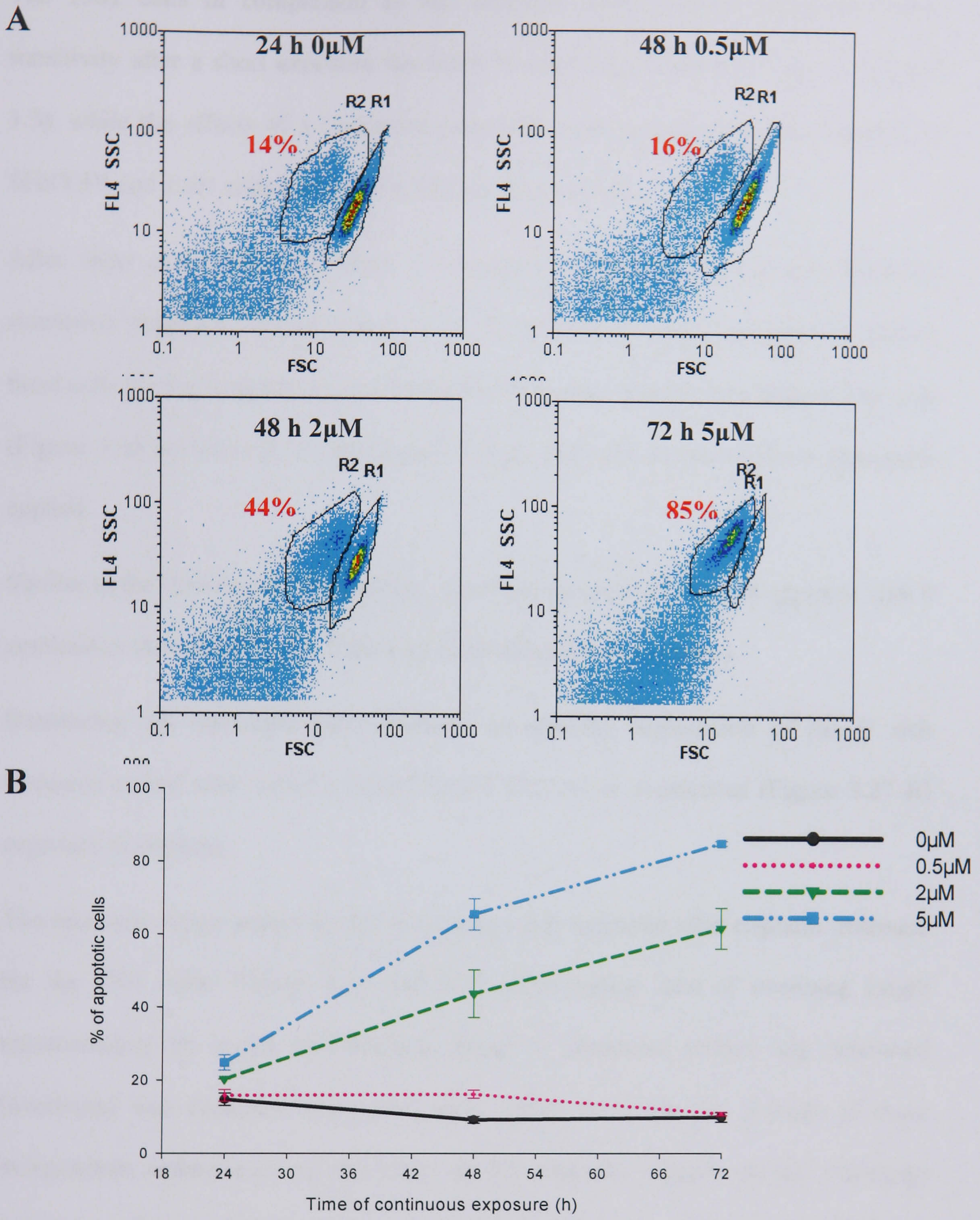

Figure 3.24 Levels of apoptosis after continuous exposure cisplatin treatment on 1301 cells. Apoptotic cells were measured by flow cytometry according to their size (forward scatter; FSC) and granularity (light scattered sideways; SSC). (A) Examples of gated apoptotic cells R2, to non apoptotic cells R1 after cisplatin treatment. Time after treatment and concentration of cisplatin indicated. % of apoptotic cells are shown in red. (B) % of apoptotic cells after cisplatin treatment average graph. Data are mean ± SEM from triplicate experiments with three replicates in each experiment.

The 1301 cells in comparison to the SHSY5Y cells showed a slightly higher sensitivity after a short exposure treatment to cisplatin (compare to Figures 3.2 and 3.3), while the effects of a continuous exposure were quantitatively very similar in SHSY5Y and 1301 cells (compare to Figures 3.2 and 3.4).

After short exposures to a range of cisplatin concentrations, the 1301 telomere restriction fragment lengths (Figure 3.25 A) showed no visible shortening, despite these cells having long telomeres. The average telomere lengths from at least four gels (Figure 3.25 B) showed no significant change after any of the cisplatin treatments applied.

Similar to the short exposure treatment, telomere degradation was not apparent after a continuous exposure (Figure 3.26) even after induction of apoptosis.

Denaturing gel electrophoresis exhibited no specific degradation of the G rich telomeric strand after either a short (Figure 3.27 A) or continuous (Figure 3.27 B) exposure to cisplatin.

The telomeric single strand G rich overhangs were measured after cisplatin treatment for the 1301 cells. Figures 3.28 and 3.29 show typical data of overhang length measurements by in-gel hybridisation. Panel A illustrates probed non denatured (overhang) and denatured (telomere) gels. Panel B shows the average of three independent experiments of the ratio of the intensity signals of the overhang/ telomeres after cisplatin treatment. The 1301 cells after short (Figure 3.28) or continuous (Figure 3.29) exposure to cisplatin displayed no significant change in overhang lengths.

A

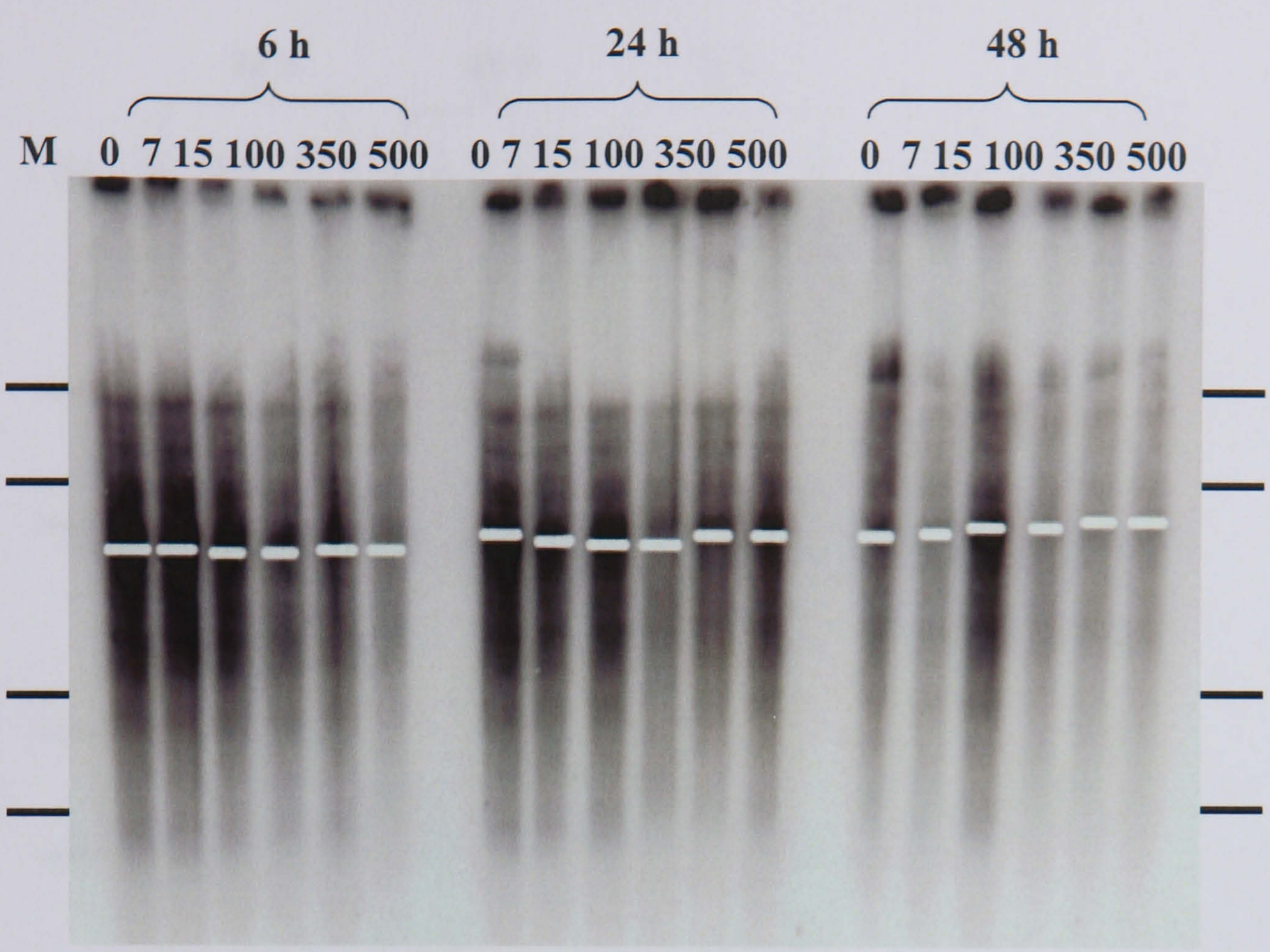

B

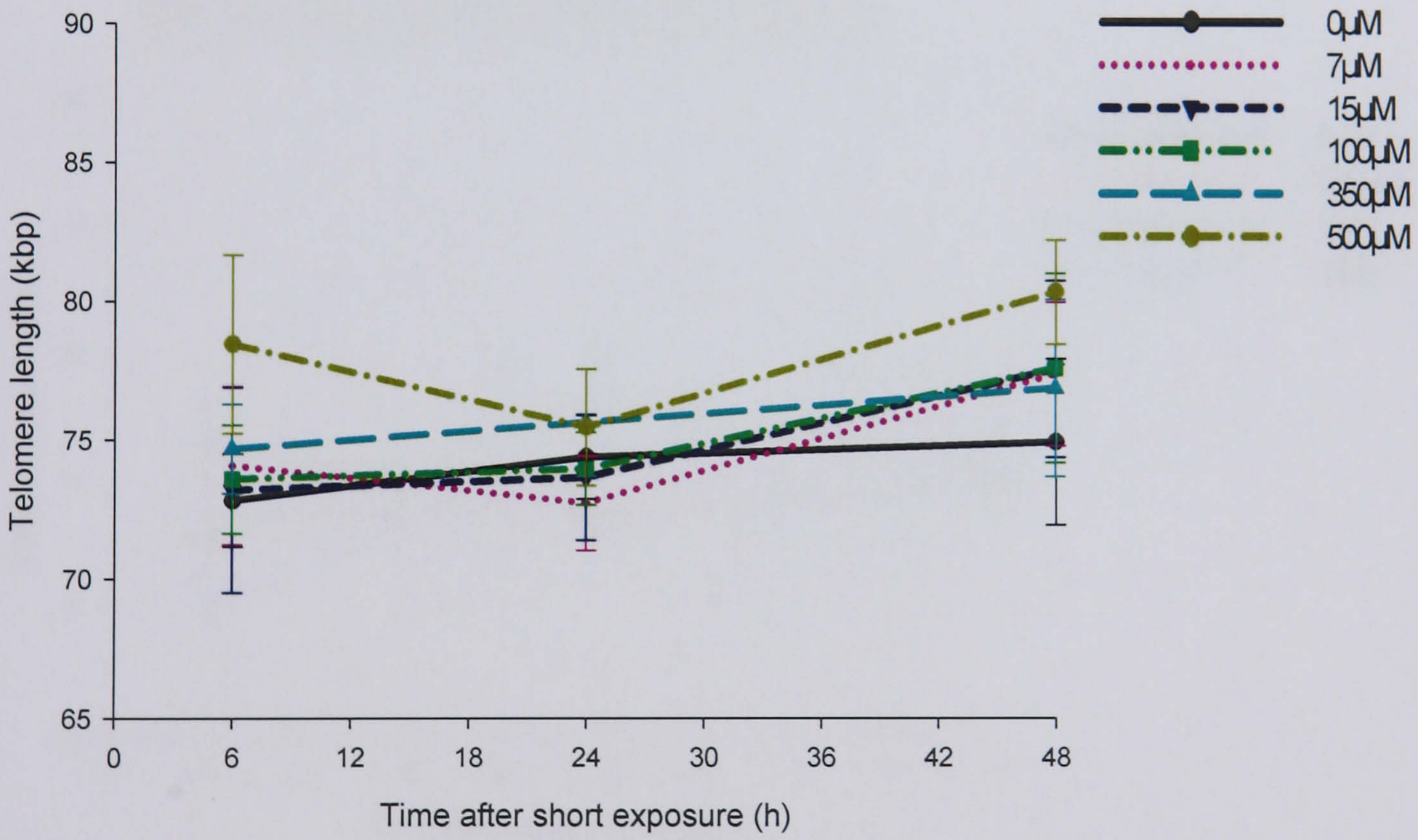

Figure 3.25 Telomere restriction fragment lengths after short exposure cisplatin treatment on 1301 cells. (A) Telomere gel. Cisplatin concentrations (in µM) and times after onset of treatment (in h) are indicated on top of the figure. White bars indicate average telomere length. The positions of the size markers (194, 97, 48.5, 23.1 kbp) are shown by black bars. (B) Average telomere length. Gels were normalised to a standard and average fragment lengths of at least four experiments were calculated. Data are ± SEM.

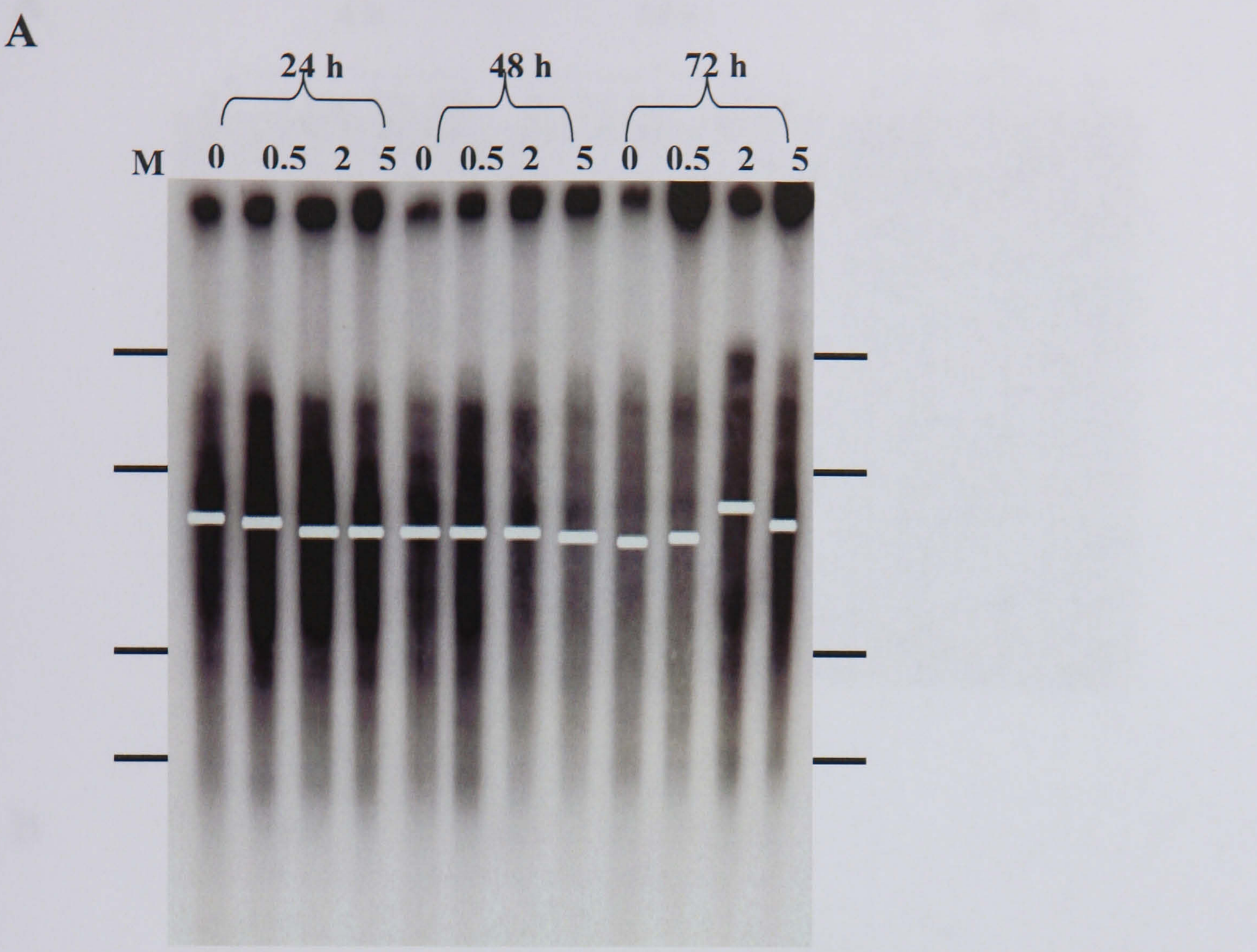

Figure 3.26 Telomere restriction fragment lengths after continuous exposure cisplatin treatment on 1301 cells. (A) Telomere gel. Cisplatin concentrations (in µM) and times after onset of treatment (in h) are indicated on top of the figure. White bars indicate average telomere length. The positions of the size markers (194, 97, 48.5, 23.1 kbp) are shown by black bars. (B) Average telomere length. Gels were normalised to a standard and average fragment lengths of at least four experiments were calculated. Data are ± SEM.

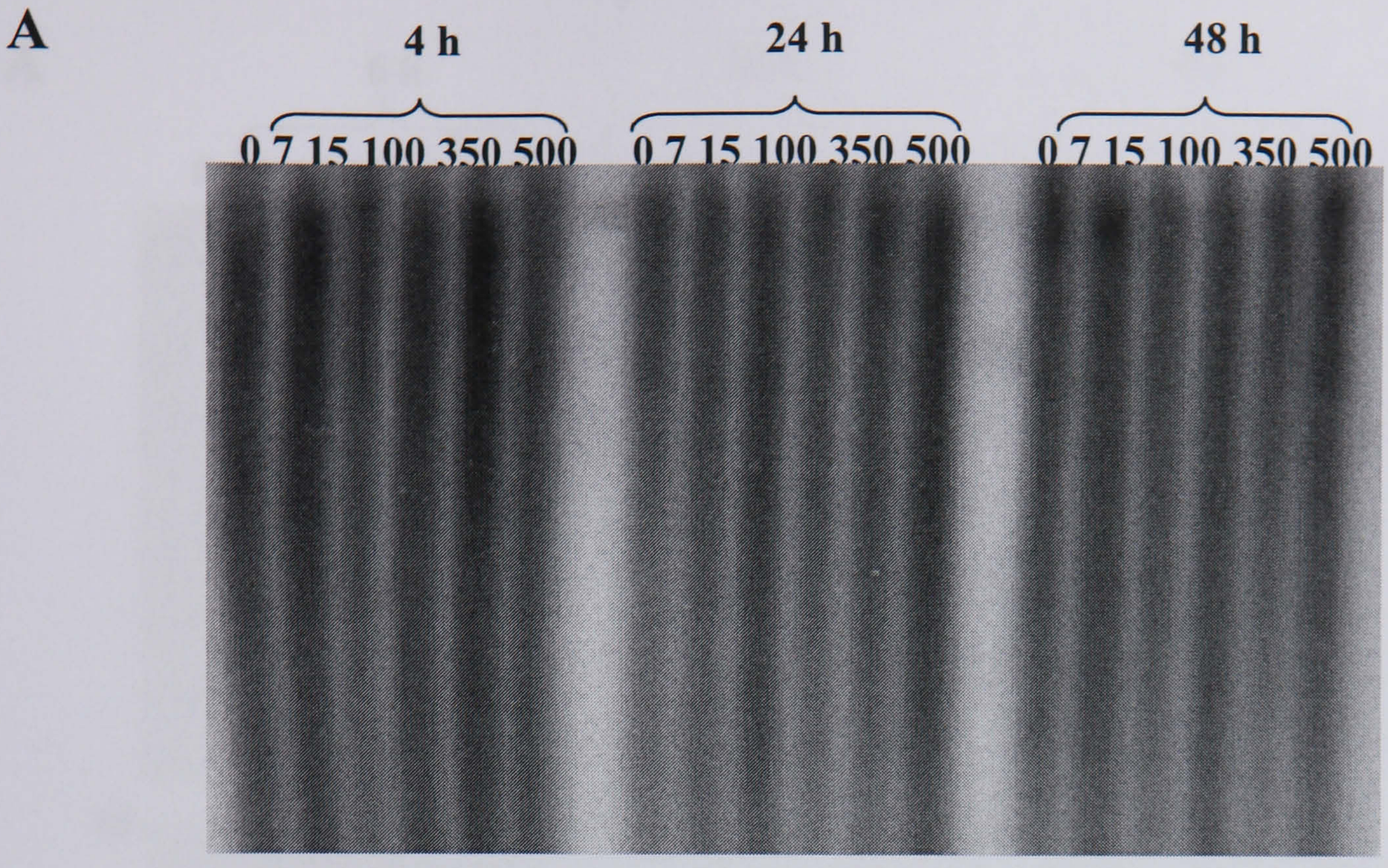

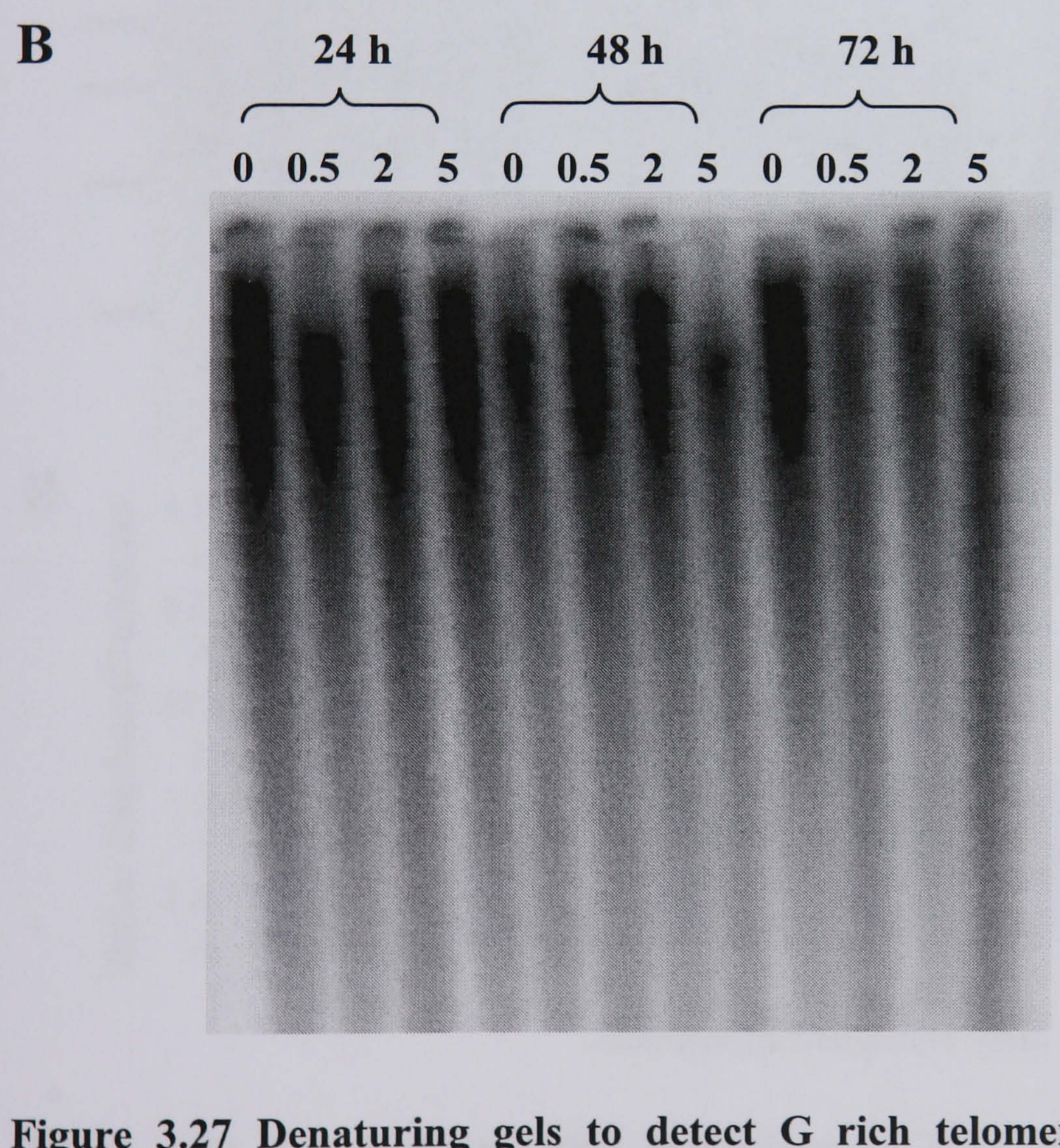

Figure 3.27 Denaturing gels to detect G rich telomeric strand breaks after cisplatin treatment on 1301 cells. Examples of denaturing gel after short (A) and continuous (B) cisplatin treatment. Cisplatin concentrations (in μM) and times after onset of treatment (in h) are indicated on top of the figures.

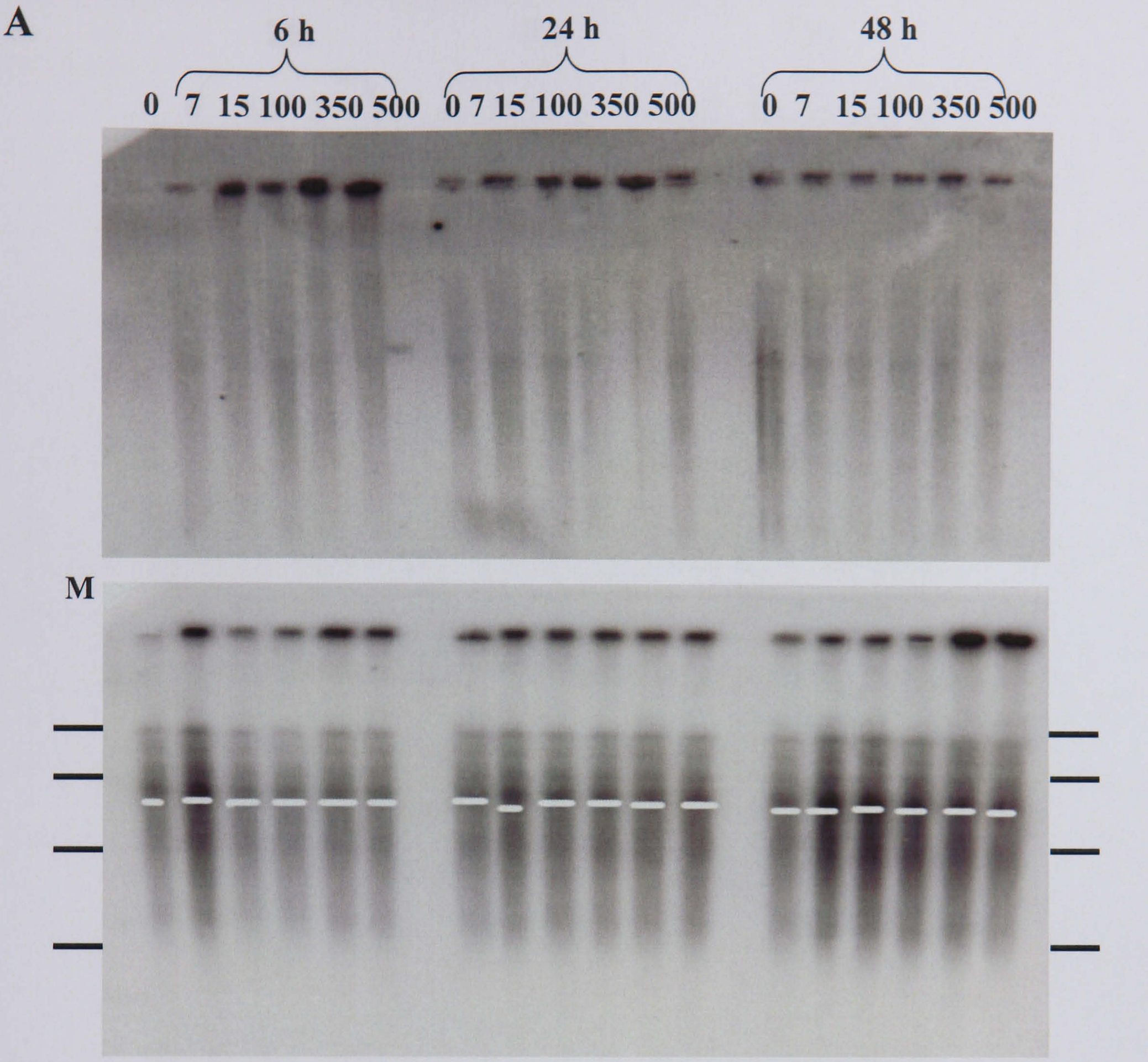

Figure 3.28 Telomeric G- rich overhangs in 1301 cells after short exposure cisplatin treatment. The overhang length is measured as the ratio of hybridisation intensities to the overhang alone vs whole telomere. (A) Example of an overhang and telomere gel. The position of the size markers (194, 97, 48.5, 23.1 kbp) are shown by black bars. M = markers. White bar indicates average telomere length. (B) Graph showing ratios. Data are mean ± SEM from at least three experiments.

A

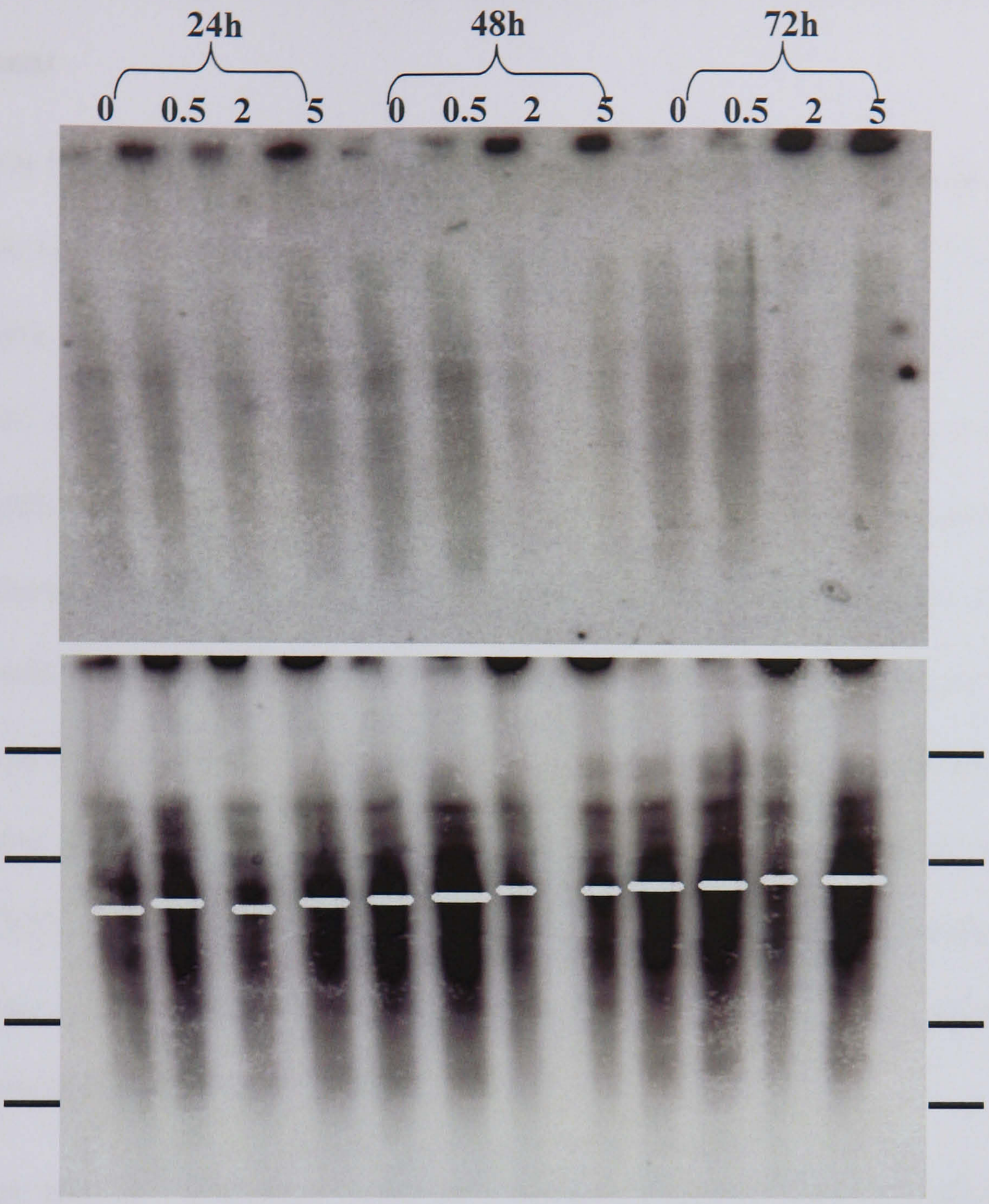

B

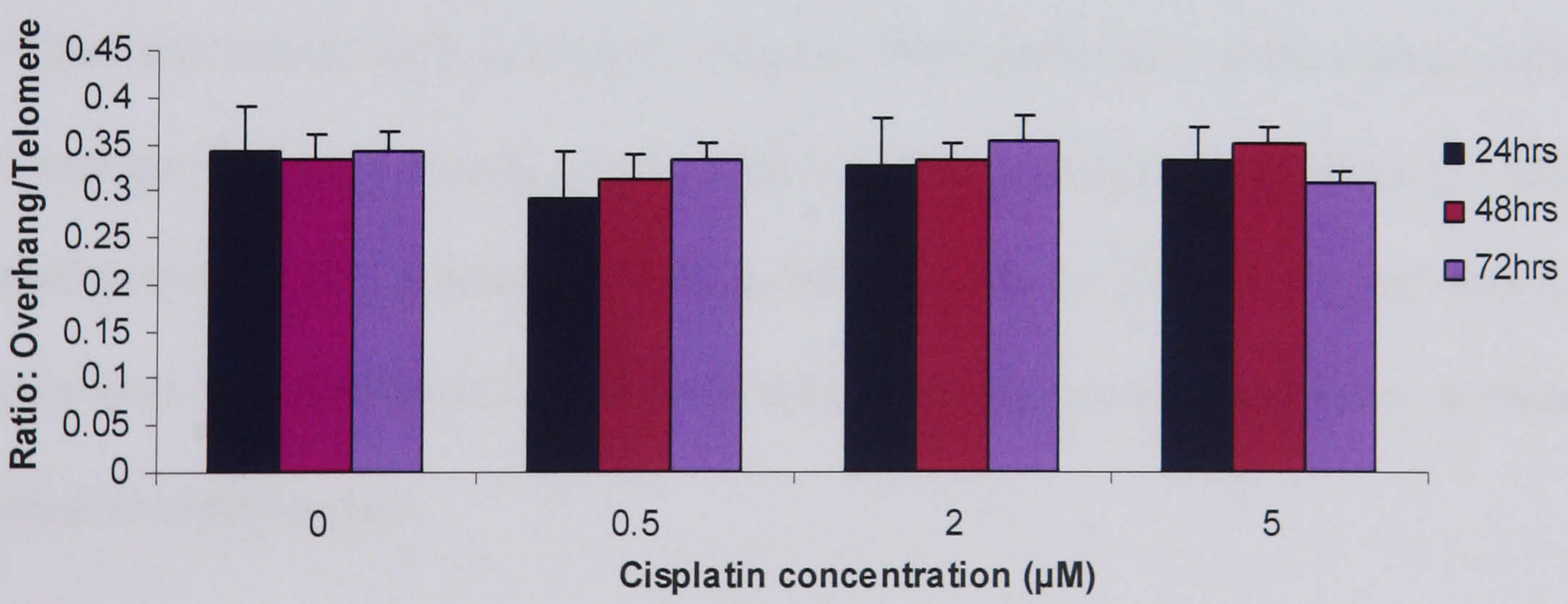

Figure 3.29 Telomeric G- rich overhangs in 1301 cells after continuous exposure cisplatin treatment. The overhang length is measured as the ratio of hybridisation intensities to the overhang alone vs whole telomere. (A) Example of an overhang and telomere gel. The position of the size markers (194, 97, 48.5, 23.1 kbp) are indicated. M = markers. White bar indicates average telomere length. (B) Graph showing ratios. Data are mean ± SEM from at least three experiments.

3.3.9 DNA damage foci are not localised at the telomeres after cisplatin treatment

Cisplatin treatment induces delayed strand breakage and a DNA damage response in the form of histone H2A.X phosphorylation as confirmed in Section 3.2.3. In order to determine whether foci of histone H2A.X phosphorylation induced in response to cisplatin occurs preferentially on telomeres, an immunoFISH procedure was developed and applied to drug treated 1301 cells. This procedure assesses γ- H2A.X DNA damage foci by immunohistochemistry and telomeric DNA by FISH in the same individual cells. As the FISH procedure requires a PNA probe to bind to the telomeric DNA, the 1301 cells with telomere lengths of greater than 80 kbp it seemed likely that they would have be an easier target and more clearly visible compared to the SHY5Y cells which have telomere lengths of less than 5 kbp. Therefore the 1301 cells were used to detect whether the DNA strand breaks induced by cisplatin localise at telomeric DNA.

14 hours after a 7 μM short exposure cisplatin treatment (Figure 3.30), 1301 cells were fixed and stained with γ- H2A.X, telomere PNA probe and DAPI nuclear stain. DNA damage foci were clearly present after cisplatin treatment and telomeric DNA was also detectable. Merged images display that the majority of DNA damage foci do not colocalise to the telomeric DNA (≥ 7 cells out of 10 in triplicate fields in three independent experiments).

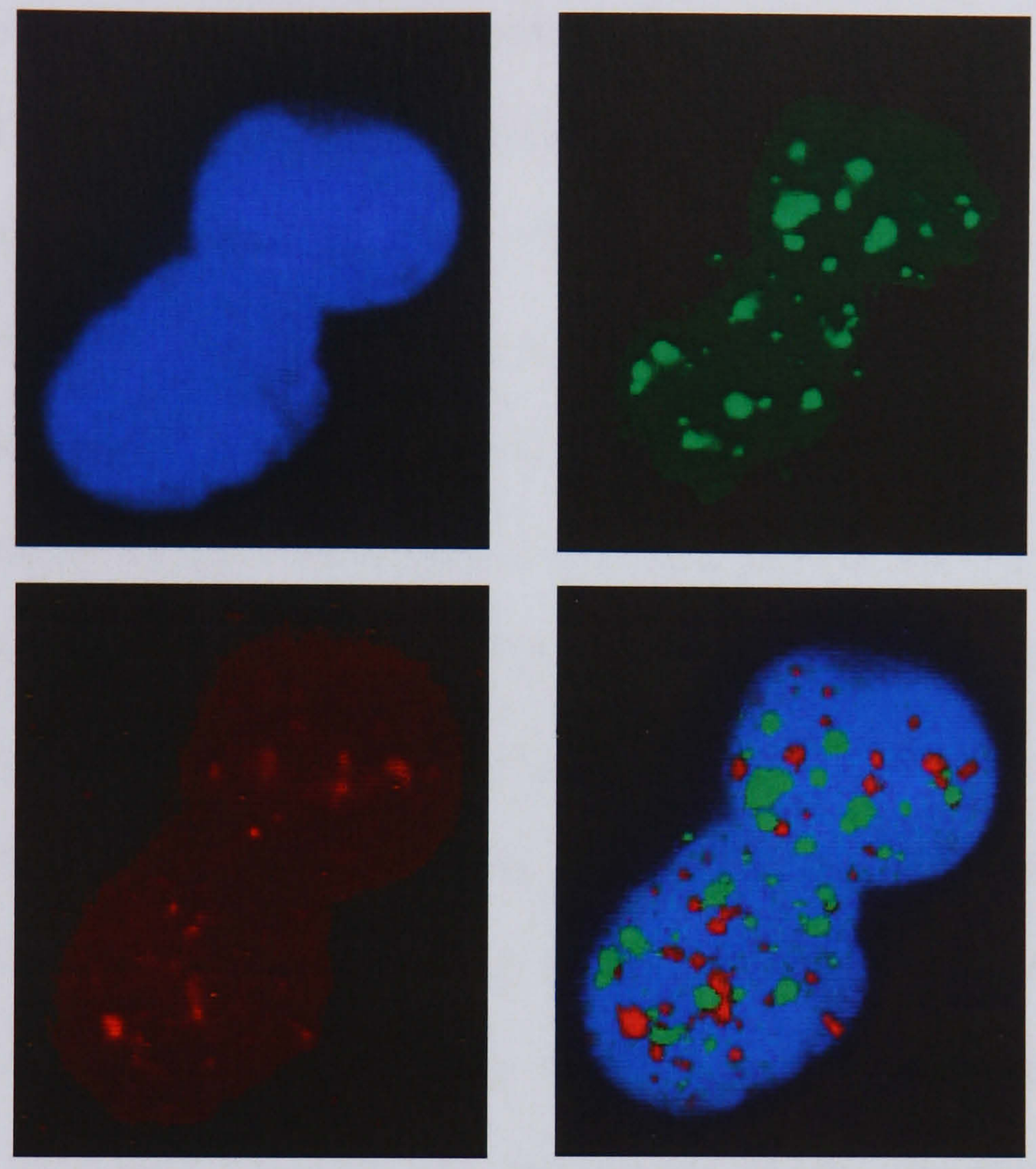

Figure 3.30 DNA damage foci do not colocalise with telomeres after a short exposure cisplatin treatment. 1301 cells were fixed 14 hours after a 4 hour treatment with 7 μM cisplatin and stained as specified. The merged images show lack of colocalisation between DNA damage foci and telomeres. x 100 objective

3.4 Discussion

As discussed in Chapter 1, there is much evidence to suggest a link between the interaction of DNA damaging drugs and telomeres. More specifically, there are indications to suggest a relationship between cisplatin and telomeres (Grimaldi *et al.*, 1994). A DNA repair yeast mutant exhibited a gradual shortening of the telomere in the presence of cisplatin (Ishii *et al.*, 2000). In human hepatoma cells (Zhang *et al.*, 2002) and HeLa cells (Ishibashi and Lippard, 1998) telomeres shortened after cisplatin treatment. Though long term cultivation of colorectal cancer cells with cisplatin led to telomere elongation at the same time as the cultures became drug resistant (Kuranaga *et al.*, 2001). Additionally, cisplatin treatment led to a reduction in telomerase activity in some cell lines like human testicular tumour cells (Burger *et al.*, 1997). Other studies established that this decline in telomerase activity was a consequence of apoptosis (Akiyama *et al.*, 1999; Cressey *et al.*, 2002). Therefore the aim of the study described here was to investigate the effects of cisplatin on the telomere/ telomerase complex and determine whether telomeres have a role in cisplatin mediated cell death.

As expected (see Chapter 1), cisplatin did not induce DNA strand breakage immediately after drug exposure but strand breaks and DNA damage foci were detected 14 hours after treatment. The H2A.X phosphorylation and strand breaks detected in cisplatin treated cells over time was probably associated with DNA repair. This has been suggested by Huang and colleagues who have reported H2A.X phosphorylation after cisplatin exposure (Huang *et al.*, 2004). Evidently, cisplatin-induced cross-links do not induce DNA damage foci formation by itself. However, strand breaks and γ-H2A.X foci are found later, indicating that they are the result of processing of the original lesions.

The experiments described in this chapter included an assessment of the effect of cisplatin exposure on total telomere length and also on the length of the single-stranded telomeric overhangs. A wide range of drug concentrations, decided by the IC_{50} values were employed for both short and continuous drug exposures. For samples taken at various times after this wide range of conditions, no evidence was found for an effect of cisplatin on telomere length or integrity. This contrasts with the publication by Ishibashi and colleague (Ishibashi and Lippard, 1998) who reported telomere length reduction in cells exposed to cisplatin and attributed the reduction of length to replication blocking. Another study showed a decrease of telomeres in BEL-7404 human hepatoma cells, whereby the telomere shortening in cisplatin treated cells was independent of time or dose and did not correlate with the induction of apoptosis (Zhang *et al.*, 2002). The discrepancy in the results could be due to the difference in cell lines examined and/ or experimental protocols and any changes may be dependent on initial telomere length. A particularly relevant difference between the cell lines was their telomere lengths which averaged 20 kbp for the HeLa cells used by Ishibashi and Lippard (1998) and ~4.2 kbp for the BEL-7404 cells used by Zhang *et al* (2002). The SHSY5Y cells used here showed an average telomere fragment length of ~4 kbp. Therefore, we examined further an acute lymphoblastic T cell line, 1301, with telomere lengths of ~80 kbp to discriminate between any discrepancies in cells with either long or short telomeres. Again, like the SHSY5Y cells, the 1301 cells showed that apoptosis induction by cisplatin treatment was not telomere dependent.

There are conflicting data on the relationship between effects of cisplatin and changes in telomerase activity. Telomerase inhibition has been shown in testicular tumour cells after cisplatin treatment, whereby cisplatin effected gene transcription by decreasing the hTR expression (Burger *et al.*, 1997). Akeshima and colleagues

demonstrated that hTERT expression did not change with time after cisplatin treatment in ovarian cancer cells (Akeshima *et al.*, 2001). Whilst another study found an inhibition of telomerase activity after cisplatin treatment in BEL-7404 human hepatoma (Zhang *et al.*, 2002). This occurred with no changes in expression level of hTR or hTERT mRNA but with a change in cell growth (Zhang *et al.*, 2002), in accordance with others (Faraoni *et al.*, 1997). However, in testicular teratoma and haematopoietic cell lines the decline in telomerase activity following cisplatin treatment was shown to be a consequence of, rather than a cause for, apoptosis (Akiyama *et al.*, 1999; Cressey *et al.*, 2002). Though others did not see an inhibition of telomerase activity after cisplatin treatment in human nasopharyngeal cells (Ku *et al.*, 1997) and there has been a report of an increase in hTERT mRNA and protein during cisplatin treatment (Lin *et al.*, 2001). Therefore, telomerase activity was examined after a short exposure cisplatin treatment. In the SHSY5Y cells the telomerase activity levels decreased significantly only where the highest concentrations of cisplatin were used. Comparison of data on apoptosis induction (Figure 3.3) with data on telomerase activity (Figure 3.21) shows that loss of telomerase activity only occurred after the majority of cells were in apoptosis, in accordance with others (Akiyama *et al.*, 1999; Cressey *et al.*, 2002). These findings indicate that down regulation of telomerase activity appears to be a consequence and not a possible cause of cisplatin induced apoptosis or growth arrest.

Dysfunctional telomeres trigger growth arrest and/ or apoptosis via telomere-specific induction of DNA damage foci, also termed senescence-associated DNA damage foci (d'Adda di Fagagna *et al.*, 2003). Therefore, DNA damage foci were assessed after cisplatin treatment on the telomeric DNA. DNA damage foci did not colocalise to telomeric DNA in the 1301 cells after a short exposure treatment.

3.5 Conclusions

In conclusion, the data presented here show the characterisation of the response to a short exposure and continuous cisplatin treatment as a combination of S phase arrest and apoptosis in high concentration cisplatin treated cells and no indication for a specific role of telomeric damage in the execution of this response. Therefore we find no indication that telomeres and/ or telomeric damage play any preferential role as signal transducers. This is in disagreement with another study which has led to the proposal that telomeric damage plays a particularly important role in the cytotoxic effects of cisplatin (Ishibashi and Lippard, 1998). The study described here reveals that the telomere/ telomerase complex is not involved in cisplatin induced apoptosis. Rather, our data suggest that DNA strand breaks elsewhere in the genome, occurring as a result of attempted repair induce DNA damage foci formation leading to apoptosis and/ or cell cycle arrest.

CHAPTER FOUR

THE ROLE OF TELOMERES IN ETOPOSIDE INDUCED TUMOUR CELL DEATH

4.1 Introduction

Topoisomerase II enzymes (Gellert, 1976) break double strands of DNA and induce topological changes in DNA (Wang *et al.*, 1996). Etoposide, a topoisomerase II poison, stabilises the cleavable complexes formed by topoisomerases, converting them into physiological toxins that take the form of protein associated breaks in the genome of treated cells (Kaufmann *et al.*, 1998). This effect is reversible and etoposide has a short elimination half life (Hsiang and Liu, 1989). Levels of topoisomerase II are generally elevated in cells that are undergoing rapid proliferation and due to the mechanism of drug action, the higher the physiological concentration of topoisomerase II, the more lethal the poison becomes.

Human telomeres, the specialised DNA-protein structures on the end region of chromosomes, are composed of the repeat sequence TTAGGG. Evidence indicates that their shortening with each round of DNA replication is caused by several mechanisms, one of these being their sensitivity to DNA damage. Thus, telomere shortening can greatly be accelerated or decelerated by controlling oxidative stress within the cells (von Zglinicki *et al.*, 2002). Telomeres end in single stranded overhangs of the G-rich strand, which appear to be essential for telomeric higher order structure (Griffith *et al.*, 1999) and possibly for the generation of DNA damage signals from telomeres (Stewart *et al.*, 2003; Saretzki *et al.*, 1999; von Zglinicki, 2000). In the vast majority of cancer cells, telomere shortening is counteracted by telomerase (Greider *et al.*, 1987; 1989). Inhibition of telomerase by different methods

has been shown to lead not only to progressive telomere shortening and ensuing cell death (Herbert *et al.*, 1999) but also to telomere length independent apoptosis induction (Saretzki *et al.*, 2001).

Etoposide has been shown to generate topoisomerase-DNA cleavable sites in telomeres *in vitro* and *in vivo* (Yoon *et al.*, 1998). Contradictory data exists on the interaction between etoposide and telomerase. Upregulation of telomerase activity was observed in the human leukemic cell line HL60 (Moriarty *et al.*, 2002; Klapper *et al.*, 2003) and a number of pancreatic tumour cell lines after etoposide treatment (Sato *et al.*, 2000). However a decrease in telomerase activity was observed in hepatocarcinomas and other leukemic cell lines (Li *et al.*, 2002) and no change in levels of telomerase in haematopoietic (Akiyama *et al.*, 1999) and nasopharyngeal carcinoma cells (Ku *et al.*, 1997). Though the decline in telomerase activity following DNA damaging drug treatments was shown to be a consequence of, rather than a cause for, apoptosis (Akiyama *et al.*, 1999; Cressey *et al.*, 2002). There is evidence that inhibition of telomerase sensitises cells to topoisomerase II poisons including etoposide (Ludwig *et al.*, 2001; Misawa *et al.*, 2002) and that overexpression of the catalytic subunit of telomerase (hTERT) in cells that also expressed the telomerase template RNA (hTR) led to an increased resistance against etoposide (Ludwig *et al.*, 2001; Zhang *et al.,* 2003). Conversely, others could not confirm a telomerase dependency of the sensitivity of various tumour cells to etoposide (Chen *et al.*, 2003; Folini *et al.*, 2000).

Given these inconsistent results, the aim of the work presented in this chapter was to test the hypothesis that a role exists for the telomere/ telomerase complex in etoposide induced cell death. Neither telomere length, telomere strand break frequency, or length of G-rich telomeric single-stranded overhangs changed in etoposide treated

cells before onset of apoptosis. Overall the results indicate that telomeres are not directly involved in the signalling pathway to etoposide induced tumour cell growth arrest or apoptosis.

4.2 Methods

All methods used in this study are described in Chapter 2.

4.3 Results

4.3.1 Growth inhibition effect of etoposide

It was important to establish the relationship between etoposide exposure and growth inhibitory effects as a basis for experiments on mechanism of action. The cytotoxicty levels of etoposide on the SHSY5Y and 1301 cells were unknown, therefore initially cells were exposed to a broad range of drug concentrations and the IC_{50} values were measured by the SRB assay and/ or cell counting after etoposide treatment.

Growth curve data for the SHSY5Y cells were used to determine the optimal inoculum density for the SRB assay (see Figure 3.1 A). The cytotoxicty levels of etoposide on the SHSY5Y cells were then examined by exposing cells to a short (4 hour) exposure treatment and incubating for a further 6 days before fixing and staining with the SRB reagents (Section 2.5). The control cells (untreated) optical density (OD) was set at 100%. The OD of the treated cells were converted into percentages of the control and plotted against etoposide concentration (see Figure 3.1 B for example of a typical graph after a drug treatment), producing an IC_{50} value of 7.1 μM.

In independent cell count experiments the IC_{50} values were determined by cell counting for both a short (48 hours after treatment) and continuous (72 hours after treatment) exposure for both the SHSY5Y and 1301 cells. The mean results from 3 separate cell count experiments are shown in Table 4.1. The IC_{50} values suggest the 1301 cells are more sensitive to etoposide exposure for both a short and continuous treatment compared to the SHSY5Y cells.

For all subsequent etoposide experiments, cells were exposed to either a short treatment, which lasted for 4 hours then further incubation for up to 48 hours or a continuous treatment for up to 72 hours. These two regimens used the concentration ranges 0, 3, 7, 15, 100 and 350 μM for the short treatment and 0, 0.25, 0.5, 1, 2 and 5 μM for the continuous treatment.

Table 4.1 Growth inhibitory concentrations (IC_{50}) after etoposide treatment assessed by cell counting

IC50 Values	Exposure/ μM	
Cell Lines	*Short*	*Continuous*
SHSY5Y	56.1	1.4
1301	16.4	0.6

Changes in cell number with time after exposure to various etoposide concentrations are shown in Figure 4.1 (short exposure) and Figure 4.2 (continuous exposure). For the SHSY5Y cells (Figure 4.1 A), cell growth occurred for treatments ≤ 15 μM over the 48 hour time course similar to the untreated cells in a time and concentration dependent manner. Whereas concentrations ≥ 100 μM displayed no increase in cell number after exposure for the whole 48 hour period. The 1301 cells (Figure 4.1 B) exhibited a similar relationship after short exposure etoposide treatment, with net growth for treatments of ≤ 15 μM and arrest with concentrations ≥ 100 μM.

Cell numbers after a continuous exposure for both cell lines (Figure 4.2) showed a similar time and concentration dependent pattern. For the SHSY5Y cells (Figure 4.2 A) an increase in cell growth arose at concentrations ≤ 0.5 μM, though for the 1301 cells (Figure 4.2 B) an increase in growth occurred only at a 0.25 μM exposure.

In conclusion, the relationships between etoposide concentration and growth inhibition have been defined for short and continuous exposure treatments.

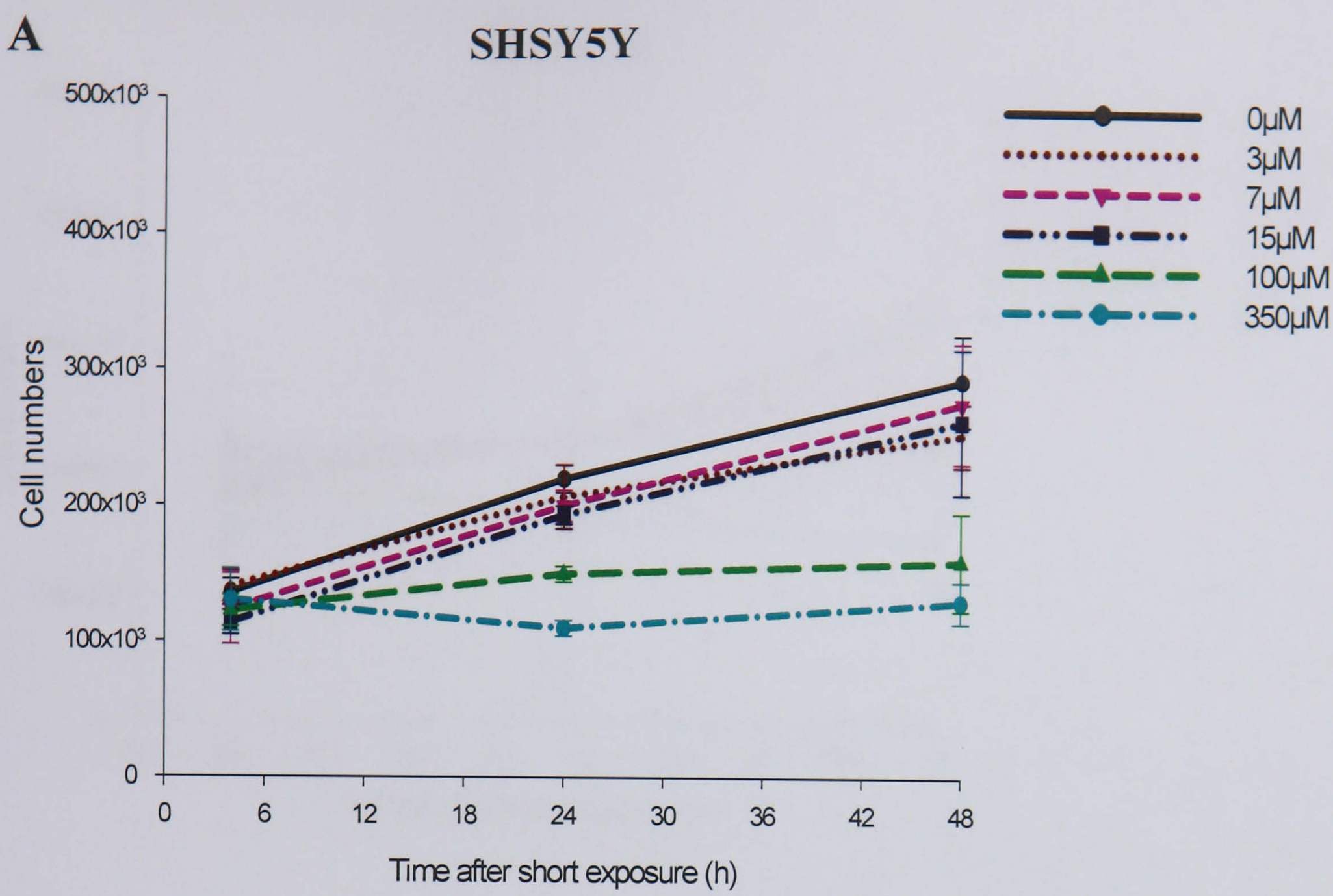

Figure 4.1 Cell numbers of SHSY5Y and 1301 cells after a short exposure etoposide treatment. SHSY5Y (A) and 1301 (B) cells were exposed to etoposide for 4 hours and cell numbers per flask were counted 4- 48 hours after. Data are mean ± SEM from triplicate experiments.

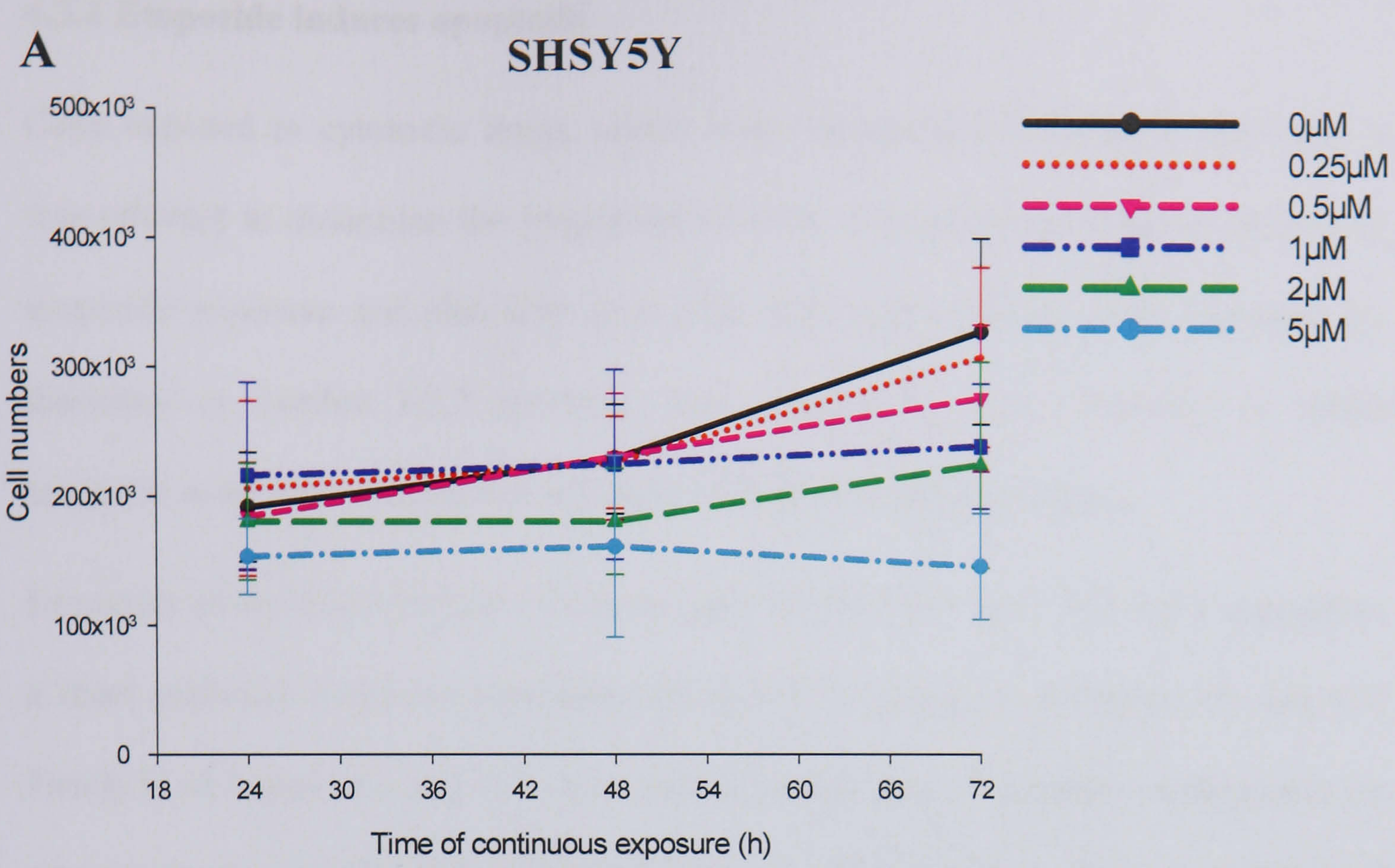

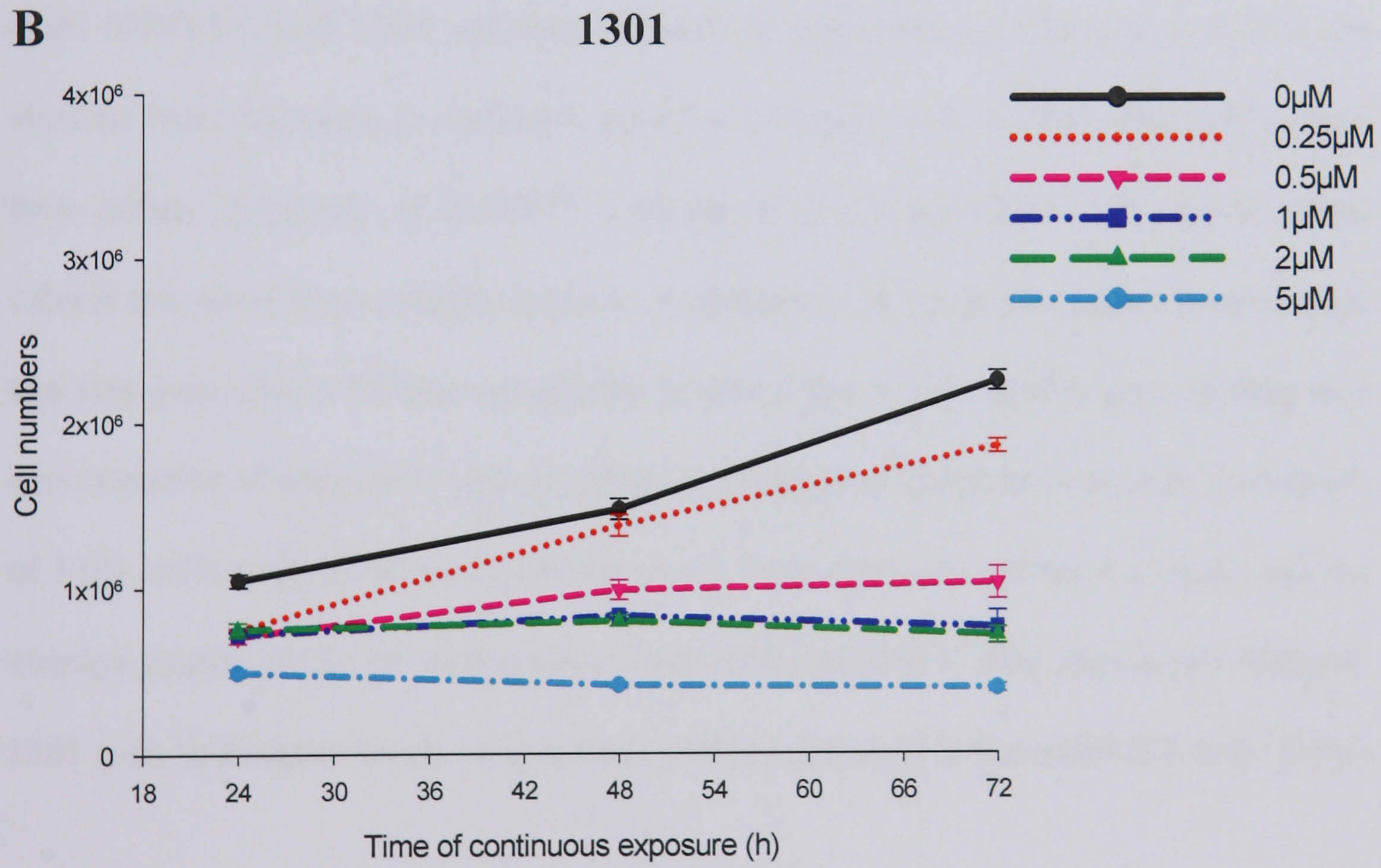

Figure 4.2 Cell numbers of SHSY5Y and 1301 cells after a continuous exposure etoposide treatment. SHSY5Y (A) and 1301 (B) cells were exposed to etoposide continuously and cell numbers per flask were counted 24- 72 hours after. Data are mean ± SEM from triplicate experiments.

4.3.2 Etoposide induces apoptosis

Cells exposed to cytotoxic drugs, under many circumstances undergo apoptosis. It was relevant to determine the proportion of cells with apoptotic features induced by etoposide exposure and also how soon after treatment apoptotic cells appeared. As discussed in Section 3.2.2 apoptosis was detected by flow cytometry in which apoptotic cells were detected on the basis of their size and granularity.

Examples of dot plots of flow cytometry data for SHSY5Y and 1301 cells exposed to a short exposure etoposide treatment are shown in panels A of Figure 4.3 and 4.4. Panels B of Figure 4.3 and 4.4 show averaged data from 3 separate experiments for percentage of apoptotic cells. SHSY5Y cells not exposed to drug showed an increased frequency of apoptotic cells by 72 hours, thought to be due to confluency of the cells. Both SHSY5Y and 1301 cultures exposed to etoposide at 100 μM and 350 μM showed clear increases in apoptotic cells by 24 hours, with further increases at later time points. Exposure of SHSY5Y cultures to concentrations of 15 μM or below caused not more than a slight increase in frequency of apoptotic cells above control and that only after a 48 hour incubation period (Figure 4.3). Following exposure to a concentration of drug of 15 μM or lower, no increase in apoptosis was seen in cultures of 1301 cells even at 48 hours (Figure 4.4). From both the scatter dot plots and the average graphs, it can be distinguished that 48 hours after a short exposure treatment, 1301 cells had higher levels of apoptosis (74%) compared to the SHSY5Y cells (64%).

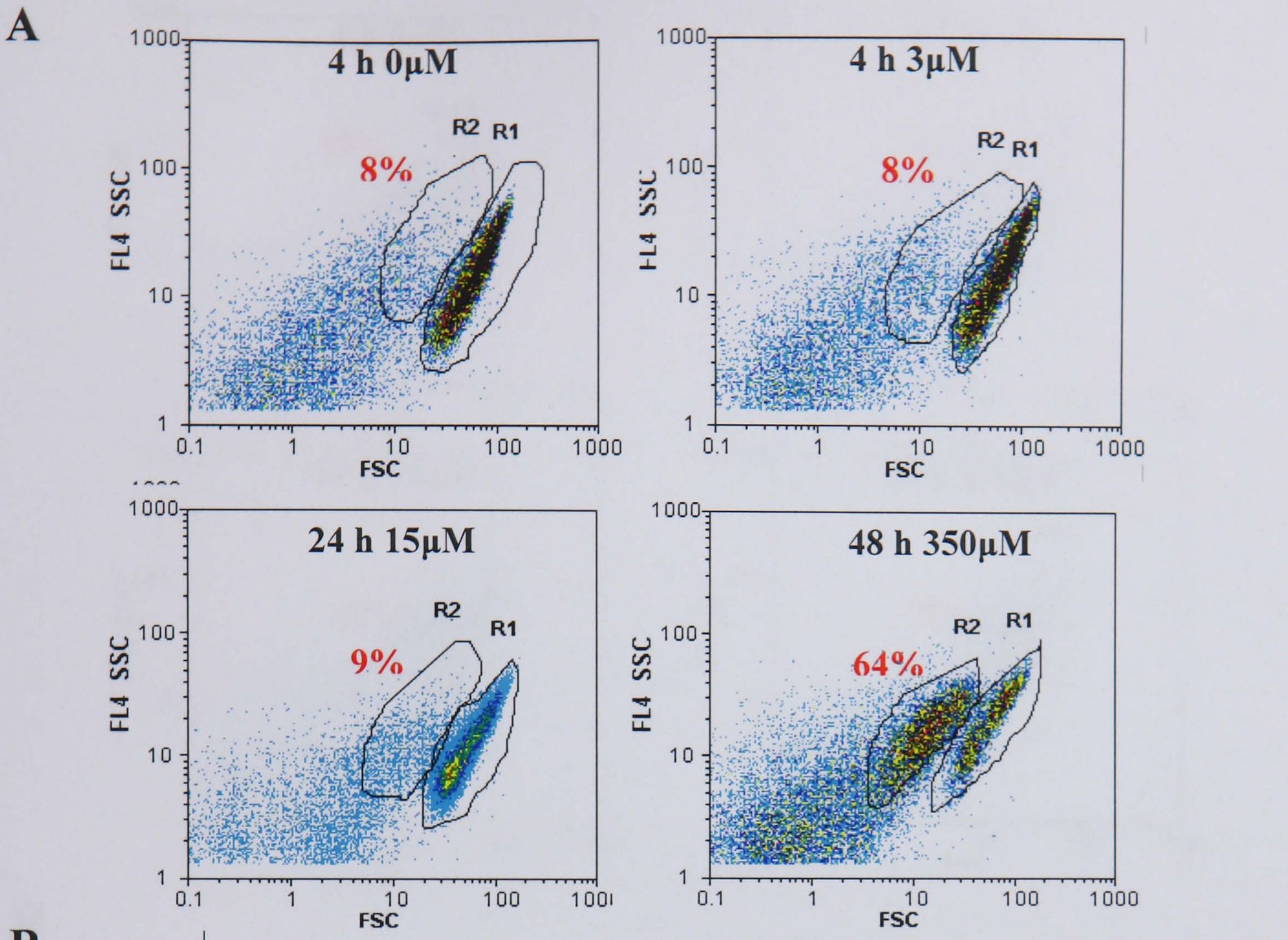

Figure 4.3 Levels of apoptosis after short exposure etoposide treatment on SHSY5Y cells. Apoptotic cells were measured by flow cytometry according to their size (forward scatter; FSC) and granularity (light scattered sideways; SSC). (A) Examples of gated apoptotic cells R2, to non apoptotic cells R1 after etoposide treatment. Time after treatment and concentration of etoposide indicated. % of apoptotic cells are shown in red. (B) % of apoptotic cells after etoposide treatment average graph. Data are mean ± SEM from triplicate experiments with three replicates in each experiment.

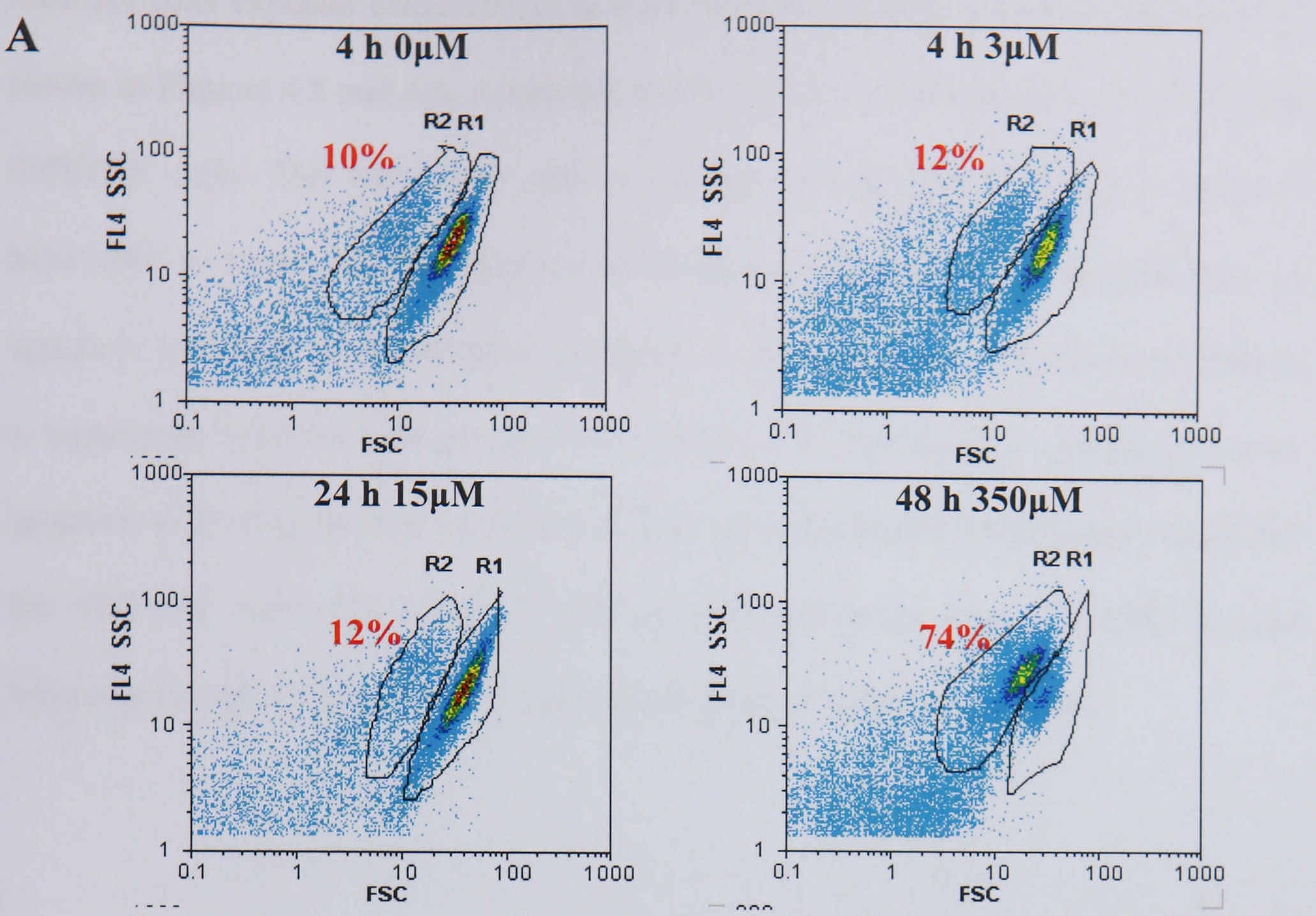

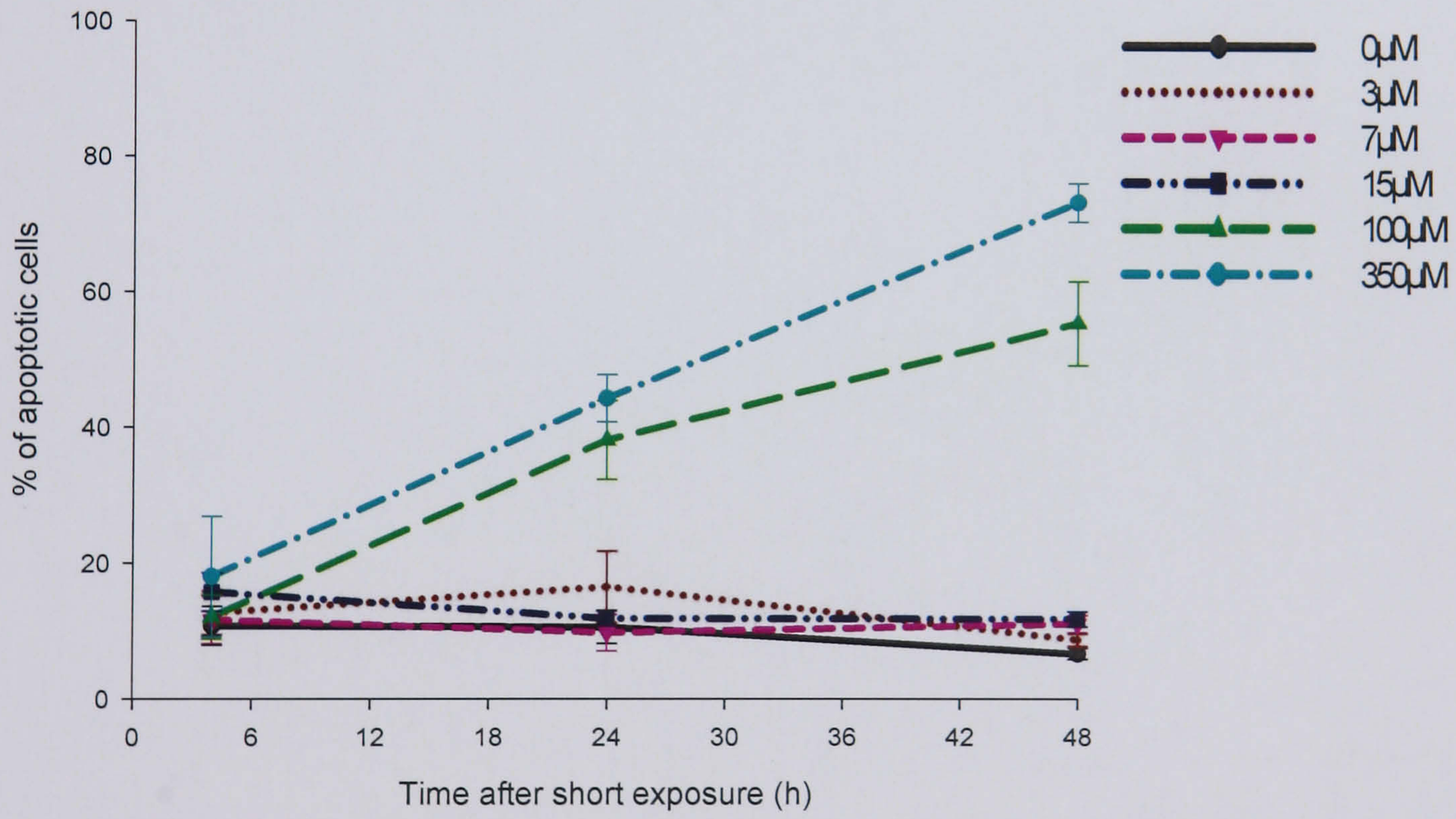

Figure 4.4 Levels of apoptosis after short exposure etoposide treatment on 1301 cells. Apoptotic cells were measured by flow cytometry according to their size (forward scatter; FSC) and granularity (light scattered sideways; SSC). (A) Examples of gated apoptotic cells R2, to non apoptotic cells R1 after etoposide treatment. Time after treatment and concentration of etoposide indicated. % of apoptotic cells are shown in red. (B) % of apoptotic cells after etoposide treatment average graph. Data are mean ± SEM from triplicate experiments with three replicates in each experiment.

Data for cells exposed continuously to a lower range of etoposide concentrations are shown in Figures 4.5 and 4.6. Apoptosis was induced at concentrations above 1 μM in SHSY5Y cells. The 1301 cells after a continuous exposure exhibited a different behaviour in terms of the induction of apoptosis (Figure 4.6). The proportion of apoptotic cells only increased after the highest concentration (5 μM) treatment despite a significant inhibition of net growth (Table 4.1). In fact the majority of non-apoptotic cells were growth arrested at 2 days after the onset of treatments. Again like the SHSY5Y cells, the highest levels of apoptosis were after a 5 μM 72 hour treatment though this time with a much lower level of apoptosis present.

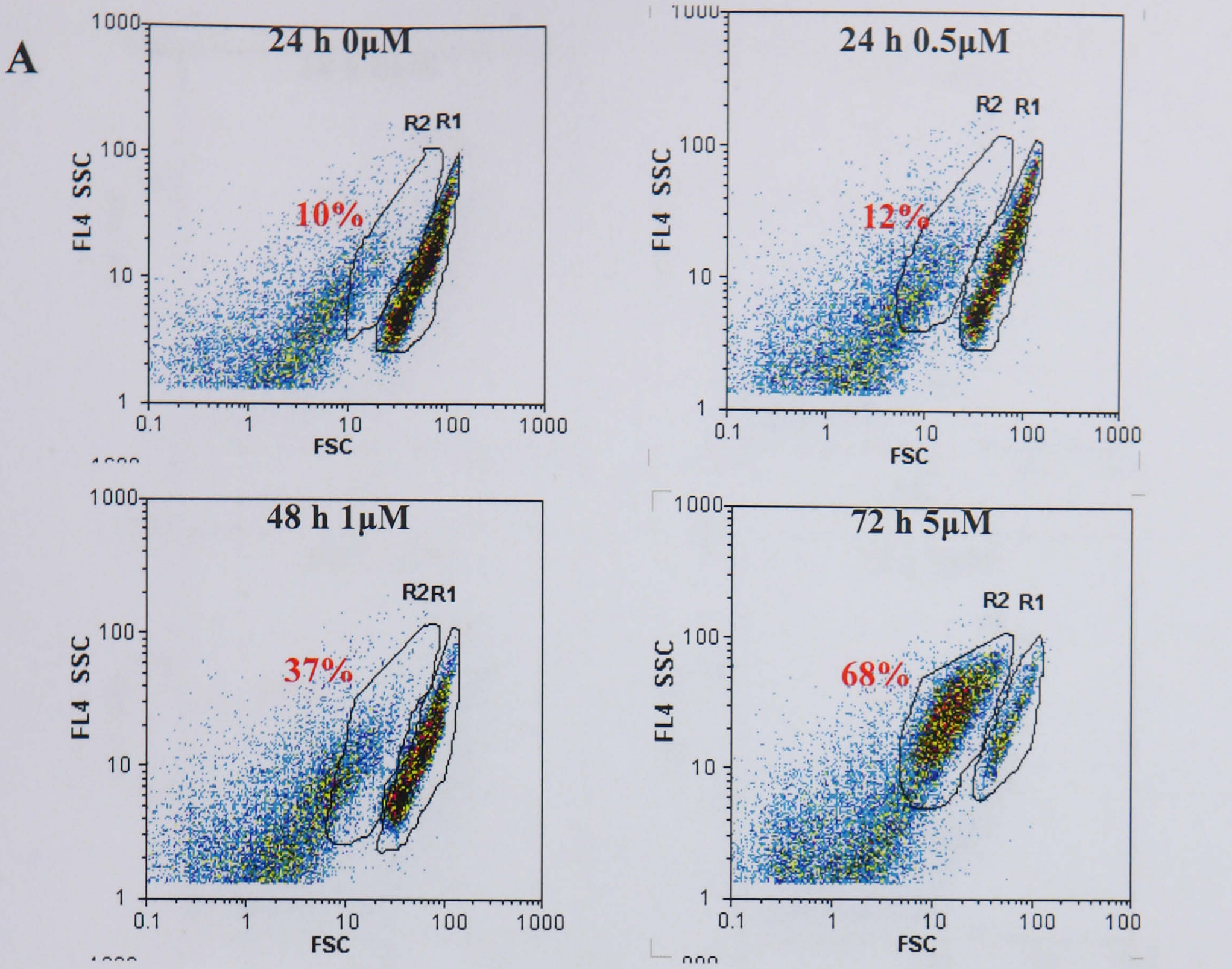

Figure 4.5 Levels of apoptosis after continuous exposure etoposide treatment on SHSY5Y cells. Apoptotic cells were measured by flow cytometry according to their size (forward scatter; FSC) and granularity (light scattered sideways; SSC). (A) Examples of gated apoptotic cells R2, to non apoptotic cells R1 after etoposide treatment. Time after treatment and concentration of etoposide indicated. % of apoptotic cells are shown in red. (B) % of apoptotic cells after etoposide treatment average graph. Data are mean ± SEM from triplicate experiments.

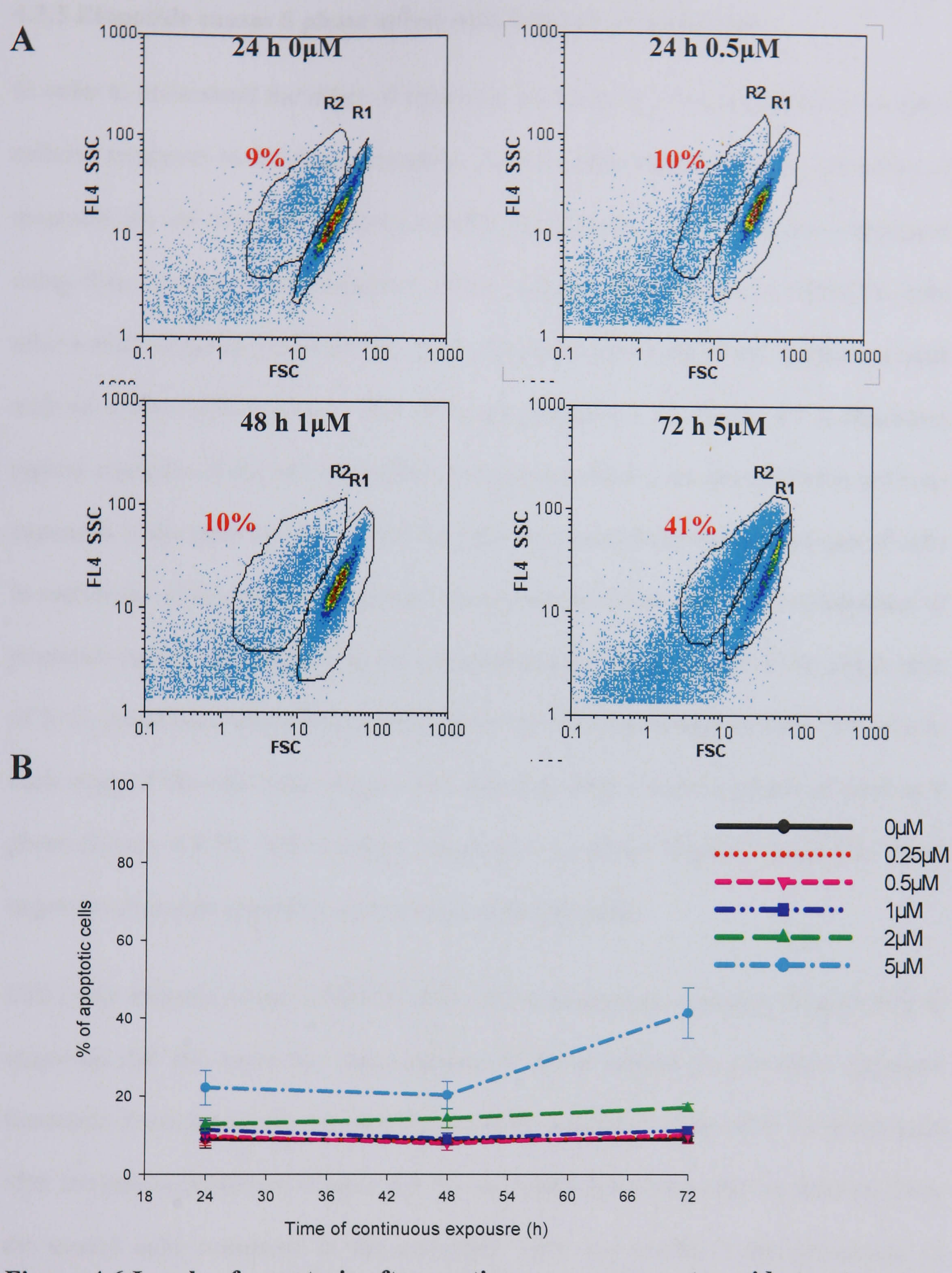

Figure 4.6 Levels of apoptosis after continuous exposure etoposide treatment on 1301 cells. Apoptotic cells were measured by flow cytometry according to their size (forward scatter; FSC) and granularity (light scattered sideways; SSC). (A) Examples of gated apoptotic cells R2, to non apoptotic cells R1 after etoposide treatment. Time after treatment and concentration of etoposide indicated. % of apoptotic cells are shown in red. (B) % of apoptotic cells after etoposide treatment average graph. Data are mean ± SEM from triplicate experiments.

4.3.3 Etoposide causes S phase arrest with features of senescence

In order to understand the effect of etoposide on the cells it was important to compare cellular responses to the drug exposures. An important aspect of this is the effect of etoposide on cell cycle progression. Initially the kinetics of cell cycle were measured using flow cytometry. Measurement of the cellular DNA content in SHSY5Y cells after a short exposure treatment revealed significant increases of the fraction of cells with an S phase DNA content after 48 hours (Figure 4.7 A). Figure 4.7 A illustrates typical examples of the cell cycle DNA histograms which were obtained after a 4 hour exposure. If the ratio of S/ G_1 phase cells are calculated from the percentages of cells in each stage of the cell cycle it can be clearly observed that after all concentrations of etoposide treatment compared to the untreated control there appears to be a high ratio of S/ G_1 phase cells after 48 hours (Figure 4.7 B). The percentage of SHSY5Y cells in each stage of the cell cycle (Figure 4.8) also indicated a slight increase of cells in S phase (Figure 4.8 B), with a minor decrease in G_1 phase (Figure 4.8 A) after short exposure etoposide treatment compared to untreated cells.

Cell cycle analysis of the SHSY5Y cells after a continuous exposure (Figure 4.9) to etoposide did not show the same pattern of DNA content as the short exposure treatment. From the histograms and the graph examining the ratio of S/ G_1 phase cells after continuous treatment (Figure 4.9 B), no significant change can be detected from the treated cells compared to the untreated. This was visible if the percentage of SHSY5Y cells in each stage of the cell cycle are assessed individually (Figure 4.10). The fall in S/ G_1 ratio between 4- 24 hours after short exposure treatment (Figure 4.7 B) could be a result of changing medium as this decrease was not detected after continuous exposure (Figure 4.9 B).

A

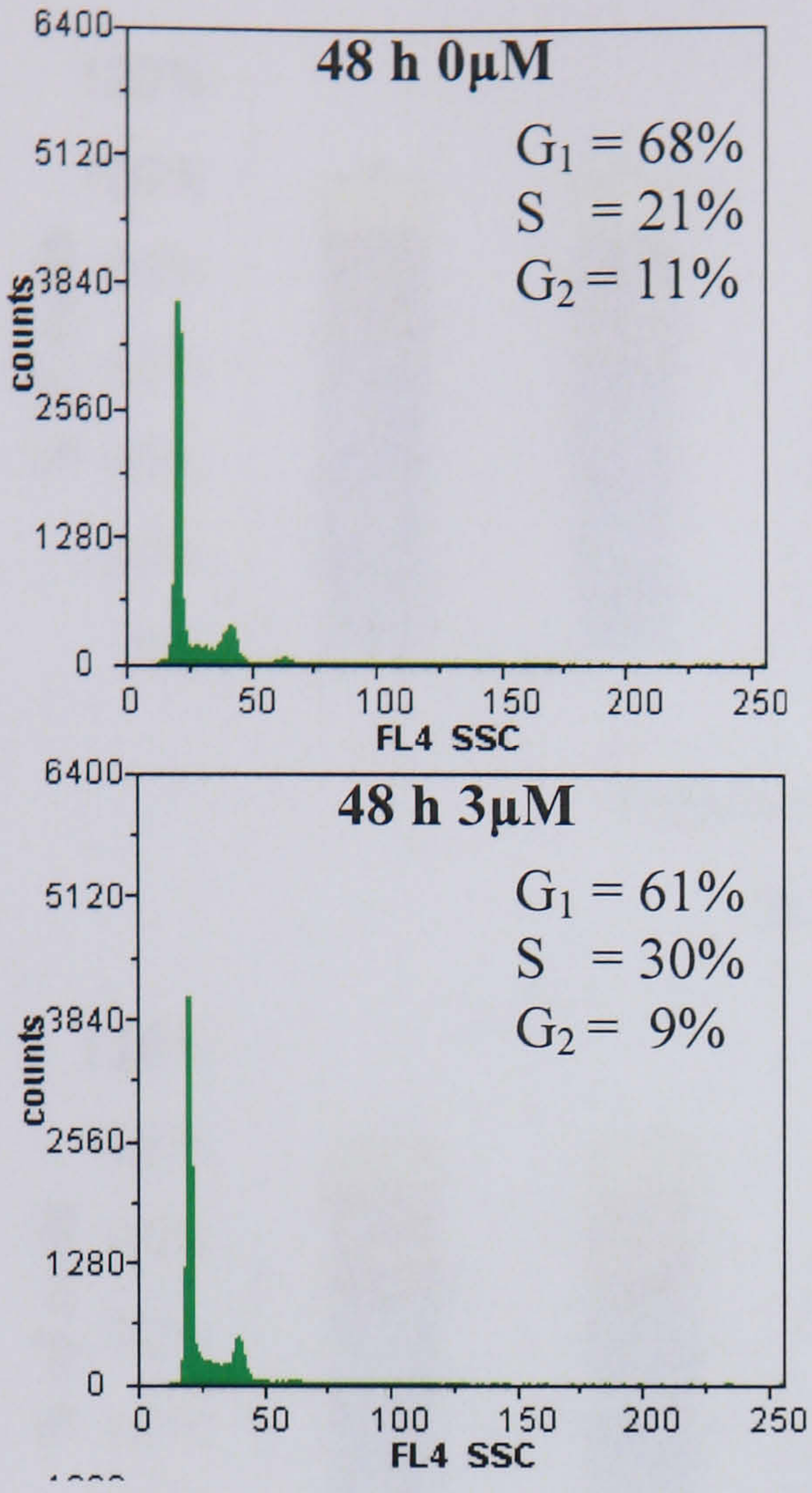

B

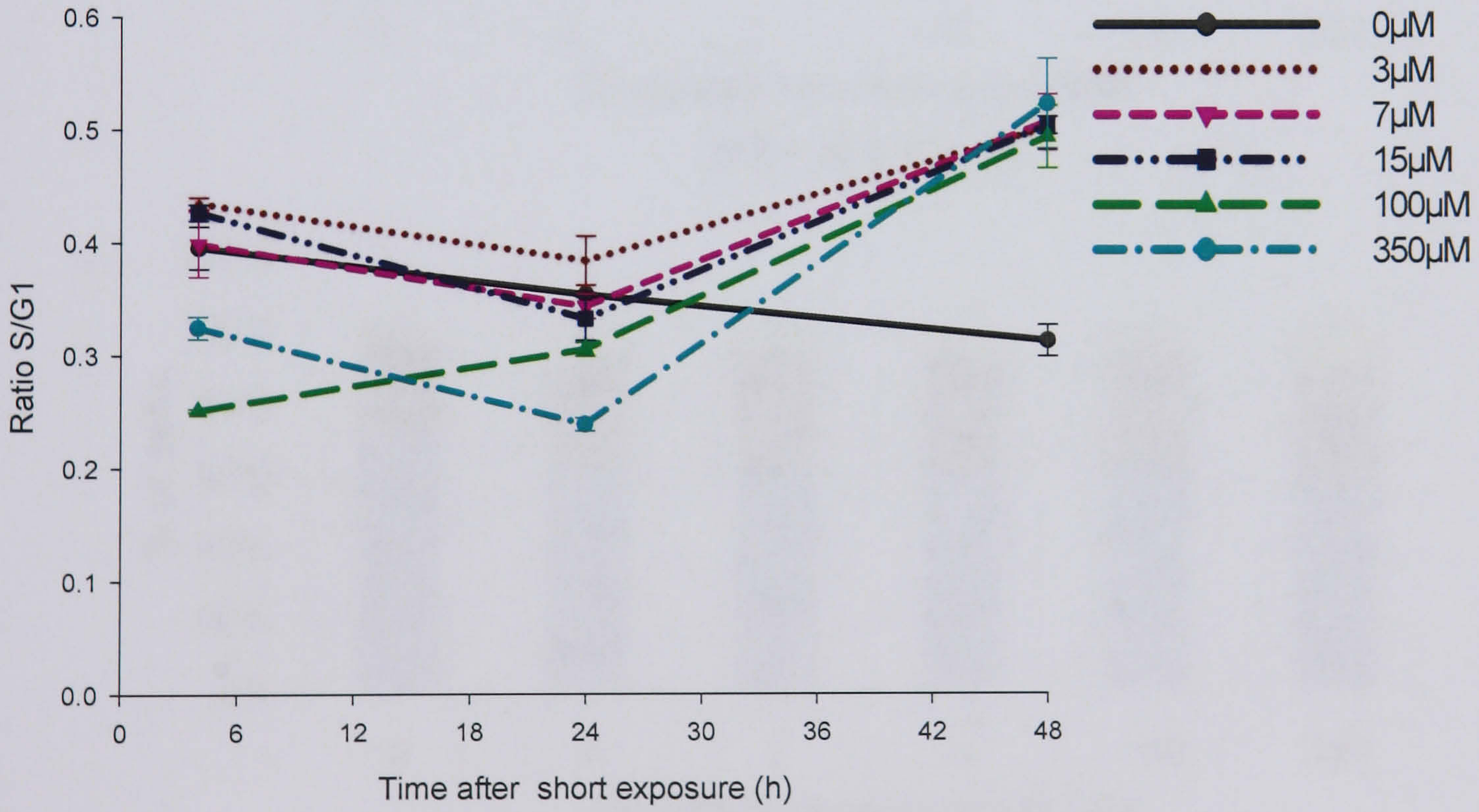

Figure 4.7 Cell cycle analysis of SHSY5Y cells exposed to etoposide for four hours. (A) Typical DNA histograms from DAPI stained cells using UV light, at the indicated times after treatment. (B) Change in ratio of S/ G_1 with time after short exposure to etoposide. Data are mean ± SEM from triplicate experiments with three replicates in each experiment.

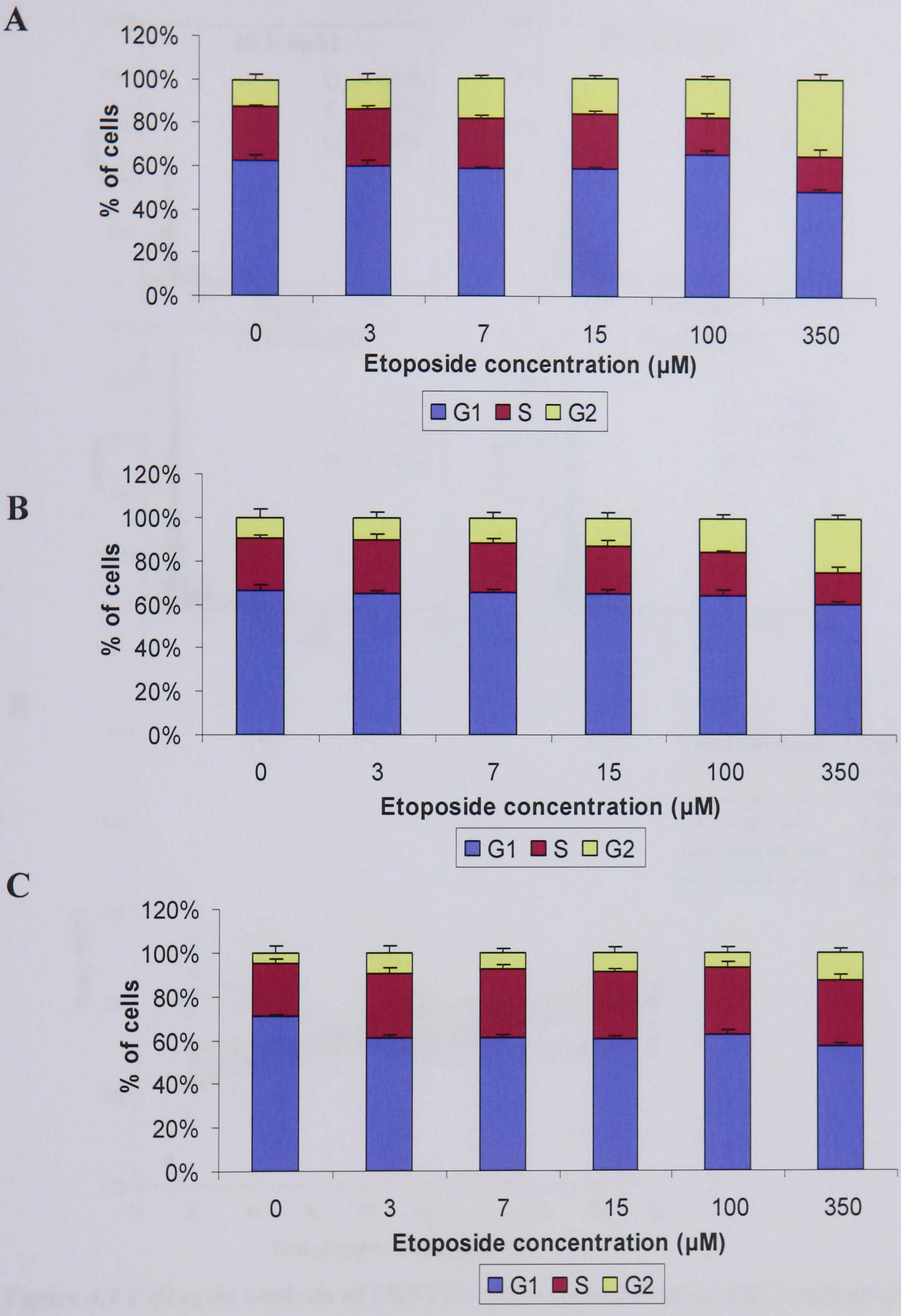

Figure 4.8 Stages of SHSY5Y cells in the cell cycle after a four hour exposure to etoposide. Percentage of cells in G_1 (blue), S (purple) and G_2 (yellow) phase 4 hours (A), 24 hours (B) and 48 hours (C) after a 4 hour etoposide treatment at the indicated etoposide concentrations, assessed by flow cytometry. Data are mean ± SEM from triplicate experiments with three replicates in each experiment.

A

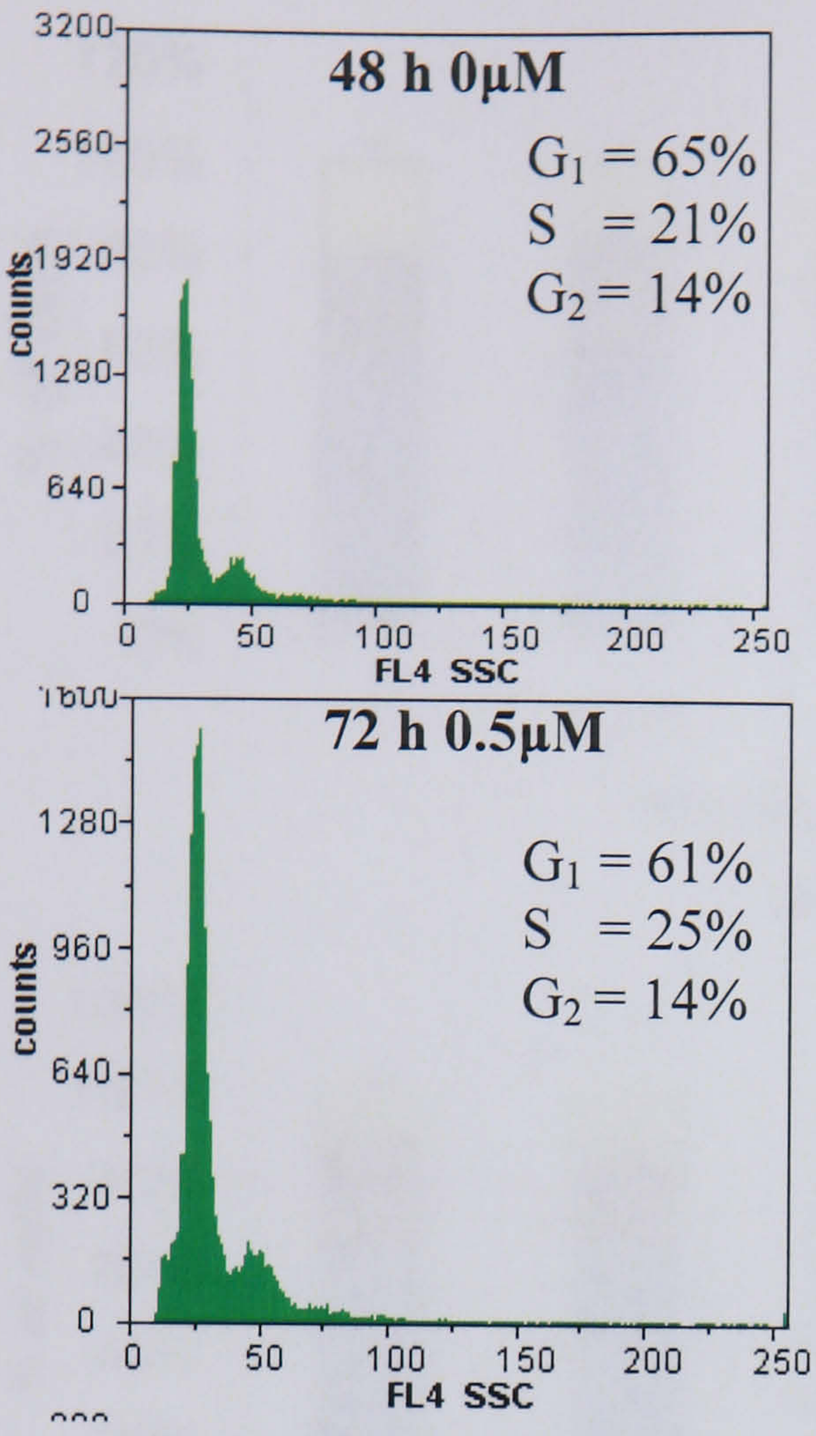

B

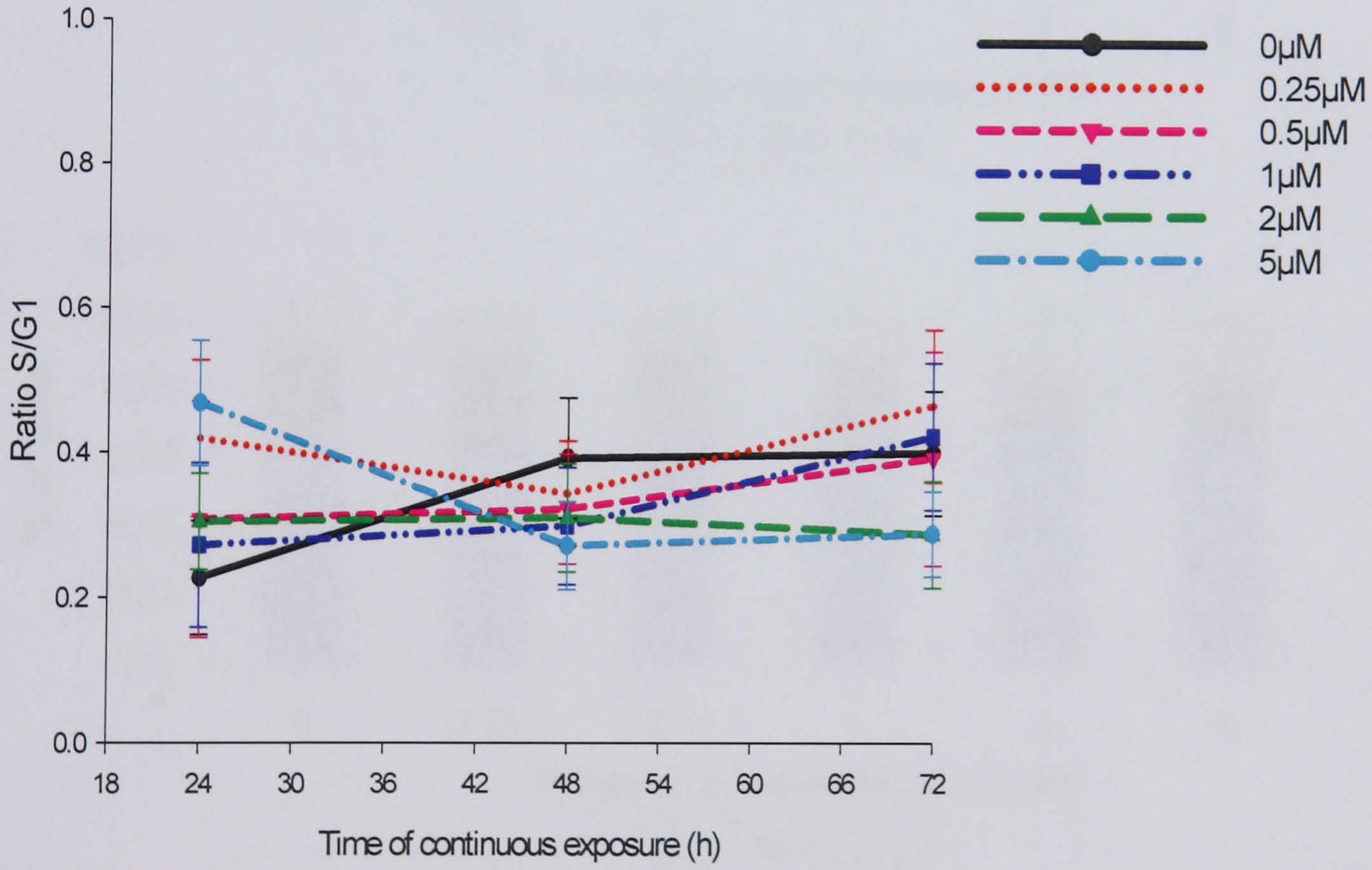

Figure 4.9 Cell cycle analysis of SHSY5Y cells exposed to etoposide continuously. (A) Typical DNA histograms from DAPI stained cells at the indicated times using UV light after treatment. (B) Graph showing change in ratio of S/ G_1 with time after continuous exposure to etoposide. Data are mean ± SEM from triplicate experiments with three replicates in each experiment.

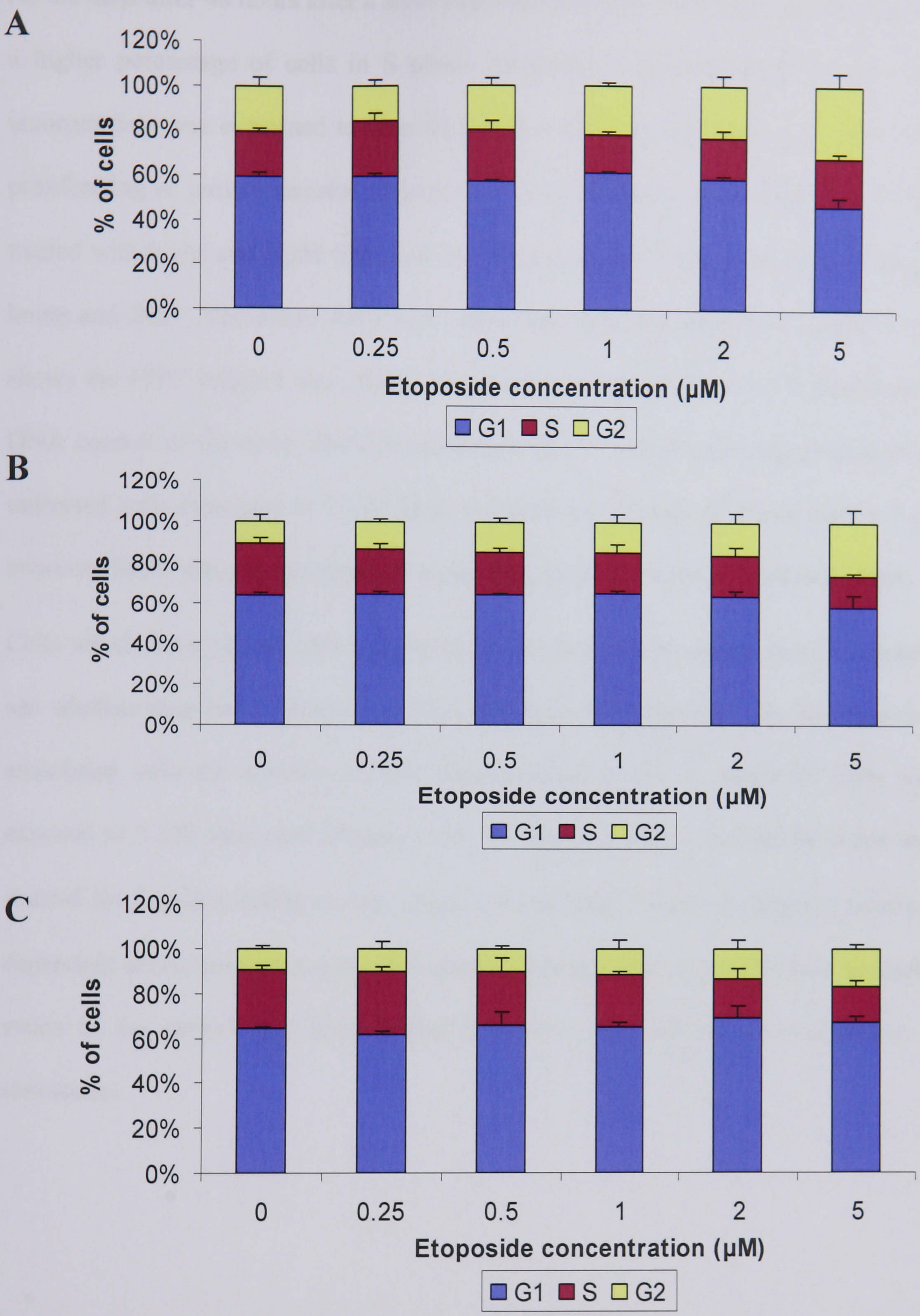

Figure 4.10 Stages of SHSY5Y cells in the cell cycle after a continuous exposure to etoposide. Percentage of cells in G_1 (blue), S (purple) and G_2 (yellow) phase 24 hours (A), 48 hours (B) and 72 hours (C) after continuous etoposide treatment at the indicated etoposide concentrations, assessed by flow cytometry. Data are mean ± SEM from triplicate experiments with three replicates in each experiment.

As the cells after 48 hours after a short exposure etoposide treatment appeared to have a higher percentage of cells in S phase compared to the untreated control, BrdU incorporation was examined to identify whether the cells that were in S phase were proliferating or growth arrested (Figure 4.11). For the BrdU incorporation cells were treated with 0 μM and 3 μM etoposide for 4 hours and then incubated for a further 48 hours and BrdU was added for 1 hour after treatment was complete. Figure 4.11 A shows the FITC labelled anti- BrdU fluorescence whilst Figure 4.11 B identifies the DNA content of the cells after the treatments. BrdU is distinctly incorporated in the untreated cells (compare to 0 μM IgG) as expected. Though 48 hours after a 3 μM exposure BrdU was not incorporated suggesting that cells were arrested in S phase.

Cells which were treated with a short exposure etoposide treatment were assessed to see whether they had a senescence-like phenotype (See Section 1.7). Senescence is associated with the activity of beta galactosidase at pH 6. SHSY5Y cells were exposed to 3 μM etoposide treatment for 4 hours and after a further 48 hours were stained for β galactosidase activity (Figure 4.12). MRC5 cells undergoing telomere-dependent senescence were used as a positive control. The results showed detectable stains in the control and drug treated SHSY5Y cells and therefore evidence of senescence.

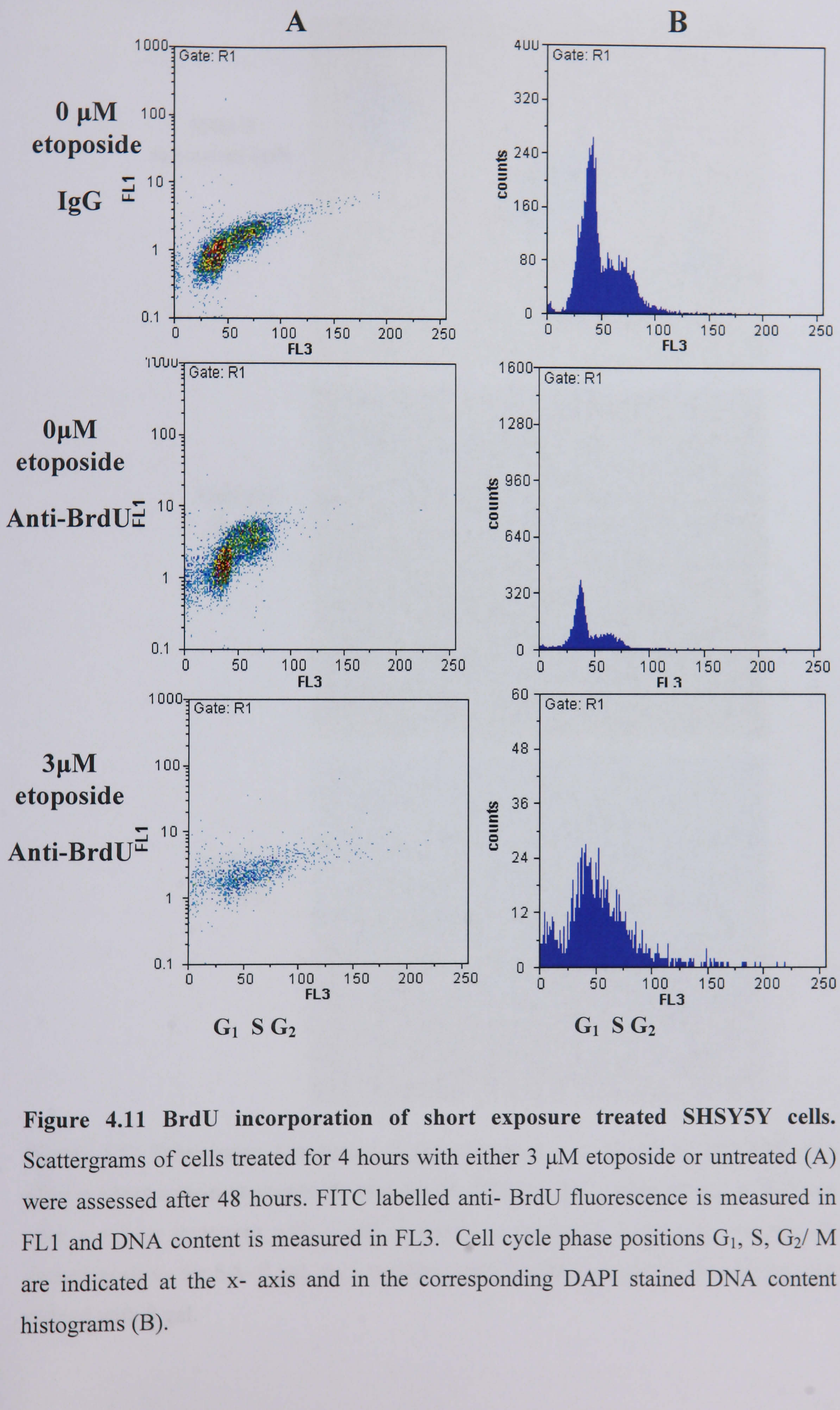

Figure 4.11 BrdU incorporation of short exposure treated SHSY5Y cells. Scattergrams of cells treated for 4 hours with either 3 µM etoposide or untreated (A) were assessed after 48 hours. FITC labelled anti- BrdU fluorescence is measured in FL1 and DNA content is measured in FL3. Cell cycle phase positions G_1, S, G_2/ M are indicated at the x- axis and in the corresponding DAPI stained DNA content histograms (B).

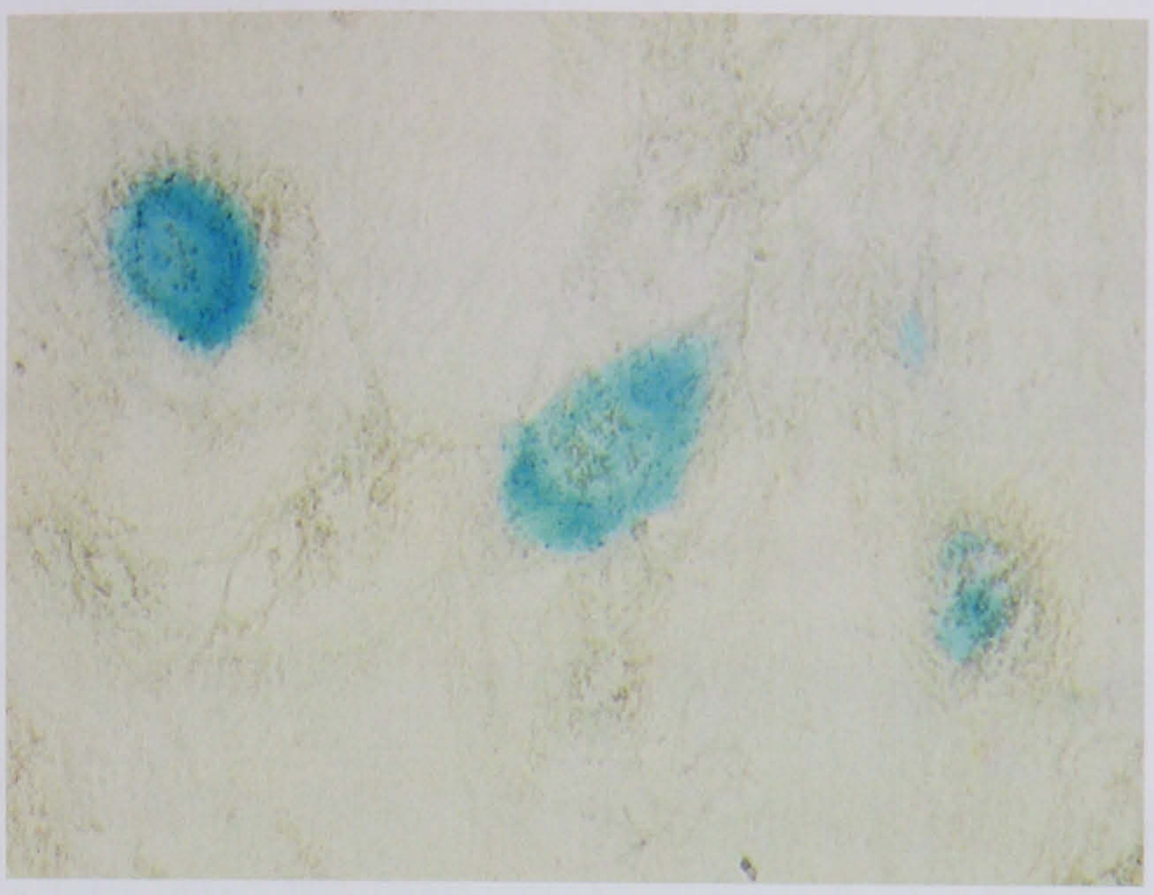

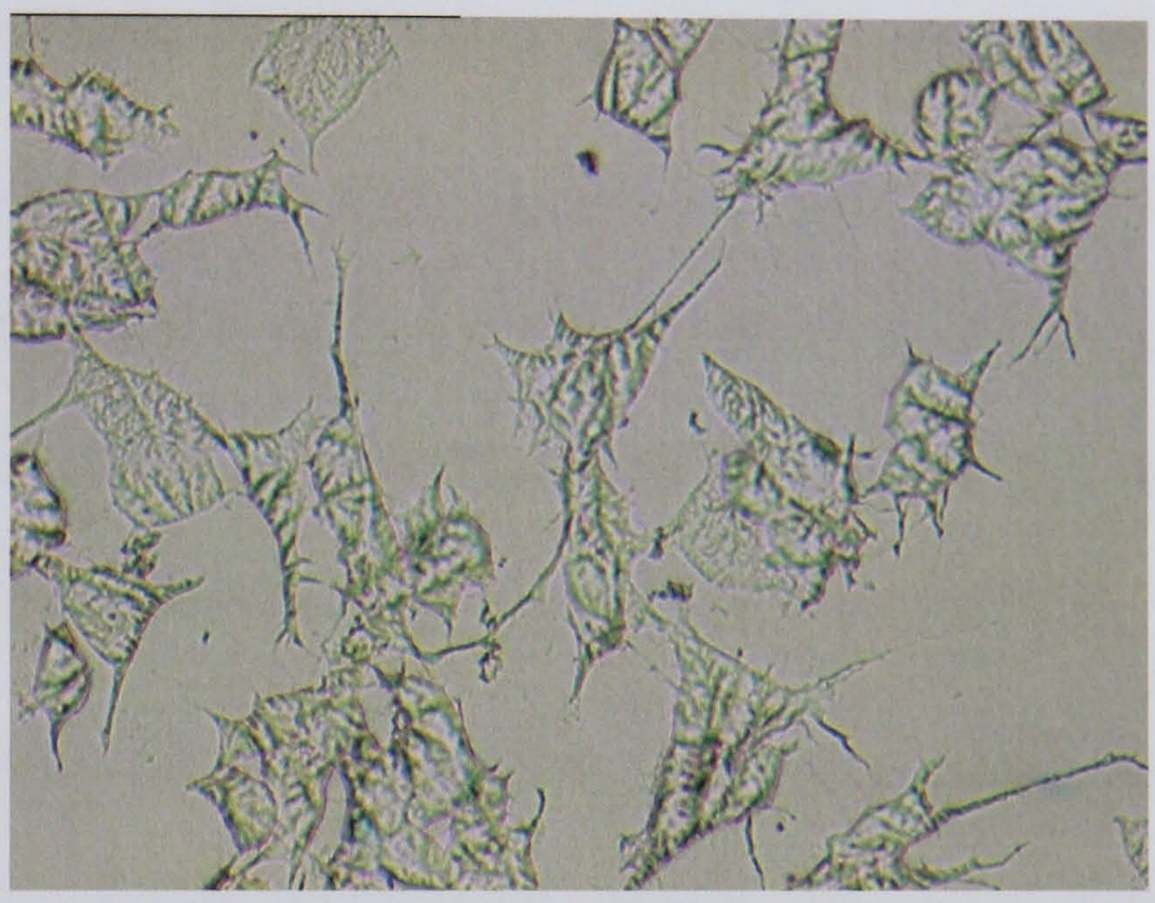

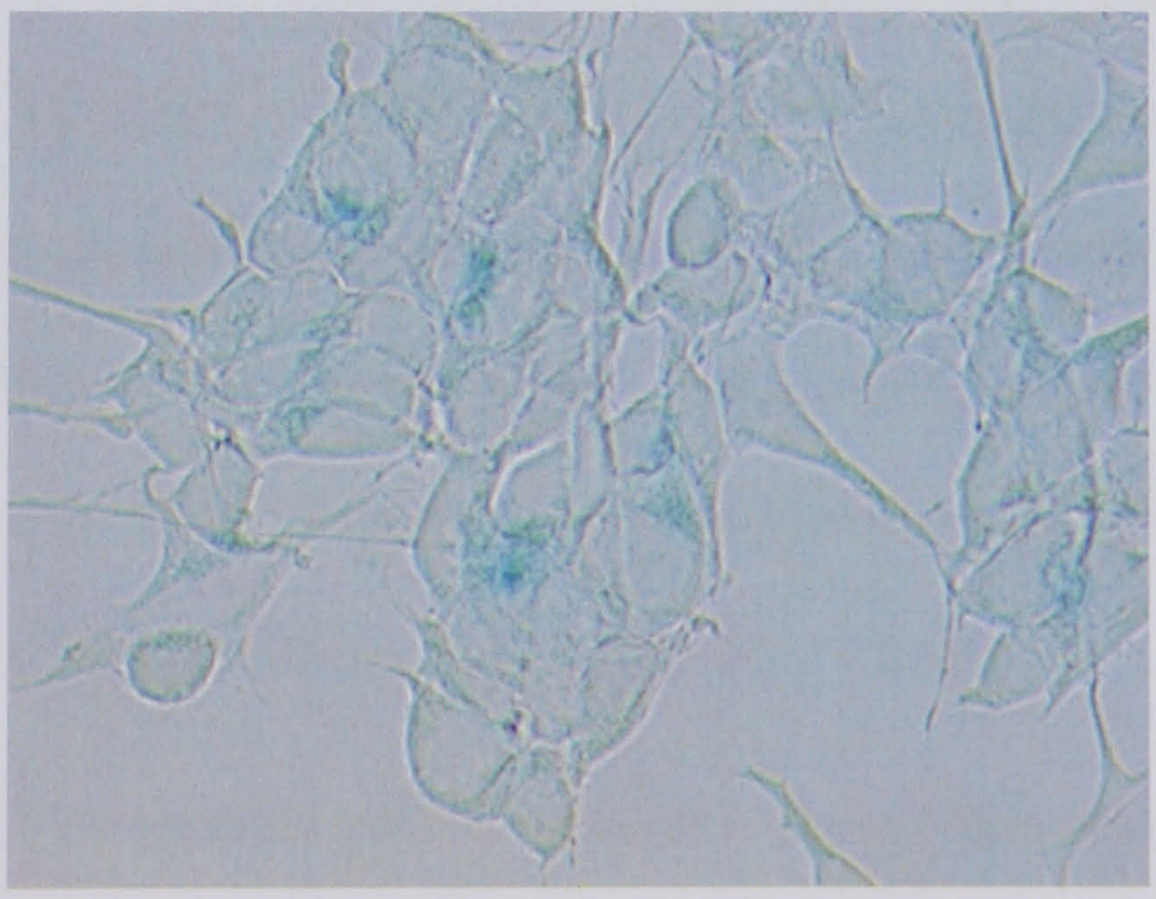

Figure 4.12 Senescence Associated -β galactosidase (SA- β gal) of SHSY5Y cells after a short exposure etoposide treatment. SHSY5Y cells were stained at 48 hours after a 4 hour treatment with 3 µM etoposide or untreated. Etoposide treated cells stained positive for SA- β gal. As a positive control MRC5 senescent fibroblasts were stained with β gal.

4.3.4 Etoposide triggers a DNA damage response

Etoposide induces stabilisation of topoisomerase II cleavable complexes and their associated double and single DNA strand breaks. Results described in Section 4.3.2 indicate that exposure of cells to a wide range of concentrations of etoposide resulted in apoptosis. In order to confirm that under the conditions in this work general damage to the overall genome is induced by etoposide, DNA strand breaks and the DNA damage response was investigated by the FADU assay and an antibody recognising the phosphorylated form of histone H2A.X (γ-H2A.X) respectively.

FADU measurements confirmed the expected concentration dependent rise of DNA strand breaks immediately after a 4 hour treatment in both SHSY5Y cells (Figure 4.13 A) and 1301 cells (Figure 4.13 B), which correlates well with the observed frequencies of apoptotic cells after short term treatment (Figures 4.3 and 4.4).

The 1301 cells religated strand breaks more efficiently, resulting in significantly less breaks remaining after a further 4 hour incubation (compare Figure 4.13 A and 4.13 B), which might be related to the ability of 1301 cells to redirect their response to low etoposide concentrations from apoptosis towards growth arrest. The significance of religation capacity was confirmed by paired t-tests. The SHSY5Y cells show significant religation effects only after 350 μM short etoposide exposure, whilst the 1301 cells show a significant religation effect at concentrations ≥ 15 μM.

After a 15 μM short exposure to etoposide, cells were fixed 24 hours later and stained with a DAPI nuclear stain and an antibody against γ-H2A.X (Figure 4.14) to examine the DNA damage response. DNA damage foci were clearly evident in the majority of the cells after 24 hours after a short treatment with as low as 15 μM etoposide.

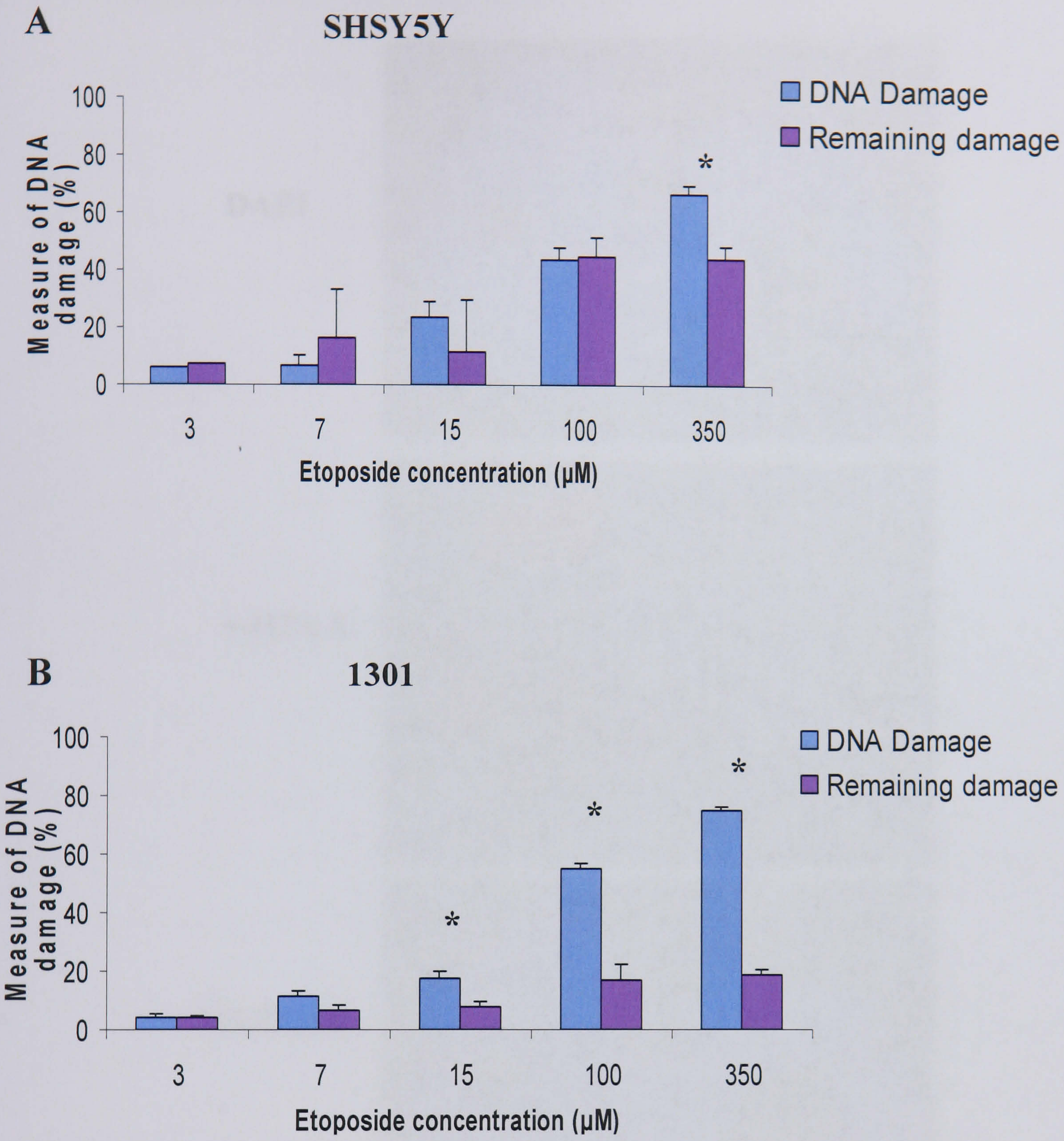

Figure 4.13 Measurement of DNA strand breaks in etoposide treated cells. DNA strand breaks were measured by FADU after a 4 hour etoposide treatment (blue bars) and after a further 4 hours recovery time allowing for religation of cleavable complexes (purple bars) in SHSY5Y (A) and 1301 (B) cells. Data are mean ± SEM from six parallel measurements. Significant repair effects are denoted by an asterisk ($p < 0.05$, paired t-test).

DAPI

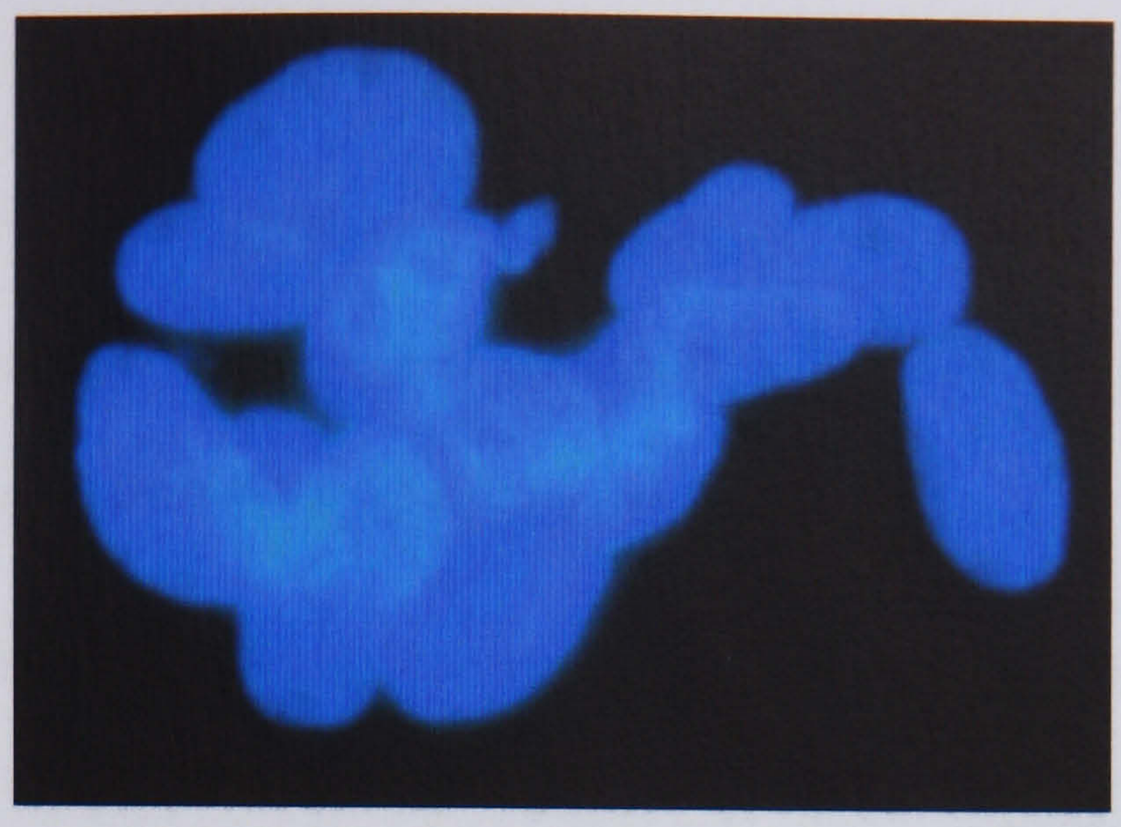

γ-H2A.X

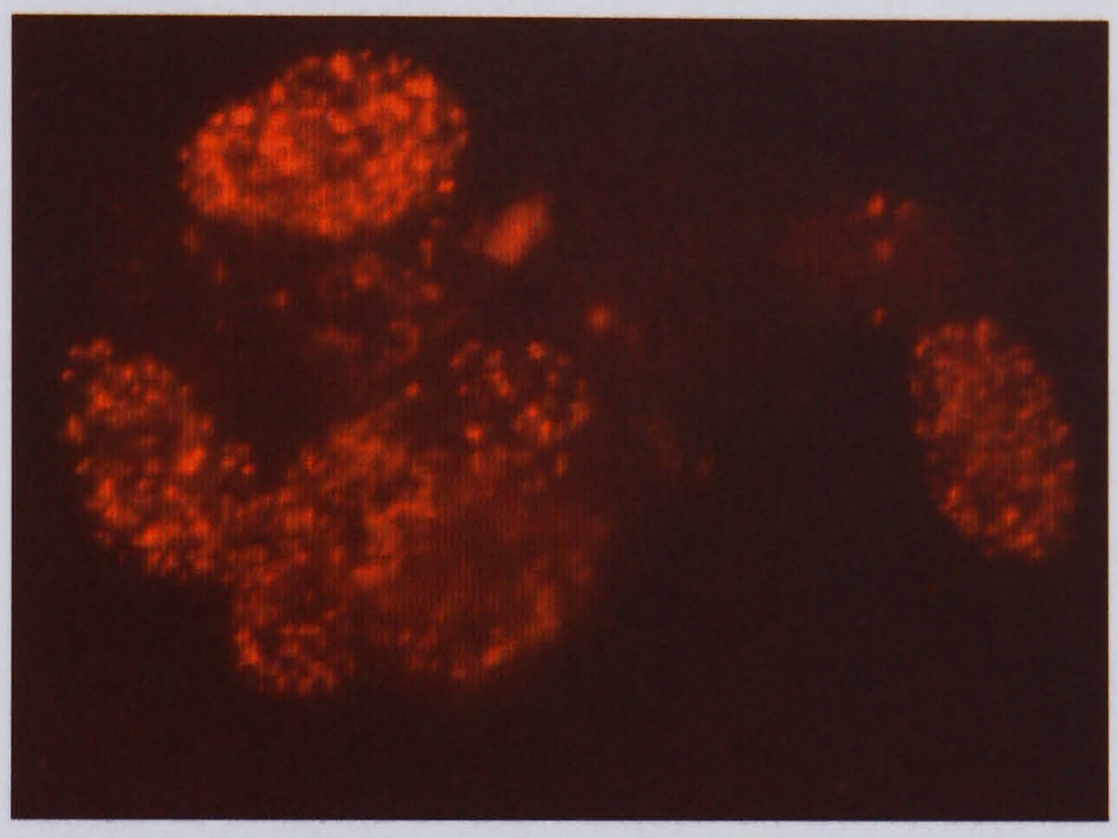

MERGED

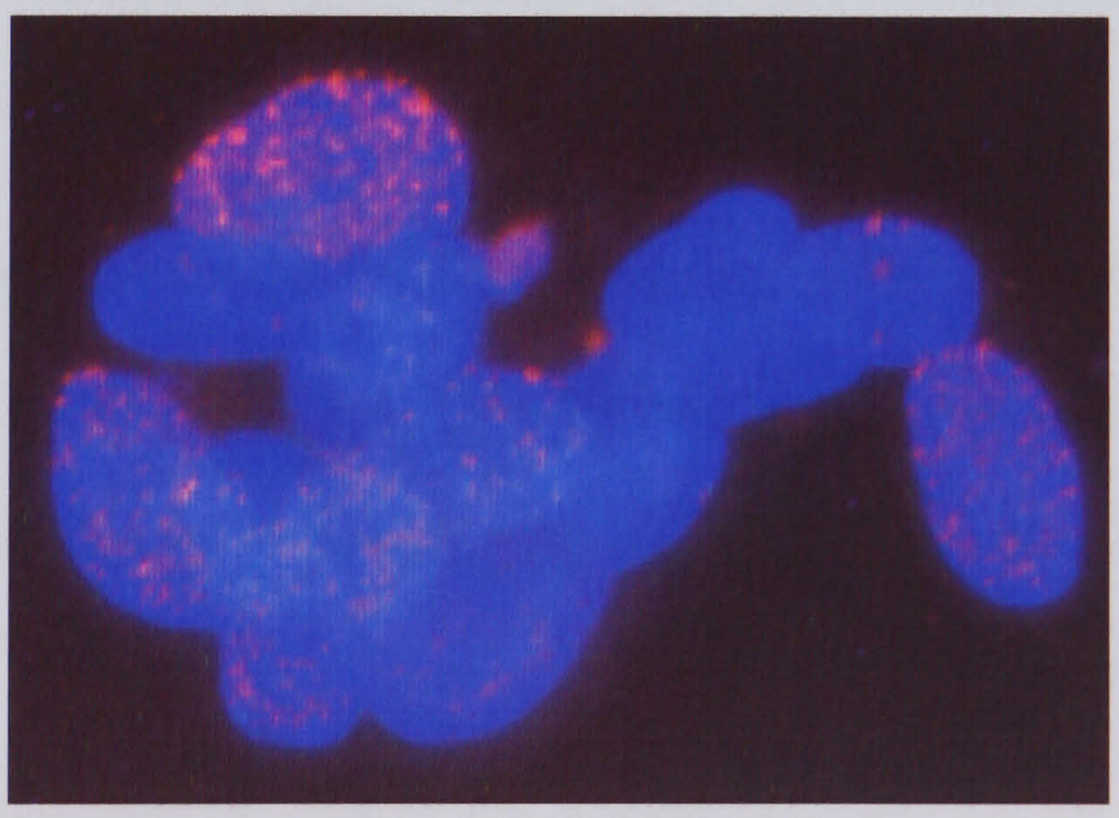

Figure 4.14 DNA damage response in etoposide treated SHSY5Y cells. Cells were fixed at 24 hours after a 4 hour treatment with 15 μM etoposide and stained with an antibody against the phosphorylated form of H2A.X (γ-H2A.X) and DAPI nuclear stain. x 40 objective

4.3.5 Etoposide does not influence telomere length

The main hypothesis being tested in this chapter was that the cytotoxic effects of etoposide induce growth arrest/ apoptosis via the telomere/ telomerase complex. Topoisomerase II cleavable complexes in telomeres would cause DNA double strand breaks and hence directly lead to shortening of telomeres.

The aim of the following experiments was to determine telomere lengths using an in-gel hybridisation technique at various times after exposure of cells to etoposide and to find out whether etoposide induced growth arrest/ apoptosis was preceded or accompanied by telomere shortening.

The SHSY5Y cells have telomere lengths of ~4 kbp while the 1301 cells have telomere lengths of ~80 kbp. The cell lines were chosen for this investigation, due to the large difference in the telomere lengths, as any changes that may occur may not be detectable in SHSY5Y cells with the shorter telomeres, though more pronounced in the 1301 cells with longer telomeres.

Cells were exposed to etoposide for either 4 hours (0, 3, 7, 15, 100 and 350 μM) or continuously (0, 0.25, 0.5, 1, 2, 5 μM). At 4, 24 and 48 hours after short exposure and 24, 48 and 72 hours after continuous exposure mean telomere restriction fragment lengths were measured.

Figures 4.14 to 4.18 show typical data. Panel A illustrates images of ethidium bromide fluorescence from electrophoresis gels to indicate distribution of total cellular DNA and MW markers. The intensity signal was proportional to the amount of DNA loaded, which was kept constant throughout.

Panel B demonstrates the telomere restriction fragment length gel. The calculated average telomere lengths are superimposed as white bars. Panel C shows the average

of at least three separate determinations of mean telomere length plotted against time after exposure to a range of etoposide concentrations.

SHSY5Y cells exposed to etoposide for 4 hours (Figure 4.15) or continuously (Figure 4.17) show no significant change in telomere length at any concentrations or time points. 1301 cells exposed to etoposide for 4 hours (Figure 4.16) or continuously (Figure 4.18) also showed no changes to the length of telomeres following exposure to any of the drug concentrations used. Measurement of telomere length at times up to 48 hours after exposure revealed no drug induced changes in telomeric restriction fragment lengths. This indicates that topoisomerase II cleavable complexes were not present in the telomere terminal repeat at a level sufficiently high to significantly reduce telomere length directly as a result of inherent double strand breaks. This is particularly relevant for the highest concentrations where the acute level of cleavable complexes is expected to be considerable. At the lower drug concentrations, telomere shortening might be expected as consequence of stalled DNA replication forks or other mechanisms.

A

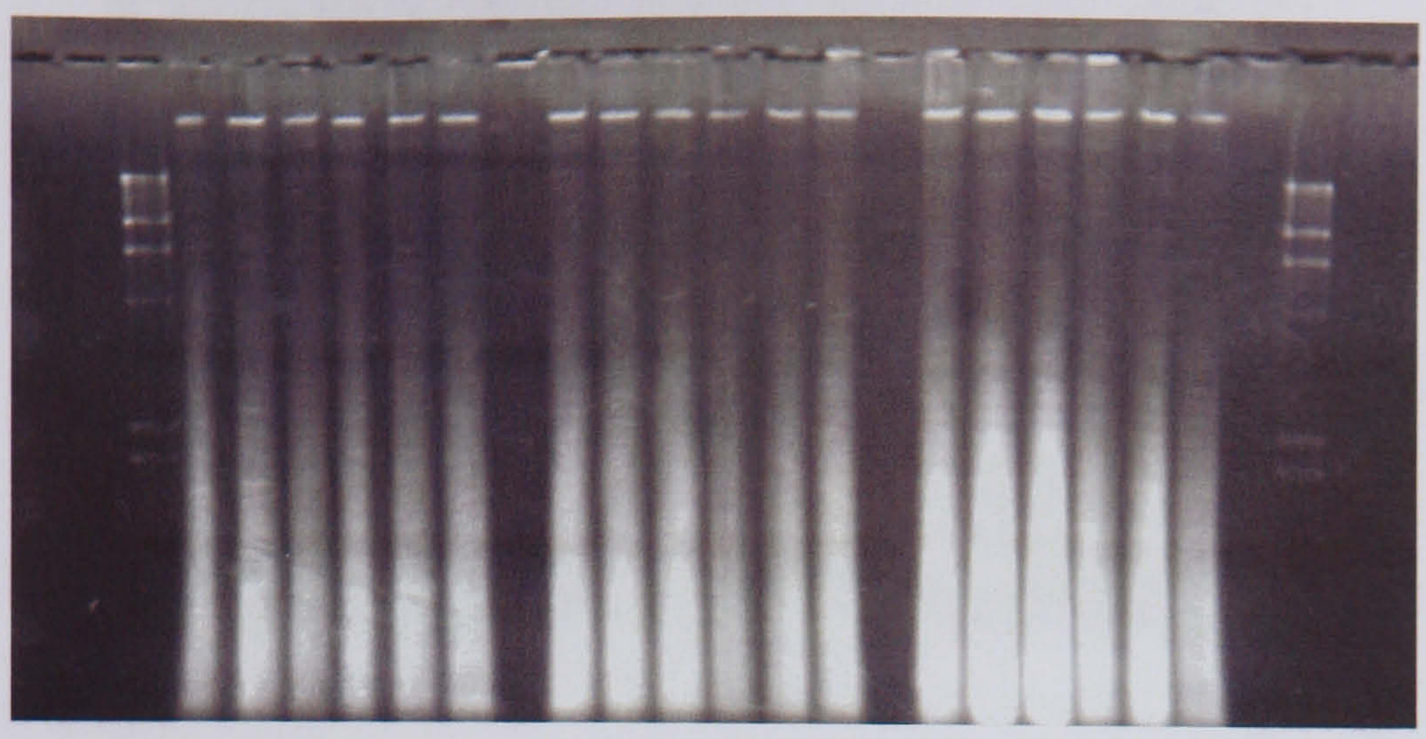

B

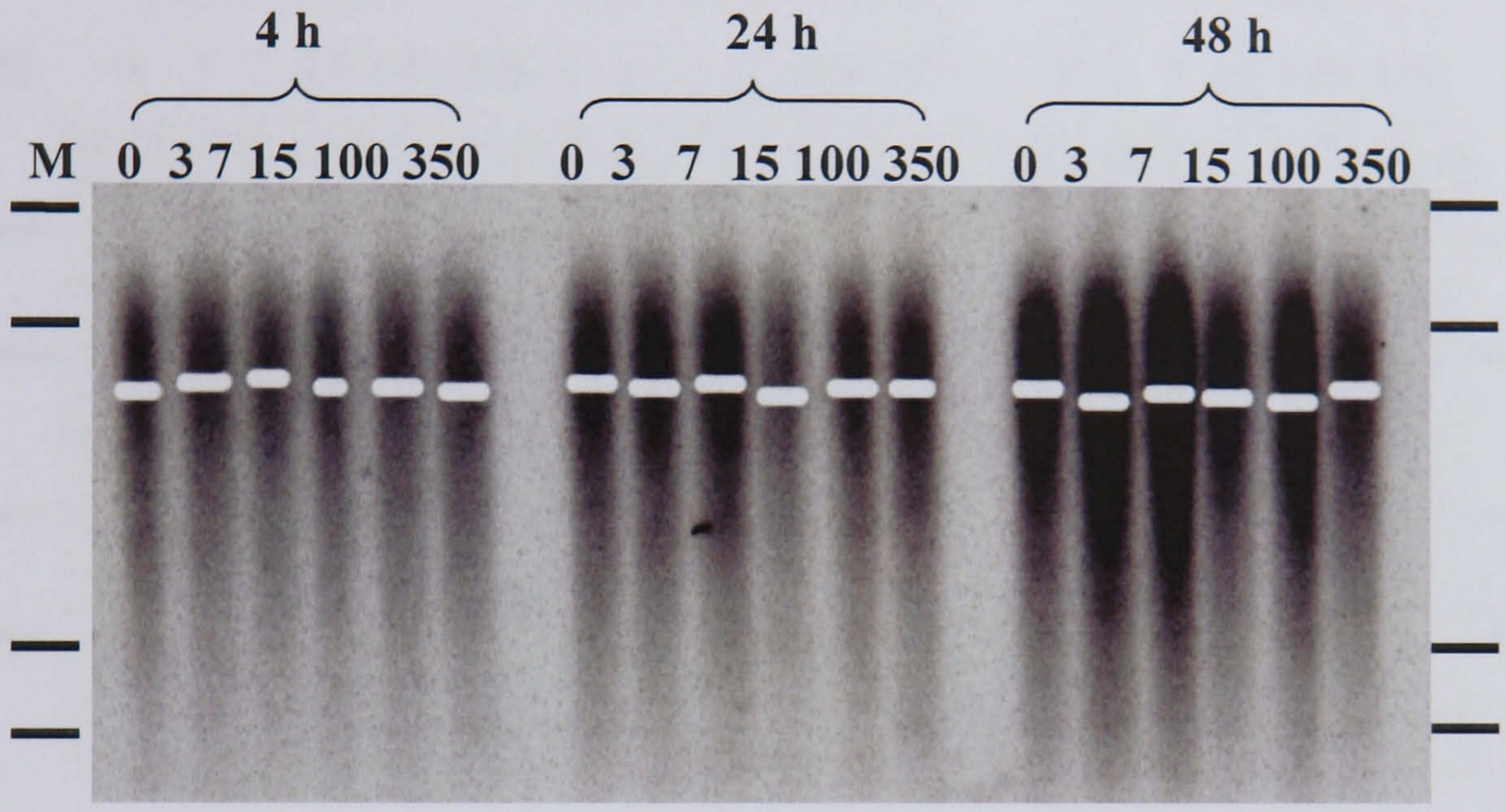

C

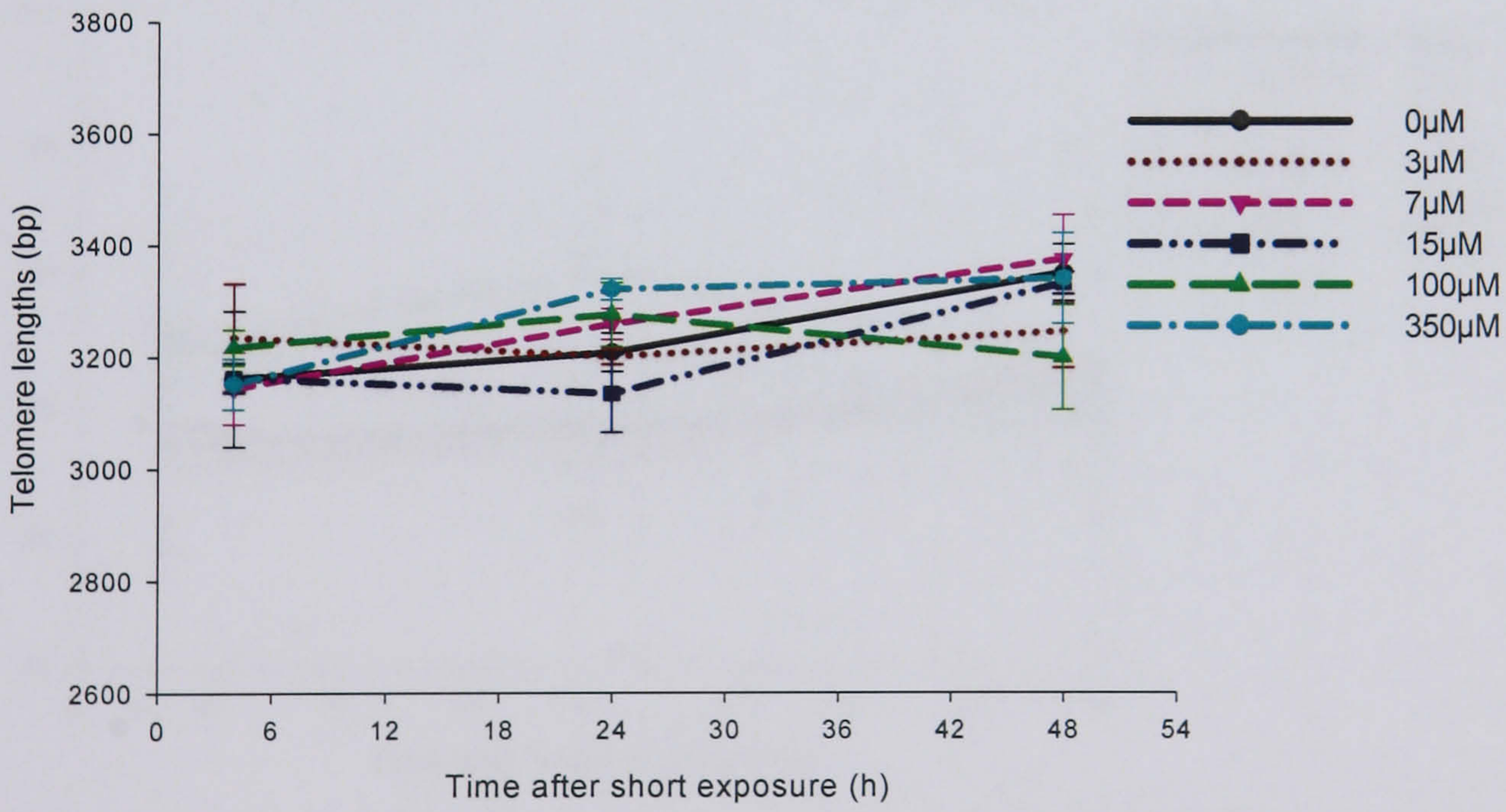

Figure 4.15 Telomere restriction fragment lengths after short exposure etoposide treatment on SHSY5Y cells. (A) Ethidium bromide fluorescence of genomic DNA. (B) Telomere gel. Etoposide concentrations (in μM) and times after onset of treatment (in h) are indicated on top of the figure. White bars indicate average telomere length. The positions of the size markers (23.1, 4.36, 2.32, 2.03 kbp) are shown by black bars. (C) Average telomere length. Gels were normalised to a standard and average fragment lengths of at least four experiments were calculated. Data are ± SEM.

Figure 4.16 Telomere restriction fragment lengths after short exposure etoposide treatment on 1301 cells. (A) Ethidium bromide fluorescence of genomic DNA. (B) Telomere gel. Etoposide concentrations (in µM) and times after onset of treatment (in h) are indicated on top of the figure. White bars indicate average telomere length. The positions of the size markers 194, 97, 48.5, 23.1 kbp) are shown by black bars. (C) Average telomere length. Gels were normalised to a standard and average fragment lengths of at least four experiments were calculated. Data are ± SEM.

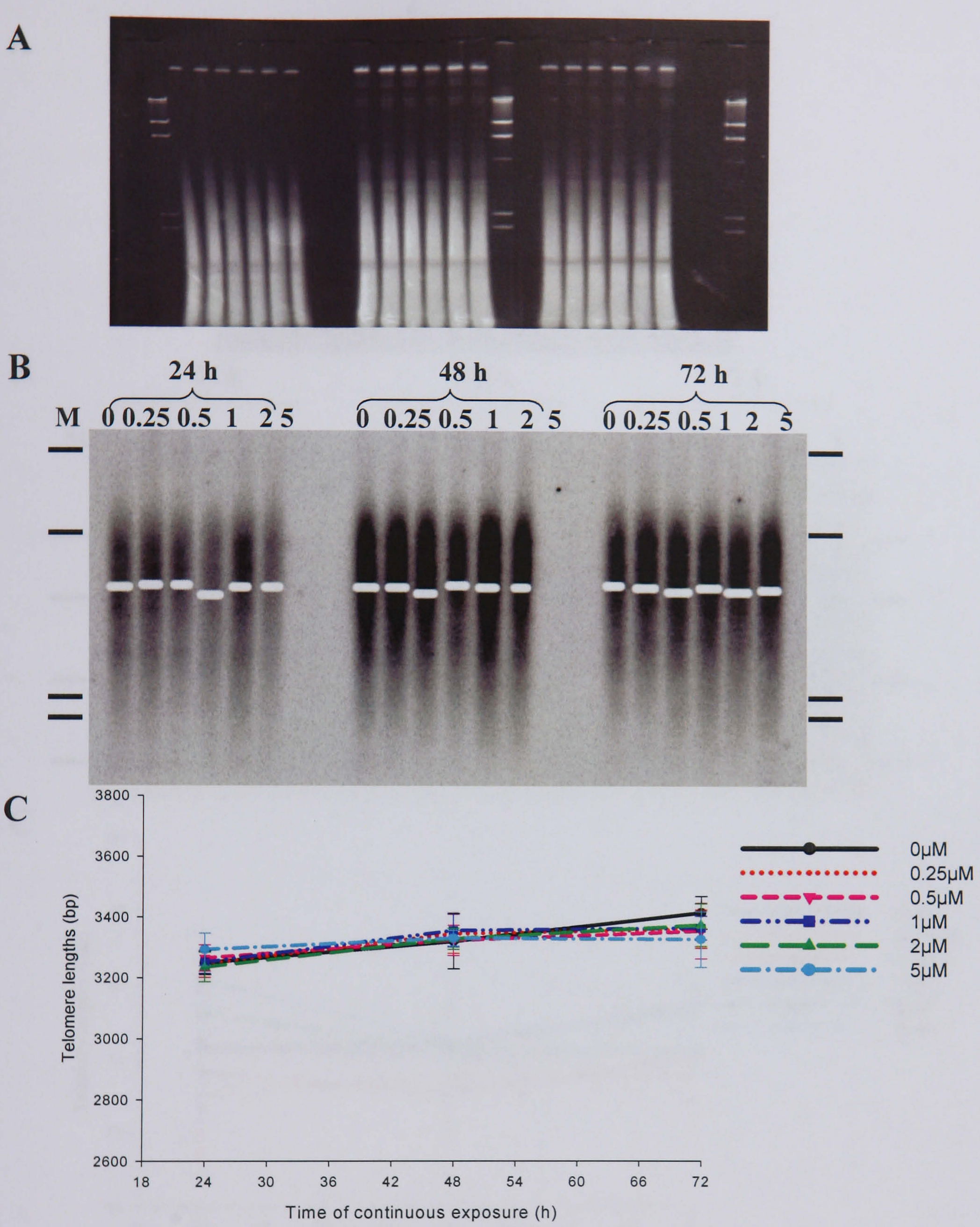

Figure 4.17 Telomere restriction fragment lengths after continuous exposure etoposide treatment on SHSY5Y cells. (A) Ethidium bromide fluorescence of genomic DNA. (B) Telomere gel. Etoposide concentrations (in μM) and times after onset of treatment (in h) are indicated on top of the figure. White bars indicate average telomere length. The positions of the size markers (23.1, 4.36, 2.32, 2.03 kbp) are specified. (C) Average telomere length. Gels were normalised to a standard and average fragment lengths of four experiments were calculated. Data are ± SEM.

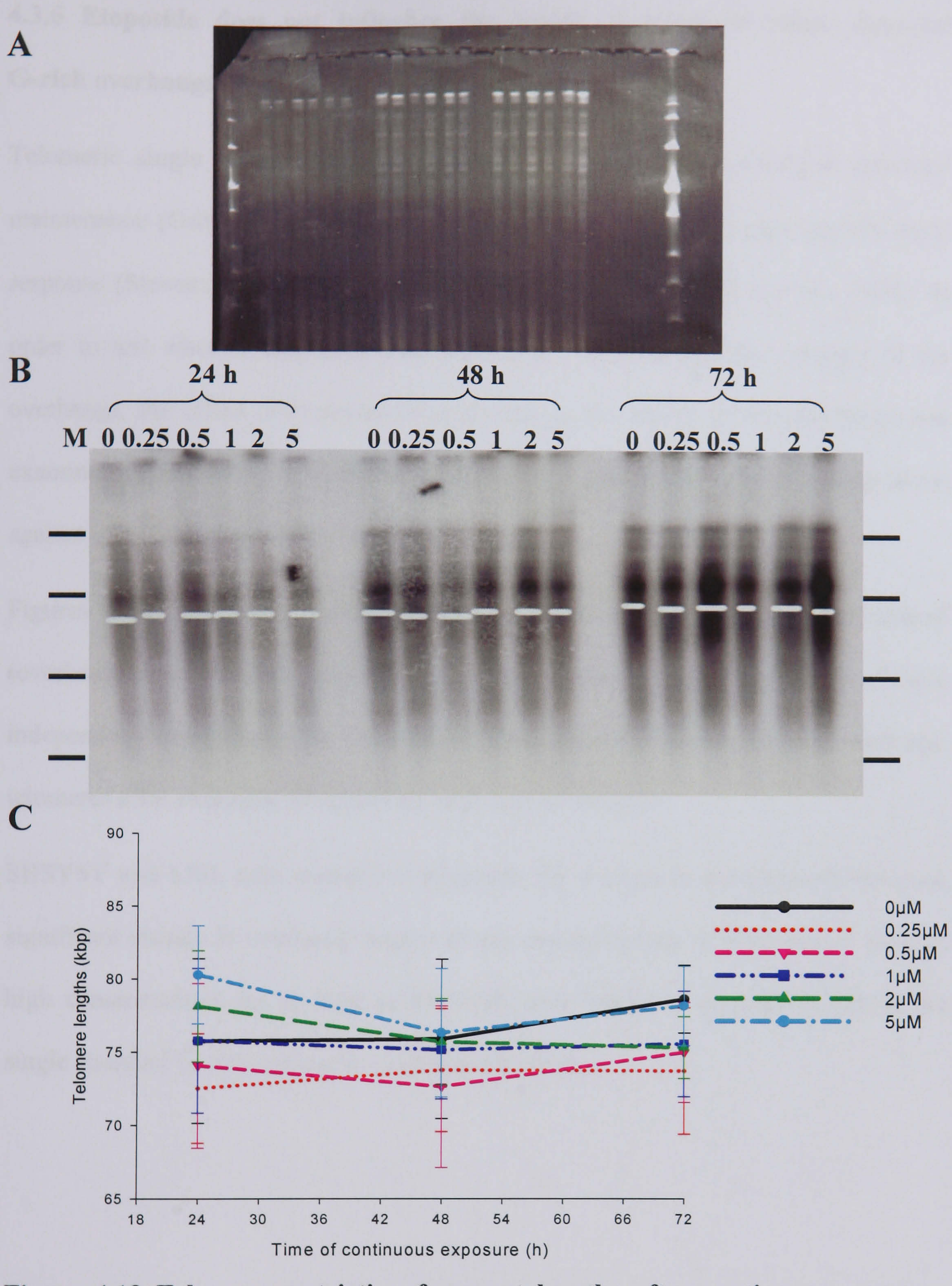

Figure 4.18 Telomere restriction fragment lengths after continuous exposure etoposide treatment on 1301 cells. (A) Ethidium bromide fluorescence of genomic DNA. (B) Telomere gel. Etoposide concentrations (in μM) and times after onset of treatment (in h) are indicated on top of the figure. White bars indicate average telomere length. The positions of the size markers (194, 97, 48.5, 23.1 kbp) are specified. (C) Average telomere length. Gels were normalised to a standard and average fragment lengths of four experiments were calculated. Data are ± SEM.

4.3.6 Etoposide does not influence the length of telomeric single stranded G-rich overhangs

Telomeric single stranded overhangs have been implicated in telomere structural maintenance (Griffith *et al.*, 1999) and generation of a DNA damage/ growth arrest response (Stewart *et al.*, 2003; Saretzki *et al.*, 1999; von Zglinicki *et al.*, 2001). In order to test whether etoposide treatment might interfere with the integrity of the overhangs, the effect of exposure to etoposide on the length of the overhangs was examined by measuring the relative hybridisation signal intensity of overhangs alone against whole telomeres (Keys *et al.*, 2004).

Figures 4.19- 4.22 show typical data. Panel A illustrates probed non denatured (overhang) and denatured (telomere) gels. Panel B shows the average graph of three independent experiments of the ratio of the intensity signals of the overhang/ telomeres after etoposide treatment on each type of analysis.

SHSY5Y and 1301 cells exposed to etoposide for 4 hours or continuously show no significant change in overhang lengths at any concentrations or time points. Even at high concentrations for as long as 48 hours after treatment no degradation of the single stranded G- rich telomeric overhang occurred.

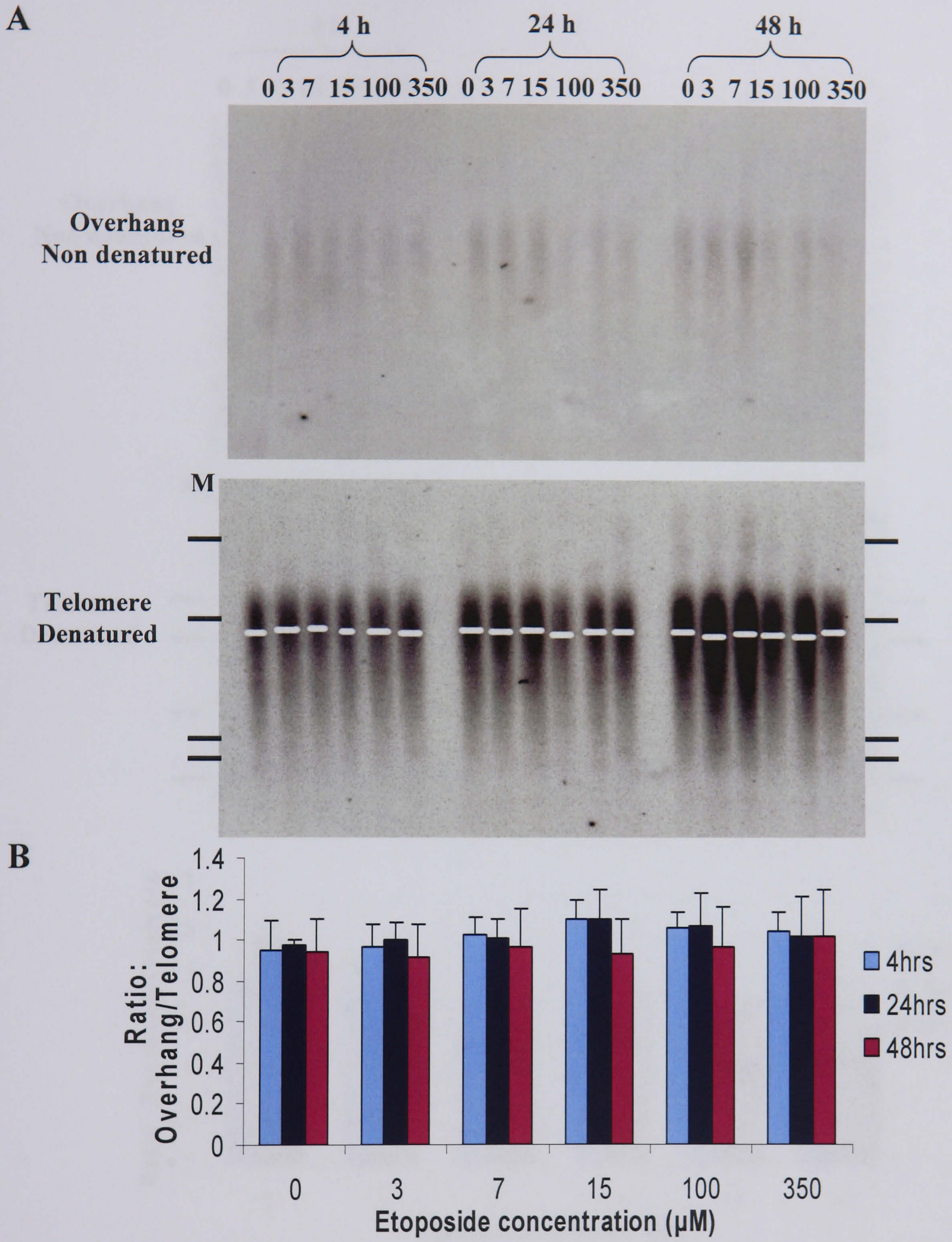

Figure 4.19 Telomeric G-rich overhangs in SHSY5Y cells after short exposure to etoposide. The overhang length is measured as the ratio of hybridisation intensities to the overhang alone vs whole telomere. (A) Example of an overhang and telomere gel. The position of size markers (23.1, 4.36, 2.32, 2.03 kbp) are shown by black bars. M = markers. White bars indicate average telomere length. (B) Graph showing ratios. Data are mean ± SEM from four experiments.

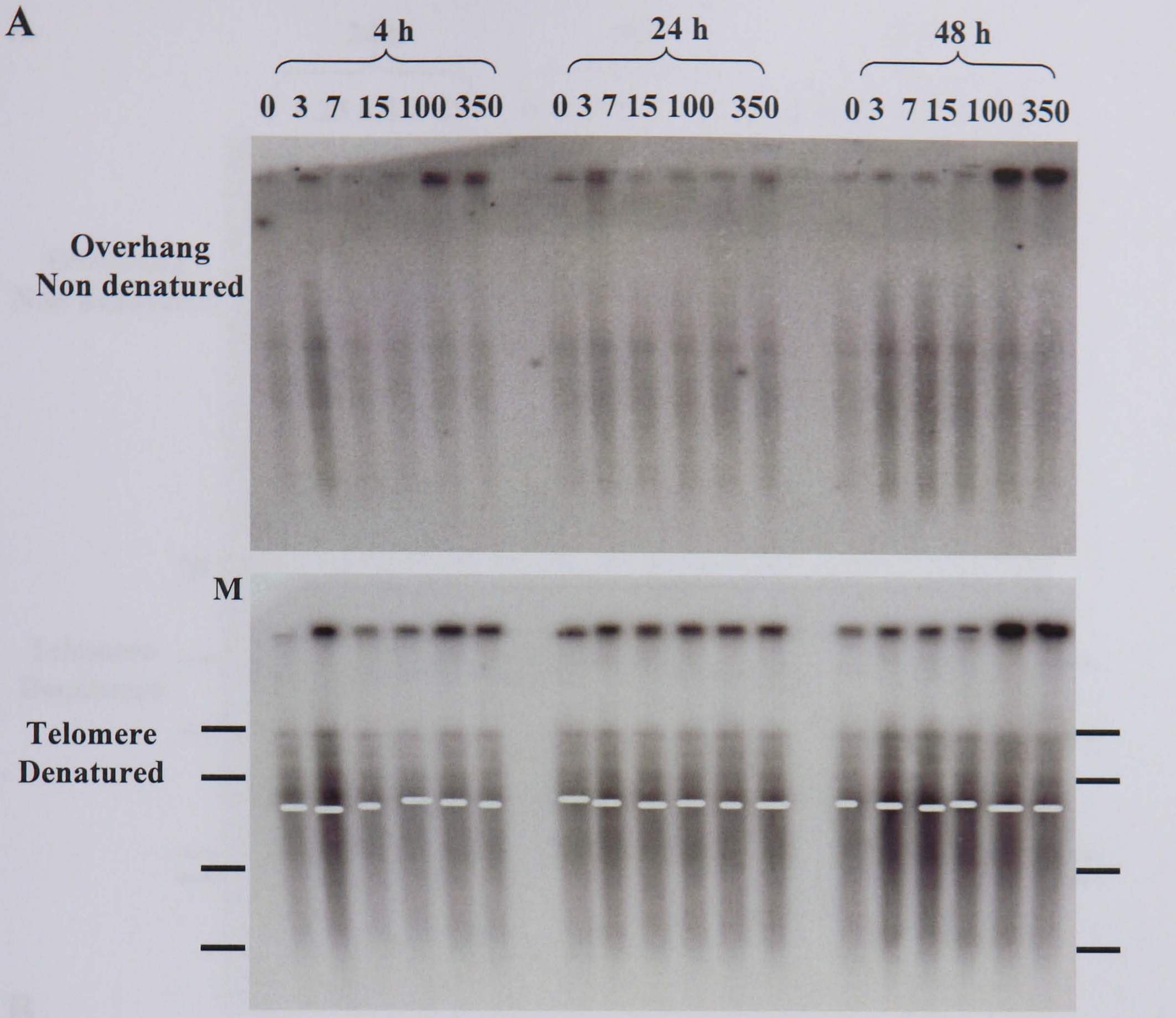

Figure 4.20 Telomeric G-rich overhangs in 1301 cells after short exposure to etoposide. The overhang length is measured as the ratio of hybridisation intensities to the overhang alone vs whole telomere. (A) Example of an overhang and telomere gel. The position of the size markers (194, 97, 48.5, 23.1) kbp are shown by black bars. M = markers. White bar indicates average telomere length. (B) Graph showing ratios. Data are mean ± SEM from five experiments.

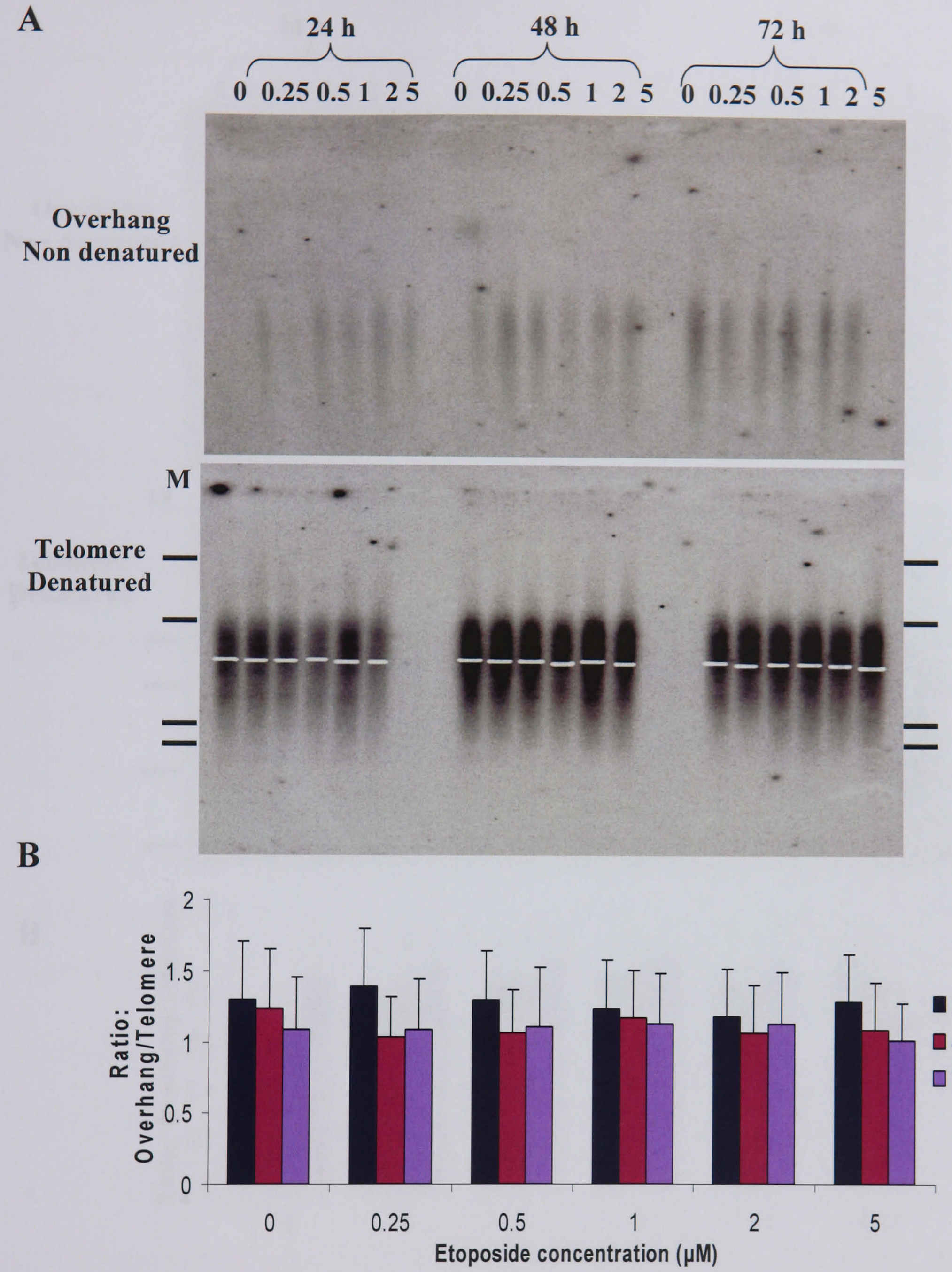

Figure 4.21 Telomeric G-rich overhangs in SHSY5Y cells after continuous exposure to etoposide. The overhang length is measured as the ratio of hybridisation intensities to the overhang alone vs whole telomere. (A) Example of an overhang and telomere gel. The position of the size markers (23.1, 4.36, 2.32, 2.03 kbp) are shown by black bars. M = markers. White bars indicate average telomere length. (B) Graph showing ratios. Data are mean ± SEM from four experiments.

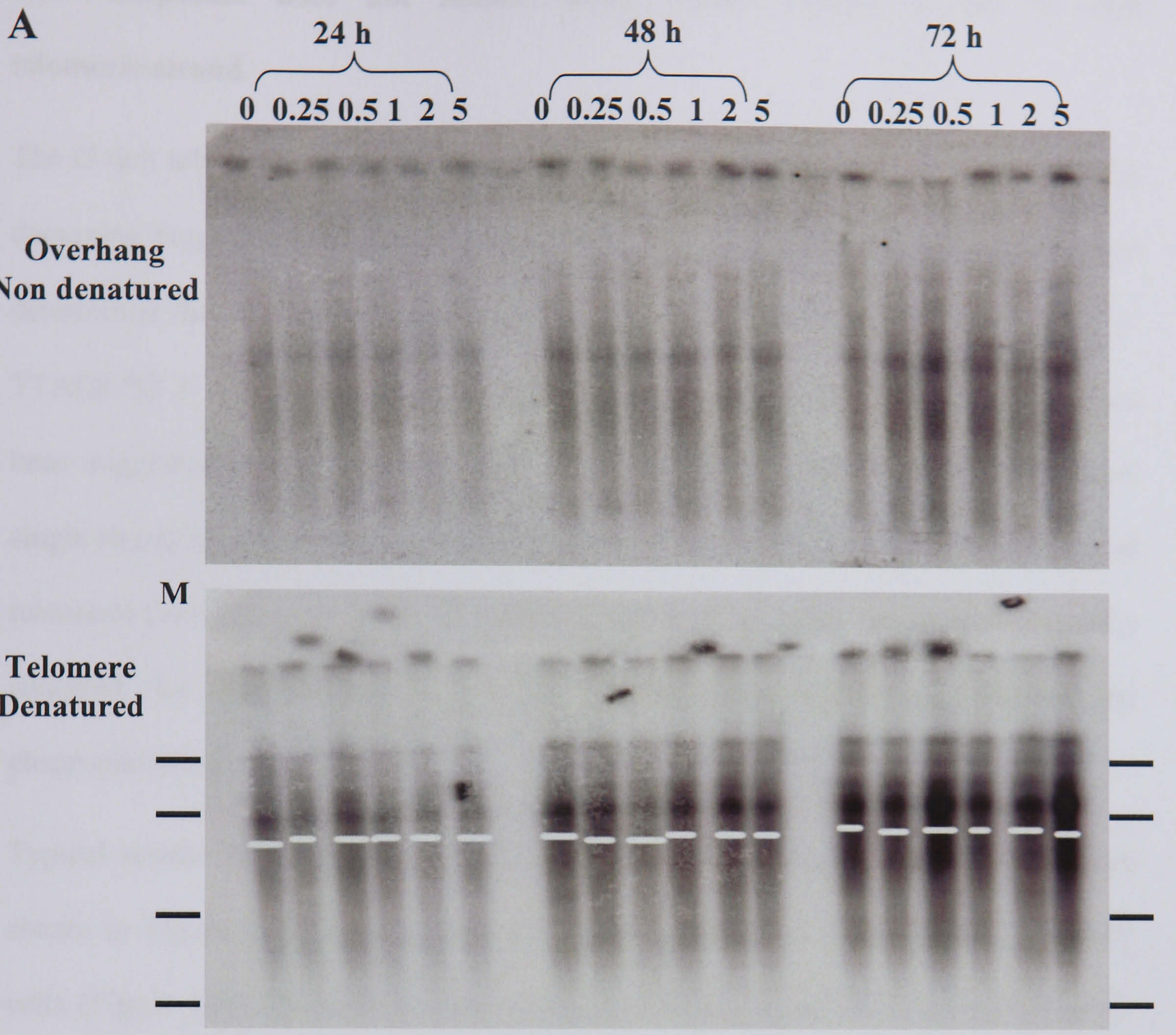

Figure 4.22 Telomeric G-rich overhangs in 1301 cells after continuous exposure to etoposide. The overhang length is measured as the ratio of hybridisation intensities to the overhang alone vs whole telomere. (A) Example of an overhang and telomere gel. The position of the size markers (194, 97, 48.5, 23.1 kbp) are shown by black bars. M = markers. White bars indicate average telomere length. (B) Graph showing ratios. Data are mean ± SEM from five experiments.

4.3.7 Etoposide does not induce single strand breaks in the G rich telomeric strand

The G rich telomeric strand has been suggested to be preferentially targeted by DNA damaging drugs due to its partial composition of guanine residues. For example it was determined that the topoisomerase II cleavage sites occurred in telomeric DNA 5' TTAGG*G 3' when etoposide was present (Yoon *et al.*, 1998). Additionally, it has been suggested that not only telomere shortening, but also an abundance of DNA single strand breaks in telomeres could lead to opening of the t-loop and uncapping of telomeres (von Zglinicki, 2001). Therefore, the G rich telomeric strand was separately analysed for the presence of strand breaks using denaturing alkaline gel electrophoresis.

Typical results for SHSY5Y and 1301 cells exposed to etoposide for 4 hours are shown in Figure 4.23. After a short exposure etoposide treatment on the SHSY5Y cells (Figure 4.23 A), there was no evidence of single stranded DNA breaks on the telomeric G rich strand. This was also the case for the 1301 cells after short exposure treatment (Figure 4.23 B).

A continuous exposure of the SHSY5Y and 1301 cells to etoposide at all time points and concentrations again showed no detectable G rich strand breaks (Figure 4.24).

Under a wide variety of drug exposures and incubation times, the mean length of G rich strand of terminal repeat fragments remained unchanged. The results indicate that even following very high concentrations of etoposide, no detectable single strand breaks were present in the G rich telomeric strand.

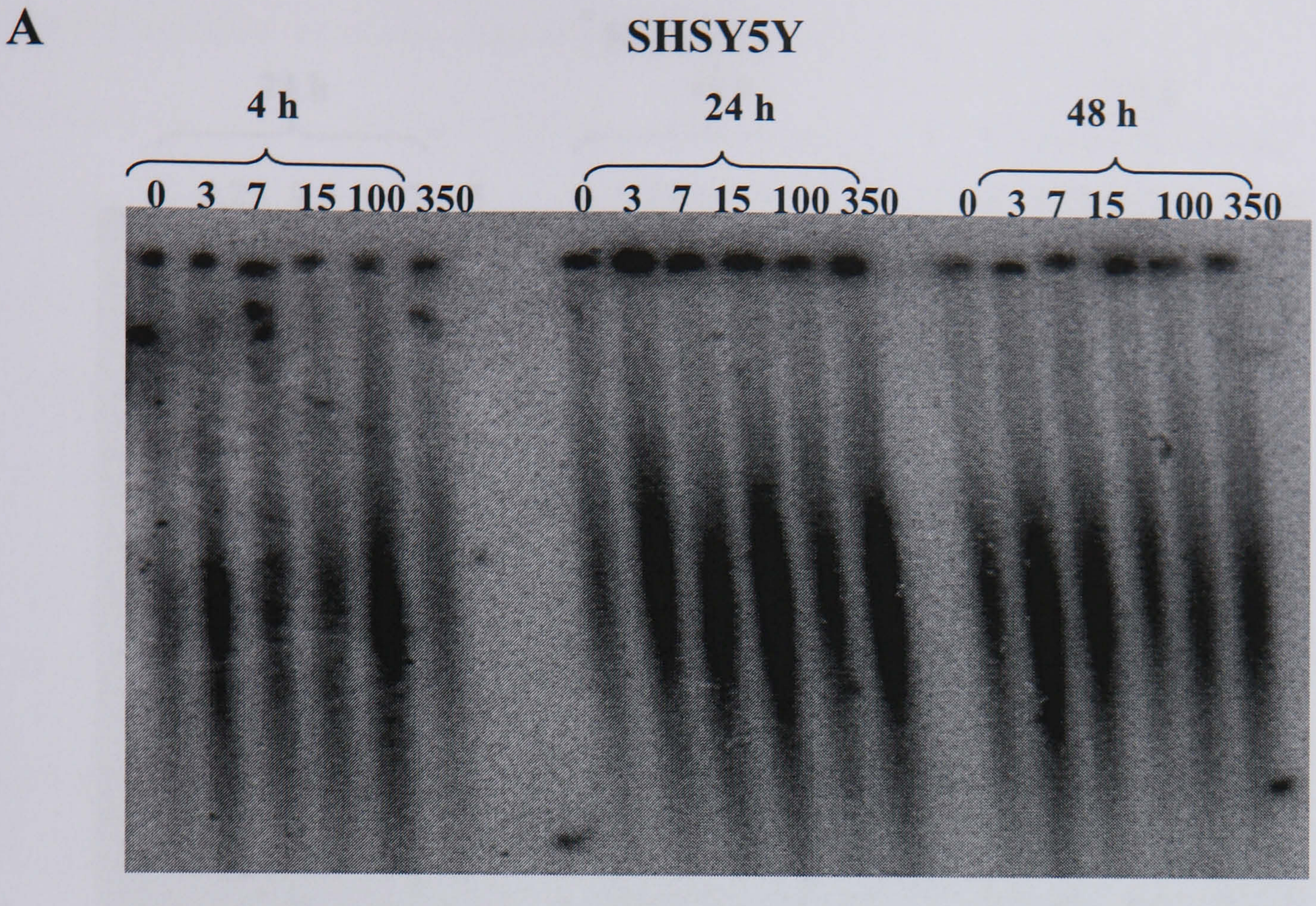

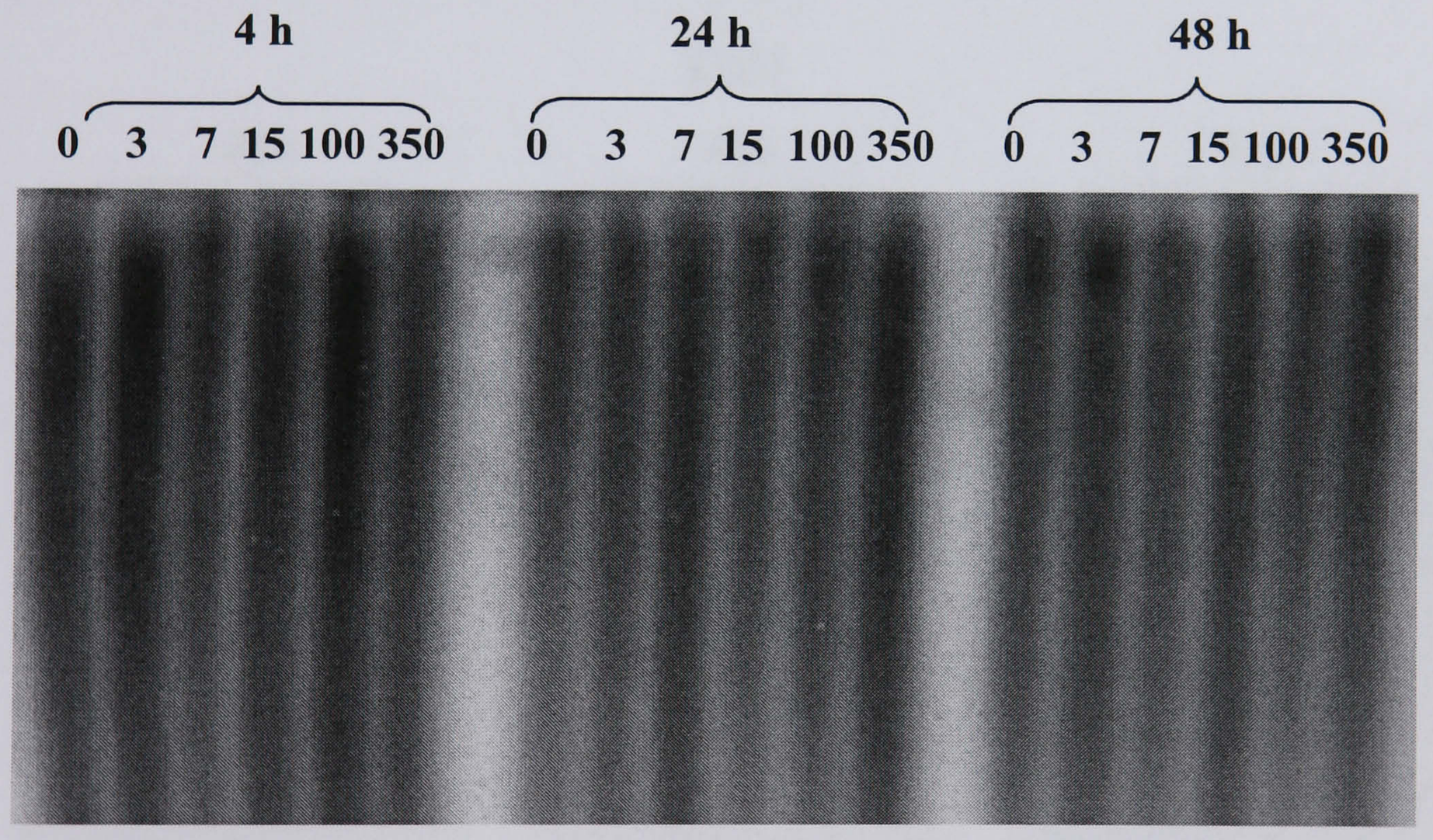

Figure 4.23 Denaturing gel to detect G rich telomeric strand breaks after short exposure etoposide treatment. Examples of gels, SHSY5Y (A) and 1301 (B) cells. Etoposide concentrations (in μM) and times after onset of treatment (in h) are indicated on top of the figures.

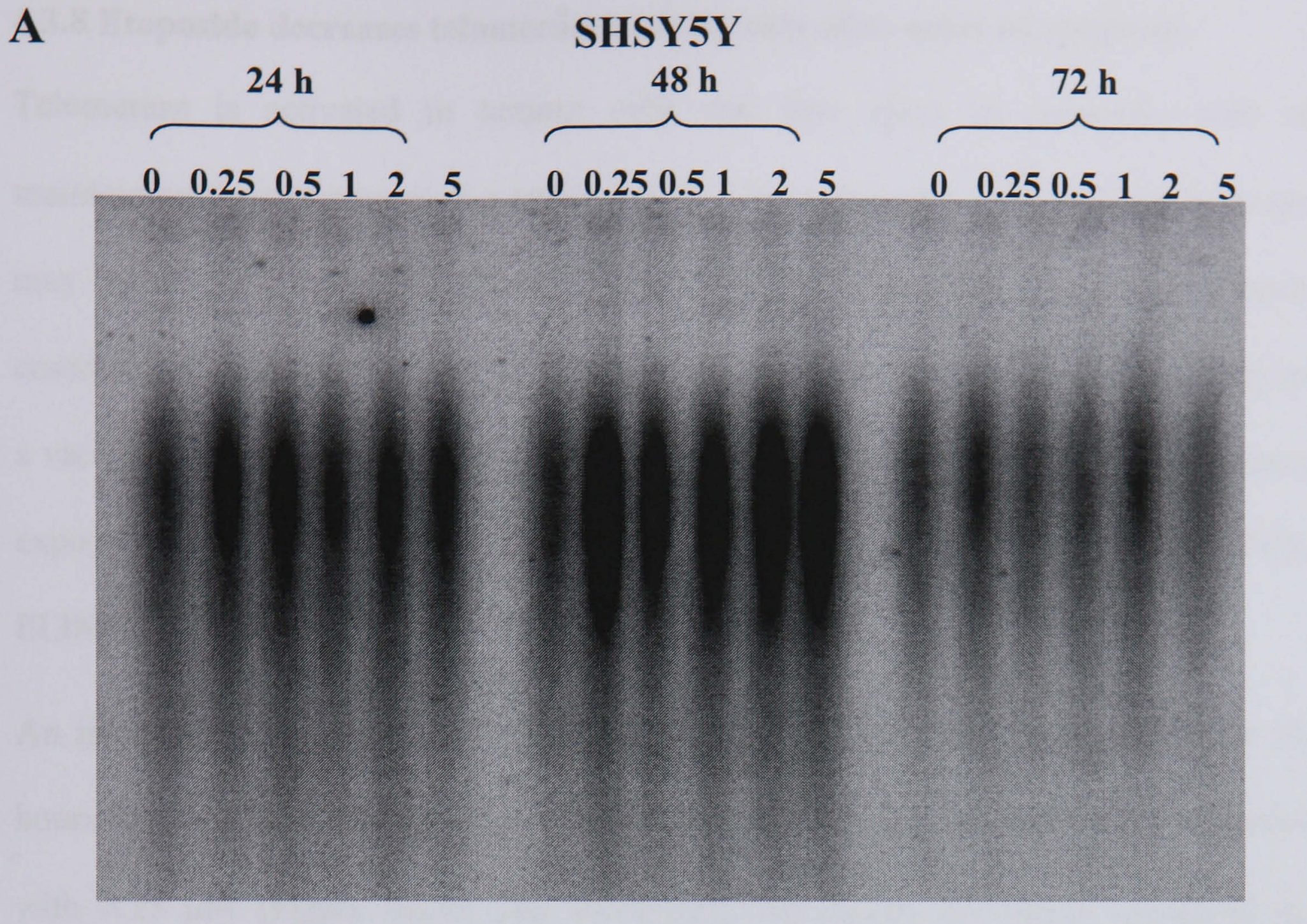

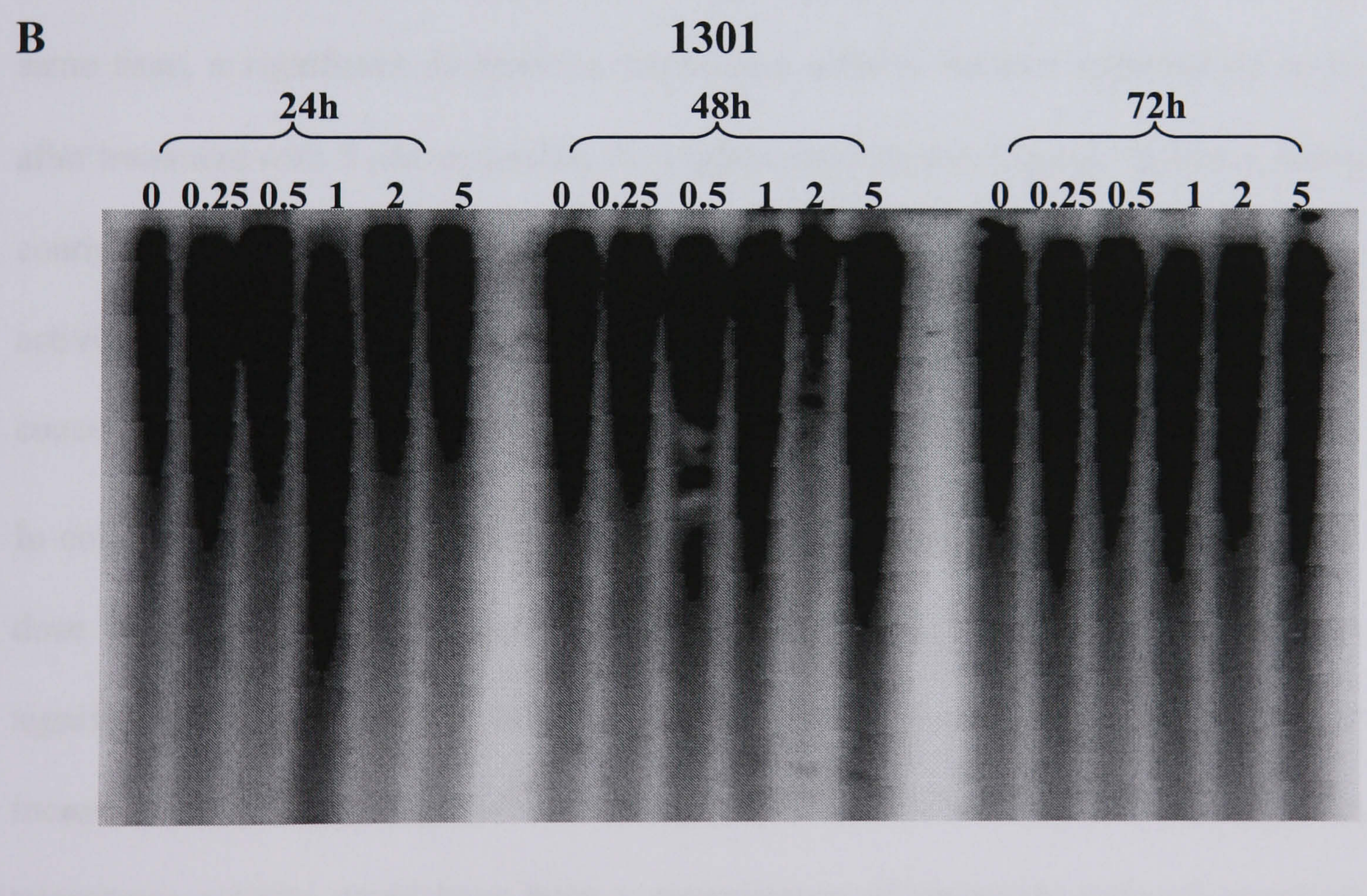

Figure 4.24 Denaturing gel to detect G rich telomeric strand breaks after continuous exposure etoposide treatment. Examples of gels, SHSY5Y (A) and 1301 (B) cells. Etoposide concentrations (in μM) and times after onset of treatment (in h) are indicated on top of the figures.

4.3.8 Etoposide decreases telomerase activity only after onset of apoptosis

Telomerase is activated in tumour cells and thus plays an important role in maintaining their telomeres at a stable length. Conventionally used anti-cancer drugs may induce their cytotoxic effects via the telomere/ telomerase complex and much contradictory data exists on the effect of etoposide treatment on telomerase activity in a variety of cell lines. Therefore telomerase activity was examined after a continuous exposure to etoposide on the SHSY5Y cells by the semi-quantitative TRAP PCR ELISA.

An increase in telomerase activity was found in the SHSY5Y cells treated for 48 hours with low concentrations of etoposide, which was significant for the treatment with 0.25 μM (Figure 4.25). The statistically significant differences compared to untreated controls were confirmed by one way analysis of variance (ANOVA). At the same time, a significant decrease in telomerase activity became apparent 48 hours after treatment with 5 μM etoposide, the highest concentration tested. 72 hours after a continuous treatment with etoposide in concentrations at or above 2 μM telomerase activity significantly decreased as well (Figure 4.25). At these time points and concentrations more than 50% of the cells are in apoptosis (Figure 4.5).

In conclusion telomerase activity was significantly upregulated 48 hours after a low dose continuous etoposide treatment on the SHSY5Y cells, at the same time a significant decrease was also detected at the highest concentrations. This significant increase could be a response to the cytotoxic treatment. The later decrease in telomerase activity could have been a consequence of etoposide induced apoptosis rather than a cause of cell death.

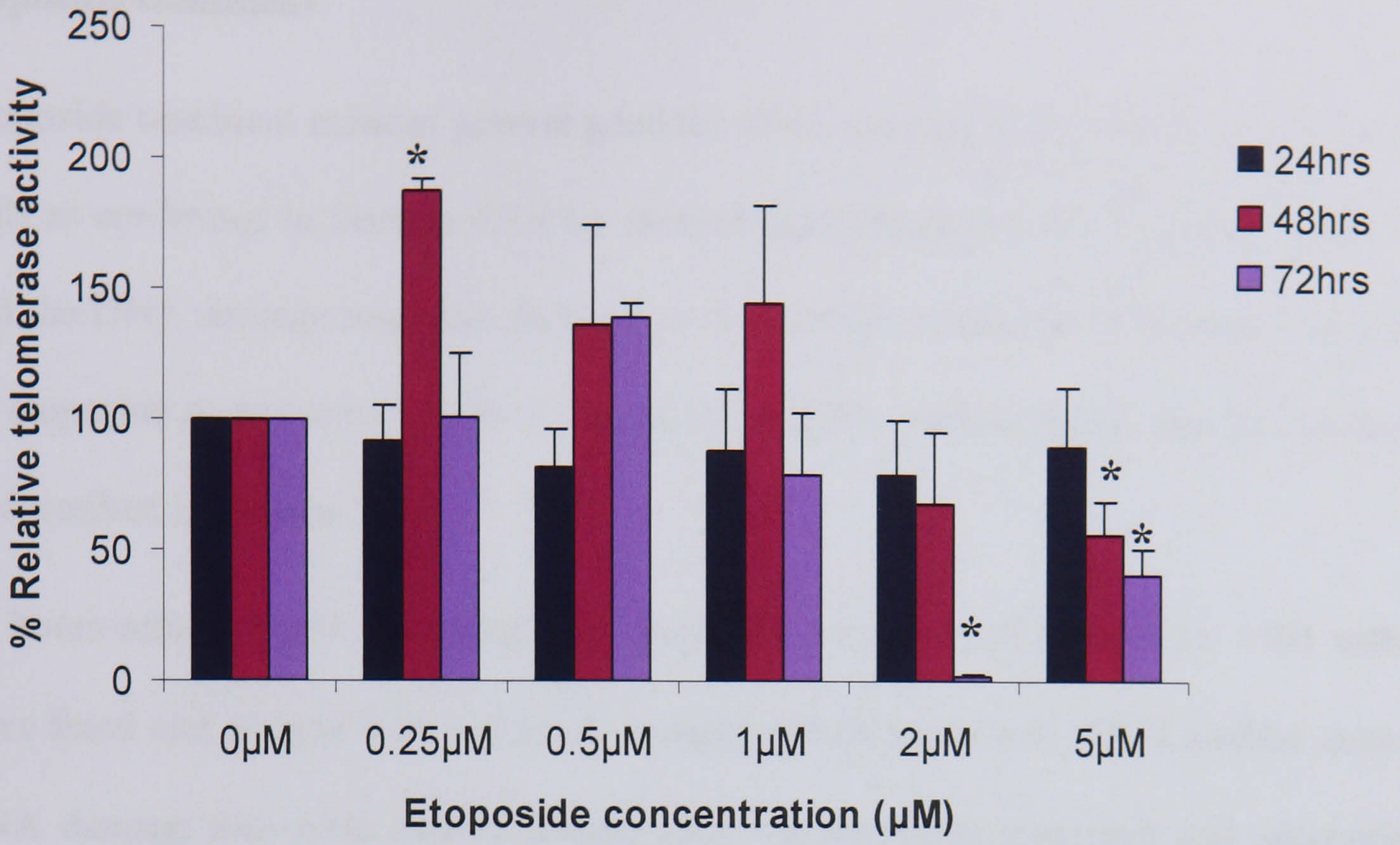

Figure 4.25 Telomerase activity in SHSY5Y cells after continuous etoposide treatment. Relative telomerase activity was measured using a telomerase PCR ELISA. Data are mean ± SEM from at least four independent experiments. For each experiment, activities measured in untreated control samples were set as 100%. Statistically significant differences towards untreated controls are marked by an asterisk ($p < 0.05$, ANOVA).

4.3.9 DNA damage foci do not colocalise to the telomeres after etoposide treatment

Etoposide treatment induces general genomic DNA damage in the SHSY5Y and 1301 cells as confirmed in Section 4.3.4 by assessing the frequency of DNA strand breaks and the DNA damage response. In order to determine whether DNA damage induced by etoposide occurs specifically in the telomeric DNA, immunoFISH was undertaken as described in Section 3.3.9.

14 hours after a 3 μM short exposure etoposide treatment (Figure 4.26), 1301 cells were fixed and stained with γ-H2A.X, telomere PNA probe and DAPI nuclear stain. DNA damage foci were clearly present after the etoposide treatment and telomeric DNA was also detectable. Merged images display that the majority of DNA damage foci do not colocalise to the telomeric DNA (≥ 8 cells out of 10 in triplicate fields in three independent experiments).

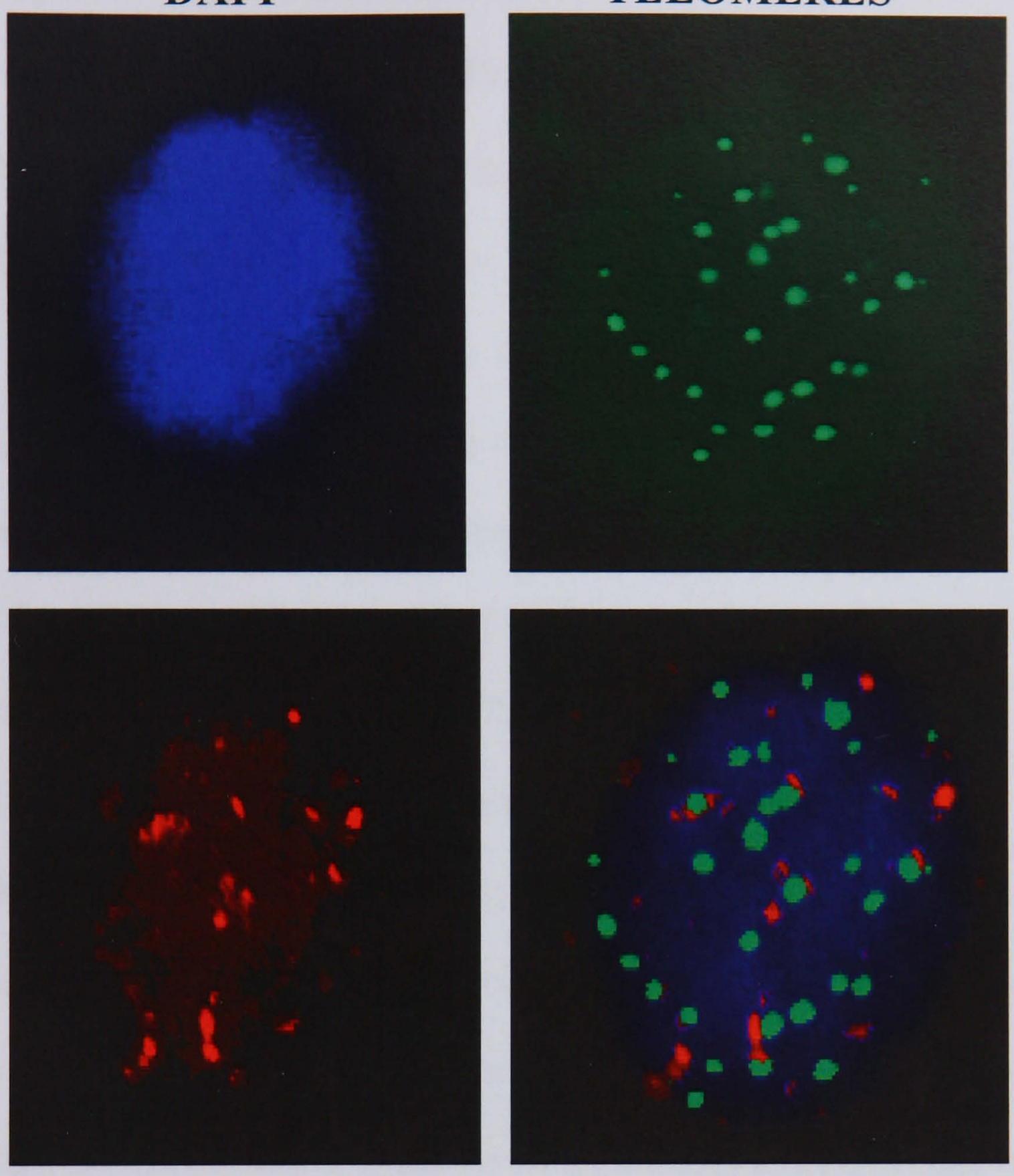

Figure 4.26 DNA damage foci do not colocalise with telomeres after a short exposure etoposide treatment. 1301 cells were fixed 14 hours after a 4 hour treatment with 3 μM etoposide and stained as indicated. The merged image, show lack of colocalisation between DNA damage foci and telomeres. x 100 objective

4.4 Discussion

There are several lines of evidence to suggest that telomere/ telomerase complexes could be important signal transduction intermediates in drug induced cell growth arrest and apoptosis (see Chapter 1). The telomere/ telomerase complex has been shown to be sensitive to etoposide treatment. For example, etoposide treatment of tumour cells has been claimed to shorten telomeres (Yoon *et al.*, 1998) and modify telomerase expression and/ or activity (Spiropoulou *et al.*, 2004). Inhibition of telomerase sensitised mice cells (Lee *et al.*, 2001) and human cells (Ludwig *et al.*, 2001; Misawa *et al.*, 2002) towards cytotoxic drugs including etoposide. Accordingly, overexpression of the catalytic subunit of telomerase increased the resistance of cells against etoposide (Ludwig *et al.*, 2001; Zhang *et al.*, 2003). However, a number of published results are contradictory. Some data, both in mice (Lee *et al.*, 2001) and in human cells (Chen *et al.*, 2003) suggest that it is telomere length rather than telomerase activity that modifies the sensitivity of cells to anti-cancer drugs. In contrast to that, arguments for a telomere length independent protective action of telomerase per se were found in a number of different systems (Saretzki *et al.*, 2001; Ludwig *et al.*, 2001; Sharma *et al.*, 2003). Other authors, however, did not detect any effect of telomerase inhibition on the sensitivity of tumour cells to etoposide (Chen *et al.*, 2003; Folini *et al.*, 2000).

The FADU data in Figure 4.13 confirms that, in the cells used here, etoposide induced widespread DNA strand breaks. Also the formation of foci of phosphorylated histone H2A.X (Figure 4.14) confirmed the classical DNA damage response. This was followed by a combination of growth arrest and apoptosis in a concentration and cell strain dependent manner.

To establish the role of telomeres in this process, we measured not only telomere length, but also length of single stranded telomeric G rich overhangs and the frequency of single strand breaks in the G-rich strand of telomeres. Since the importance of a telomere-dependent signal transduction pathway, if it existed at all, might be different in cells with long and short telomeres, we examined one cell line with very short (SHSY5Y, average telomere length ~4 kbp) and one with extremely long (1301, average telomere length ~80 kbp) telomeres. None of the parameters mentioned above changed significantly in either cell line under the treatments despite induction of growth arrest and/ or apoptosis. This is not in accordance with Yoon *et al* who show a slight shortening of telomeres in HeLa cells with telomere lengths of ~ 20 kbp after a 30 minute 100 μM treatment with etoposide (Yoon *et al.*, 1998). Whether this discrepancy to our results might be cell line specific, is not clear. However, our data clearly establish that measurable telomeric damage, might it be shortening, accumulation of single strand breaks or deterioration of the G-rich overhang, is not necessary as a signal transduction intermediate in etoposide induced tumour cell growth arrest and apoptosis. Additionally, there was no co-localisation of γ-H2A.X foci with telomeric DNA after etoposide treatment.

We next examined telomerase activity levels in SHSY5Y cells after continuous exposure to etoposide. Previous studies on telomerase activity after etoposide treatment have been somewhat contradictory. An upregulation of telomerase activity after etoposide treatment was reported in a human leukemic cell line, HL60 (Moriaty *et al.*, 2002 and Klapper *et al.*, 2003) and pancreatic tumour cell lines (Sato *et al.*, 2000). While a decrease was detected in hepatocarcinomas (Li *et al.*, 2002) there was no change in haematopoietic (Akiyama *et al.*, 1999) and nasopharyngeal cancer cells (Ku *et al.*, 1997). Under our conditions of continuous treatment, we found a transient

increase of telomerase activity after 48 hours, which was significant under the lowest etoposide concentration. Even high concentrations of etoposide did not induce any immediate change in telomerase activity. However, a decrease of telomerase activity was observed with increasing concentration of etoposide and with increasing time of treatment. Comparison of telomerase data (Figure 4.5) with the time course of induction of apoptosis (Figure 4.25) reveals that telomerase activity only became reduced after the appearance of a high frequency of apoptotic cells. This indicates that loss of telomerase did not trigger apoptosis but was probably a consequence of apoptotic changes in cells. These results are in accordance with others (Akiyama *et al.*, 1999). Thus, downregulation of telomerase is a consequence, not a possible cause of etoposide induced apoptosis or growth arrest. However, the possibility remains that telomerase is upregulated also in response to higher etoposide concentrations, but that this is masked by a parallel induction of apoptosis. Thus, upregulation of telomerase might be part of a compensatory response of tumour cells to cytotoxic treatments. Telomerase could promote survival by a telomere-independent mechanism (See Section 1.8.3). In fact, upregulation of telomerase has been demonstrated in response to etoposide in previous studies (Moriarty *et al.*, 2002; Klapper *et al.*, 2003; Sato *et al.*, 2000). This is consistent with the idea of telomerase acting as a "survival factor" (Saretzki *et al.*, 2001; Zhang *et al.*, 2003; Sharma *et al.*, 2003).

Telomerase working as a protective factor has also been observed in MRC5 human fibroblasts which had been stably transfected with hTERT. The response after etoposide treatment between parental MRC5 and MRC5-hTERT cells indicated that hTERT expressing fibroblasts were efficiently protected from apoptosis (Jeyapalan *et al.*, 2004). A similar protective effect of hTERT overexpression against the cytotoxcity of etoposide, other topoisomerase II poisons and cisplatin has been shown

before in other human cell lines (Ludwig *et al.*, 2001; Zhang *et al.*, 2003; Biroccio *et al.*, 2003).

4.5 Conclusions

In conclusion, our data suggest that DNA strand breaks elsewhere in the genome (not in the telomeric region) occurring as direct consequence of etoposide treatment induce DNA damage foci formation leading to apoptosis and/ or cell cycle arrest. While a transient activation of telomerase is evident under some conditions, which might be part of an attempted survival response, we find no indication that telomeres and/ or telomeric damage play any preferential role as a signal transducer towards apoptosis and/ or growth arrest in etoposide treated tumour cells.

CHAPTER 5

FINAL DISCUSSION

5.1 Introduction

Telomeres appear to be particularly sensitive to DNA damage demonstrated by a number of factors. Firstly, telomeres are sensitive to DNA damage induced by UV (Kruk *et al.*, 1995), oxidative stress (von Zglinicki *et al.*, 1995; Stewart *et al.*, 2003) and possibly, chemotherapeutic drugs (Yoon *et al.*, 1998). Secondly, dysfunctional telomeres trigger growth arrest and/ or apoptosis via telomere-specific induction of DNA damage foci, also termed senescence-associated DNA damage foci (d'Adda di Fagagna *et al.*, 2003). Thirdly, inhibition of telomerase sensitises mice cells (Lee et al., 2001) and human cells (Ludwig *et al.*, 2001; Misawa *et al.*, 2002) towards cytotoxic drugs. Accordingly, overexpression of the catalytic subunit of telomerase increased the resistance of cells (Ludwig *et al.*, 2001; Zhang *et al.*, 2003). Fourthly, drug treatment of tumour cells has been claimed to shorten telomeres (Yoon *et al.*, 1998) or to modify telomerase expression and/ or activity (Spiropoulou *et al.*, 2004). Some data, both in mice (Lee *et al.*, 2001) and in human cells (Chen *et al.*, 2003) suggest that it is telomere length rather than telomerase activity that modifies the sensitivity of cells to anti-cancer drugs.

There have been indications that at least two classes of established anti-cancer drugs act on telomeric DNA, namely cisplatin (Section 3.1) and etoposide (Section 4.1). Though there are many contradicting studies. Therefore, the relationship between conventionally used DNA damaging drugs and the telomere/ telomerase complex are not at all clear.

5.2 Aim

The aim of the work described in this study was to establish to what extent the telomere/ telomerase complex plays a role in the cytotoxic effects of the widely used anti-cancer drugs, cisplatin and etoposide. This has be done using cells with either short or long telomeres. An important aspect of the work was to distinguish effects of apoptotic changes from the direct effects of the drugs on telomere biology. This was approached by determining whether or not induction of growth arrest and apoptosis preceded effects on telomeres and telomerase after drug treatments. Secondly, the work involved the determination of the spatial relationship between telomeres and DNA damage foci after drug exposure by development of an immunoFISH technique to detect telomeric DNA and DNA damage foci simultaneously.

The cell lines used in this investigation were SHSY5Y, an adherent neuroblastoma cell line which has telomere lengths of ~4-5 kbp and 1301, a non adherent acute lymphoblastic T cell line with telomere lengths of ~80 kbp. Both cell lines are telomerase positive. The p53 status of the SHSY5Y is wildtype but it is thought to be not fully functional and the 1301 cell line has not been tested specifically but it is thought to be mutant for p53.

5.3 Outline of Results

5.3.1 Cisplatin

The details of how cisplatin kills cancer cells are not fully understood but there is evidence to suggest that cisplatin binding to form DNA adducts is the central process (Section 1.10). The adducts so formed might act by blocking replication or by directly triggering a variety of DNA damage responses. Therefore one of the primary

objectives of this study was to determine whether cisplatin induces growth arrest/ apoptosis via the telomere/ telomerase complex which previous studies had suggested (Ishibashi and Lippard, 1998). In the present study the nature of the cytotoxic effect was confirmed and the relationship between drug exposure and cytotoxicity of cisplatin on the SHSY5Y cells was defined. As expected, cisplatin induced apoptosis and an S phase arrest was detected after high concentrations of cisplatin with either short or continuous treatment. Cisplatin treatment did not induce strand breaks after initial drug exposure but strand breaks and DNA damage foci were detected 24 hours after treatment in the SHSY5Y cells. The H2A.X phosphorylation and strand damage detected in cisplatin treated cells over time may be associated with DNA repair, which has also been suggested by others who have seen H2A.X phosphorylation after cisplatin exposure (Huang *et al.*, 2004). This possibility could be investigated by inhibiting ATM and measuring the effect on apoptosis i.e. to determine whether there is a delay.

Telomere restriction fragment lengths, single stranded G rich overhang lengths and single strand breaks on the G rich telomeric strand after cisplatin treatment were measured and no detectable telomeric DNA damage was observed in the SHSY5Y cells. This does not confirm the work of others which is fully discussed in Chapter 3 Section 3.4 (Ishibashi and Lippard, 1998; Zhang *et al.*, 2002).

In the present study a decrease in telomerase activity was detected in the SHSY5Y cells at the highest concentrations and after the longest time points, where a large majority of the cells were in apoptosis in line with others (Akiyama *et al.*, 1999; Cressey *et al.*, 2002) and discussed in Chapter 3 Section 3.4.

The examination of DNA damage foci formation simultaneously with a telomeric DNA PNA probe in the 1301 cells after cisplatin treatment showed no localisation of DNA damage foci on telomeric DNA.

5.3.2 Etoposide

Etoposide, a topoisomerase II poison stabilises cleavable complex formation, inducing double strand breaks into a cell. In Chapter 4 the role of the telomere/ telomerase complex in etoposide induced cell death was examined, as previous work had suggested a link (Yoon *et al.*, 1998). The cytotoxic effect of etoposide on the SHSY5Y and 1301 cells were confirmed with the induction of apoptosis. SHSY5Y cells were arrested in S phase, 48 hours after etoposide treatment and cells at this time point also had a senescence like phenotype. Etoposide treatment induced strand breaks after initial drug exposure and DNA damage foci were detected 24 hours after treatment.

Telomere restriction fragment lengths, single stranded G rich overhangs and the G rich telomeric strand after cisplatin treatment were measured in both the SHSY5Y and 1301 cells and no detectable specific, telomeric DNA damage was observed. This is not in accordance with another study (Yoon *et al.*, 1998) and is fully discussed in Chapter 4 Section 4.4.

Previous studies on telomerase activity after etoposide treatment have been somewhat contradictory (Section 4.1). In this investigation telomerase activity after a continuous etoposide treatment in the SHSY5Y cells was upregulated at low doses and at the same time decreased at the high concentrations. This upregulation of telomerase activity could be due to a protective factor of telomerase working in a telomere independent mechanism (Section 1.8.3) and the cells initial response to the cytotoxic

drug treatment. The decrease in telomerase activity levels is a consequence of high drug treatments and high apoptosis levels rather than a cause and is discussed fully in Chapter 4 Section 4.4.

The examination of DNA damage foci formation simultaneously with a telomeric DNA PNA probe in the 1301 cells after etoposide treatment showed no colocalisation of DNA damage foci to telomeric DNA.

5.4 Summary

Under conditions where exposure to etoposide or cisplatin was shown to induce general DNA damage and H2A.X foci , at no time after drug exposure were there any detectable changes in lengths of telomeres or telomeric overhangs and no detectable level of single strand breaks in the G-rich telomeric DNA. This was shown to be true for cells with either long or short telomeres and for cells exposed to a wide range of drug concentrations. Exposure to the drugs generated both growth arrest and apoptosis in a concentration and time-dependent manner. Telomerase activity decreased only after onset of apoptosis.

Although there was induction of genome wide DNA strand breaks but no strand breaks in telomeric DNA (telomere lengths, single stranded G rich overhang lengths, single strand breaks in G rich telomeric strand) were detected, there is no contradiction in the data. This is because the sensitivity of the telomere restriction fragment measurements to detect telomeric strand breaks (single or double strand) is in the order of 1 break per Mb. This is significantly lower than the sensitivity of the FADU assay where one strand break per chromosome can be detected (Birnboim and Jevcak, 1981). This may suggest that we are unable to detect the telomere damage which may lead to growth arrest/ apoptosis due to the low sensitivity of the procedure

for telomere restriction fragment length analysis. Though in senescence studies any effect on telomere length which has been induced were large and easily measurable using the southern hybridisation technique. Also, cisplatin and etoposide induced DNA damage foci did not localise at the telomeres.

The two cell lines, SHSY5Y and 1301 showed some differences in IC_{50} values and in levels of drug-induced apoptosis. Overall however, the telomeres/ telomerase complex in the SHSY5Y and 1301 cell lines generally displayed similar characteristics in response to cisplatin and etoposide treatment, in the sense that there is no role of the telomeres/ telomerase complex in cisplatin or etoposide induced cell death.

5.5 Conclusions

This study has extensively investigated the role of the telomere/ telomerase complex in drug induced DNA cell death by investigating two types of conventionally used anti-cancer drugs, cisplatin and etoposide whose mode of action target DNA through contrasting mechanisms. Furthermore, the response was evaluated on cell lines with either short (SHSY5Y) or long telomeres (1301).

In conclusion, this thesis has demonstrated that there was no preferential damage to telomeres as a result of exposure to cisplatin or etoposide. Consequently, telomeres do not play an exceptionally important role as signal transducers towards apoptosis and/ or growth arrest in these cell lines following exposure to these drugs, unless low levels of damage in telomeres triggers a particularly important type of damage response. The cell lines responded to the drug treatments by a combination of S phase arrest and apoptosis. A transient activation of telomerase was evident after some conditions of etoposide treatment which might be part of an attempted survival

response. However, the main drug induced changes in telomerase activity were decreases in activity levels following high drug exposures and long treatment times. These decreases were rather a consequence of than a cause of, apoptosis.

The thesis studies suggest that DNA strand breaks are not occurring on telomeric DNA and the cytotoxicty observed must therefore have resulted from damage in other regions of the genome, inducing DNA damage foci formation and leading to apoptosis and/ or cell cycle arrest.

REFERENCES

Adams, P.D., Sellers, W.R., Sharma, S.K., Wu, A.D., Nalin, C.M. and Kaelin, W.G.J. (1996) Identification of a cyclin-cdk2 recognition motif present in substrates and p21 like cyclin dependent kinase inhibitors. *Molecular and Celluar Biology* **16**: 6623-6633.

Adimoolam, S. and Ford, J.M. (2003) p53 and regulation of DNA damage recognition during nucleotide excision repair. *DNA Repair* **2**: 947-954.

Adrain, C. and Martin, S.J. (2001) The mitochondrial apoptosome: a killer unleashed by the cytochrome seas. *Trends in Biochemical Sciences* **26**: 390-397.

Agarwal, M.L., Agarwal, A., Taylor, W.R. and Stark, G.R. (1995) p53 controls both the G_2/M and the G_1 cell cycle checkpoints and mediates reversible growth arrest in human fibroblasts. *Proceedings of the National Academy of Sciences USA* **92**: 8493-8497.

Akeshima, R., Kigawa, J., Takahashi, M., Oishi, T., Kanamori, Y., Itamochi, H., Shimada, M., Kamazawa, S., Sato, S. and Terakawa, N. (2001) Telomerase activity and p53-dependent apoptosis in ovarian cancer cells. *British Journal of Cancer* **84**: 1551-1555.

Akiyama, M., Horiguchi-Yamada, J., Saito, S., Hoshi, Y., Yamada, O., Mizoguchi, H. and Yamada, H. (1999) Cytostatic concentrations of anticancer agents do not affect telomerase activity of leukaemic cells in vitro. *European Journal of Cancer* **35**: 309-315.

Allshire, R.C., Gosden, J.R., Cross, S.H., Cranston, G., Rout, D., Sugawara, N., Szostak, J.W., Fantes, P.A. and Hastie, N.D. (1988) Telomeric repeats from T.thermophila cross hybridizes with human telomeres. *Nature* **332**: 656-659.

Allshire, R.C., Dempster, M. and Hastie, N.D. (1989) Human telomeres contain at least three types of G-rich repeat distributed non randomly. *Nucleic Acids Research* **17** (12): 4611-4627.

Ambros, I.M., Zellner, A., Roald, B., Amann, G., Ladenstein, R., Printz, D., Gadner, H. and Ambros, P.F. (1996) Role of ploidy, chromosome 1p and Schwann cells in the maturation of neuroblastoma. *New England Journal of Medicine* **334**: 1505-1511.

Arends, M.J. and Wyllie, A.H. (1991) Apoptosis: mechanisms and roles in pathology. *Int Rev Exp Pathol* **32**: 223-254.

Bailey, S.M., Meyne, J., Chen, D.J., Kurimasa, A., Li, G.C., Lehnert, B.E. and Goodwin, E.H. (1999) DNA double strand break repair proteins are required to cap the ends of mammalian chromosomes. *Proceedings of the National Academy of Sciences USA* **96** (26): 14899-14904.

Baird, D.M., Rowson, J., Wynford-Thomas, D. and Kipling, D. (2003) Extensive allelic variation and ultrashort telomeres in senescent human cells. *Nature Genetics* **33**: 203-207.

Baumann, P. and Cech, T.R. (2001) Pot1, the putative telomere end binding protein in fission yeast and humans. *Science* **292** (5519): 1171-1175.

Beattie, T.L., Zhou, W., Robinson, M.O. and Harrington, L. (1998) Reconstitution of human telomerase activity in vitro. *Current Biology* **8**: 177-180.

Bechter, O.E., Zou, Y., Walker, W., Wright, W.E. and Shay, J.W. (2004) Telomeric recombination in mismatch repair deficient human colon cancer cells after telomerase inhibition. *Cancer Research* **64**: 3444-3451.

Beck, D.J. and Brubaker, R.R. (1973) Effect of cis-platinum(II)diamminodichloride on wild type and deoxyribonucleic acid repair deficient mutants of Escherichia coli. *Journal of Bacteriology* **116**: 1247-1252.

Bellon, S.F., Coleman, J.H. and Lippard, S.J. (1991) DNA unwinding produced by site-specific intrastrand cross-links of the anti-tumor drug cis-diammine dichloroplatinum(II). *Biochemistry* **30**: 8026-8035.

Benanti, J.A. and Galloway, D.A. (2004) Normal human fibroblasts are resistant to RAS-induced senescence. *Molecular and Celluar Biology* **24**: 2842-2852.

Bernd, K. (2003) DNA damage triggered apoptosis: critical role of DNA repair double strand breaks, cell proliferation and signaling. *Biochemical Pharmacology* **66**: 1547-1554.

Bianchi, A. and de Lange, T. (1999) Ku binds telomeric DNA in vitro. *The Journal of Biological Chemistry* **274**: 21223-21227.

Bilaud, T., Brun, C., Ancelin, K., Koering, C.E., Laroche, T. and Gilson, E. (1997) Telomeric localization of TRF2, a novel human telobox protein. *Nature Genetics* **17**: 231-235.

Birnboim, H.C. and Jevcak, J.J. (1981) Fluorometric method for rapid detection of DNA strand breaks in human white blood cells produced by low doses of radiation. *Cancer Research* **41** (5): 1189-1192.

Biroccio, A., Gabellini, C., Amodei, S., Benassi, B., Del Bufalo, D., Elli, R., Antonelli, A., D' Incalci, M. and Zupi, G. (2003) Telomere dysfunction increases cisplatin and ecteinascidin- 743 sensitivity of melanoma cells. *Molecular Phamacology* **63** (3): 632-638.

Blackburn, E. (1999) The telomere and telomerase: How do they interact? *The Mount Sinai Journal of Medicine* **66**: 292-300.

Blackburn, E.H. (1984) Telomeres: do the ends justify the means? *Cell* **37**: 7-8.

Blackburn, E.H. (2000) Telomere states and cell fates. *Nature* **408**: 53-56.

Blackburn, E.H. (2001) Switching and signalling at the telomere. *Cell* **106**: 661-673.

Blackburn, E.H. and Greider, C.W. (1985) Identification of a specific telomere terminal transferase activity in Tetrahymena extracts. *Cell* **43**: 405-413.

Blackburn, E.H. and Szostak, J.W. (1984) The molecular structure of centromeres and telomeres. *Annual Reviews in Biochemistry* **53**: 163-194.

Bodnar, A.G., Ouellette, M., Frolkis, M., Holt, S.E., Chiu, C.P., Morin, G.B., Harley, C.B., Shay, J.W., Lichtsteiner, S. and Wright, W.E. (1998) Extension of lifespan by introduction of telomerase into normal human cells. *Science* **279**: 349-352.

Bonelli, G., Sacchi, M.C., Barbiero, G., Durati, F., Golgi, G., Verdun di Cantogna, L., Amenta, J.S., Piacentini, M., Tacchetti, C. and Baccino, F.M. (1996) Apoptosis of L929 cells by etoposide: a quantitative and kinetic approach. *Experimental Cell Research* **228**: 292-305.

Bown, N., Cotterill, S., Lastowska, M., O'Neill, S., Pearson, A.D., Plantaz, D., Meddeb, M., Danglot, G., Brinkschmidt, C., Christiansen, H., Laureys, G. and Speleman, F. (1999) Gain of chromosome arm 17q and adverse outcome in patients with neuroblastoma. *New England Journal of Medicine* **340**: 1954-1961.

Brabeck, C., Pfeiffer, R., Leake, A., Beneke, S., Meyer, R. and Burkle, A. (2003) L-selegiline potentiates the cellular poly(ADP-ribosyl)ation response to ionizing radiation. *The Journal of Pharmacology and Experimental Therapeutics* **306**: 973-979.

Brinkschmidt, C., Poremba, C., Christiansen, H., Simon, R., Schafer, K.L., Tepe, H.J., Lampert, F., Boecker, W. and Dockhorn-Dworniczak, B. (1998) Comparative genomic hybridization and telomerase activity analysis identify two biologically different groups of four neuroblastomas. *British Journal of Cancer* **77**: 2223-2229.

Broccoli, D., Smorgorzewska, A., Chong, L. and de Lange, T. (1997) Human telomeres contain two distinct Myb-related proteins, TRF1 and TRF2. *Nature Genetics* **17**: 231-235.

Brodeur, G.M., Seege, R.C., Schwab, M., Varmus, H.E. and Bishop, J.M. (1984) Amplification of N-myc in untreated human neuroblastomas correlates with advanced disease stage. *Science* **224**: 1121-1124.

Brown, W.R.A. (1989) Molecular cloning of human telomeres in yeast. *Nature* **338**: 774-776.

Bryan, T.M., Englezou, A., Gupta, J., Bacchetti, S. and Reddel, R.R. (1995) Telomere elongation in immortal human cells without detectable telomerase activity. *The EMBO Journal* **14** (17): 4240-4248.

Bryan, T.M., Englezou, A., Dalla-Pozza, L., Dunham, M.A. and Reddel, R.R. (1997) Evidence for an alternative mechanism for maintaining telomere length in human tumors and tumor derived cell lines. *Nature Medicine* **3** (11): 1271-1274.

Bryan, T.M. and Reddel, R.R. (1997) Telomere dynamics and telomerase activity in in vitro immortalised human cells. *European Journal of Cancer* **33** (5): 767-773.

Bullock, A.N. and Fersht, A.R. (2001) Rescuing the function of mutant p53. *Nature Reviews Cancer* **1**: 68-76.

Burger, A.M., Double, J.A. and Newell, D.R. (1997) Inhibition of telomerase activity by cisplatin in human testicular cancer cells. *European Journal of Cancer* **33**: 638-644.

Burger, A.M., Fiebig, H.H., Kuettel, M.R., Lautenberger, J.A., Kung, H.F. and Rhim, J.S. (1998) Effect of oncogene expression on telomerase activation and telomere length in human endothelial, fibroblast and prostate epithelial cells. *International Journal of Oncology* **13**: 1043-1048.

Butt, A.J., Harvey, N.L., Parasivam, G. and Kumar, S. (1998) Dimerization and autoprocessing of the Nedd2 (caspase-2) precursor requires both the prodomain and the carboxyl-terminal regions. *Journal of Biological Chemistry* **273**: 6763-6768.

Calvert, A.H., Newell, D.R. and Tilby, M.J. (1995). Cisplatin and analogues: discovery, mechanism of action and clinical pharmacology. Oxford Textbook of Oncology. M. Peckham, H. Pinedo and U. Veronesi, Oxford University Press.

Campisi, J. (1997) The biology of replicative senescence. *European Journal of Cancer* **33** (5): 703-709.

Campisi, J. (2000) Cancer, aging and cellular senescence. *In vivo* **14**: 183-188.

Cao, Y., Li, H., Deb, S. and Liu, J.P. (2002) TERT regulates cell survival independent of telomerase enzymatic activity. *Oncogene* **21**: 3130-3138.

Caron, H., van Sluis, P., de Kraker, J., Bokkerink, J., Egeler, M., Laureys, G., Slater, R., Westerveld, A., Voute, P.A. and Versteeg, R. (1996) Allelic loss of chromosme 1p as a predictor of unfavourable outcome in patients with neuroblastoma. *New England Journal of Medicine* **334**: 225-230.

Chaney, S.G. and Vaisman, A. (1999) Specificity of platinum-DNA adduct repair. *Journal of Inorganic Biochemistry* **77**: 71-81.

Chang, B.D., Broude, E.V., Dokmanovic, M., Zhu, H., Ruth, A., Xuan, Y., Kandel, E.S., Lausch, E., Christov, K. and Roninson, I.B. (1999) A senescence-like phenotype distinguishes tumor cells that undergo terminal proliferation arrest after exposure to anticancer agents. *Cancer Research* **59**: 3761-7.

Chen, J., Saha, P., Kornbluth, S., Dynlacht, B.D. and Dutta, A. (1996) Cyclin binding motifs are essential for the function of p21CIP1. *Molecular and Celluar Biology* **16**: 4673-4682.

Chen, Z., Koeneman, K.S. and Corey, D.R. (2003) Consequences of telomerase inhibition and combination treatments for the proliferation of cancer cells. *Cancer Research* **63**: 5917-5925.

Chi, N.W. and Lodish, H.F. (2000) Tankyrase is a golgi associated mitogen activated protein kinase substrate that interacts with IRAP in GLUT4 vesicles. *The Journal of Biological Chemistry* **275** (49): 38437-3844.

Chin, L., Artandi, S.E., Shen, Q., Tam, A., Lee, S.L., Gottlieb, G.J., Greider, C.W. and DePinho, R.A. (1999) p53 deficiency rescues the adverse effects of telomere loss and cooperates with telomere dysfunction to accelerate carcinogenesis. *Cell* **97**: 527-538.

Cooke, H.J. and Smith, B.A. (1986) Variability at the telomeres of the human X/Y pseudoautosomal region. *Cold Spring Harbor Symposia On Quantitative Biology* **LI**: 213-219.

Cory, S. and Adams, J.M. (2002) The Bcl2 family: regulators of the cellular life-or-death switch. *Nature Reviews Cancer* **2**: 647-656.

Counter, C.M., Meyerson, M., Eaton, E.N., Ellisen, L.W., Caddle, S.D., Haber, D.A. and Weinberg, R.A. (1998) Telomerase activity is restored in human cells by ectopic expression of hTERT (hEST2) the catalytic subunit of telomerase. *Oncogene* **16**: 1217-1222.

Cressey, T.R., Tilby, M.J. and Newell, D.R. (2002) Decreased telomerase activity is not a reliable indicator of chemosensitivity in testicular cancer cell lines. *European Journal of Cancer* **38**: 586-593.

Cross, S.H., Allshire, R.C., McKay, S.J., McGill, N.I. and Cooke, H.J. (1989) Cloning of human telomeres by complementation in yeast. *Nature Biotechnology* **338**: 771-774.

Daboussi, F., Dumay, A., Delacote, F. and Lopez, B.S. (2002) DNA double-strand break repair signalling: the case of RAD51 post-translational regulation. *Cell Signalling* **14**: 969-75.

d'Adda di Fagagna, F., Hande, M.P., Tong, W.M., Lansdorp, P.M., Wang, Z.Q. and Jackson, S.P. (1999) Functions of poly(ADP-ribose) polymerase in controlling telomere length and chromosomal stability. *Nature Genetics* **23**: 76-80.

d'Adda di Fagagna, F., Reaper, P.M., Clay-Farrace, L., Fiegler, H., Carr, P., von Zglinicki, T., Saretzki, G., Carter, N.P. and Jackson, S.P. (2003) A DNA damage checkpoint response in telomere-initiated senescence. *Nature* **426**: 194-198.

D'Arpa, P., Beardmore, C. and Liu, L.F. (1990) Involvement of nucleic acid synthesis in cell killing mechanisms of topoisomerase poisons. *Cancer Research* **50**: 6919-6924.

Davies, S.M., Robson, C.N., Davies, S.L. and Hickson, I.D. (1988) Nuclear topoisomerase II levels correlate with the sensitivity of mammalian cells to intercalating agents and epipodophyllotoxins. *Journal of Biological Chemistry* **263**: 17724-17729.

de Lange, T. (1992) Human telomeres are attached to the nuclear matrix. *The EMBO Journal* **11**: 717-724.

de Lange, T. (1995). Telomere dynamics and genome instability in human cancer. Telomeres. E. H. Blackburn and C. W. Greider, Cold Spring Harbour Press, New York: 265-293.

de Lange, T. (2001) Telomere capping-one strand fits all. *Science* **292** (5519): 1075-1076.

de Lange, T., Shiue, L., Myers, R.M., Cox, D.R., Naylor, S.L., Killery, A.M. and Varmus, H.E. (1990) Structure and variability of human chromosome ends. *Molecular and Cellular Biology* **10** (2): 518-527.

Degen, W.G., Pruijn, G.J., Raats, J.M. and van Venrooij, W.J. (2000) Caspase-dependent cleavage of nucleic acids. **7**: 616-627.

Deleo, A.B., Jay, G., Appella, E., Dubois, G.C., Law, L.W. and Old, L.J. (1979) Detection of a transformation-related antigen in chemically induced sarcomas and other transformed cells of the mouse. *Proceedings of the National Academy of Sciences USA* **76**: 2420-2424.

Dierick, J.F., Kalume, D.E., Wenders, F., Salmon, M., Dieu, M., Raes, M., Roepstorff, P. and Toussaint, O. (2002) Identification of 30 protein species involved in replicative senescence and stress induced premature senescence. *Febs Letters* **531**: 499-504.

Dijt, F.J., Fichtinger-Schepman, A.M., Berends, F. and Reedijk, J. (1988) Formation and repair of cisplatin-induced adducts to DNA in cultured normal and repair deficient human fibroblasts. *Cancer Research* **48**: 6058-6062.

Dimri, G.P., Lee, X., Basile, G., Acosta, M., Scott, G., Roskelley, C., Medrano, E.E., Linskens, M., Rubelj, I., Pereir-Smith, O., Peacocke, M. and Campisi, J. (1995) A biomarker that identifies senescent human cells in culture and in aging skin in vivo. *Proceedings of the National Academy of Sciences USA* **92**: 9363-9367.

Dimri, G.P., Martinez, J.L., Jacobs, J.J., Keblusek, P., Itahana, K., van Lohuizen, M., Campisi, J., Wazer, D.E. and Band, V. (2002) The Bmi-1 oncogene induces telomerase activity and immortalises human mammary epithelial cells. *Cancer Research* **62**: 4736-4745.

Donehower, L.A., Harvey, M., Slagle, B.L., McArthur, M.J., Montgomery, C.A.J., Butel, J.S. and Bradley, A. (1992) Mice deficient for p53 are developmentally normal but susceptible to spontaneous tumours. *Nature* **356**: 215-221.

Dubrana, K., Perrod, S. and Gasser, S.M. (2001) Turning telomeres off and on. *Current Opinion in Cell Biology* **13**: 281-289.

Dudognon, C., Pendino, F., Hillion, J., Saumet, A., Lanotte, M. and Segal-Bendirdjian, E. (2004) Death receptor signaling regulatory function for telomerase: hTERT abolishes TRAIL-induced apoptosis, independently of telomere maintenance. *Oncogene* **23**: 7469-7474.

Eastman, A. and Barry, M.A. (1987) Interaction of trans-diamminedichloroplatinum (II) with DNA: formation of monfunctional adducts and their reaction with gluthione. *Biochemistry* **26**: 3303-3307.

Elmore, L.W., Rehder, C.W., Di, X., McChesney, P.A., Jackson-Cook, C.K., Gewirtz, D.A. and Holt, S.E. (2002) Adriamycin-induced senescence in breast tumor cells involves functional p53 and telomere dysfunction. *Journal of Biological Chemistry* **277**: 35509-15.

Estey, E., Adlalcha, R.C., Hittleman, W.N. and Zwelling, L.A. (1987) Cell cycle stage dependent variations in drug-induced topoisomerase II mediated DNA cleavage and cytotoxicity. *Biochemistry* **26**: 4338-4344.

Falck, J., Mailand, N., Syljuasen, R.G., Bartek, J. and Lukas, J. (2001) The ATM-CHK2-CDC25A checkpoint pathway guards against radiosensitive DNA synthesis. *Nature* **410**: 842-847.

Fan, S., El Deiry, W.S., Bae, I., Freeman, J., Jondle, D., Bhatia, K., Fornace, A.J.J., Magrath, I., Kohn, K.W. and O'Connor, P.M. (1994) p53 gene mutations are associated with decreased sensitivity of human lymphoma cells to DNA damaging agents. *Cancer Research* **54**: 5824-5830.

Faraoni, I., Turriziani, M., Masci, G., De Vecchis, L., Shay, J.W., Bonmassar, E. and Graziani, G. (1997) Decline in telomerase activity as a measure of tumour cell killing by antineoplastic agents in vitro. *Clinical Cancer Research* **3**: 579-585.

Feng, J., Funk, W.D., Wang, S.S., Weinrich, S.L., Avilion, A.A., Chiu, C.P., Adams, R.R., Chang, E., Allsopp, R.C., Yu, J., Le, S., West, M.D., Harley, C.B., Andrews, W.H., Greider, C.W. and Villiponteau, B. (1995) The RNA component of human telomerase. *Science* **269**: 1236-1241.

Ferbeyre, G., de Stanchina, E., Lin, A.W., Querido, E., McCurrach, M.E., Hannon, G.J. and Lowe, S.W. (2002) Oncogenic ras and p53 cooperate to induce cellular senescence. *Molecular and Celluar Biology* **22**: 3947-3508.

Fichtinger-Schepman, A.M., van der Veer, J.L., den Hartog, J.H., Lohman, P.H. and Reedijk, J. (1985) Adducts of the antitumour drug cis-diammine dichloroplatinum (II) with DNA: formation, identification and pharmacologically active agents. *Biochemistry* **24**: 707-713.

Fink, D., Aebi, S. and Howell, S.B. (1998) The role of DNA mismatch repair in drug resistance. *Clinical Cancer Research* **4**: 1-6.

Flore, O., Rafii, S., Ely, S., O'Leary, J.J., Hyjek, E.M. and Cesarman, E. (1998) Transformation of primary human endothelial cells by Kaposi's sarcoma-associated herpesvirus. *Nature* **394**: 588-592.

Folini, M., De Marco, C., Orlandi, M.L., Daidone, M.G. and Zaffaroni, N. (2000) Attenuation of telomerase activity does not increase sensitivity of human melanoma cells to anticancer agents. *European Journal of Cancer* **36**: 2137-2145.

Fraval, H.N. and Roberts, J.J. (1979) Excision repair of cis-diammine dichloroplatinum(II) induced damage to DNA of Chinese hamster cells. *Cancer Research* **39**: 1793-1797.

Frei, E., Elias, A., Wheeler, C., Richardson, P. and Hryniuk, W. (1998) The relationship between high dose treatment and combination chemotherapy: the concept of summation dose intensity. *Clinical Cancer Research* **4**: 2027-2037.

Froelich-Ammon, S.J. and Oshesoff, N. (1995) Topoisomerase poisons: harressing the darkside of enzyme mechanisms. *Journal of Biological Chemistry* **270**: 21429-21432.

Fu, W., Killen, M., Culmsee, C., Dhar, S., Pandita, T.K. and Mattson, M.P. (2000) The catalytic subunit of telomerase is expressed in developing brain neurons and serves a cell survival-promoting function. *Journal of Molecular Neuroscience* **14**: 3-15.

Furuta, T., Takemura, H., Liao, Z.Y., Aune, G.J., Redon, C., Sedelnikova, O.A., Pilch, D.R., Rogakou, E.P., Celeste, A., Chen, H.T., Nussenzweig, A., Aladjem, M.I., Bonner, W.M. and Pommier, Y. (2003) Phosphorylation of histone H2AX and activation of Mre11, Rad50 and Nbs1 in response to replication dependent DNA double strand breaks induces by mammalian topoisomerase I cleavage complexes. *Journal of Biological Chemistry* **278**: 20303-20312.

Gellert, M., Mitzuuchi, K., O'Dea, M.H. and Nash, H.A. (1976) DNA gyrase: An enzyme that integrates superhelical turns into DNA. *Proceedings of the National Academy of Sciences USA* **73** (11): 3872-3876.

Givan, A.L. (2001). Flow cytometry. First Principles, Wiley-liss.

Goldstein, S. (1990) Replicative senescence: the human fibroblast comes of age. *Science* **249**: 1129-1133.

Goldstein, S. and Singal, D.P. (1974) Senescence of cultured human fibroblasts: mitotic versus metabolic time. *Experimental Cell Research* **88**: 359-364.

Gorbunova, V., Seluanov, A. and Pereira-Smith, O.M. (2002) Expression of human telomerase (hTERT) does not prevent stress-induced senescence in normal human fibroblasts but protects the cells from stress-induced apoptosis and necrosis. *Journal of Biological Chemistry* **277**: 38540-9.

Gottschling, D.E., Aparicio, O.M., Billington, B.L. and Zakian, V.A. (1990) Position effect at S. cerevisiae telomeres: reversible repression of Pol II transcription. *Cell* **63**: 751-762.

Green, D.R. and Reed, J.C. (1998) Mitochondria and apoptosis. *Science* **281**: 1309-12.

Greider, C.W. (1991) Telomeres. *Current Opinion in Cell Biology* **3**: 444-451.

Greider, C.W. and Blackburn, E.H. (1985) Identification of a specific telomere terminal transferase activity in Tetrahymena extracts. *Cell* **43**: 405-413.

Greider, C.W. and Blackburn, E.H. (1987) The telomere terminal transferase of Tetrahymena is a ribonucleoprotein enzyme with two kinds of primer specificity. *Cell* **51**: 887-898.

Greider, C.W. and Blackburn, E.H. (1989) A telomeric sequence in the RNA of Tetrahymena telomerase required for telomere repeat synthesis. *Nature* **337**: 331-337.

Griffith, J., Bianchi, A. and de Lange, T. (1998) TRF1 promotes parallel pairing of telomeric tracts in vitro. *Journal of Molecular Biology* **278**: 79-88.

Griffith, J.D., Comeau, L., Rosenfield, S., Stansel, R.M., Bianchi, A., Moss, H. and de Lange, T. (1999) Mammalian telomeres end in a large duplex loop. *Cell* **97**: 503- 514.

Grimaldi, K.A., McAdam, S.R., Souhami, R.L. and Hartley, J.A. (1994) DNA damage by anti-cancer agents resolved at the nucleotide level of a single copy gene: evidence for a novel binding site for cisplatin in cells. *Nucleic Acids Research* **22** (12): 2311-2317.

Grobelny, J.V., Kulp-McEliece, M. and Broccoli, D. (2001) Effects of reconstitution of telomerase activity on telomere maintenance by the alternative lengthening of telomeres (ALT) pathway. *Human Molecular Genetics* **10** (18): 1953-1961.

Gu, W. and Roeder, R.G. (1997) Activation of p53 sequence-specific DNA binding by acetylation of the p53 C-terminal domain. *Cell* **90**: 595-606.

Haber, J.E. (2000) Partners and pathways repairing a double-strand break. *Trends in Genetics* **16**: 259-264.

Haendeler, J., Hoffmann, J., Rahman, S., Zeiher, A.M. and Dimmeler, S. (2003) Regulation of telomerase activity and anti-apoptotic function by protein-protein interaction and phosphorylation. *Febs Letters* **536**: 180-186.

Hahn, W.C., Counter, C.M., Lundberg, A.S., Beijersbergen, R.L., Brooks, M.W. and Weinberg, R.A. (1999) Creation of human tumour cells with defined genetic elements. *Nature* **400**: 464-468.

Han, Z., Wei, W., Dunaway, S., Darnowski, J.W., Calabresi, P., Sedivy, J., Hendrickson, E.A., Balan, K.V., Pantazis, P. and Wyche, J.H. (2002) Role of p21 in apoptosis and senescence of human colon cancer cells treated with camptothecin. *Journal of Biological Chemistry* **277**: 17154-60.

Hanahan, D. and Weinberg, R.A. (2000) The hallmarks of cancer. *Cell* **100**: 57-70.

Hande, K.R. (1998a) Clinical applications of anti-cancer drugs targeted to topoisomerase II. *Biochimica et Biophysica Acta* **1400**: 173-184.

Hande, K.R. (1998b) Etoposide: four decades of development of a topoisomerase II inhibitor. *European Journal of Cancer* **34**: 1514-1521.

Hansson, J. and Wood, R.D. (1989) Repair synthesis by human cell extracts in DNA damaged by cis- and trans-diamminedichloroplatinum(II). *Nucleic Acids Research* **17**: 8073-8091.

Haq, R., Brenton, J.D., Takahashi, M., Finan, D., Finkielsztein, A., Damaraju, S., Rottapel, R. and Zanke, B. (2002) Constitutive p38HOG mitogen-activated protein kinase activation induces permanent cell cycle arrest and senescence. *Cancer Research* **62**: 5076-82.

Hardy, C.F., Sussel, L. and Shore, D. (1992) A RAP1-interacting protein involved in transcriptional silencing and telomere length regulation. *Genes and Development* **6** (5): 801-814.

Harley, C.B. (1991) Telomere loss: mitotic clock or genetic time bomb? *Mutation Research* **256**: 271-282.

Harley, C.B., Futcher, A.B. and Greider, C.W. (1990) Telomeres shorten during ageing of human fibrolasts. *Nature* **345**: 458-460.

Harley, C.B., Vaziri, H., Counter, C. and Allsopp, R.C. (1992) The telomere hypothesis of cellular ageing. *Experimental Gerontology* **27**: 375-382.

Harrington, L. (2004) Those dam-aged telomeres! *Current Opinion in Genetics & Development* **14**: 22-28.

Harrington, L., McPhail, T., Mar, V., Zhou, W., Oulton, R., Bass, M.B., Arruda, I. and Robinson, M.O. (1997) A mammalian telomerase associated protein. *Science* **275**: 973-977.

Hastie, N.D., Dempster, M., Dunlop, M.G., Thompson, A.M., Green, D.K. and Allshire, R.C. (1990) Telomere reduction in human colorectal carcinoma and with ageing. *Nature* **346**: 866-868.

Hayes, D.M., Cvitkovic, E., Golbey, R.B., Scheiner, E., Helson, L. and Krakoff, I.H. (1977) High dose cis-platinumdiamminedichloride: amelioration of renal toxicity by mannitol diuresis. *Cancer* **39**: 1372-1381.

Hayflick, L. (1965) The limited in vitro lifetime of human diploid cell strains. *Experimental Cell Research* **37**: 614-636.

Hazelrigg, T., Levis, R. and Rubin, G.M. (1984) Transformation of white locus DNA in drosophila: dosage compensation, zeste interaction, and position effects. *Cell* **36**: 469-481.

Hemann, M.T., Strong, M.A., Hao, L.Y. and Greider, C.W. (2001) The shortest telomere, not average telomere length, is critical for cell viability and chromosome stability. *Cell* **107**: 67-77.

Henkels, K.M. and Turchi, J.J. (1997) Induction of apoptosis in cisplatin-sensitive and resistant human ovarian cancer cell lines. *Cancer Research* **57**: 4488-4492.

Herbert, B.S., Pitts, A.E., Baker, S.I., Hamiliton, S.E., Wright, W.E., Shay, J.W. and Corey, D.R. (1999) Inhibition of human telomerase in immortal human cells leads to progressive telomere shortening and cell death. *Proceedings of the National Academy of Sciences USA* **96**: 14276-14281.

Higby, D.J., Wallace, H.J.J., Albert, D.J. and Holland, J.F. (1974) Diamine dichloroplatinum: a phase I study showing responses in testicular and other tumors. *Cancer* **33**: 1219-1225.

Hiyama, E., Hiyama, K., Yokoyama, T., Matsuura, Y., Piatyszek, M.A. and Shay, J.W. (1995) Correlating telomerase activity levels with human neuroblastoma outcomes. *Nature Medicine* **1**: 249-255.

Hiyama, E., Hiyama, K., Nishiyama, M., Reynolds, C.P., Shay, J.W. and Yokoyama, T. (2003) Differential gene expression profiles between neuroblastomas with high telomerase activity and low telomerase activity. *Journal of Pediatric Surgery* **38**: 1730-4.

Hofseth, L.J., Perwez Hussain, S. and Harris, C.C. (2004) p53: 25 years after its discovery. *Trends in Pharmacological Sciences* **25**: 177-181.

Holliday, R. and Tarrant, G.M. (1972) Altered enzymes in ageing human fibroblasts. *Nature* **238**: 26-30.

Hollstein, M., Sidransky, D., Vogelstein, B. and Harris, C.C. (1991) p53 mutations in human cancers. *Science* **253**: 49-53.

Holt, S.E., Glinsky, V., Ivanova, A.B. and Glinsky, G.V. (1999) Resistance to apoptosis in human cells conferred by telomerase function and telomere stability. *Molecular Carcinogenesis* **25**: 241-248.

Hsiang, Y.H. and Liu, L.F. (1989) Evidence for the reversibility of cellular DNA lesion induced by mammalian topoisomerase II poisons. *Journal of Biological Chemistry* **264**: 9713-9715.

Hsu, H.L., Gilley, D., Blackburn, E.H. and Chen, D.J. (1999) Ku is associated with the telomere in mammals. *Proceedings of the National Academy of Sciences USA* **96** (22): 12454-12458.

Hsu, H.L., Gilley, D., Galande, S.A., Hande, M.P., Allen, B., Kim, S.H., Li, G.C., Campisi, J., Shigematsu, T.K. and Chen, D.J. (2000) Ku acts in a unique way at the mammalian telomere to prevent end joining. *Genes & Development* **14**: 2807-2812.

Huang, X., Okafuji, M., Traganos, F., Luther, E., Holden, E. and Darzynkiewicz, Z. (2004) Assessment of histone H2AX phosphorylation induced by DNA topoisomerase I and II inhibitors topotecan and mitoxantrone and by the DNA cross-linking agent cisplatin. *Cytometry Part A* **58A**: 99-110.

Hultdin, M., Gronlund, E., Worrback, K.F., Lindstrom, E.E., Just, T. and Roos, G. (1998) Telomere analysis by fluoresence in situ hybridization and flow cytometry. *Nucleic Acids Research* **26** (16): 3651-3656.

Hurlin, P.J., Maher, V.M. and McCormick, J.J. (1989) Malignant transformation of human fibroblasts caused by expression of a transfected T24 HRAS oncogene. *Proceedings of the National Academy of Sciences USA* **86**: 187-191.

Igney, F.H. and Krammer, P.H. (2002) Death and anti-death: tumour resistance to apoptosis. *Nature Reviews Cancer* **2**: 277-288.

Ishibashi, T. and Lippard, S.J. (1998) Telomere loss in cells treated with cisplatin. *Proceedings of the National Academy of Sciences USA* **95**: 4219-4223.

Ishii, K., Yang, W.L., Cvijic, M.E., Kikuchi, Y., Nagata, I. and Chin, K.V. (2000) Telomere shortening by cisplatin in yeast nucleotide excision repair mutant. *Experimental Cell Research* **255**: 95-101.

Jackson, S.P. and Jeggo, P.A. (1995) DNA double-strand break repair and V(D)J recombination: involvement of DNA-PK. *Trends in Biochemical Sciences* **20**: 412-415.

Jamieson, E.R. and Lippard, S.J. (1999) Structure, recognition and processing of cisplatin-DNA adducts. *Chemical Reviews* **99**: 2467-2498.

Jeyapalan, J., Leake, A., Ahmed, S., Saretzki, G., Tilby, M.J. and von Zglinicki, T. (2004) The role of telomeres in etoposide induced tumour cell death. *Cell Cycle* **3**: 1169-76

Johnson, R.D. and Jasin, M. (2001) Double-strand-break-induced homologous recombination in mammalian cells. *Biochem Soc Trans* **29**: 196-201.

Jordan, P. and Carmo-Fonseca, M. (2000) Molecular mechanisms involved in cisplatin cytotoxicity. *Cell Molecular Life Sciences* **57**: 1229-35.

Kakuo, S., Asaoka, K. and Ide, T. (1999) Human is a unique species among primates in terms of telomere length. *Biochemical and Biophysical Research Communications* **263**: 308-314.

Kaminker, P.G., Kim, S.H., Taylors, R., Zebarjadians, Y., Funk, W.D., Morins, G.B., Yaswen, P. and Campisi, J. (2001) TANK2 a new TRF1 associated poly (ADP-ribose) polymerase causes rapid induction of cell death upon overexpression. *The Journal of Biological Chemistry* **276**: 35891-35899.

Kanaar, R., Hoeijmakers, J.H. and van Gent, D.C. (1998) Molecular mechanisms of DNA double strand break repair. *Trend in Cell Biology* **8**: 483-489.

Kang, K.S., Sun, W., Nomata, K., Morita, I., Cruz, A., Liu, C.J., Trosko, J.E. and Chang, C.C. (1998) Involvement of tyrosine phosphorylation of p185(c-erbB2/neu) in tumorigenicity induced by X-rays and the neu oncogene in human breast epithelial cells. *Molecular Carcinogenesis* **21**: 225-33.

Kaplan, D.R., Hempstead, B.L., Martin Zanca, D., Chao, M.V. and Parada, L.F. (1991) The trk proto-oncogene product: a signal transducing receptor for nerve growth factor. *Science* **252**: 554-558.

Karlseder, J., Broccoli, D., Dai, Y., Hardy, S. and de Lange, T. (1999) p53 and ATM dependent apoptosis induced by telomeres lacking TRF2. *Science* **283** (5406): 1321-1325.

Karlseder, J., Hoke, K., Mirzoeva, O.K., Bakkenist, C., Kastan, M.B., Petrini, J.H. and de Lange, T. (2004) The telomeric protein TRF2 binds the ATM kinase and can inhibit the ATM-dependent DNA damage response. *PLOS* **2**: Epub.

Kastan, M.B., Onyekwere, O., Sidransky, D., Vogelstein, B. and Craig, R.W. (1991) Participation of p53 protein in the cellular response to DNA damage. *Cancer Research* **51**: 6304-6311.

Kaufmann, S.H. (1998) Cell death induced by topoisomerase targeted drugs: more questions than answers. *Biochimica et Biophysica Acta* **1400**: 195-211.

Keith, W.N., Bilsland, A., Evans, T.R.J. and Glasspool, R.M. (2002) Telomerase-directed molecular therapeutics. *Expert Reviews in Molecular Medicine* **http://www.expertreviews.org/02004507h.htm**.

Kelland, L.R. (1993) New platinum antitumor complexes. *Crit Rev Oncol Hematol* **15**: 191-219.

Kelland, L.R. (2000) Preclinical perspectives on platinum resistance. *Drugs* **59**: 1-8.

Keys, B., Serra, V., Saretzki, G. and von Zglinicki, T. (2004) Telomere shortening in human fibroblasts is not dependent on the size of the telomeric-3'-overhang. *Aging Cell* **3**: 103-109.

Kidgell, A.E., Butcher, M.E. and Brown, G.W. (1990) Antiemetic control: 5-HT3 antagonists: review of clinical results, with particular emphasis on ondansetron. *Cancer Treatment Reviews* **17**: 311-317.

Kill, I.R., Faragher, R.G., Lawrence, K. and Shall, S. (1994) The expression of proliferation-dependent antigens during the lifespan of normal and progeroid human fibroblasts in culture. *Journal of Cell Science* **107**: 571-579.

Kim, N.W., Piatyzek, M.A., Prowse, K.R., Harley, C.B., West, M.D., Ho, P.L.C., Oviello, G.M., Wright, W.E., Weinrich, S.L. and Shay, J.W. (1994) Specific association of human telomerase activity with immortal cells and cancer. *Science* **266**: 2011-2014.

Kim, S.H., Kaminker, P. and Campisi, J. (1999) TIN2 a new regulator of telomere length in human cells. *Nature Genetics* **23**: 405-412.

Kipling, D. (1995) Telomerase: immortality enzyme or oncogene? *Nature Genetics* **9**: 104-106.

Kirkwood, T.B.L. and Austad, S.N. (2000) Why do we age? *Nature* **408** (6809): 233-238.

Kishi, S., Zhou, X.Z., Ziv, Y., Khoo, C., Hill, D.E., Shiloh, Y. and Lu, K.P. (2001) Telomeric protein Pin2/TRF1 as an important ATM target in response to double strand DNA breaks. *Journal of Biological Chemistry* **276**: 29282-91.

Kiyono, T., Foster, S.A., Koop, J.I., McDougall, J.K., Galloway, D.A. and Klingelhutz, A.J. (1998) Both Rb/p16INK4 inactivation and telomerase activation are required to immortalize human epithelial cells. *Nature* **396**: 84-88.

Klapper, W., Qian, W., Schukte, C. and Parwaresch, R. (2003) DNA damage transiently increases TRF2 mRNA expression and telomerase activity. *Leukemia* **17**: 2007-2015.

Klotbutcher, L.A., Swanton, M.T., Donini, P. and Prescott, D.M. (1981) All gene sized DNA molecules in 4 species of hypotrichs have the same terminal sequence and an unusual 3' terminus. *Proceedings of the National Academy of Sciences USA* **78**: 3015-3019.

Knox, R.J., Friedlos, F., Lydall, D.A. and Roberts, J.J. (1986) Mechanism of cytotoxicity of anticancer platinum drugs: evidence that cis-diammine dichloroplatinum(II) and cis-diammine-(1,1-cyclobutanedicarboxylato) platinum(II) differ only in the kinetics of their interaction with DNA. *Cancer Research* **46**: 1972-1979.

Kolodner, R.D. and Marsischky, G.T. (1999) Eukaryotic DNA mismatch repair. *Current Opinion in Genetics & Development* **9**: 89-96.

Kondo, S., Tanaka, Y., Kondo, Y., Hitomi, M., Barnett, G.H., Ishizaka, Y., Liu, J., Haqqi, T., Nishiyama, A., Villeponteau, B., Cowell, J.K. and Barna, B.P. (1998) Antisense telomerase treatment: induction of two distinct pathways, apoptosis and differentiation. *The FASEB Journal* **12**: 801-811.

Kondo, Y., Komata, T. and Kondo, S. (2001) Combination therapy of 2-5A antisense against telomerase RNA and cisplatin for malignant gliomas. *International Journal of Oncology* **18**: 1287-1292.

Koomagi, R., Stammler, G., Manegold, C., Mattern, J. and Volm, M. (1996) Expression of resistance related proteins in tumoral and peritumoral tissues of patients with lung cancer. *Cancer Letters* **110**: 129-136.

Kraemer, K.H., Lee, M.M. and Scotto, J. (1987) Xeroderma pigmentosum. Cutaneous, ocular, and neurologic abnormalities in 830 published cases. *Arch Dermatol* **123**: 241-250.

Kroemer, G. and Reed, J.C. (2000) Mitochondrial control of cell death. *Nature Medicine* **6**: 513-519.

Kruk, P.A., Rampino, N.J. and Bohr, V.A. (1995) DNA damage and repair in telomeres: relation to aging. *Proceedings of the National Academy of Sciences USA* **92**: 258-262.

Ku, W.C., Cheng, A.J. and Wang, T.C. (1997) Inhibition of telomerase activity by PKC inhibitors in human nasoparyngeal cancer cells in culture. *Biochemical and Biophysical Research Communications* **241**: 730-736.

Kunifuji, Y., Gotoh, S., Abe, T., Miura, M. and Karasaki, Y. (2002) Down regulation of telomerase activity by anticancer drugs in human ovarian cancer cells. *Anti-Cancer Drugs* **13**: 595-598.

Kuranaga, N., Shinomiya, N. and Mochizuki, H. (2001) Long term cultivation of colorectal carcinoma cells with anticancer drugs induces drug resistance and telomere elongation: an in vitro study. *Biomedical Central Cancer* **1**: 10.

Lai, G.M., Ozols, R.F., Smyth, J.F., Young, R.C. and Hamilton, T.C. (1988) Enhanced DNA repair and resistance to cisplatin in human ovarian cancer. *Biochem Pharmacol* **37**: 4597-4600.

Land, H., Parada, L.F. and Weinberg, R.A. (1983) Tumorigenic conversion of primary embryo fibroblasts requires at least two cooperating oncogenes. *Nature* **304**: 596-602.

Lane, D.P. (1992) Cancer. p53, guardian of the genome. *Nature* **358**: 15-16.

Lane, D.P. and Crawford, L.V. (1979) T antigen is bound to a host protein in SV40 transformed cells. *Nature* **278**: 261-263.

Lansdorp, P.M., Verwoerd, N.P., Van de Rijke, F.M., Dragowska, V., Little, M.T., Dirks, R.W., Raap, A.K. and Tanke, H.J. (1996) Heterogeneity in telomere length of human chromosomes. *Human Molecular Genetics* **5**: 685-691.

Laroche, T., Martin, S.G., Gotta, M., Gorham, H.C., Pryde, F.E., Louis, E.J. and Gasser, S.G. (1998) Mutation of yeast Ku genes disrupts the subnuclear organization of telomeres. *Current Biology* **8**: 653-656.

Lee, K., Rudolph, L., Ju, Y., Greenberg, R.A., Cannizzaro, L., Chin, L., Weiler, S.R. and DePinho, R.A. (2001) Telomere dysfunction alters the chemotherapeutic profile of transformed cells. *Proceedings of the National Academy of Sciences USA* **98**: 3381-3386.

Lee, S., Cavallo, L. and Griffith, J. (1997) Human p53 binds Holliday junctions strongly and facilitates their cleavage. *Journal of Biological Chemistry* **272**: 7532-7539.

Levine, A.J. (1997) p53, the cellular gatekeeper for growth and division. *Cell* **88**: 323-331.

Levine, A.J., Momand, J. and Finlay, C.A. (1991) The p53 tumour suppressor gene. *Nature* **351**: 453-456.

Levy, M.Z., Allsopp, R.C., Futcher, A.B., Greider, C.W. and Harley, C.B. (1992) Telomere end replication problem and aging. *Journal of Molecular Biology* **225**: 951-960.

Li, B., Oestreich, S. and de Lange, T. (2000) Identification of human Rap1: implications for telomere evolution. *Cell* **101**: 471-483.

Li, D., Zhang, Y., Cao, W., Sun, L., Xu, H. and Lu, W. (2002) Regulative function of telomerase and extracellular regulated protein kinases to leukemic cell apoptosis. *J Huazhong Univ Sci Technolog Med Sci* **22** (4): 292-301.

Li, L.F. and Chen, A.Y. (1994) DNA topoisomerases: essential enzymes and lethal targets. *Annual Reviews of Pharmological Toxicology* **34**: 191-218.

Li, P., Nijhawan, D., Budihardjo, I., Srinivasula, S.M., Ahmad, M., Alnemri, E.S. and Wang, X. (1997) Cytochrome c and dATP-dependent formation of Apaf-1/caspase-9 complex initiates an apoptotic protease cascade. *Cell* **91**: 479-489.

Lin, A.W., Barradas, M., Stone, J.C., van Aelst, L., Serrano, M. and Lowe, S.W. (1998) Premature senescence involving p53 and p16 is activated in response to constitutive MEK/ MAPK mitogenic signalling. *Genes and Development* **12**: 3008-3019.

Lin, Z., Lim, S., Viani, M.A., Sapp, M. and Lim, M.S. (2001) Down regulation of telomerase activity in malignant lymphomas by radiation and chemotherapeutic agents. *American Journal of Pathology* **159**: 711-719.

Linzer, D.I. and Levine, A.J. (1979) Characterization of a 54K dalton cellular SV40 tumor antigen present in SV40 transformed cells and uninfected embryonal carcinoma cells. *Cell* **17**: 43-52.

Liu, D., Safari, A., O'Connor, M.S., Chan, D.W., Laegeler, A., Qin, J. and Songyang, Z. (2004) PTOP interacts with POT1 and regulates its localization to telomeres. *Nature Cell Biology* **6**: 673-680.

Lowe, S.W., Schmitt, E.M., Smith, S.W., Osborne, B.A. and Jacks, T. (1993) p53 is required for radiation-induced apoptosis in mouse thymocytes. *Nature* **362**: 847-849.

Ludwig, A., Saretzki, G., Holm, P.S., Tiemann, F., Lorenz, M., Emrich, T., Harley, C.B. and von Zglinicki, T. (2001) Ribozyme cleavage of telomerase mRNA sensitizes breast epithelial cells to inhibitors of topoiomerase. *Cancer Research* **61**: 3053-3061.

Makarov, V.L., Hirose, Y. and Langmore, J.P. (1997) Long G tails at both ends of human chromosomes suggest a C strand degradation mechanism for telomere shortening. *Cell* **88**: 657-666.

Malkin, D., Li, F.P., Strong, L.C., Fraumeni, J.F.J., Nelson, C.E., Kim, D.H., Kassel, J., Gryka, M.A., Bischoff, F.Z. and Tainsky, M.A. (1990) Germ line p53 mutations in a familial syndrome of breast cancer, sarcomas, and other neoplasms. *Science* **250**: 1233-1238.

Maris, J.M. and Matthay, K.K. (1999) Molecular biology of neuroblastoma. *Journal of Clinical Oncology* **17**: 2264-2279.

Martens, U.M., Chavez, E.A., Poons, S.S.S., Schmoor, C. and Lansdorp, P.M. (2000) Accumulation of short telomeres in human fibroblasts prior to replicative senescence. *Experimental Cell Research* **256**: 291-299.

Martin-Ruiz, C., Saretzki, G., Petrie, J., Ladhoff, J., Jeyapalan, J., Wei, W., Sedivy, J. and von Zglinicki, T. (2004) Stochastic variation in telomere shortening rate causes heterogeneity of human fibroblast replicative life span. *Journal of Biological Chemistry* **279**: 17826-33.

Mason, J.M. and Biessmann, H. (1995) The unusual telomeres of Drosophila. *Trends In Genetics* **11**: 58-62.

Masutomi, K., Yu, E.Y., Khurts, S., Ben-Porath, I., Currier, J.L., Metz, G.B., Brooks, M.W., Kaneko, S., Murakami, S., DeCaprio, J.A., Weinberg, R.A., Stewart, S.A. and Hahn, W.C. (2003) Telomerase maintains telomere structure in normal human cells. *Cell* **114**: 241-253.

McClintock, B. (1941) The stability of broken ends of chromosmes in Zea Mays. *Genetics* **41**: 234-282.

Medema, J.P., Scaffidi, C., Kischkel, F.C., Shevchenko, A., Mann, M., Krammer, P.H. and Peter, M.E. (1997) FLICE is activated by association with the CD95 death-inducing signaling complex (DISC). *EMBO Journal* **16**: 2794-804.

Mehle, C., Piatyszek, M.A., Ljungberg, B., Shay, J.W. and Roos, G. (1996) Telomerase activity in human renal cell carcinoma. *Oncogene* **13**: 161-166.

Mellon, I. and Hanavalt, P.C. (1989) Induction of the Escherichia coli lactose operon selectively increases repair of its transcribed DNA strand. *Nature* **342**: 95-98.

Meyerson, M., Counter, C., Eaton, E.N., Ellisen, L.W., Steiner, P., Caddle, S.D., Ziaugra, L., Beijersbergen, R.L., Daividoff, M.J., Liu, Z., Bacchetti, S., Haber, D.A. and Weinberg, R.A. (1997) hEST2, the putative human telomerase catalytic subunit gene, is upregulated in tumor cells and during immortalization. *Cell* **90**: 785-795.

Michishita, E., Nakabayashi, K., Ogino, H., Suzuki, T., Fuji, M. and Ayusawa, D. (1998) DNA topoisomerase inhibitors induce reversible senescence in normal human fibroblasts. *Biochemical and Biophysical Research Communications* **253**: 667-671.

Michishita, E., Nakabayashi, K., Suzuki, T., Kaul, S.C., Ogino, H., Fujii, M., Mitsui, Y. and Ayusawa, D. (1999) 5-Bromodeoxyuridine induces senescence-like phenomena in mammalian cells regardless of cell type or species. *Journal of Biochemistry* **126**: 1052-1059.

Misawa, M., Tauchi, T., Sashida, G., Nakajima, A., Abe, K., Ohyashiki, J.H. and Ohyashiki, K. (2002) Inhibition of human telomerase enhances the effect of chemotherapeutic agents in lung cancer cells. *International Journal of Oncology* **21**: 1087-92.

Montaser, A. (1998). Inductively coupled plasma mass spectrometry, Wiley-VCH.

Morales, C.P., Holt, S.E., Ouellette, M., Kaur, K.J., Yan, Y., Wilson, K.S., White, M.A., Wright, W.E. and Shay, J.W. (1999) Absence of cancer associated changes in human fibroblasts immortalized with telomerase. *Nature Genetics* **21**: 115-118.

Morgan, S.E. and Kastan, M.B. (1997) Dissociation of radiation-induced phosphorylation of replication protein A from the S-phase checkpoint. *Cancer Research* **57**: 3386-3389.

Moriarty, T.J., Dupuis, S. and Autexier, C. (2002) Rapid upregulation of telomerase activity in human leukemia HL-60 cells treated with clinical doses of the DNA damaging drug etoposide. *Leukemia* **16**: 1112-1120.

Muller, H.J. (1938) The remaking of chromosomes. *Collecting Net* **13**: 1181-1198.

Murakami, J., Nagai, N., Shigemasa, K. and Ohama, K. (1999) Inhibition of telomerase activity and cell proliferation by a reverse transcriptase inhibitor in gynaecological cancer cell lines. *European Journal of Cancer* **35**: 1027-1034.

Murnane, J.P., Sabatier, L., Marder, B.A. and Morgan, W.F. (1994) Telomere dynamics in an immortal human cell line. *EMBO Journal* **13**: 4953-4956.

Nakabayashi, K., Ogata, T., Fujii, M., Tahara, H., Ide, T., Wadhwa, R., Kaul, S.C., Mitsui, Y. and Ayusawa, D. (1997) Decrease in amplified telomeric sequences and induction of senescence markers by introduction of human chromosome 7 or its segments in SUSM-1. *Experimental Cell Research* **235**: 345-353.

Nakagawara, A., Arim- Nakagawara, M., Scavarda, N.J., Azar, C.G., Cantor, A.B. and Brodeur, G.M. (1993) Association between high levels of expression of the TRK gene and favourable outcome in human neuroblastoma. *The New England Journal of Medicine* **328** (12): 847-854.

Nakamura, T.M., Morin, G.B., Chapman, K.B., Weinrich, S.L., Andrews, W.H., Lingner, J., Harley, C.B. and Cech, T.R. (1997) Telomerase catalytic subunit homologs from fission yeast and human. *Science* **277** (5328): 955-959.

Nakayama, J., Tahara, H., Tahara, E., Saito, M., Ito, K., Nakamura, H., Nakanishi, T., Ide, T. and Ishikawa, F. (1998) Telomerase activation by hTRT in human normal fibroblasts and hepatocellular carcinomas. *Nature Genetics* **18**: 65-68.

Narita, M., Nunez, S., Heard, E., Narita, M., Lin, A.W., Hearn, S.A., Spector, D.L., Hannon, G.J. and Lowe, S.W. (2003) Rb-mediated heterochromatin formation and silencing of E2F target genes during cellular senescence. *Cell* **113**: 703-716.

Nozaki, C., Horibe, K., Iwata, H., Ishiguro, Y., Hamaguchi, M. and Takahashi, M. (2000) Prognostic impact of telomerase activity in patients with neuroblastoma. *International Journal of Oncology* **17**: 341-345.

Offer, H., Wolkowicz, R., Matas, D., Blumenstein, S., Livneh, Z. and Rotter, V. (1999) Direct involvement of p53 in the base excision repair pathway of the DNA repair machinery. *Febs Letters* **450**: 197-204.

Oka, Y., Shiota, S., Nakai, S., Nishida, Y. and Okubo, S. (1980) Inverted terminal repeat sequence in the macronuclear DNA of Stylonychia pustulaton. *Genetics* **10**: 301-306.

Okamoto-Kubo, S., Nishio, K., Heike, Y., Yoshida, M., Ohimori, T. and Saijo, N. (1994) Apoptosis induced by etoposide in small cell lung cancer cell lines. *Chemotherapy Pharmacology* **33**: 385-390.

Olovnikov, A.M. (1971) Principles of marginotomy in template synthesis of polynucleotides. *Doklady Akad. Nauk SSSR* **201**: 1496-1499.

Opresko, P.L., von Kobbe, C., Laine, J.P., Harrigan, J., Hickson, I.D. and Bohr, V.A. (2002) Telomere-binding protein TRF2 binds to and stimulates the Werner and Bloom syndrome helicases. *Journal of Biological Chemistry* **277**: 41110-9.

Oren, M. and Rotter, V. (1999) Introduction: p53- the first twenty years. *Cell Molecular Life Sciences* **55**: 9-11.

Ormerod, M.G. (2000). Flow cytometry, Oxford University Press.

Ormerod, M.G., O'Neill, C., Robertson, D., Kelland, L.R. and Harrap, K.R. (1996) cis-Diamminedichloroplatinum(II)-induced cell death through apoptosis in sensitive and resistant human ovarian carcinoma cell lines. *Cancer Chemotherapy and Pharmacology* **37**: 463-471.

Ouellette, M.M., Liao, M., Herbert, B.S., Johnson, M., Holt, S.E., Liss, H.S., Shay, J.W. and Wright, W.E. (2000) Subsenescent telomere lengths in fibroblasts immortalized by limiting amounts of telomerase. *The Journal of Biological Chemistry* **275** (14): 10072-10076.

Page, J.D., Husain, I., Sancar, A. and Chaney, S.G. (1990) Effect of the diaminocyclohexane carrier ligand on platinum adduct formation, repair, and lethality. *Biochemistry* **29**: 1016-1024.

Park, E.J., Chan, D.W., Park, J.H., Oettinger, M.A. and Kwon, J. (2003) DNA-PK is activated by nucleosomes and phosphorylated H2AX within the nucleosomes in an acetylated dependent manner. *Nucleic Acids Research* **31**: 6819-6827.

Park, J.I., Jeong, J.S., Han, J.Y., Kim, D.I., Gao, Y.H., Park, S.C., Rodgers, G.P. and Kim, I.H. (2000) Hydroxyurea induces a senescence-like change of K562 human erythroleukemia cell. *J Cancer Res Clin Oncol* **126**: 455-460.

Park, K.H., Rha, S.Y., Kim, C.H., Kim, T.S., Yoo, N.C., Kim, J.H., Roh, J.K., Noh, S.H., Min, J.S., Lee, K.S., Kim, B.S. and Chung, H.C. (1998) Telomerase activity and telomere lengths in various cell lines: changes of telomerase activity can be another method for chemosensitivity evaluation. *International Journal of Oncology* **13**: 489-495.

Paull, T.T., Rogakou, E.P., Yanazaki, V., Kirchgessner, C.U., Gellet, M. and Bonner, W.M. (2000) A critical role for histone H2AX in recruitment of repair factors to nuclear foci after DNA damage. *Current Biology* **10**: 886-895.

Perrem, K., Colgin, L.M., Neumann, A.A., Yeager, T.R. and R.R, R. (2001) Coexistence of alternative lengthening of telomeres and telomerase in hTERT-transfected GM847 cells. *Molecular and Cellular Biology* **21**: 3862-3875.

Petersen, S., Saretzki, G. and von Zglinicki, T. (1998) Preferential accumulation of single stranded regions in telomeres of human fibroblasts. *Experimental Cell Research* **239**: 152-160.

Pinto, A.L. and Lippard, S.J. (1985) Binding of the antitumor drug cis-diamminedichloroplatinum(II) (cisplatin) to DNA. *Biochim Biophys Acta* **780**.

Poremba, C., Willenbring, H., Hero, B., Christiansen, H., Schafer, K.L., Brinkschmidt, H.J., Bocker, W. and Dworniczak, B.D. (1999) Telomerase activity distinguishes between neuroblastomas with good and poor prognosis. *Annals of Oncology* **10**: 715-721.

Poremba, C., Hero, B., Heine, B., Scheel, C., Schaefer, K.L., Christiansen, H., Berthold, F., Kneif, S., Stein, H., Juergens, H., Boecker, W. and Dockhorn-Dworniczak, B. (2000) Telomerase is a strong indicator for assessing the proneness to progression in neuroblastomas. *Medical and Pediatric Oncology* **35**: 651-655.

Reuter, G. and Spierer, P.S. (1992) Position effect variegation and chromatin proteins. *Bioessays* **14**: 605-612.

Rhim, J.S., Jay, G., Arnstein, P., Price, F.M., Sanford, K.K. and Aaronson, S.A. (1985) Neoplastic transformation of human epidermal keratinocytes by AD12-SV40 and Kirsten sarcoma viruses. *Science* **227**: 1250-2.

Roberts, P.A. (1974) A cytogenetic analysis of X-ray induced 'visible' mutations at the yellow locus of Drosophila melanogaster. *Mutation Research* **22**: 139-144.

Robles, S.J. and Adami, G.R. (1998) Agents that cause DNA double strand breaks lead to p16INK4a enrichment and the premature senescence of normal fibroblasts. *Oncogene* **16**: 1113-1123.

Rogakou, E.P., Boon, C., Redon, C. and Bonner, W.M. (1999) Megabase chromatin domains involved in DNA double strand breaks in vivo. *Journal of Cell Biology* **146**: 905-916.

Rosenberg, B., Vancamp, L. and Krigas, T. (1965) Inhibition of cell division in Escherichia coli by electrolysis products from a platinum electrode. *Nature* **13**: 698-699.

Rosenberg, B., Vancamp, L., Grimley, E.B. and Thomson, A.J. (1967) The inhibition of growth or cell division in Escherichia coli by different ionic species of platinum (IV) complexes. *Journal of Biological Chemistry* **25**: 1347-1352.

Rosenberg, B., Vancamp, L., Trosko, J.E. and Mansour, V.H. (1969) Platinum compounds: a new class of potent antitumour agents. *Nature* **222**: 385-386.

Ross, R.A., Spengler, B.A. and Biedler, J.L. (1983) Coordinate morphological and biochemical interconversion of human neuroblastoma. *Journal of the National Cancer Institute* **71** (4): 741-747.

Roy, S. and Nicholson, D.W. (2000) Cross-talk in cell death signaling. *Journal of Experimental Medicine* **192**: 21-26.

Ruley, H.E. (1983) Adenovirus early region 1A enables viral and cellular transforming genes to transform primary cells in culture. *Nature* **304**: 602-606.

Santos, J.H., Meyer, J.N., Skorvaga, M., Annab, L.A. and Van Houten, B. (2004) Mitochondrial hTERT exacerbates free-radical-mediated mtDNA damage. *Aging Cell* **3**: 399-411.

Saretzki, G. (2003) Telomerase inhibition as cancer therapy. *Cancer Letters* **194**: 209-219.

Saretzki, G., Sitte, N., Merkel, U., Wurm, R.E. and von Zglinicki, T. (1999) Telomere shortening triggers a p53-dependent cell cycle arrest via accumulation of G-rich single stranded DNA fragments. *Oncogene* **18**: 5148-5158.

Saretzki, G., Ludwig, A., von Zglinicki, T. and Runebaum, I.B. (2001) Ribozyme mediated telomerase inhibition induces immediate cell loss but not telomere shortening in ovarian cancer cells. *Cancer Gene Therapy* **8**: 27-34.

Sato, N., Mizumoto, K., Nishio, S., Maehara, N., Urashima, T., Ogawa, T. and Tanuka, M. (2000) Up-regulation of telomerase activity in human pancreatic cancer cells after exposure to etoposide. *British Journal of Cancer* **82**: 1819-1826.

Scheel, C., Schaefer, K.L., Jauch, A., Keller, M., Wai, D., Brinkschmidt, C., van Valen, F., Boecker, W., Dockhorn-Dworniczak, B. and Poremba, C. (2001) Alternative lengthening of telomeres is associated with chromosomal instability in osteosarcomas. *Oncogene* **20**: 3835-3844.

Scheidtmann, K.H., Mumby, M.C., Rundell, K. and Walter, G. (1991) Dephosphorylation of simian virus 40 large-T antigen and p53 protein by protein phosphatase 2A: inhibition by small-t antigen. *Molecular and Celluar Biology* **11**: 1996-2003.

Schulze-Osthoff, K., Ferrari, D., Los, M., Wesselborg, S. and Peter, M.E. (1998) Apoptosis signaling by death receptors. *European Journal of Biochemistry* **254**: 439-459.

Serra, V. and von Zglinicki, T. (2002) Human fibroblasts in vitro senesce with a donor specific telomere length. *Febs Letters*.

Sgonc, R. and Gruber, J. (1998) Apoptosis Detection: An overview. *Experimental Gerontology* **33** (6): 525-533.

Sharma, G., Gupta, J., Wang, H., Scherthan, H., Dhar, S., Gandhi, V., Iliakis, G., Shay, J.W., Young, C.S.H. and Pandita, T.K. (2003) hTERT associates with human telomeres and enhances genomic stability and DNA repair. *Oncogene* **22**: 131-146.

Shay, J.W. and Bacchetti, S. (1997) A survey of telomerase activity in human cancer. *European Journal of Cancer* **33** (5): 787-791.

Shay, J.W., Pereira-Smith, O.M. and Wright, W.E. (1991) A role for both Rb and p53 in the regulation of human cellular senescence. *Experimental Cell Research* **196**: 33-39.

Shay, J.W., Wright, W.E., Braiskyle, D. and Van der Haegen, B.A. (1993) E6 of human papillomavirus type 16 can overcome the M1 stage of immortalization in human mammary epithelial cells but not in human fibroblasts. *Oncogene* **8**: 1407-1412.

Shay, J.W., Brasiskyte, D., Ouellette, M., Piatyszek, M.A., Werbin, H., Ying, Y. and Wright, W.E. (1994) Analysis of telomerase and telomeres. *Methods in Molecular Genetics* **5**: 263-280.

Shen, M., Haggblom, C., Vogt, M., Hunter, T. and Lu, K.P. (1997) Characterization and cell cycle regulation of the related human telomeric proteins PIN2 and TRF1 suggest a role in mitosis. *Proceedings of the National Academy of Sciences USA* **94**: 13618-13623.

Shin, K.H., Kang, M.K., Dicterow, E., Kameta, A., Baluda, M.A. and Park, N.H. (2004) Introduction of human telomerase reverse transcriptase to normal human fibroblasts enhances DNA repair capacity. *Clinical Cancer Research* **10**: 2551-2560.

Siddik, Z.H. (2003) Cisplatin: mode of cytotoxic action and molecular basis of resistance. *Oncogene* **22**: 7265-7269.

Sitte, N., Saretzki, G. and von Zglinicki, T. (1998) Accelerated telomere shortening in fibroblasts after extended periods of confluency. *Free Radical Biology and Medicine* **24**: 885-893.

Skenhan, P., Storeng, R., Scudiero, D.A., Monks, A., McMahon, J., Vistica, D.,

Warren, J.T., Bokesch, H., Kenney, S. and Boyd, M.R. (1990) New colorimetric cytotoxicity assay for anticancer drug screening. *Journal of the National Cancer Insitute* **82**: 1107-1112.

Smith, G.C.M. and Jackson, S.P. (1999) The DNA dependent protein kinase. *Genes & Development* **13**: 916-934.

Smith, S. and de Lange, T. (1997) TRF1, a mammalian telomeric protein. *Trends In Genetics* **13** (1): 21-26.

Smith, S. and de Lange, T. (2000) Tankyrase promotes telomere elongation in human cells. *Current Biology* **10**: 1299-1302.

Smith, S., Giriat, I., Schmitt, A. and de Lange, T. (1998) Tankyrase a PARP at human telomeres. *Science* **282** (5393): 1484-1487.

Smogorzewska, A. and de Lange, T. (2002) Different telomere damage signalling pathways in human and mouse cells. *The EMBO Journal* **21** (16): 4338-4348.

Smogorzewska, A. and de Lange, T. (2004) Regulation of telomerase by telomeric proteins. *Annual Reviews in Biochemistry* **73**: 177-208.

Song, K., Jung, D., Jung, Y., Lee, S.G. and Lee, I. (2000) Interaction of human Ku70 with TRF2. *Febs Letters* **481**: 81-85.

Spiropoulou, T., Ferekidou, L., Angelopoulou, K., Stathopoulou, A., Talieri, M. and Lianidou, E.S. (2004) Effect of antineoplastic agents on the expression of human telomerase reverse transcriptase beta plus transcript in MCF-7 cells. *Clinical Biochemistry* **37**: 299-304.

Srivastava, S., Zou, Z.Q., Pirollo, K., Blattner, W. and Chang, E.H. (1990) Germ-line transmission of a mutated p53 gene in a cancer-prone family with Li-Fraumeni syndrome. *Nature* **348**: 747-749.

Stampfer, M.R. and Yaswen, P. (2003) Human epithelial cell immortalization as a step in carcinogenesis. *Cancer Letters* **194**: 199-208.

Stein, G.H., Drullinger, L.F., Soulard, A. and Dulic, V. (1999) Differential roles for cyclin dependent kinase inhibitors p21 and p16 in the mechanisms of senescence and differentiation in human fibroblasts. *Molecular and Cellular Biology* **19** (3): 2109-2117.

Stewart, N., Hicks, G.G., Paraskevas, F. and Mowat, M. (1995) Evidence for a second cell cycle block at G_2/M by p53. *Oncogene* **10**: 109-115.

Stewart, S.A., Ben-Porath, I., Carey, V.J., O'Connor, B.F., Hahn, W.C. and Weinberg, R.A. (2003) Erosion of the telomeric single stranded overhang at replicative senescence. *Nature Genetics* **33**: 492-496.

Stoyanovsky, D., Yalowich, J., Gantchev, T. and Kagan, V. (1993) Tyrosinase-induced phenoxyl radicals of etoposide (VP-16): interaction with reductants in model systems, K562 leukemic cell and nuclear homogenates. *Free Radic Res Commun* **19**: 371-86.

Strahl, C. and Blackburn, E.H. (1996) Effects of reverse transcriptase inhibitors on telomere length and telomerase activity in two immortalized human cell lines. *Molecular and Cellular Biology* **16**: 53-65.

Suzuki, T., Minagawa, S., Michishita, E., Ogino, H., Fujii, M., Mitsui, Y. and Ayusawa, D. (2001) Induction of senescence-associated genes by 5-bromodeoxyuridine in HeLa cells. *Experimental Gerontology* **36**: 465-474.

Szymkowski, D.E., Yarema, K., Essigmann, J.M., Lippard, S.J. and Wood, R.D. (1992) An intrastrand d(GpG) platinum crosslink in duplex M13 DNA is refractory to repair by human cell extracts. *Proc Natl Acad Sci U S A* **89**: 10772-19776.

Takai, H., Smorgorzewska, A. and de Lange, T. (2003) DNA damage foci at dysfunctional telomeres. *Current Biology* **13**: 1549-1556.

Takata, M., Sasaki, M.S., Sonoda, E., Morrison, C., Hashimoto, M., Utsumi, H., Yamaguchi-Iwai, Y., Shinohara, A. and Takeda, S. (1998) Homologous recombination and non-homologous end-joining pathways of DNA double-strand break repair have overlapping roles in the maintenance of chromosomal integrity in vertebrate cells. *EMBO Journal* **17**: 5497-508.

Tanaka, T., Slamon, D.J., Shimada, H., Shimoda, H., Fujisawa, T., Ida, N. and Seeger, R.C. (1991) A significant association of Ha-ras p21 in neuroblastoma cells with patient prognosis. *Cancer* **68**: 1296-1302.

Thompson, M.J. and Walsh, J.N. (1983). A Handbook of ICP-MS, Blackie USA: Chapman & Hall, New York.

Thornberry, N.A. (1999) Caspases: a decade of death research. *Cell Death Differentiation* **6**: 1023-1027.

Todo, T., Ryo, H., Yamamoto, K., Toh, H., Inui, T., Ayaki, H., Nomura, T. and Ikenaga, M. (1996) Similarity among the Drosophila (6-4)photolyase, a human photolyase homolog, and the DNA photolyase-blue-light photoreceptor family. *Oncogene* **22**: 5792-5812.

Toussaint, O., Medrano, E.E. and von Zglinicki, T. (2000) Cellular and molecular mechanisms of stress induced premature senescence (SIPS) of human diploid fibroblasts and melanocytes. *Experimental Gerontology* **35**: 927-945.

Ulaner, G.A., Hu, J.F., Vu, T.H., Giudice, L.C. and Hoffman, A.R. (1998) Telomerase activity in human development is regulated by human telomerase reverse transcriptase (hTERT) transcription and by alternate splicing of hTERT transcripts. *Cancer Research* **58**: 4168-4172.

van Steensel, B. and de Lange, T. (1997) Control of telomere length by the human telomeric protein TRF1. *Nature* **385** (6618): 740-743.

van Steensel, B., Smogorzeska, A. and de Lange, T. (1998) TRF2 protects human telomeres from end to end fusions. *Cell* **92**: 401-413.

Vaziri, H. and Benchimol, S. (1998) Reconstitution of telomerase activity in normal cells leads to elongation of telomeres and extended replicative lifespan. *Current Biology* **8**: 279-282.

Vaziri, H., Squire, J.A., Pandita, T.K., Bradley, G., Kuba, R.M., Zhang, H., Gulyas, S., Hill, R.P., Nolan, G.P. and Benchimol, S. (1999) Analysis of genomic integrity and p53 dependent G_1 checkpoint in telomere induced extended life span in human fibroblasts. *Molecular and Cellular Biology* **19**: 2373-2379.

von Zglinicki, T. (2000) Role of oxidative stress in telomere length regulation and replicative senescence. *Annals New York Academy of Sciences* **908**: 99-110.

von Zglinicki, T. (2001) Telomeres and replicative senescence: is it only length that counts ? *Cancer Letters* **168**: 111-116.

von Zglinicki, T. (2002) Oxidative stress shortens telomeres. *Trends in Biochemical Sciences* **27** (7): 339-344.

von Zglinicki, T., Saretzki, G., Docke, W. and Lotze, C. (1995) Mild hyperoxia shortens telomeres and inhibits proliferation of fibroblast: A model for senescence? *Experimental Cell Research* **220**: 186-193.

von Zglinicki, T., Pilger, R. and Sitte, N. (2000) Accumulation of single stand breaks is the major cause of telomere shortening in human fibroblasts. *Free Radical Biology and Medicine* **28**: 64-74.

Wang, J.C. (1971) Interaction between DNA and E. Coli: protein omega. *Journal of Molecular Biology* **55**: 523-533.

Wang, J.C. (1996) DNA topoisomerases. *Annual Reviews in Biochemistry* **65**: 635-692.

Wang, X., Wong, S.C., Pan, J., Tsao, S.W., Fung, K.H., Kwong, D.L., Sham, J.S. and Nicholls, J.M. (1998) Evidence of cisplatin-induced senescent-like growth arrest in nasopharyngeal carcinoma cells. *Cancer Research* **58**: 5019-5022.

Watson, J.D. (1972) Origin of concatemeric T7 DNA. *Nat. N. Biol.* **239**: 197-201.

Wei, W. and Sedivy, J.M. (1999) Differentiation between senescence (M1) and crisis (M2) in human fibroblast cultures. *Experimental Cell Research* **253**: 519-522.

Weinrich, S.L., Pruzan, R., Ma, L., Ouellette, M., Tesmer, V.M., Hott, S.E., Bodnar, A.G., Lichtsteiner, S., Kim, N.W., Trager, J.B., Taylor, R.D., Carlos, R., Andrews, W.H., Wright, W.E., Shay, J.W., Harley, C.B. and Morin, G.B. (1997) Reconstitution of human telomerase with the template RNA component hTR and the catalytic protein subunit hTRT. *Nature Genetics* **17**: 498-502.

Wen, J., Cong, Y.S. and Bacchetti, S. (1998) Reconstitution of wild type or mutant telomerase activity in telomerase negative immortal human cells. *Human Molecular Genetics* **7**: 1137-1141.

West, M.D., Pereira-Smith, O.M. and Smith, J.R. (1989) Replicative senescence of human skin fibroblasts correlates with a loss of regulation an overexpression of collagenase activity. *Experimental Cell Research* **184**: 138-147.

Wiltshaw, E. and Carr, B. (1974) cis-Platinum(II)diamminedichloride: clinical experience of the Royal Marsden Hospital and Institute of Cancer Research. *Recent Results in Cancer Research* **48**: 178.

Wolf, C.R., Hayward, I.P., Lawrie, S.S., Buckton, K., McIntyre, M.A., Adams, D.J., Lewis, A.D., Scott, A.R. and Smyth, J.F. (1987) Cellular heterogeneity and drug resistance in two ovarian adenocarcinoma cell lines derived from a single patient. *International Journal of Cancer* **39**: 695-702.

Wong, J.M., Kusdra, L. and Collins, K. (2002) Subnuclear shuttling of human telomerase induced by transformation and DNA damage. *Nature Cell Biology* **4**: 731-736.

Wright, W.E., Tesmer, V.M., Huffmann, K.E., Leverne, S.D. and Shay, J.W. (1997) Normal human chromosomes have long G rich telomeric overhangs at one end. *Genes and Development* **11**: 2801-2809.

Wyllie, A.H. (1997) Apoptosis: an overview. *British Medical Bulletin* **53** (3): 451-465.

Wyllie, A.H., Kerr, J.F. and Currie, A.R. (1980) Cell death: the significance of apoptosis. *Int. Rev. Cytol* **68**: 251-306.

Ye, J.Z. and de Lange, T. (2004) TIN2 is a tankyrase 1 PARP modulator in the TRF1 telomere length control complex. *Nature Genetics* **36**: 618-623.

Ye, J.Z., Donigian, J.R., van Overbeek, M., Loayza, D., Luo, Y., Krutchinsky, A.N., Chait, B.T. and de Lange, T. (2004b) TIN2 binds TRF1 and TRF2 simultaneously and stabilizes the TRF2 complex on telomeres. *Journal of Biological Chemistry* **279**: 47264-47271.

Ye, J.Z., Hockemeyer, D., Krutchinsky, A.N., Loayza, D., Hooper, S.M., Chait, B.T. and de Lange, T. (2004a) POT1-interacting protein PIP1: a telomere length regulator that recruits POT1 to the TIN2/TRF1 complex. *Genes and Development* **18**: 1649-1654.

Yoakum, G.H., Lechner, J.F., Gabrielson, E.W., Korba, B.E., Malan-Shibley, L., Willey, J.C., Valerio, M.G., Shamsuddin, A.M., Trump, B.F. and Harris, C.C. (1985) Transformation of human bronchial epithelial cells transfected by Harvey ras oncogene. *Science* **227**: 1174-9.

Yoon, H.J., Choi, I.Y., Kang, M.R., Kim, S.S., Muller, M.T., Spitzner, J.R. and Chung, I.K. (1998) DNA topoisomerases II cleavage of telomeres in vitro and in vivo. *Biochimica et Biophysica Acta* **1395**: 110-120.

Zakian, V.A. (1989) Structure and function of telomeres. *Annual Reviews In Genetics* **23**: 579-604.

Zhang, P., Chan, S.L., Fu, W., Mendoza, M. and Mattson, M.P. (2003) TERT suppresses apoptosis at a premitochondrial step by a mechanism requiring reverse transcriptase activity and 14-3-3 protein binding activity. *The FASEB Journal* **17**: 767-769.

Zhang, R.G., Zhang, R.P., Wang, X.W. and Xie, H. (2002) Effects of cisplatin on telomerase activity and telomere length in BEL-7404 human hepatoma cells. *Cell Research* **12** (1): 55-62.

Zhao, X., Liu, J., Hsu, D.S., Zhao, S., Taylor, J.S. and Sancar, A. (1997) Reaction mechanism of (6-4) photolyase. *Journal of Biological Chemistry* **272**: 32580-32590.

Zhou, J., Ahn, J., Wilson, S.H. and Prives, C. (2001) A role for p53 in base excision repair. *EMBO Journal* **20**: 914-923.

Zhou, X.Z. and Lu, K.P. (2001) The Pin2/TRF1-interacting protein PinX1 is a potent telomerase inhibitor. *Cell* **107**: 347-59.

Zhu, L., Harlow, E. and Dynlacht, B.D. (1995) p107 uses a p21CIP1 related domain to bind cyclin/cdk2 and regulate interactions with E2F. *Genes and Development* **9**: 1740-1752.

Zhu, X.D., Kuster, B., Mann, M., Petrini, J.h.J. and de Lange, T. (2000) Cell-cycle-regulated association of RAD50/MRE11/NBS1 with TRF2 and human telomeres. *Nature Genetics* **25**: 347-351.

Zhu, X.D., Niedernhofer, L., Kuster, B., Mann, M., Hoeijmakers, J.H. and de Lange, T. (2003) ERCC1/XPF removes the 3' overhang from uncapped telomeres and represses formation of telomeric DNA-containing double minute chromosomes. *Molecular Cell* **12**: 1489-1498.